



Supporting Information

Palladium-Catalyzed Directed *meta*-Selective C–H Allylation of Arenes: Unactivated Internal Olefins as Allyl Surrogates

Tapas Kumar Achar⁺, Xinglong Zhang⁺, Rahul Mondal, M. S. Shanavas, Siddhartha Maiti, Sabyasachi Maity, Nityananda Pal, Robert S. Paton,* and Debabrata Maiti*

anie_201904608_sm_miscellaneous_information.pdf

Supporting Information
©Wiley-VCH 2016
69451 Weinheim, Germany

Palladium-Catalyzed Directed *meta*-Selective C–H Allylation of Arenes: Unactivated Internal Olefins as Allyl Surrogates

Tapas Kumar Achar,^{[a],†} Xinglong Zhang,^{[b],†} Rahul Mondal,^[a] Shanavas M. S.,^[a] Siddhartha Maiti,^[c] Sabyasachi Maity,^[a] Nityananda Pal,^[a] Robert S. Paton, *^[b] and Debabrata Maiti*^[a]

^[a]Department of Chemistry, Indian Institute of Technology Bombay, Powai, Mumbai 400076, India

^[b]Chemistry Research Laboratory, University of Oxford, Mansfield Road, Oxford OX1 3TA, United Kingdom

^[c]BSBE, Indian Institute of Technology Bombay, Powai, Mumbai 400076, India

† These authors contributed equally.

* Debabrata Maiti: dmaiti@chem.iitb.ac.in

* Robert S. Paton: robert.paton@colostate.edu

Abstract: Palladium(II)-catalyzed *meta*-selective C–H allylation of arenes has been developed utilizing synthetically inert unactivated acyclic internal olefins as allylic surrogates. The strong σ-donating and π-accepting ability of pyrimidine-based directing group facilitates the olefin insertion by overcoming inertness of the typical unactivated internal olefins. Exclusive allyl over styrenyl product selectivity as well as *E*-stereoselectivity were achieved with broad substrate scope, wide functional group tolerance and good to excellent yields. Late-stage functionalisations of pharmaceuticals were demonstrated. Experimental and computational studies shed insights on the mechanism and pointed to key palladacyclic steric control in determining product selectivities.

Table of Content

Section	Title	Page No
1	General consideration	S3
2	Experimental section	S3
2.1	Preparation of starting materials	S3 – S9
2.2	Optimization details for <i>meta</i> -C–H allylation with aliphatic olefins	S10 – S16
2.3	NMR spectra of the representative allylated compound, 3a	S17 – S18
2.4	Determination of <i>meta</i> -selectivity	S19
2.5	General procedure for palladium catalyzed <i>meta</i> -selective C–H allylation of arene	S19
2.6	Characterization data of <i>meta</i> -allylated products	S20 – S47
2.7	Mechanistic studies	S48 – S56
2.8	General procedure for palladium catalyzed <i>meta</i> -selective C–H allylation with terminal olefin	S56 – S57
2.9	Computational methods	S58 – S101
3	References	S101 – 103
4	Author contributions	S104
5	NMR spectra	S105 – S168

1. General Consideration:

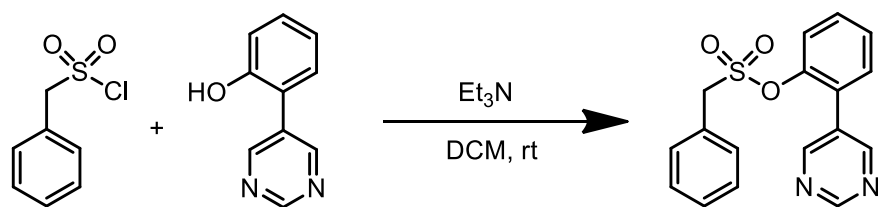
Reagent Information. Unless otherwise stated, all reactions were carried out in screw cap reaction tubes under aerobic condition. All the chemicals were purchased from Sigma Aldrich, Alfa Aesar and TCI-India. Solvents were bought from commercial sources and were used without further purification. Silica gel (100–200 mesh), obtained from Merck, was used for column chromatography. Products and starting materials were visualized on TLC plate (Merck, TLC silica gel 60 F₂₅₄) using UV-light or by staining with PMA (Phosphomolybdic acid). Petroleum ether and ethyl acetate mixture was used as a gradient elution for column chromatography.

Analytical Information. Isolated compounds were characterized by ¹H NMR, ¹³C NMR spectroscopy, and high-resolution mass spectra (HRMS). Unless otherwise stated, all Nuclear Magnetic Resonance spectra were recorded on a Bruker 400 MHz and 500 MHz instrument. NMR spectra are reported in parts per million (ppm), and were measured relative to the signals for residual solvent (7.26 ppm for ¹H NMR and 77.16 ppm for ¹³C NMR in CDCl₃) in the deuterated solvent, unless otherwise stated. All ¹³C NMR spectra were obtained with ¹H decoupling. HRMS were recorded on a micro-mass ESI TOF (time of flight) mass spectrometer.

2. Experimental Section

2.1. Preparation of Starting materials

2.1.1. Synthesis of sulfonyl ester scaffolds:



Step 1: Preparation of phenylmethanesulfonyl chloride

An oven dried clean round bottom flask was charged with magnetic stir-bar, benzyl chloride/bromide (10 mmol) and thiourea (10 mmol, 760 mg). 10 ml of absolute ethanol was added and refluxed at 96 °C. After 3 h the reaction was taken out and solvent was evaporated under

reduced pressure to obtained white solid thiouric salt. The obtained solid salt was suspended in 14 ml of MeCN and 3 ml 2M HCl was added to it. The mixture was stirred at 0 °C for 15 min. N-chlorosuccinimide (NCS) (40 mmol; 5.34 g) was added in portion to the suspension in order to obtain a clear solution. The solution was stirred for another 30 min at room temperature. The solution was evaporated under reduced pressure to remove the MeCN. The remaining aqueous portion was extracted with ethyl acetate. The organic portion was dried over anhydrous Na₂SO₄ and the crude mixture was evaporated and purified by column chromatography using silica gel (100-200 mesh size) and petroleum ether/ ethyl acetate as an eluent. Quantitative yield.

Step 2: Preparation of 2-(pyrimidin-5-yl)phenol

2-(pyrimidin-5-yl)phenol was prepared by following Suzuki cross coupling reaction condition. A clean, oven-dried screw cap reaction tube with previously placed magnetic stir-bar was charged with 5-bromopyrimidine (1 equiv.), 2-hydroxyphenyl boronic acid (1.2 equiv.), palladium (II) acetate (2 mol%), SPhos (4 mol%) and K₃PO₄ (2 equiv.). The cap was fitted with a rubber septum and the reaction tube was evacuated and back filled with nitrogen and this sequence was repeated three additional times. Now under the positive flow of nitrogen, 6 mL THF was added to the reaction mixture. Several reactions were carried out in different reaction tubes (2 mmol/reaction tube). The reaction mixture was vigorously stirred on an oil bath at 75 °C for 24 h. The reaction mixture was subsequently dried using rotary evaporator. The reaction mixture was extracted thrice with ethyl acetate (3 x 20 mL) and brine solution (3 x 10 mL). The organic layer was collected and dried over anhydrous Na₂SO₄. The solvent was evaporated under reduced pressure. The crude mixture was purified by column chromatography using neutral alumina and petroleum ether/ethyl acetate (80/20, v/v) as an eluent; white solid, 72%

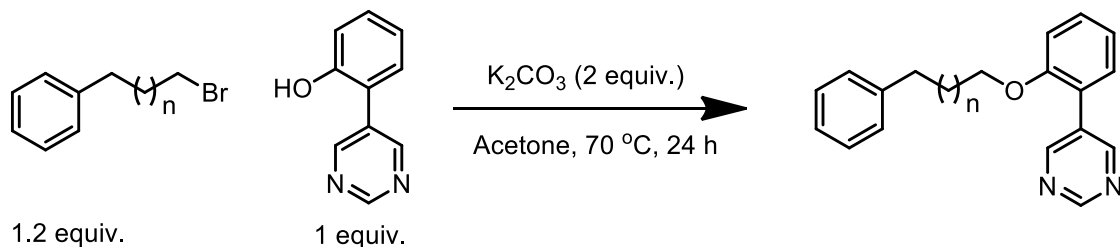
Step 3: To an ice-cold solution of 2-(pyrimidin-5-yl)phenol (5 mmol) and triethylamine (1.5 equiv, 1.04 mL) in 10 mL dichloromethane under nitrogen atmosphere, phenylmethanesulfonyl chloride was added portion wise. Stirring was continued for an additional 20 minutes, after that the ice bath was removed and the reaction mixture was left for vigorous stirring at room temperature overnight. DCM was removed under reduced pressure. The residual was diluted and extracted with ethyl acetate (3 x 20 mL) and brine solution (3 x 10 mL). The organic layer was collected and dried over anhydrous Na₂SO₄. After filtration and evaporation of the solvent, the crude mixture was purified

by column chromatography using neutral alumina and petroleum-ether/ethyl acetate (85/15, v/v) as an eluent. White solid, 74%; ^1H NMR (400 MHz, CDCl_3) δ 9.21 (s, 1H), 8.81 (s, 2H), 7.46 – 7.41 (m, 2H), 7.41 – 7.35 (m, 4H), 7.33 – 7.29 (m, 3H), 4.33 (s, 2H); ^{13}C NMR (101 MHz, CDCl_3) δ 157.95, 156.86, 146.16, 131.32, 131.15, 130.88, 130.83, 129.66, 129.25, 128.81, 127.97, 126.71, 123.44, 57.85.

All the sulfonyl esters were synthesized following the above procedures and characterized by ^1H and ^{13}C NMR spectroscopy, characterization data matched with our previous reports (*Angew. Chem. Int. Ed.* **2017**, *56*, 3182–3186; *Angew. Chem. Int. Ed.* **2017**, *56*, 12538–12542).

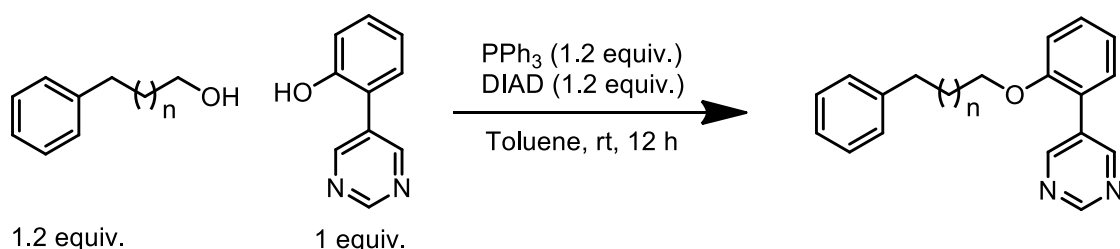
2.1.2. Synthesis of ether scaffolds:

General procedure A



A clean, oven-dried screw cap reaction tube with previously placed magnetic stir-bar was charged with 2-(pyrimidin-5-yl)phenol (1 equiv, 2.4 mmol), and K_2CO_3 (2 equiv, 4 mmol). The cap was fitted with a rubber septum and the reaction tube was evacuated and back filled with nitrogen and this sequence was repeated three additional times. Now under the positive flow of nitrogen, 6 mL acetone was added to the reaction mixture. Then, phenyl alkyl bromide (1.2 equiv, 2 mmol) was added by using syringe. The reaction mixture was vigorously stirred at 70°C for 24 h. The reaction mixture was dried under rotary evaporator. The reaction mixture was extracted thrice with ethyl acetate (3 x 20 mL) and brine solution (3 x 10 mL). The organic layer was collected and dried over anhydrous Na_2SO_4 . The solvent was evaporated under reduced pressure. The crude mixture was purified by column chromatography using neutral alumina and petroleum-ether/ethyl acetate (95/5, v/v) as an eluent.

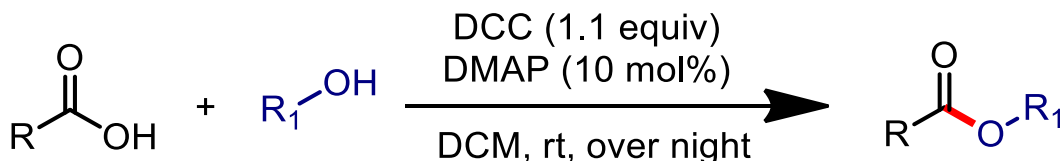
General procedure B



To a 20-mL reaction tube, starting alcohol (1.2 equiv), 2-(pyrimidin-5-yl)phenol (1 equiv), triphenylphosphine (1.2 equiv), diisopropyl diazene-1,2-dicarboxylate (DIAD, 1.2 equiv) and toluene (2 mL) were added. The mixture was stirred at room temperature and monitored by TLC. Upon completion of the reaction, 5 mL water was added and the layers were separated. The aqueous phase was extracted twice with ethyl acetate (10 mL). The combined organic phase was washed with brine solution and dried over anhydrous Na_2SO_4 . After filtration and removal of solvent under vacuum, the residue was purified through column chromatography with hexane/ethyl acetate as an eluent. The target substrates were obtained generally in good to excellent yields.

All the synthesized ether scaffolds were characterized by ^1H and ^{13}C NMR spectroscopy and characterization data matched with previous reports (*Angew. Chem. Int. Ed.* **2017**, *56*, 3182–3186; *Angew. Chem. Int. Ed.* **2017**, *56*, 12538–12542; *Angew. Chem. Int. Ed.* **2018**, *57*, 7659 – 7663).

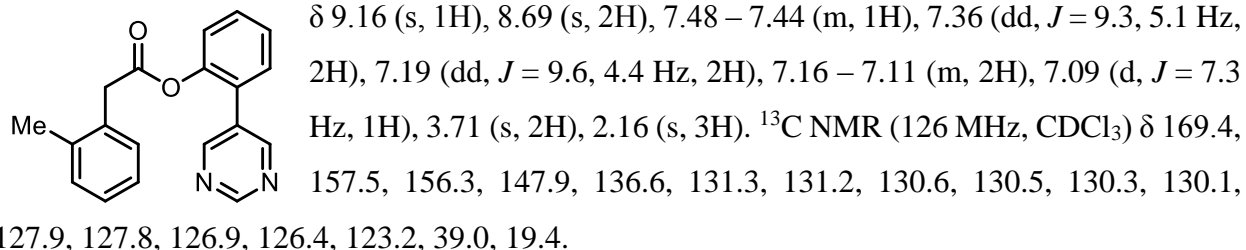
2.1.3. General Procedure for Synthesis of Carbonyl Ester:



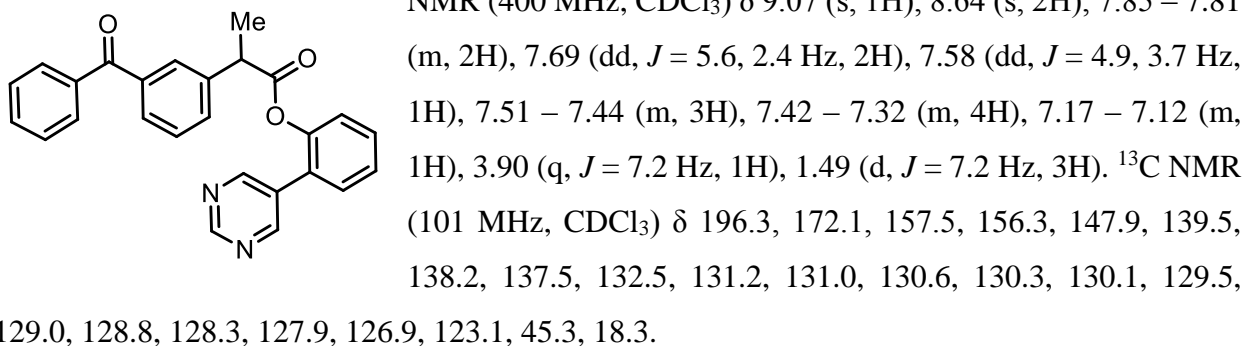
To a stirred solution of carboxylic acid (10 mmol) and DMAP (1 mmol) in 30 mL anhydrous DCM, alcohol (15 mmol) was added. After 15 minutes of stirring, DCC (11 mmol) was added to the reaction mixture at 0°C, and then allowed to stir overnight at room temperature. Upon completion of reaction, precipitated urea is then filtered off. Filtrate is evaporated and the residue

was dissolved in DCM and washed with saturated NaHCO_3 solution, and then dried over anhydrous Na_2SO_4 . The solvent was removed under reduced pressure and the residue was purified by column chromatography on silica gel (eluent: Petroleum ether/EtOAc) to give the desired ester.

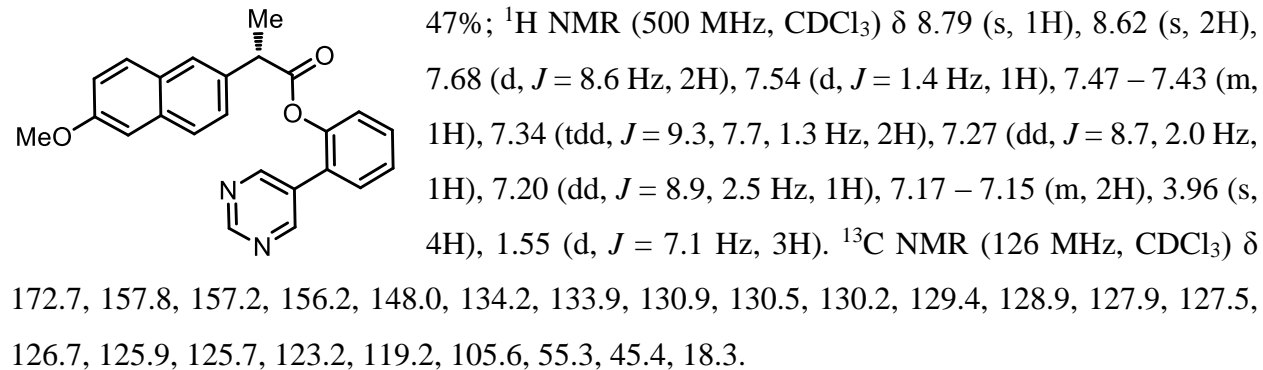
2-(pyrimidin-5-yl)phenyl 2-(o-tolyl)acetate: Yellow oil; yield 68%; ^1H NMR (500 MHz, CDCl_3)



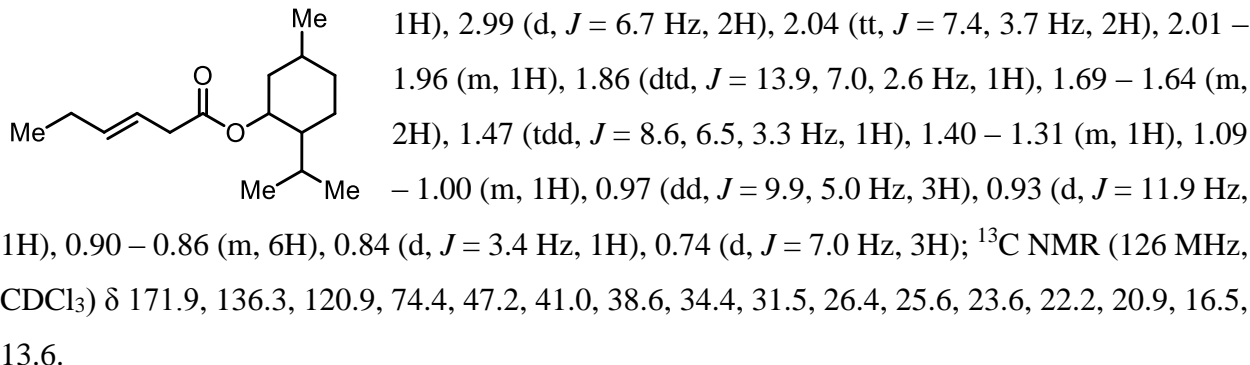
2-(pyrimidin-5-yl)phenyl 2-(3-benzoylphenyl)propanoate: Off-white solid; yield 74%; ^1H



(S)-2-(pyrimidin-5-yl)phenyl 2-(6-methoxynaphthalen-2-yl)propanoate: Yellow solid; yield



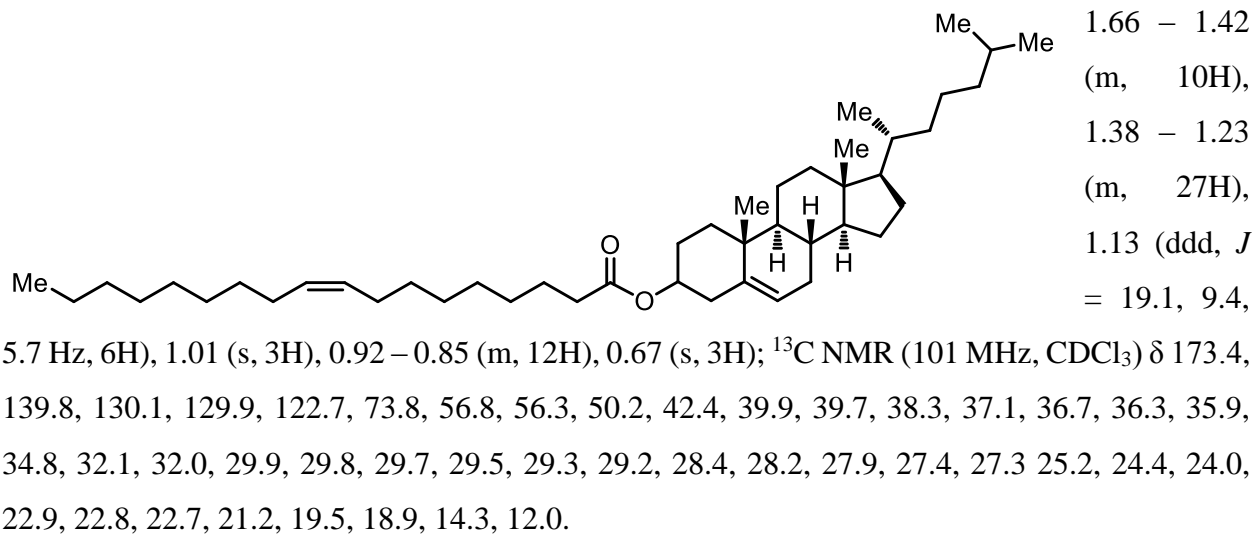
(E)-2-isopropyl-5-methylcyclohexyl hex-3-enoate: Colorless oil; yield 86%; ¹H NMR (500 MHz, CDCl₃) δ 5.60 (dt, *J* = 15.2, 6.1 Hz, 1H), 5.55 – 5.46 (m, 1H), 4.66 (td, *J* = 10.9, 4.4 Hz, 1H), 2.99 (d, *J* = 6.7 Hz, 2H), 2.04 (tt, *J* = 7.4, 3.7 Hz, 2H), 2.01 – 1.96 (m, 1H), 1.86 (dtd, *J* = 13.9, 7.0, 2.6 Hz, 1H), 1.69 – 1.64 (m, 2H), 1.47 (tdd, *J* = 8.6, 6.5, 3.3 Hz, 1H), 1.40 – 1.31 (m, 1H), 1.09 – 1.00 (m, 1H), 0.97 (dd, *J* = 9.9, 5.0 Hz, 3H), 0.93 (d, *J* = 11.9 Hz, 1H), 0.90 – 0.86 (m, 6H), 0.84 (d, *J* = 3.4 Hz, 1H), 0.74 (d, *J* = 7.0 Hz, 3H); ¹³C NMR (126 MHz, CDCl₃) δ 171.9, 136.3, 120.9, 74.4, 47.2, 41.0, 38.6, 34.4, 31.5, 26.4, 25.6, 23.6, 22.2, 20.9, 16.5, 13.6.



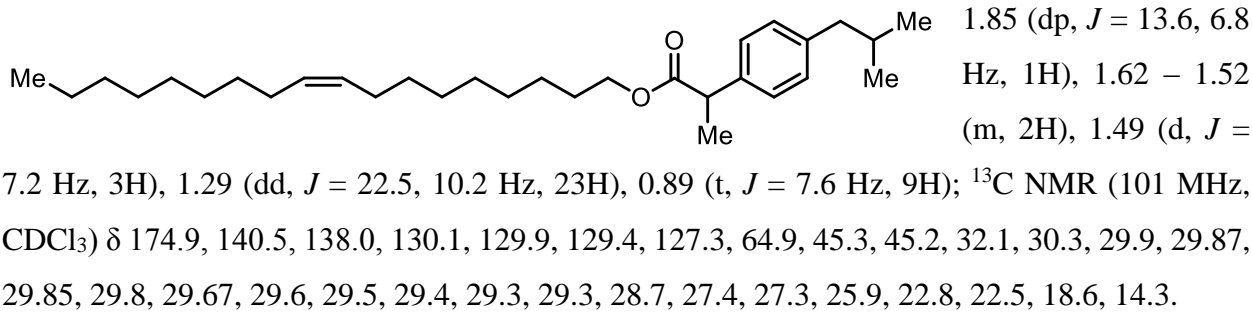
(E)-(Z)-3,7-dimethylocta-2,6-dien-1-yl hex-3-enoate: Colorless oil; yield 82%; ¹H NMR (500 MHz, CDCl₃) δ 5.58 (dt, *J* = 15.3, 6.0 Hz, 1H), 5.55 – 5.47 (m, 1H), 5.35 (t, *J* = 7.2 Hz, 1H), 5.08 (ddd, *J* = 5.5, 4.7, 1.2 Hz, 1H), 4.56 (d, *J* = 7.2 Hz, 2H), 3.01 (dd, *J* = 6.6, 0.9 Hz, 2H), 2.06 (ddd, *J* = 14.7, 9.1, 3.7 Hz, 6H), 1.75 (s, 3H), 1.67 (s, 3H), 1.59 (s, 3H), 0.97 (t, *J* = 7.5 Hz, 3H); ¹³C NMR (126 MHz, CDCl₃) δ 172.4, 142.7, 136.4, 132.3, 123.7, 120.8, 119.3, 61.3, 38.2, 32.3, 26.8, 25.8, 25.6, 23.6, 17.8, 13.6.

(E)-Dec-5-en-1-yl adamantane-1-carboxylate: Colorless oil; yield 87%; ¹H NMR (400 MHz, CDCl₃) δ 5.44 – 5.25 (m, 2H), 3.99 (t, *J* = 6.5 Hz, 2H), 1.96 (s, 7H), 1.84 (s, 6H), 1.73 – 1.62 (m, 6H), 1.56 (dd, *J* = 14.6, 6.9 Hz, 2H), 1.37 (dd, *J* = 14.9, 7.5 Hz, 2H), 1.27 (d, *J* = 2.2 Hz, 4H), 0.84 (t, *J* = 6.5 Hz, 3H); ¹³C NMR (101 MHz, CDCl₃) δ 177.7, 130.9, 129.6, 64.0, 40.7, 38.9, 36.6, 32.3, 32.1, 31.8, 28.1, 28.0, 25.9, 22.2, 13.9.

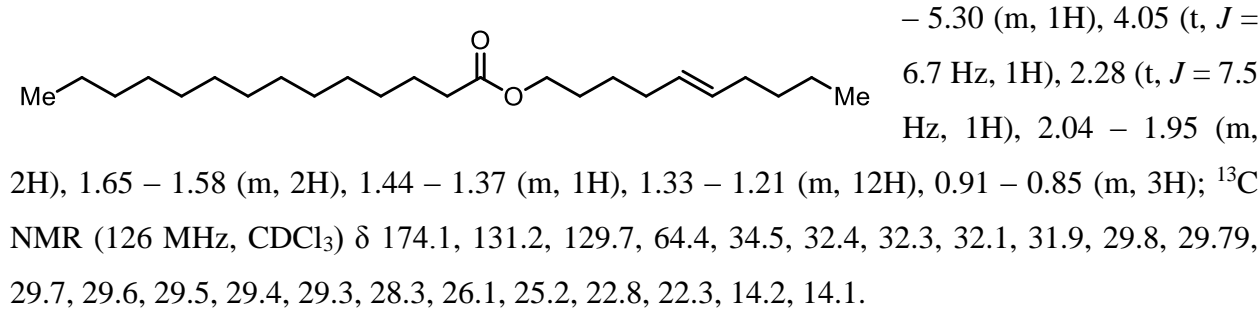
Cholesterol oleate: White solid; yield 85%; ^1H NMR (400 MHz, CDCl_3) δ 5.39 – 5.31 (m, 3H), 4.66 – 4.55 (m, 1H), 2.34 – 2.23 (m, 4H), 1.98 (dd, $J = 17.2, 10.8$ Hz, 7H), 1.89 – 1.80 (m, 3H),



(Z)-octadec-9-en-1-yl 2-(4-isobutylphenyl)propanoate: Colorless oil; yield 91%; ^1H NMR (400 MHz, CDCl_3) δ 7.21 (d, $J = 8.1$ Hz, 2H), 7.09 (d, $J = 8.1$ Hz, 2H), 5.46 – 5.27 (m, 2H), 4.06 (t, $J = 6.7$ Hz, 2H), 3.69 (q, $J = 7.1$ Hz, 1H), 2.45 (d, $J = 7.2$ Hz, 2H), 2.02 (dt, $J = 7.5, 3.7$ Hz, 3H),



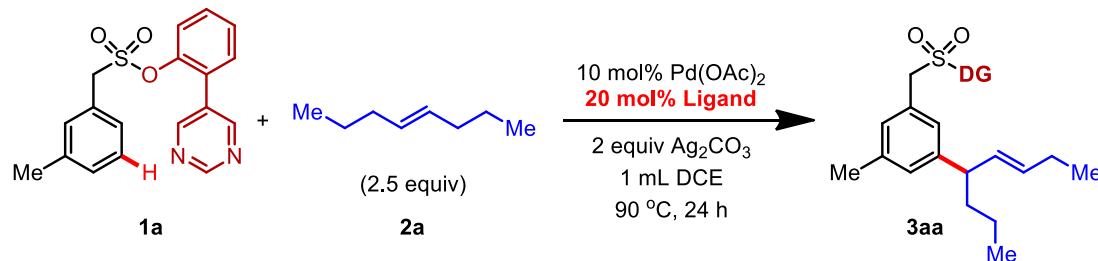
(E)-dec-5-en-1-yl tetradecanoate: Colorless oil; yield 94%; ^1H NMR (500 MHz, CDCl_3) δ 5.48



2.2. Optimization details for *meta*-C–H allylation with aliphatic olefins:

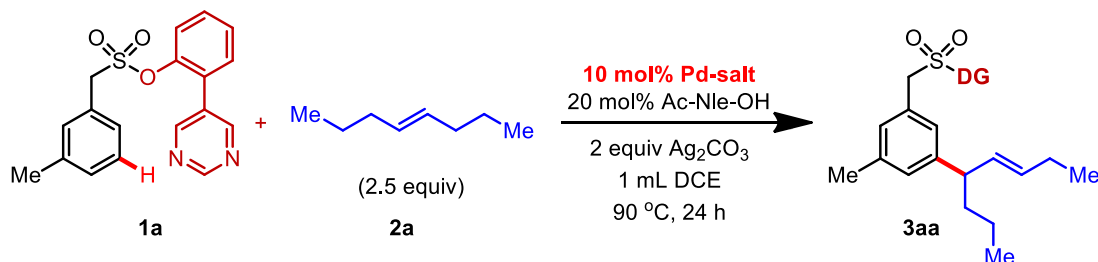
All the reactions were carried out with 0.05 mmol of **1a** in a screw cap reaction tube. Yield and selectivity are based on ¹H NMR of the crude reaction mixture using 1,3,5-trimethoxybenzene as an internal standard.

Table S1. Optimization of ligand

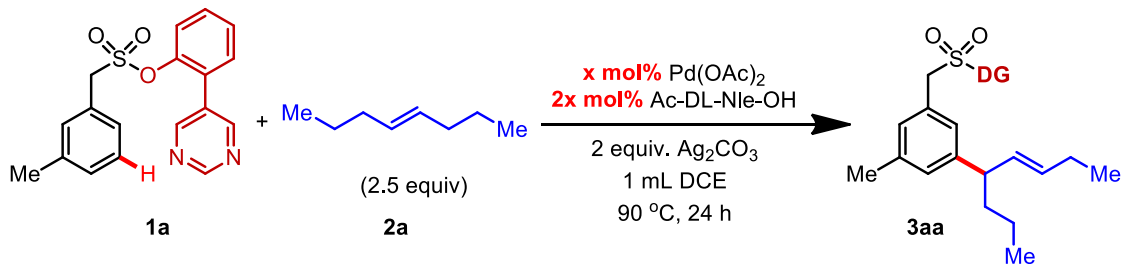


Entry	Ligands	Yield (%)	Selectivity (<i>meta</i> :others)
1	Without ligand	10	4:1
2	<i>N</i> -Acetyl Glycine	37	10:1
3	Glycine	trace	--
4	<i>N</i> -Formyl Glycine	trace	--
5	<i>N</i> -Boc Glycine	20	6:1
6	FMoc-Glycine	trace	--
7	Glycyl-Glycine	trace	--
8	<i>N</i> -Boc-Phenylglycine	trace	--
9	<i>N</i> -Acetyl Phenylglycine	trace	--
10	<i>N</i> -Acetyl-2-Phenylglycine	trace	--
11	<i>N</i> -Acetyl valine	21	6:1
12	<i>N</i> -Acetyl-4-hydroxy-proline	trace	--
13	<i>N</i> -Acetyl Leucine	35	7:1
14	<i>N</i>-Acetyl-DL-norleucine	46	13:1
15	<i>N</i> -Acetyl Tryptophan	trace	--
16	<i>N</i> -Boc <i>tert</i> -Leucine	15	4:1

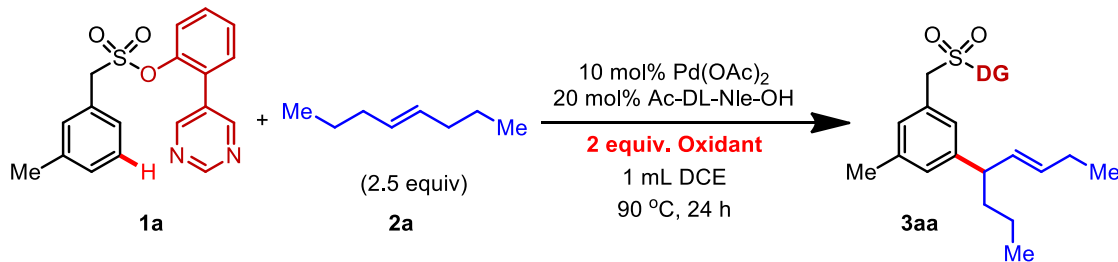
17	N-Boc Leucine	18	4:1
18	N-Boc Isoleucine	18	5:1
19	2-Hydroxy pyridine	nd	--
20	Anthranilamide	nd	--
21	rac-BINAM	nd	--
22	XPhos	nd	--
23	N-Acetyl-DL-2-Aminobutyric acid	32	2:1
24	IPr	trace	--

Table S2. Optimization of Pd-salt:

Entry	Pd-salt	Yield (%)	Selectivity (meta:others)
1	Pd(OAc)₂	46	13:1
2	PdCl ₂	trace	--
2	Pd(OPiv) ₂	28	10:1
4	Pd(CF ₃ COO) ₂	16	8:1
5	Pd(acac) ₂	nd	--
6	[PdCl(C ₃ H ₅)] ₂	nd	--
7	Pd ₂ (dba) ₃	nd	--
8	(PhCN) ₂ PdCl ₂	nd	--
9	(PPh ₃) ₂ PdCl ₂	nd	--

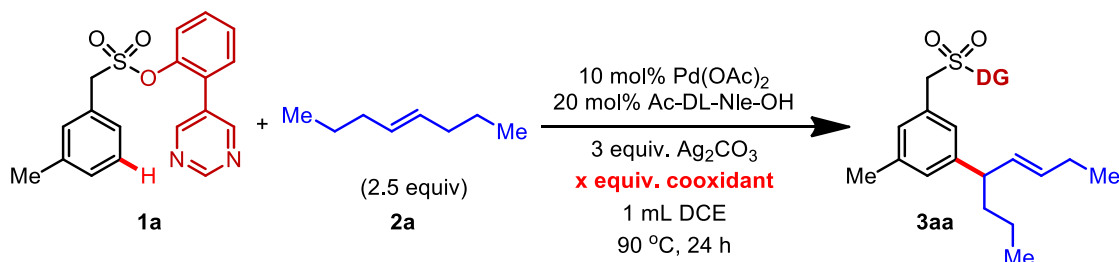
Table S3. Optimization by varying catalyst and ligand loading:

Entry	Catalyst Pd(OAc)_2	Ligand Ac-Nle-OH	Yield (%)	Selectivity (meta:others)
1	4	8	29	13:1
2	5	10	32	13:1
3	8	16	37	13:1
4	10	20	46	13:1
5	12	24	45	13:1
6	15	30	46	13:1

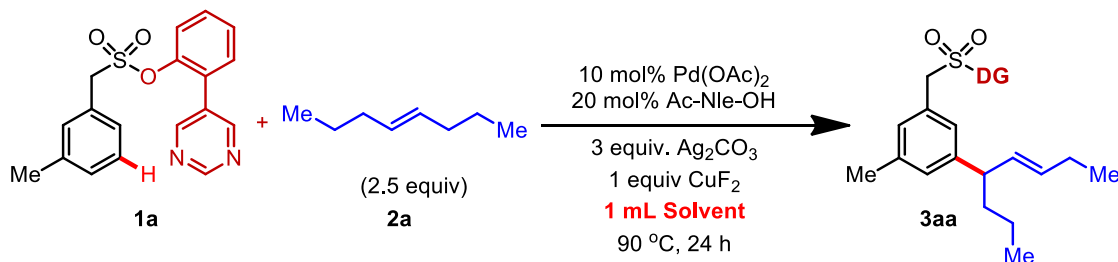
Table S4. Optimization of oxidant

Entry	Oxidant	Yield (%)	Selectivity (meta:others)
1	AgOAc	34	12:1
2	Ag_2CO_3	46	13:1
3	Ag_2SO_4	nd	--
4	AgNO_3	trace	--
5	AgOTf	nd	--
6	$\text{Cu}(\text{OAc})_2 \cdot \text{H}_2\text{O}$	44	12:1
7	BQ	trace	--
8	PIDA	nd	--

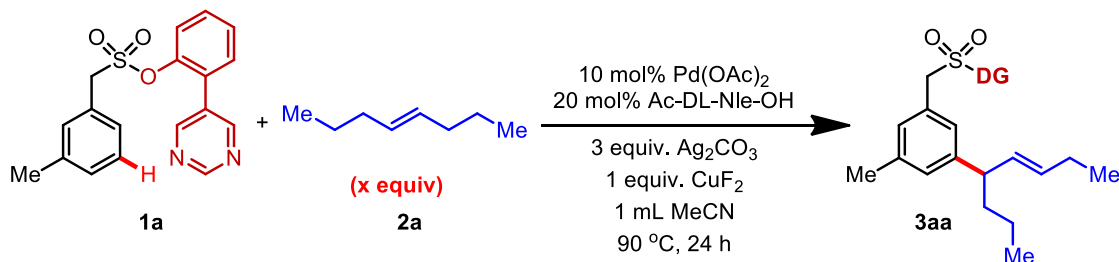
9	PIFA	nd	--
10	AgTFA	trace	--
11	K ₂ S ₂ O ₈	nd	--
12	Ag ₂ CO ₃ (2.5 equiv)	38	13:1
13	Ag₂CO₃ (3 equiv)	53	13:1
14	Ag ₂ CO ₃ (4 equiv)	48	13:1

Table S5. Optimization of additives

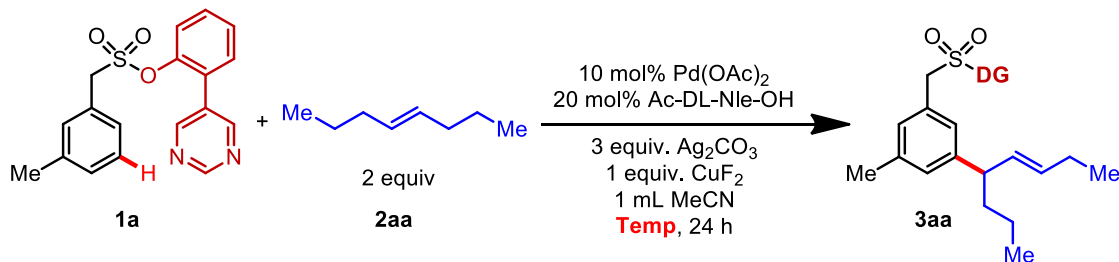
Entry	Co-oxidant (1 equiv)	Yield (%)	Selectivity (meta:others)
1	Cu ₂ (OAc).H ₂ O	44	12:1
2	CuCO ₃ .H ₂ O	38	6:1
3	CuCl ₂	36	8:1
4	CuF₂	65	13:1
5	CuO	37	6:1
6	CuOTf	trace	--
7	CuCl	49	9:1
8	Cu ₂ O	42	10:1
9	CuI	trace	--
10	O ₂ atm.	45	13:1
11	CuF ₂ (1.5 equiv)	65	13:1
12	CuF ₂ (0.75 equiv)	53	13:1

Table S6. Optimization of solvent

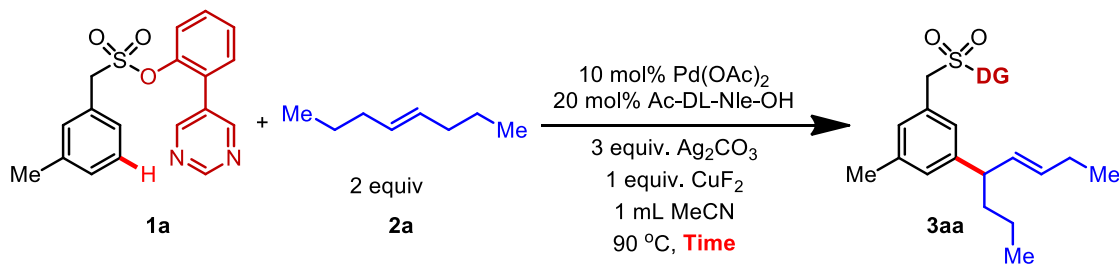
Entry	Solvent (1 mL)	Yield (%)	Selectivity (meta:others)
1	HFIP	trace	--
2	HFIP:DCE (1:1)	18	6:1
3	HFIP:DCE (1:4)	41	6:1
4	DCE	65	13:1
5	TFE	28	4:1
6	MeCN	83	13:1
7	1,4-Dioxane	trace	--
8	EtOH	--	--
9	DMSO	--	--
10	DMF	--	--
11	<i>t</i> BuOH	--	--

Table S7. Optimization of olefin amount

Entry	Trans-4-octene (equiv)	Yield (%)	Selectivity (meta:others)
1	1	65	13:1
2	1.5	71	13:1
3	2	83	13:1
4	2.5	82	13:1
5	3	84	13:1

Table S8. Temperature optimization

Entry	Temperature	Yield (%)	Selectivity (meta:others)
1	RT	--	--
2	50	33	8:1
3	70	60	12:1
4	80	75	13:1
5	90	83	13:1
6	100	78	10:1
7	110	76	9:1

Table S9. Time optimization

Entry	Time (h)	Yield (%)	Selectivity (meta:others)
1	12	65	13:1
2	18	74	13:1
3	24	83	13:1
4	30	81	13:1
5	36	82	13:1

2.3. NMR spectra of the representative allylated compound, 3a

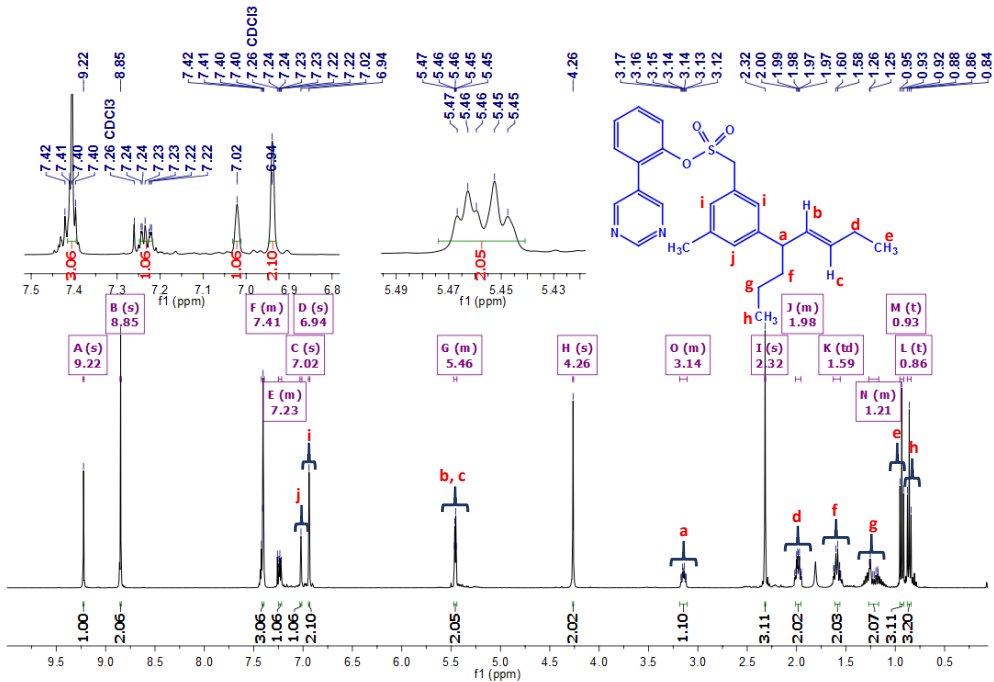


Figure S1. ^1H NMR of 3a

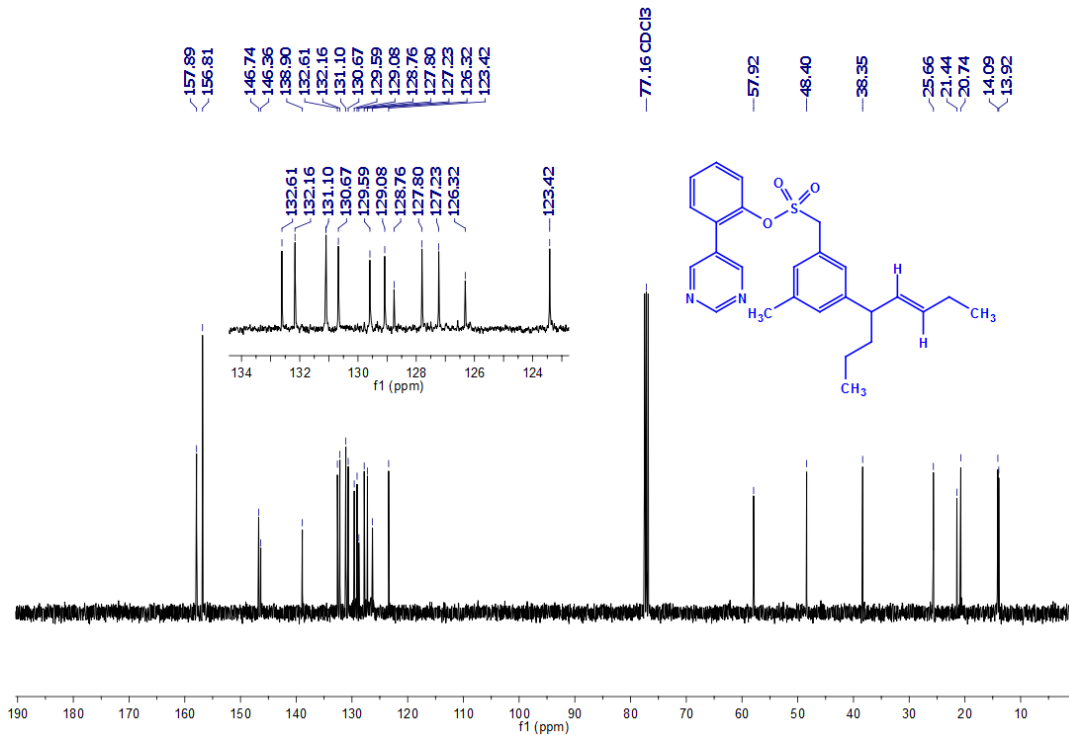


Figure S2. ^{13}C NMR of 3a

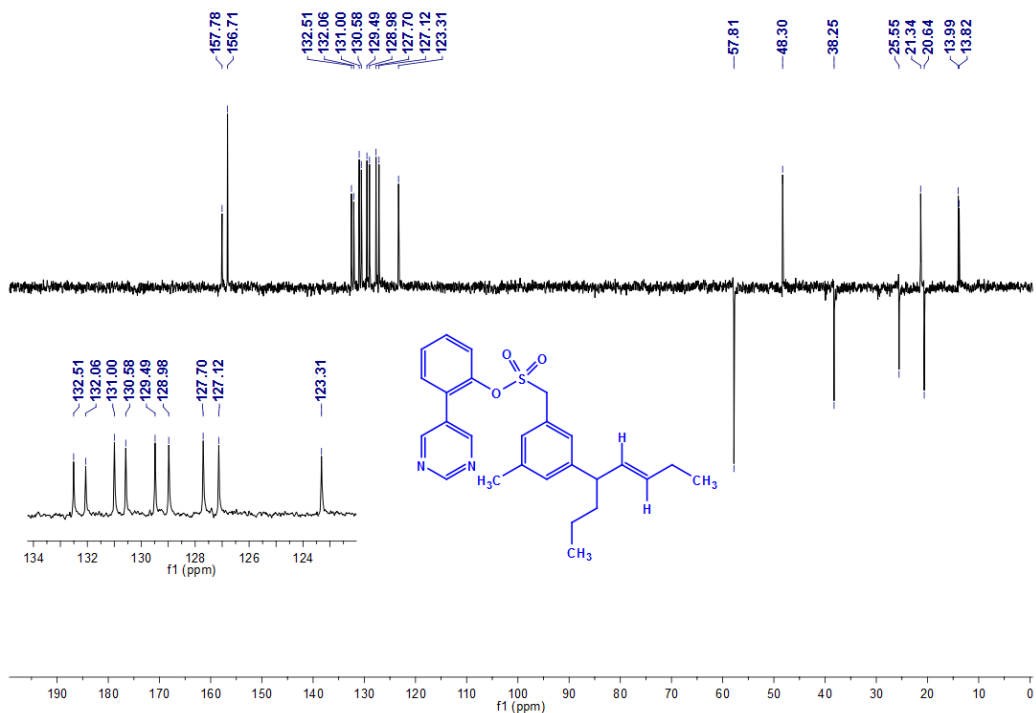
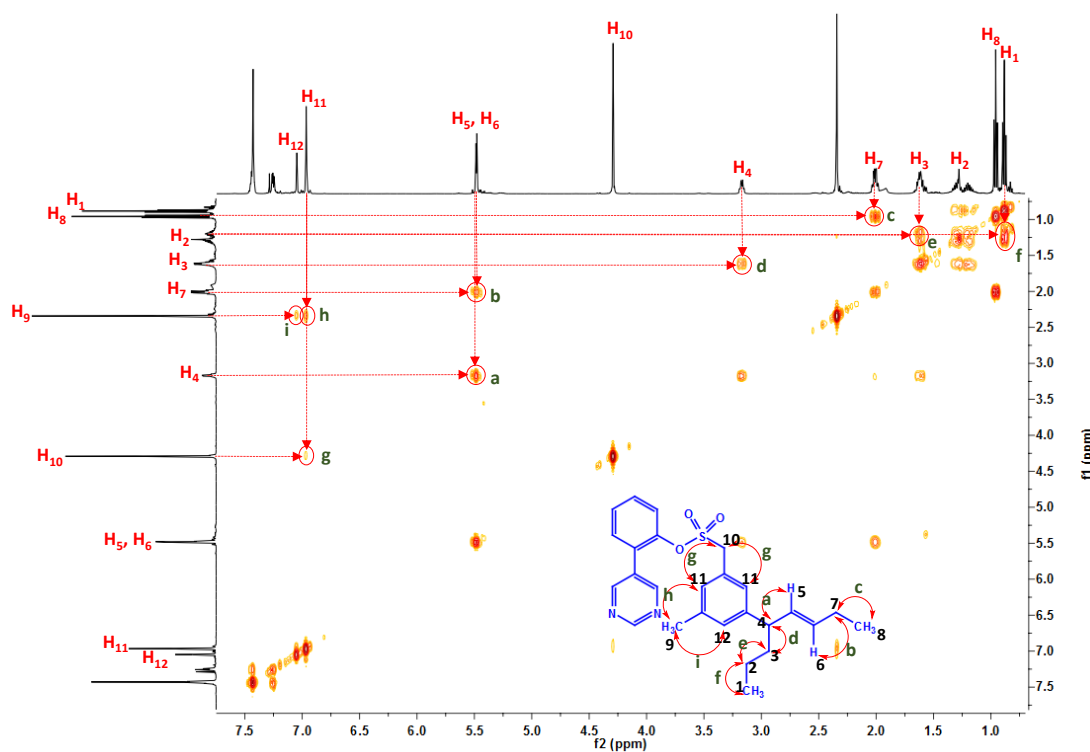


Figure S3. DEPT-135 NMR of 3a

Figure S4. ¹H-¹H COSY NMR of 3a

2.4. Determination of *meta*-selectivity: The selectivity of *meta*-C–H allylation product was determined by ^1H NMR of crude reaction mixture. The selectivity of the allyl product is determined based on characteristic –CH and –CH=CH peaks. It is relatable to note that the exact assignment of “others” (i.e. *ortho* and *para*-products, etc.) is conjectural, due to their low yields.

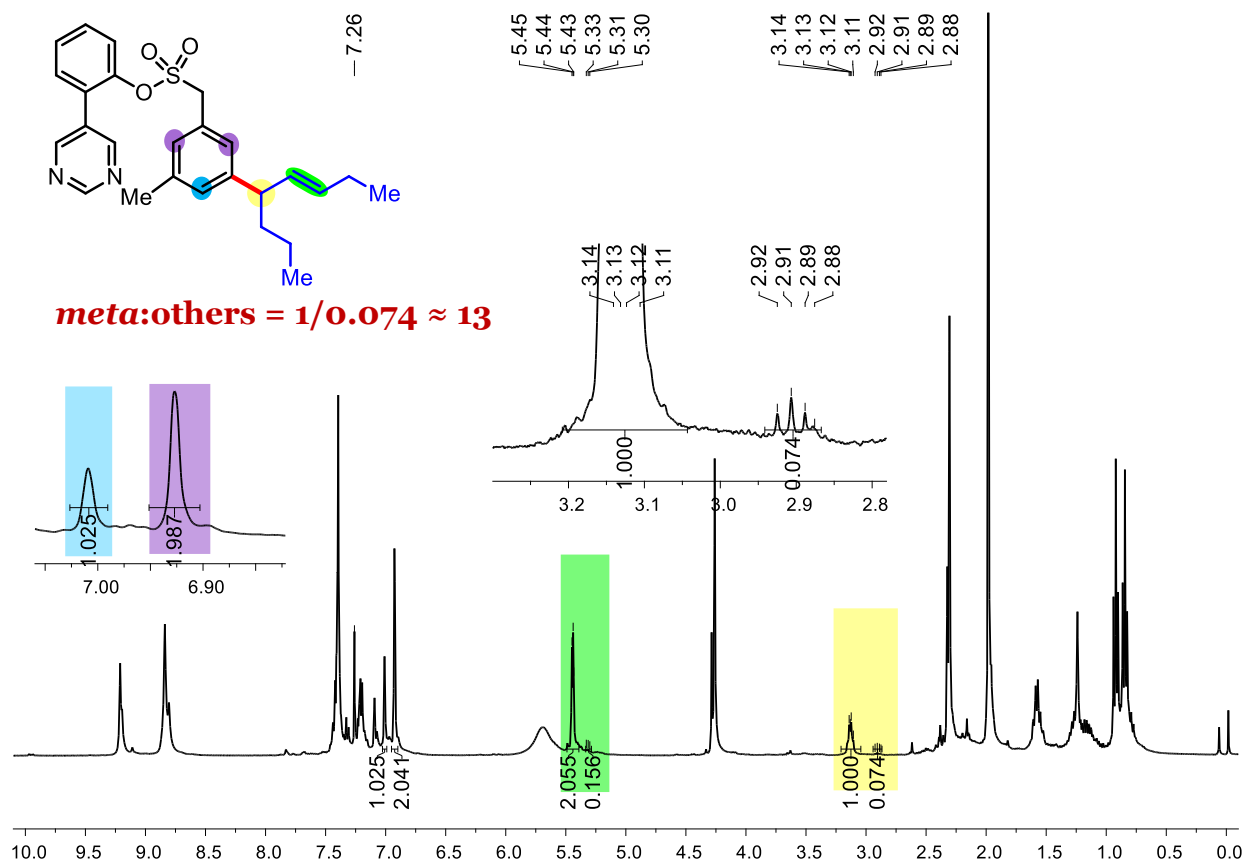


Figure S5. ^1H NMR of crude reaction mixture from the reaction of **1a** and *trans*-4-octene.

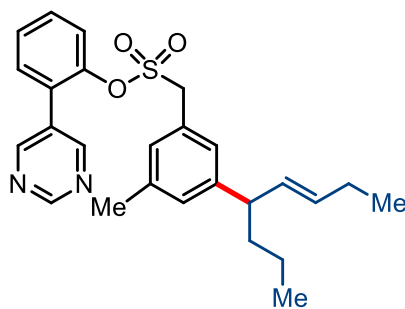
2.5. General procedure for palladium catalyzed *meta*-selective C–H allylation of arene:

To an oven-dried screw cap reaction tube charged with a magnetic stir-bar was added sulfonate ester/ether scaffold (0.25 mmol, 1 equiv), $\text{Pd}(\text{OAc})_2$ (10 mol%), N-acetylnorleucine (20 mol%), Ag_2CO_3 (3 equiv) and CuF_2 (1 equiv). Aliphatic internal olefins (2 equiv) was added with a micro litter pipette and 2 mL acetonitrile was added with a disposable laboratory syringe under aerobic condition. Note that, commercially purchased solvents were used without further purification or drying. The tube was placed in a preheated oil bath at 90 °C and the reaction mixture was stirred for 24 h. The reaction mixture was then cooled to room temperature and filtered through a celite

pad with ethyl acetate. The filtrate was concentrated and the crude compound was purified by column chromatography using silica gel (100-200 mesh size) and petroleum ether / ethyl acetate as an eluent.

2.6. Characterization data of meta-allylated compounds:

(E)-2-(pyrimidin-5-yl)phenyl (3-methyl-5-(oct-5-en-4-yl)phenyl)methanesulfonate (3a):

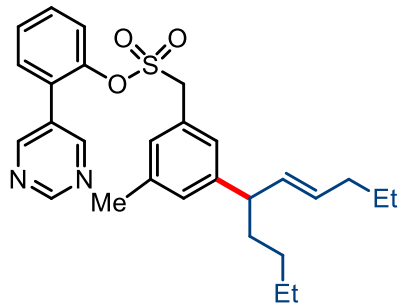


Colorless oil; yield 82%; $R_f = 0.38$ (ethyl acetate/hexane = 1:4);
 ^1H NMR (400 MHz, CDCl_3) δ 9.23 (s, 1H), 8.85 (s, 2H), 7.42 – 7.39 (m, 3H), 7.25 – 7.20 (m, 1H), 7.02 (s, 1H), 6.94 (s, 2H), 5.46 – 5.41 (m, 2H), 4.26 (s, 2H), 3.15 (dt, $J = 10.2, 5.3$ Hz, 1H), 2.32 (s, 3H), 1.98 (ddd, $J = 11.8, 6.4, 3.4$ Hz, 2H), 1.62 – 1.56 (m, 2H), 1.30 – 1.26 (m, 1H), 1.20 – 1.14 (m, 1H), 0.93 (t, $J = 7.4$ Hz, 3H), 0.86 (t, $J = 7.3$ Hz, 3H).

^{13}C NMR (100 MHz, CDCl_3) δ 157.9, 156.8, 146.7, 146.4, 138.9, 132.6, 132.2, 131.1, 130.7, 129.6, 129.1, 128.8, 127.8, 127.2, 126.3, 123.4, 57.9, 48.4, 38.4, 25.7, 21.5, 20.7, 14.1, 13.9

HRMS (m/z): [M + H]⁺ calcd for $\text{C}_{26}\text{H}_{31}\text{N}_2\text{O}_3\text{S}$: 451.2049, found: 451.2041

(E)-2-(pyrimidin-5-yl)phenyl (3-(dec-6-en-5-yl)-5-methylphenyl)methanesulfonate (3b):

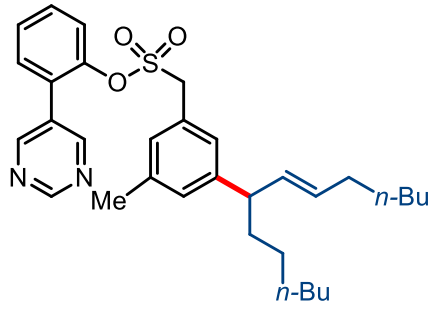


Colorless oil; yield 78%; $R_f = 0.38$ (ethyl acetate/hexane = 1:4);
 ^1H NMR (400 MHz, CDCl_3) δ 9.22 (s, 1H), 8.85 (s, 2H), 7.44 – 7.39 (m, 3H), 7.22 (dq, $J = 3.3, 2.3$ Hz, 1H), 7.02 (s, 1H), 6.94 (s, 2H), 5.50 – 5.36 (m, 2H), 4.26 (s, 2H), 3.12 (q, $J = 7.4$ Hz, 1H), 2.32 (s, 3H), 1.99 – 1.90 (m, 2H), 1.61 (dd, $J = 14.8, 7.3$ Hz, 2H), 1.31 (ddd, $J = 10.7, 7.7, 4.7$ Hz, 5H), 1.16 – 1.08 (m, 1H), 0.87 – 0.81 (m, 6H).

¹³C NMR (126 MHz, CDCl₃) δ 157.8, 156.8, 146.8, 146.3, 138.9, 133.8, 131.0, 131.1, 130.7, 130.4, 129.6, 129.1, 128.7, 127.8, 127.2, 126.3, 123.4, 57.9, 48.7, 35.8, 34.7, 29.8, 22.7, 22.6, 21.4, 14.1, 13.7.

HRMS (*m/z*): [M + H]⁺ calcd for C₂₈H₃₅N₂O₃S: 479.2362, found: 479.2371

(E)-2-(pyrimidin-5-yl)phenyl (3-methyl-5-(tetradec-8-en-7-yl)phenyl)methanesulfonate (3c):

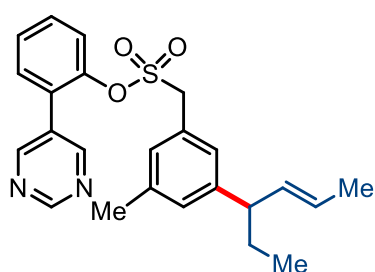


Pale-yellow oil; yield 79%; *R*_f = 0.4 (ethyl acetate/hexane = 1:4); ¹H NMR (400 MHz, CDCl₃) δ 9.23 (s, 1H), 8.85 (s, 2H), 7.43 – 7.39 (m, 3H), 7.22 (ddd, *J* = 5.2, 3.7, 2.6 Hz, 1H), 7.02 (s, 1H), 6.94 (s, 2H), 5.49 – 5.37 (m, 2H), 4.26 (s, 2H), 3.12 (q, *J* = 7.2 Hz, 1H), 2.32 (s, 3H), 1.96 (dd, *J* = 13.3, 6.4 Hz, 3H), 1.60 (dd, *J* = 14.0, 6.9 Hz, 2H), 1.37 – 1.24 (m, 10H), 1.15 (m, 4H), 0.89 – 0.83 (m, 6H).

¹³C NMR (100 MHz, CDCl₃) δ 157.9, 156.8, 146.8, 146.3, 138.9, 133.6, 131.1, 130.7, 130.6, 129.6, 129.0, 128.8, 128.7, 127.8, 127.2, 126.3, 123.4, 57.9, 48.7, 36.1, 32.6, 31.9, 31.5, 29.3, 29.2, 27.6, 22.7, 22.6, 21.4, 14.2.

HRMS (*m/z*): [M + H]⁺ calcd for C₃₃H₄₅N₂O₂S: 533.3196, found: 533.3187

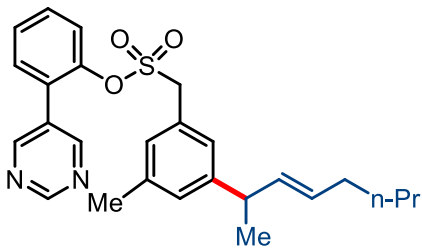
(E)-2-(pyrimidin-5-yl)phenyl (3-(hex-4-en-3-yl)-5-methylphenyl)methanesulfonate (3d):



Colorless oil; yield 66%; *R*_f = 0.35 (ethyl acetate/hexane = 1:4); ¹H NMR (400 MHz, CDCl₃) δ 9.23 (s, 1H), 8.85 (s, 2H), 7.44 – 7.39 (m, 3H), 7.26 – 7.22 (m, 1H), 7.01 (s, 1H), 6.93 (s, 2H), 5.53 – 5.38 (m, 2H), 4.26 (s, 2H), 3.03 (q, *J* = 7.4 Hz, 1H), 2.32 (s, 3H), 1.73 – 1.65 (m, 2H), 1.64 (d, *J* = 5.6 Hz, 3H), 0.81 (t, *J* = 7.3 Hz, 3H).

¹³C NMR (101 MHz, CDCl₃) δ 157.9, 156.8, 146.5, 146.4, 138.9, 134.7, 131.1, 130.7, 129.7, 129.1, 128.8, 127.8, 127.3, 126.3, 125.2, 123.4, 57.9, 50.6, 29.0, 21.5, 18.1, 12.3.

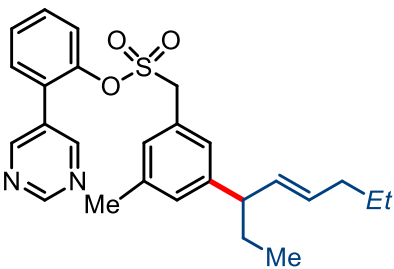
HRMS (*m/z*): [M + H]⁺ calcd for C₂₄H₂₇N₂O₃S: 423.1736, found: 423.1729

(E)-2-(pyrimidin-5-yl)phenyl (3-methyl-5-(oct-3-en-2-yl)phenyl)methanesulfonate (3e):

Pale-yellow oil; yield 67%; $R_f = 0.4$ (ethyl acetate/hexane = 1:4); ¹H NMR (400 MHz, CDCl₃) δ 9.22 (s, 1H), 8.84 (s, 2H), 7.45 – 7.38 (m, 3H), 7.28 – 7.26 (m, 1H), 7.04 (s, 1H), 6.95 (s, 1H), 6.94 (s, 1H), 5.55 – 5.34 (m, 2H), 4.26 (s, 2H), 3.36 (p, $J = 6.8$ Hz, 1H), 2.32 (s, 3H), 2.17 (s, 3H), 2.02 – 1.96 (m, 2H), 1.32 – 1.29 (m, 4H), 0.86 (t, $J = 7.1$ Hz, 3H).

¹³C NMR (101 MHz, CDCl₃) δ 157.9, 156.8, 147.6, 146.3, 138.9, 134.5, 131.1, 130.7, 129.8, 129.3, 129.1, 128.8, 127.8, 126.9, 126.3, 123.4, 57.9, 42.1, 32.3, 31.7, 31.0, 29.8, 22.3, 21.6, 21.4, 14.1.

HRMS (*m/z*): [M + H]⁺ calcd for C₂₆H₃₁N₂O₃S: 451.2049, found: 451.2046

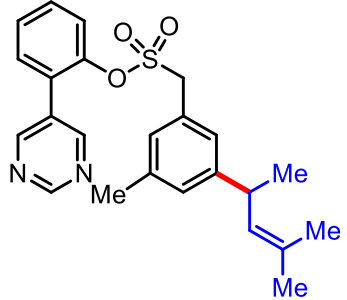
(E)-2-(pyrimidin-5-yl)phenyl (3-methyl-5-(oct-4-en-3-yl)phenyl)methanesulfonate (3f):

Pale-yellow oil; yield 75% (2:1 regioisomers); $R_f = 0.4$ (ethyl acetate/hexane = 1:4); ¹H NMR (400 MHz, CDCl₃) δ 9.23 (s, 1H), 8.85 (s, 2H), 7.44 – 7.40 (m, 3H), 7.25 – 7.22 (m, 1H), 7.02 (s, 1H), 6.94 (s, 2H), 5.51 – 5.41 (m, 2H), 4.26 (s, 2H), 3.04 (q, $J = 7.2$ Hz, 1H), 2.32 (s, 3H), 1.95 (dt, $J = 6.9, 4.3$ Hz, 2H), 1.64 – 1.62 (m, 2H), 1.36 – 1.34 (m, 1H), 1.30 – 1.26 (m, 1H), 0.86 (t, $J = 5.9$ Hz, 3H), 0.84 – 0.80 (m, 3H).

¹³C NMR (101 MHz, CDCl₃) δ 157.9, 156.8, 146.7, 146.6, 146.4, 138.9, 138.9, 135.0, 133.6, 131.1, 130.7, 130.7, 129.7, 129.6, 129.1, 128.8, 127.8, 127.3, 127.2, 126.3, 125.0, 123.5, 57.9, 50.5, 48.8, 35.8, 34.8, 29.9, 29.0, 22.7, 22.7, 21.5, 18.1, 14.1, 13.8, 12.3.

ESI-MS (*m/z*): [M + Na]⁺ calcd for C₂₆H₃₀NaN₂O₃S: 473.1869, found: 473.1827

2-(pyrimidin-5-yl)phenyl (3-methyl-5-(4-methylpent-3-en-2-yl)phenyl)methanesulfonate (3g):

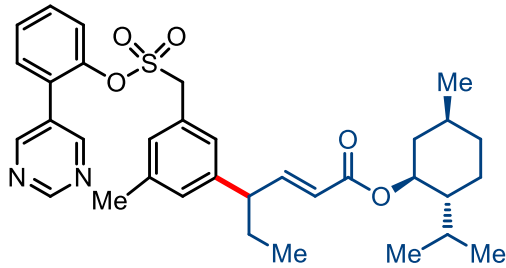


Pale-yellow oil; yield 71%; $R_f = 0.32$ (ethyl acetate/hexane = 1:4); ^1H NMR (500 MHz, CDCl_3) δ 9.2, 8.8, 7.45 – 7.40 (m, 3H), 7.25 (d, $J = 7.1$ Hz, 1H), 7.06 (s, 1H), 6.98 (s, 1H), 6.92 (s, 1H), 5.21 (d, $J = 9.2$ Hz, 1H), 4.27 (s, 2H), 3.63 – 3.58 (m, 1H), 2.32 (s, 3H), 1.68 (s, 3H), 1.64 (s, 3H), 1.26 (d, $J = 3.4$ Hz, 3H).

^{13}C NMR (126 MHz, CDCl_3) δ 157.8, 156.8, 148.3, 146.4, 138.9, 131.1, 130.7, 129.7, 129.0, 128.9, 128.7, 127.8, 126.6, 126.3, 123.5, 123.4, 57.9, 38.0, 29.8, 25.9, 22.5, 21.5, 18.1.

HRMS (m/z): [M + H]⁺ calcd for $\text{C}_{24}\text{H}_{27}\text{N}_2\text{O}_3\text{S}$: 423.1737, found: 423.1732

(E)-(1*S*,2*R*,5*S*)-2-isopropyl-5-methylcyclohexyl 4-(3-methyl-5-((2-(pyrimidin-5-yl)phenoxy)sulfonyl)methyl)phenylhex-2-enoate (3h):

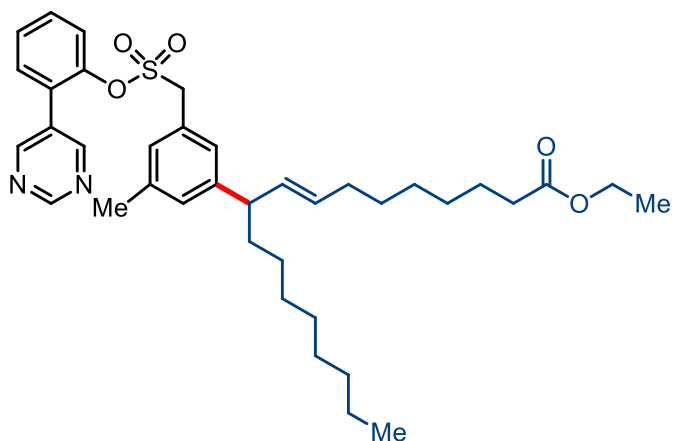


Pale-yellow oil; yield 72%; $R_f = 0.38$ (ethyl acetate/hexane = 1:4); 4:1 d.r.; ^1H NMR (500 MHz, CDCl_3) δ 9.23 (s, 1H), 8.85 (s, 2H), 7.42 (ddd, $J = 8.8, 5.3, 2.8$ Hz, 3H), 7.31 – 7.26 (m, 1H), 7.05 – 6.99 (m, 2H), 6.98 (s, 1H), 6.93 (s, 1H), 5.76 (ddd, $J = 15.6, 4.7, 1.1$ Hz, 1H), 4.71 (td, $J = 10.9, 4.0$ Hz, 1H), 4.26 (s, 2H), 3.24 (q, $J = 7.5$ Hz, 1H), 2.32 (s, 3H), 2.00 – 1.92 (m, 1H), 1.86 – 1.72 (m, 3H), 1.69 – 1.60 (m, 3H), 1.50 – 1.43 (m, 1H), 1.39 – 1.32 (m, 1H), 0.96 (dd, $J = 34.7, 23.1$ Hz, 2H), 0.88 – 0.83 (m, 9H), 0.72 (t, $J = 7.4$ Hz, 3H).

^{13}C NMR (126 MHz, CDCl_3) δ 166.3, 157.8, 156.7, 150.95, 150.9, 146.2, 143.3, 139.4, 131.1, 130.7, 129.9, 129.8, 128.8, 127.9, 127.5, 127.49, 126.7, 123.4, 121.6, 74.2, 57.7, 50.0, 47.2, 41.0, 34.3, 31.4, 28.0, 26.3, 23.6, 22.1, 21.4, 20.8, 16.5, 12.2.

HRMS (m/z): [M + H]⁺ calcd for $\text{C}_{34}\text{H}_{43}\text{N}_2\text{O}_5\text{S}$: 591.2887, found: 591.2882

(E)-ethyl 10-(3-methyl-5-(((2-(pyrimidin-5-yl)phenoxy)sulfonyl)methyl)phenyl)octadec-8-enoate (3i):



Colorless oil; yield 83%; $R_f = 0.48$ (ethyl acetate/hexane = 1:4); ^1H NMR (400 MHz, CDCl_3) δ 9.23 (s, 1H), 8.85 (s, 2H), 7.43 – 7.40 (m, 3H), 7.23 (dd, $J = 7.0, 3.9$ Hz, 1H), 7.01 (s, 1H), 6.93 (s, 2H), 5.48 – 5.36 (m, 2H), 4.26 (s, 2H), 4.11 (q, $J = 7.1$ Hz, 2H), 3.11 (q, $J = 7.2$ Hz, 1H), 2.31 (s, 3H), 2.25 (td, $J = 7.6, 2.0$ Hz, 2H), 1.96 (dd, $J = 13.1, 6.5$ Hz, 2H), 1.63 – 1.53 (m, 4H), 1.25 –

1.22 (m, 22H), 0.88 – 0.83 (m, 3H).

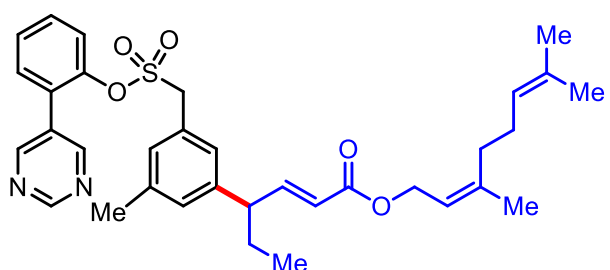
¹³C NMR (101 MHz, CDCl₃) δ 174.0, 173.9, 157.9, 156.8, 146.7, 146.3, 138.9, 133.7, 133.5, 131.1, 130.7, 130.6, 130.5, 129.5, 129.1, 128.8, 127.8, 127.2, 126.3, 123.4, 60.3, 57.9, 48.7, 36.14, 36.11, 34.5, 32.7, 32.6, 31.9, 29.67, 29.6, 29.4, 29.1, 28.9, 27.7, 27.6, 25.1, 25.0, 22.7, 21.5, 14.4, 14.2.

HRMS (*m/z*): [M + H]⁺ calcd for C₃₈H₅₃N₂O₅S: 649.3669, found: 649.3663

(E)-(Z)-3,7-dimethylocta-2,6-dien-1-yl

4-(3-methyl-5-(((2-(pyrimidin-5-

yl)phenoxy)sulfonyl)methyl)phenyl)hex-2-enoate (3j):



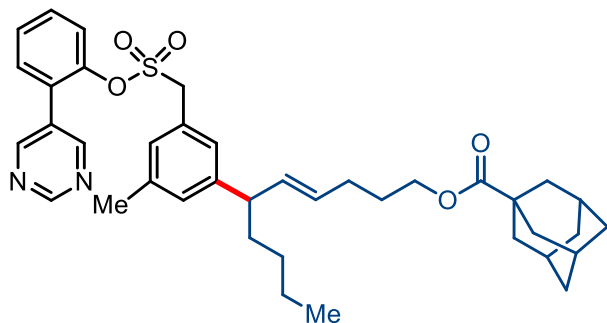
Colorless oil; yield 69%; $R_f = 0.5$ (ethyl acetate/hexane = 1:4); ^1H NMR (500 MHz, CDCl_3) δ 9.22 (s, 1H), 8.83 (s, 2H), 7.46 – 7.39 (m, 4H), 7.28 (d, $J = 1.4$ Hz, 1H), 6.98 (dd, $J = 11.9, 9.9$ Hz, 3H), 5.78 (d, $J = 15.6$ Hz, 1H), 5.35 (t, $J = 7.3$ Hz, 1H), 5.07 (t, $J = 6.3$ Hz, 1H), 4.59

(d, $J = 7.2$ Hz, 2H), 4.25 (s, 2H), 3.24 (q, $J = 7.4$ Hz, 1H), 2.32 (s, 3H), 2.09 (t, $J = 6.3$ Hz, 2H), 2.06 (d, $J = 6.0$ Hz, 2H), 1.74 (s, 3H), 1.73 (s, 2H), 1.65 (s, 3H), 1.58 (s, 3H), 0.89 – 0.81 (m, 3H).

¹³C NMR (126 MHz, CDCl₃) δ 166.7, 157.9, 156.8, 151.2, 146.2, 143.2, 142.7, 139.4, 132.3, 131.2, 130.1, 130.7, 129.9, 129.8, 128.8, 127.8, 127.5, 126.8, 123.7, 123.5, 123.4, 121.2, 119.3, 61.2, 57.7, 49.9, 32.3, 27.9, 26.7, 25.8, 23.6, 21.4, 17.8, 12.2.

HRMS (*m/z*): [M + H]⁺ calcd for C₃₄H₄₁N₂O₅S: 589.2730, found: 589.2729

(E)-6-(3-methyl-5-((2-(pyrimidin-5-yl)phenoxy)sulfonyl)methyl)phenyl)dec-4-en-1-yl adamantine-1-carboxylate (3k):

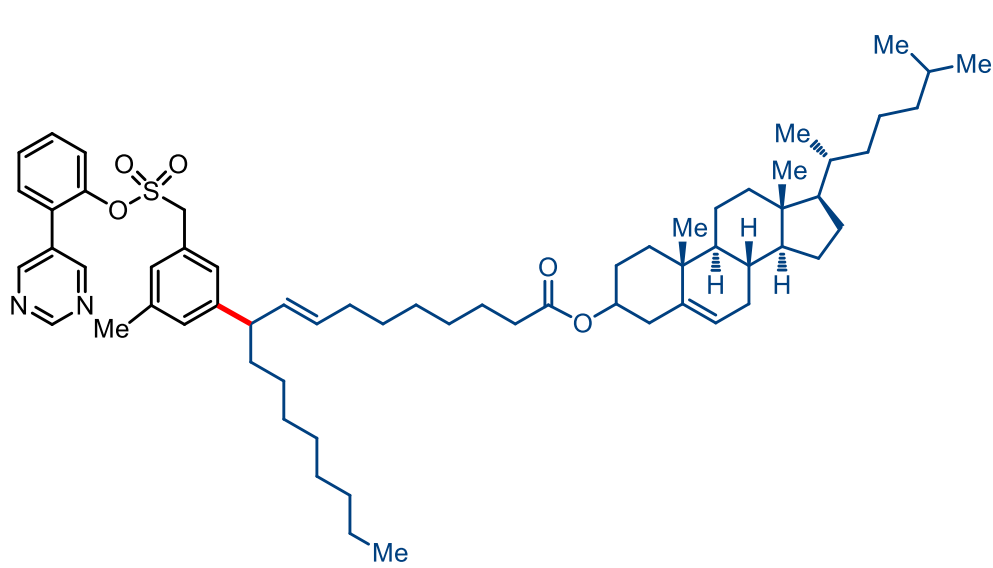


Pale-yellow oil; yield 77%; *R_f* = 0.46 (ethyl acetate/hexane = 1:4); ¹H NMR (400 MHz, CDCl₃) δ 9.22 (s, 1H), 8.85 (s, 2H), 7.42 – 7.40 (m, 3H), 7.25 (dd, *J* = 5.8, 3.8 Hz, 1H), 7.01 (s, 1H), 6.93 (s, 2H), 5.55 – 5.35 (m, 2H), 4.26 (s, 2H), 3.99 (q, *J* = 6.4 Hz, 2H), 3.16 – 3.10 (m, 1H), 2.32 (s, 3H), 2.08 – 1.92 (m, 6H), 1.86 – 1.83 (m, 8H), 1.68 – 1.53 (m, 7H), 1.36 – 1.26 (m, 3H), 1.20 – 1.13 (m, 1H), 0.86 – 0.81 (m, 3H).

¹³C NMR (126 MHz, CDCl₃) δ 177.8, 157.8, 156.8, 146.5, 146.4, 138.9, 134.8, 133.4, 131.1, 131.6, 131.7, 129.5, 129.1, 128.7, 127.8, 127.2, 127.1, 126.4, 123.4, 64.0, 63.5, 57.9, 48.6, 40.8, 40.7, 38.9, 36.6, 35.7, 34.7, 29.8, 28.9, 28.6, 28.5, 28.1, 24.0, 22.7, 21.4, 14.1, 13.8.

ESI-MS (*m/z*): [M + H]⁺ calcd for C₃₉H₄₈NaN₂O₅S: 679.3176, found: 679.2968

(10E)-10,13-dimethyl-17-(6-methylheptan-2-yl)-2,3,4,7,8,9,10,11,12,13,14,15,16,17-tetradecahydro-1H-cyclopenta[a]phenanthren-3-yl 10-(3-methyl-5-((2-(pyrimidin-5-yl)phenoxy)sulfonyl)methyl)phenyl)octadec-8-enoate (3l):



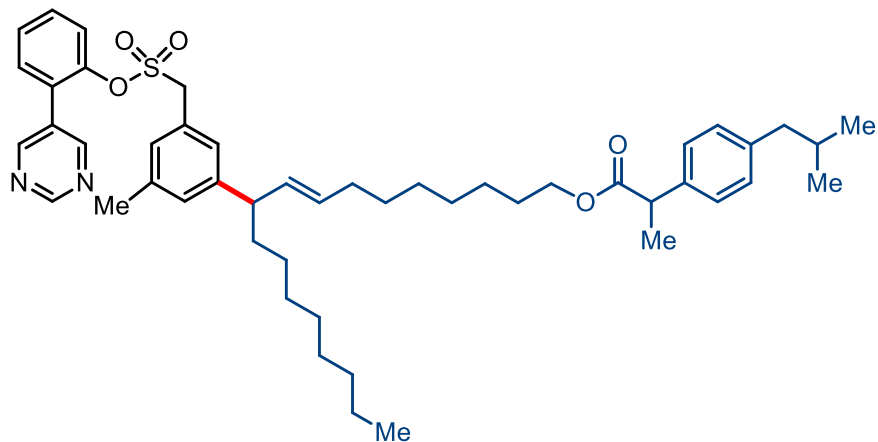
Pale-yellow oil;
yield 76%; $R_f =$
0.5 (ethyl
acetate/hexane =
1:4); 5:1 d.r.; ^1H
NMR (500
MHz, CDCl_3) δ
9.22 (s, 1H),
8.85 (s, 2H),
7.43 – 7.39 (m,
3H), 7.24 – 7.22

(m, 1H), 7.01 (s, 1H), 6.93 (s, 2H), 5.43 (dddd, $J = 11.1, 9.2, 6.2, 2.4$ Hz, 2H), 5.39 – 5.31 (m, 2H), 4.64 – 4.56 (m, 1H), 4.26 (s, 2H), 3.11 (q, $J = 7.2$ Hz, 1H), 2.34 – 2.27 (m, 7H), 2.24 (td, $J = 7.6,$ 3.0 Hz, 3H), 2.04 – 1.92 (m, 6H), 1.88 – 1.80 (m, 5H), 1.51 (ddd, $J = 22.4, 16.0, 10.3$ Hz, 14H), 1.33 (d, $J = 8.3$ Hz, 6H), 1.13 – 1.08 (m, 6H), 1.01 (s, 6H), 0.91 (d, $J = 6.5$ Hz, 5H), 0.86 (dd, $J = 6.6, 2.3$ Hz, 12H), 0.67 (s, 4H).

^{13}C NMR (126 MHz, CDCl_3) δ 173.4, 157.9, 156.8, 146.8, 146.4, 139.8, 138.9, 133.7, 133.5, 131.1, 130.8, 130.7, 130.5, 129.6, 129.1, 128.8, 127.8, 127.2, 126.3, 123.4, 122.7, 73.8, 57.9, 56.8, 56.2, 50.1, 48.7, 42.4, 39.8, 39.6, 38.3, 37.1, 36.7, 36.4, 36.1, 35.9, 34.8, 32.6, 32.5, 32.0, 29.6, 29.5, 29.4, 29.3, 29.2, 28.9, 28.3, 28.1, 27.9, 27.7, 27.6, 25.1, 24.4, 23.9, 22.9, 22.7, 21.5, 21.1, 19.4, 18.8, 14.2, 11.9.

HRMS (m/z): $[\text{M} + \text{H}]^+$ calcd for $\text{C}_{63}\text{H}_{93}\text{N}_2\text{O}_5\text{S}$: 989.6800, found: 989.6805

(E)-10-(3-methyl-5-(((2-(pyrimidin-5-yl)phenoxy)sulfonyl)methyl)phenyl)octadec-8-en-1-yl 2-(4-isobutylphenyl)propanoate (3m):

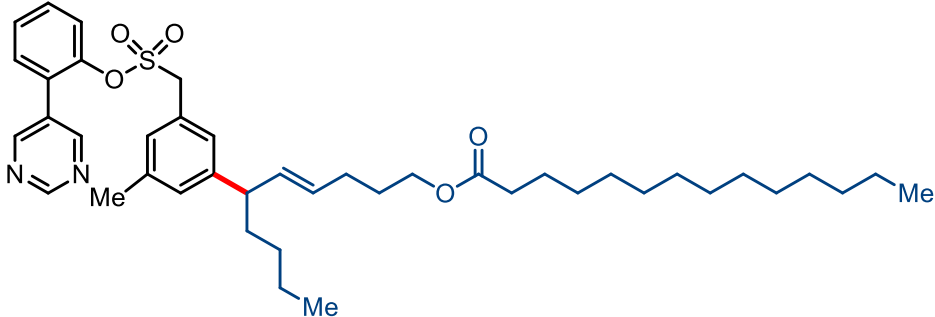


Pale-yellow oil; yield 65%; $R_f = 0.42$ (ethyl acetate/hexane = 1:4); 7:1 d.r.; ^1H NMR (500 MHz, CDCl_3) δ 9.24 (s, 1H), 8.86 (s, 2H), 7.41 (m, 3H), 7.26 – 7.22 (m, 1H), 7.19 (d, $J = 7.7$ Hz, 2H), 7.08 (d, $J = 7.7$ Hz, 2H), 7.02 (s, 1H), 6.94 (s, 2H), 5.48 – 5.36 (m, 2H), 4.26 (s, 2H), 4.03 (t, $J = 6.0$ Hz, 2H), 3.67 (q, $J = 7.0$ Hz, 1H), 3.14 – 3.10 (m, 1H), 2.43 (d, $J = 7.1$ Hz, 2H), 2.32 (s, 3H), 1.96 (dt, $J = 14.6, 7.4$ Hz, 2H), 1.83 (tt, $J = 13.5, 6.9$ Hz, 2H), 1.71 (s, 2H), 1.65 – 1.49 (m, 5H), 1.47 (s, 2H), 1.21 (s, 16H), 0.93 – 0.81 (m, 11H).

^{13}C NMR (126 MHz, CDCl_3) δ 174.9, 157.9, 156.8, 146.8, 146.3, 140.5, 138.9, 138.0, 133.7, 133.6, 131.1, 131.0, 130.7, 130.6, 129.5, 129.4, 129.1, 128.8, 127.8, 127.3, 127.2, 126.3, 123.4, 64.9, 64.8, 57.9, 48.7, 45.3, 45.1, 36.2, 32.7, 32.6, 31.9, 30.3, 29.7, 29.6, 29.4, 29.2, 28.6, 27.6, 25.9, 25.8, 22.7, 22.5, 21.4, 18.6, 14.2.

HRMS (m/z): [M + H]⁺ calcd for $\text{C}_{49}\text{H}_{67}\text{N}_2\text{O}_5\text{S}$: 795.4765, found: 795.4763

(E)-6-(3-methyl-5-(((2-(pyrimidin-5-yl)phenoxy)sulfonyl)methyl)phenyl)dec-4-en-1-yl tetradecanoate (3n):



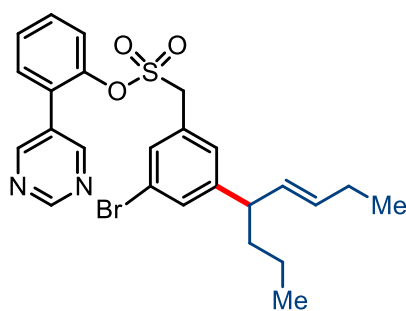
Colorless oil; yield 86%; $R_f = 0.5$ (ethyl acetate/hexane = 1:4); ^1H NMR (500 MHz, CDCl_3) δ 9.24 (s, 1H),

8.87 (s, 2H), 7.41 (s, 3H), 7.25 (d, $J = 5.9$ Hz, 1H), 7.01 (s, 1H), 6.93 (s, 2H), 5.45 (tdd, $J = 29.9$, 15.0, 7.2 Hz, 2H), 4.26 (d, $J = 5.1$ Hz, 2H), 4.02 (dd, $J = 12.2$, 6.2 Hz, 2H), 3.15 – 3.12 (m, 1H), 2.32 (s, 3H), 2.26 (dd, $J = 14.1$, 7.0 Hz, 3H), 2.08 – 2.03 (m, 1H), 1.97 – 1.93 (m, 1H), 1.69 – 1.58 (m, 8H), 1.41 – 1.26 (m, 13H), 1.16 – 1.07 (m, 2H), 0.89 – 0.82 (m, 10H).

^{13}C NMR (126 MHz, CDCl_3) δ 174.0, 157.9, 156.8, 146.4, 138.9, 134.7, 133.4, 131.1, 130.7, 129.5, 129.3, 129.2, 129.0, 128.9, 128.8, 127.8, 127.2, 126.4, 123.4, 64.3, 63.8, 57.9, 48.6, 35.7, 35.6, 34.7, 34.5, 32.0, 29.8, 29.7, 29.6, 25.13, 25.1, 24.0, 22.9, 22.7, 22.6, 21.4, 14.2, 14.1, 13.8.

HRMS (m/z): [M + H]⁺ calcd for $\text{C}_{42}\text{H}_{61}\text{N}_2\text{O}_5\text{S}$: 705.4295, found: 705.4298

(E)-2-(pyrimidin-5-yl)phenyl (3-bromo-5-(oct-5-en-4-yl)phenyl)methanesulfonate (3o):



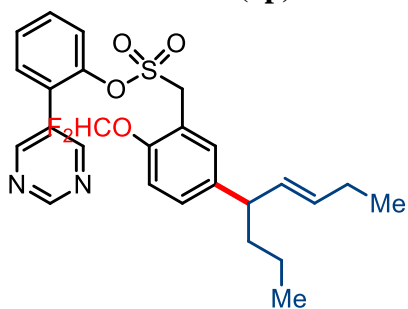
Pale yellow liquid; yield 78%; $R_f = 0.34$ (ethyl acetate/hexane = 1:4); ^1H NMR (400 MHz, CDCl_3) δ 9.23 (s, 1H), 8.84 (s, 2H), 7.46 – 7.41 (m, 3H), 7.36 (t, $J = 1.4$ Hz, 1H), 7.31 – 7.27 (m, 1H), 7.26 (d, $J = 1.7$ Hz, 1H), 7.07 (s, 1H), 5.51 – 5.39 (m, 2H), 4.25 (s, 2H), 3.16 (q, $J = 7.3$ Hz, 1H), 2.03 – 1.96 (m, 2H), 1.63 – 1.54 (m, 2H), 1.34 – 1.26 (m, 1H), 1.20 – 1.12 (m, 1H), 0.94

(t, $J = 7.4$ Hz, 3H), 0.87 (t, $J = 7.3$ Hz, 3H).

^{13}C NMR (100 MHz, CDCl_3) δ 158.0, 156.8, 149.1, 146.1, 133.1, 131.9, 131.7, 131.2, 131.1, 131.0, 130.8, 128.9, 128.8, 128.5, 128.1, 123.4, 123.0, 57.2, 48.2, 38.2, 25.7, 20.7, 14.0, 13.9.

HRMS (m/z): [M + H]⁺ calcd for $\text{C}_{25}\text{H}_{28}\text{BrN}_2\text{O}_3\text{S}$: 517.0980, found: 517.0984

(E)-2-(pyrimidin-5-yl)phenyl methanesulfonate (3p):



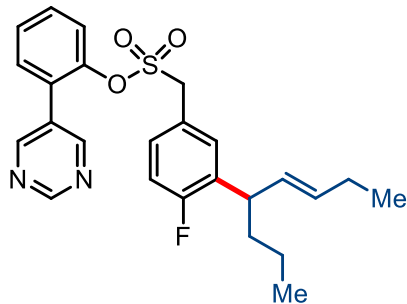
Pale-yellow oil; yield 82%; $R_f = 0.32$ (ethyl acetate/hexane = 1:4); ^1H NMR (500 MHz, CDCl_3) δ 9.21 (s, 1H), 8.85 (s, 2H), 7.46 – 7.41 (m, 3H), 7.35 – 7.31 (m, 1H), 7.24 – 7.20 (m, 2H), 7.11 (d, $J = 9.0$ Hz, 1H), 6.45 (t, $J = 73.7$ Hz, 1H), 5.45 (dd, $J = 7.7$, 5.7 Hz, 2H), 4.44 (s, 2H), 3.19 (q, $J = 7.1$ Hz, 1H), 2.04

– 1.95 (m, 2H), 1.62 – 1.54 (m, 2H), 1.30 – 1.25 (m, 1H), 1.21 – 1.14 (m, 1H), 0.94 (t, $J = 7.5$ Hz, 3H), 0.87 (t, $J = 7.3$ Hz, 3H).

^{13}C NMR (126 MHz, CDCl_3) δ 157.9, 156.8, 148.3, 146.1, 143.8, 132.7, 132.1, 131.9, 131.2, 131.1, 130.7, 130.3, 128.9, 128.0, 123.5, 119.6, 118.5, 116.4 (t, $J = 258$ Hz), 51.7, 47.7, 38.2, 25.7, 20.7, 14.1, 13.9.

HRMS (m/z): [M + H]⁺ calcd for $\text{C}_{26}\text{H}_{28}\text{F}_2\text{N}_2\text{NaO}_4\text{S}$: 525.1630, found: 525.1634

(E)-2-(pyrimidin-5-yl)phenyl (4-fluoro-3-(oct-5-en-4-yl)phenyl)methanesulfonate (3q):

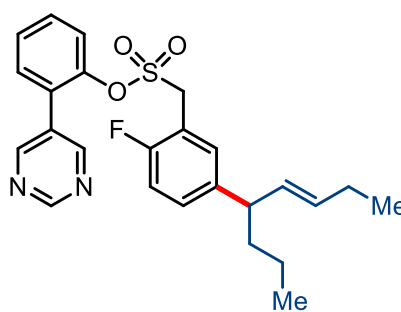


Pale-yellow oil; yield 58%; $R_f = 0.34$ (ethyl acetate/hexane = 1:4); ^1H NMR (500 MHz, CDCl_3) δ 9.24 (s, 1H), 8.85 (s, 2H), 7.42 (qd, $J = 6.1, 3.3$ Hz, 3H), 7.26 – 7.22 (m, 1H), 7.16 (dd, $J = 6.7, 2.1$ Hz, 1H), 7.12 – 7.08 (m, 1H), 7.02 – 6.97 (m, 1H), 5.52 – 5.42 (m, 2H), 4.27 (s, 2H), 3.53 (dd, $J = 13.4, 6.6$ Hz, 1H), 2.01 – 1.93 (m, 2H), 1.60 (dd, $J = 15.3, 8.4$ Hz, 2H), 1.33 – 1.27 (m, 1H), 1.20 – 1.13 (m, 1H), 0.92 (t, $J = 7.4$ Hz, 3H), 0.86 (t, $J = 7.3$ Hz, 3H).

^{13}C NMR (126 MHz, CDCl_3) δ 161.3 (d, $J = 249$ Hz), 157.8, 156.8, 146.1, 133.6, 133.5, 131.5 (d, $J = 5.9$ Hz), 131.2, 130.8, 129.8 (d, $J = 8.9$ Hz), 128.8, 127.9, 123.4, 122.4, 122.3, 116.3 (d, $J = 23.94$), 57.2, 41.4, 37.4, 25.6, 20.7, 13.92 (d, $J = 19.7$ Hz).

HRMS (m/z): [M + H]⁺ calcd for $\text{C}_{25}\text{H}_{28}\text{FN}_2\text{O}_3\text{S}$: 455.1799, found: 455.1795

(E)-2-(pyrimidin-5-yl)phenyl (2-fluoro-5-(oct-5-en-4-yl)phenyl)methanesulfonate (3r):

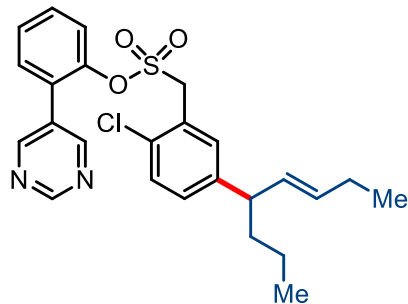


Pale-yellow oil; yield 63%; $R_f = 0.34$ (ethyl acetate/hexane = 1:4); ^1H NMR (500 MHz, CDCl_3) δ 9.21 (s, 1H), 8.84 (s, 2H), 7.42 (qd, $J = 6.5, 3.8$ Hz, 3H), 7.30 – 7.24 (m, 2H), 7.18 (dd, $J = 10.3, 3.9$ Hz, 1H), 7.10 (dd, $J = 9.4, 5.9$ Hz, 1H), 5.54 – 5.45 (m, 2H), 4.43 (s, 2H), 3.60 – 3.50 (m, 1H), 1.98 (ddd, $J = 14.8, 7.4, 4.4$ Hz, 2H), 1.62 (ddd, $J = 13.5, 9.4, 7.4$ Hz, 2H), 1.34 – 1.26 (m, 1H), 1.21 – 1.13 (m, 1H), 0.93 (t, $J = 7.4$ Hz, 3H), 0.86 (t, $J = 7.3$ Hz, 3H).

¹³C NMR (126 MHz, CDCl₃) δ 159.1 (d, *J* = 249.8 Hz), 157.8, 156.8, 146.1, 133.43 (d, *J* = 15.3 Hz), 133.0, 131.2, 131.1, 130.9, 130.7, 130.4 (d, *J* = 5.6 Hz), 129.8 (d, *J* = 2.3 Hz), 128.9, 127.9, 124.6, 124.5, 123.33 (s), 114.29 (d, *J* = 16.1 Hz), 62.3, 51.2, 41.3, 37.5, 25.6, 20.7, 14.0, 13.8.

HRMS (*m/z*): [M + H]⁺ calcd for C₂₅H₂₈FN₂O₃S: 455.1799, found: 455.1798.

(E)-2-(pyrimidin-5-yl)phenyl (2-chloro-5-(oct-5-en-4-yl)phenyl)methanesulfonate (3s):

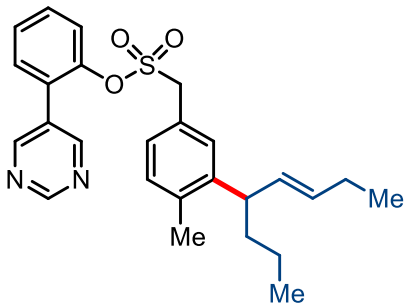


Pale-yellow oil; yield 71%; *R*_f = 0.35 (ethyl acetate/hexane = 1:4); ¹H NMR (500 MHz, CDCl₃) δ 9.21 (s, 1H), 8.85 (s, 2H), 7.42 (dd, *J* = 9.3, 5.4 Hz, 3H), 7.34 (d, *J* = 8.2 Hz, 1H), 7.27 (dd, *J* = 14.2, 7.6 Hz, 3H), 7.16 (d, *J* = 8.3 Hz, 1H), 5.50 – 5.39 (m, 2H), 4.57 (s, 2H), 3.17 (q, *J* = 7.1 Hz, 1H), 2.03 – 1.94 (m, 2H), 1.58 (dd, *J* = 15.2, 7.8 Hz, 2H), 1.30 (dd, *J* = 18.5, 10.6 Hz, 1H), 1.19 – 1.11 (m, 1H), 0.94 (t, *J* = 7.4 Hz, 3H), 0.86 (t, *J* = 7.3 Hz, 3H).

¹³C NMR (126 MHz, CDCl₃) δ 157.7, 156.8, 146.1, 145.4, 132.8, 132.6, 132.0, 131.2, 130.8, 130.3, 130.2, 128.9, 128.0, 124.7, 123.5, 54.7, 47.8, 38.2, 25.7, 20.7, 14.1, 13.9.

HRMS (*m/z*): [M + H]⁺ calcd for C₂₅H₂₈ClN₂O₃S: 471.1504, found: 471.1502.

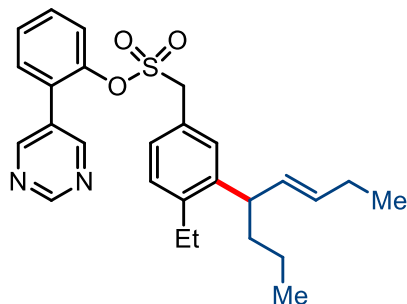
(E)-2-(pyrimidin-5-yl)phenyl (4-methyl-3-(oct-5-en-4-yl)phenyl)methanesulfonate (3t):



Colorless oil; yield 67%; *R*_f = 0.38 (ethyl acetate/hexane = 1:4); ¹H NMR (500 MHz, CDCl₃) δ 9.22 (s, 1H), 8.84 (s, 2H), 7.43 – 7.38 (m, 3H), 7.26 – 7.21 (m, 1H), 7.13 (d, *J* = 1.3 Hz, 1H), 7.11 (d, *J* = 7.8 Hz, 1H), 7.02 (dd, *J* = 7.7, 1.5 Hz, 1H), 5.43 – 5.35 (m, 2H), 4.29 (s, 2H), 3.42 (dd, *J* = 13.5, 6.8 Hz, 1H), 2.32 (s, 3H), 1.97 – 1.95 (m, 2H), 1.61 – 1.59 (m, 2H), 1.32 – 1.29 (m, 1H), 1.22 – 1.15 (m, 1H), 0.91 (t, *J* = 7.4 Hz, 3H), 0.86 (t, *J* = 7.4 Hz, 3H).

¹³C NMR (126 MHz, CDCl₃) δ 157.8, 156.8, 146.3, 144.6, 137.5, 132.3, 132.0, 131.2, 131.1, 131.0, 130.7, 128.9, 128.7, 127.9, 127.8, 124.1, 123.4, 57.9, 43.6, 37.8, 25.7, 20.7, 19.6, 14.1, 13.9.

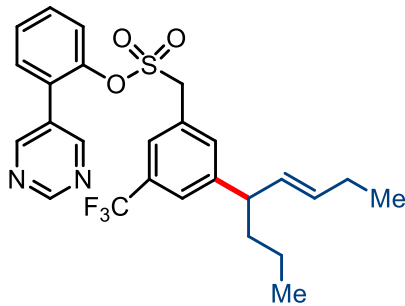
HRMS (*m/z*): [M + H]⁺ calcd for C₂₆H₃₁N₂O₃S: 451.2049, found: 451.2053

(E)-2-(pyrimidin-5-yl)phenyl (4-ethyl-3-(oct-5-en-4-yl)phenyl)methanesulfonate (3u):

Colorless oil; yield 68%; $R_f = 0.4$ (ethyl acetate/hexane = 1:4);
¹H NMR (500 MHz, CDCl₃) δ 9.23 (s, 1H), 8.86 (s, 2H), 7.40 (d, $J = 2.9$ Hz, 3H), 7.15 (d, $J = 7.6$ Hz, 3H), 7.07 (d, $J = 7.8$ Hz, 1H), 5.46 – 5.35 (m, 2H), 4.30 (s, 2H), 3.47 (q, $J = 7.1$ Hz, 1H), 2.68 (qd, $J = 14.5, 7.4$ Hz, 2H), 1.95 (dt, $J = 14.4, 7.3$ Hz, 2H), 1.65 – 1.61 (m, 1H), 1.58 – 1.55 (m, 1H), 1.33 – 1.27 (m, 2H), 1.20 (t, $J = 7.6$ Hz, 3H), 0.90 (d, $J = 7.5$ Hz, 3H), 0.85 (t, $J = 7.3$ Hz, 3H).

¹³C NMR (126 MHz, CDCl₃) δ 157.9, 156.9, 146.4, 144.2, 143.3, 132.7, 132.2, 131.2, 131.1, 130.6, 129.5, 129.4, 128.7, 128.1, 127.8, 124.0, 123.4, 57.9, 42.9, 38.5, 25.8, 25.7, 20.8, 15.6, 14.2, 13.9.

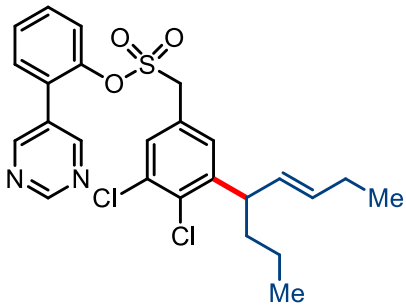
HRMS (*m/z*): [M + H]⁺ calcd for C₂₇H₃₃N₂O₃S: 465.2206, found: 465.2201

(E)-2-(pyrimidin-5-yl)phenyl (3-(oct-5-en-4-yl)-5 (trifluoromethyl)phenyl)methanesulfonate (3v):

Pale-yellow oil; yield 74%; $R_f = 0.3$ (ethyl acetate/hexane = 1:4);
¹H NMR (400 MHz, CDCl₃) δ 9.22 (s, 1H), 8.84 (s, 2H), 7.48 – 7.42 (m, 4H), 7.39 (s, 1H), 7.34 (s, 1H), 7.31 – 7.27 (m, 1H), 5.55 – 5.40 (m, 2H), 4.33 (s, 2H), 3.27 (q, $J = 7.2$ Hz, 1H), 2.05 – 1.95 (m, 2H), 1.67 – 1.58 (m, 2H), 1.34 – 1.27 (m, 1H), 1.18 (ddd, $J = 9.4, 7.1, 3.0$ Hz, 1H), 0.94 (t, $J = 7.4$ Hz, 3H), 0.88 (t, $J = 7.3$ Hz, 3H).

¹³C NMR (101 MHz, CDCl₃) δ 157.9, 156.7, 148.1, 146.0, 133.4, 131.8 (q, $J = 50.5$ Hz), 130.8, 128.8, 128.1, 127.5, 125.5 (q, $J = 271$ Hz), 123.4, 57.3, 48.3, 38.1, 25.6, 20.7, 14.0, 13.8.

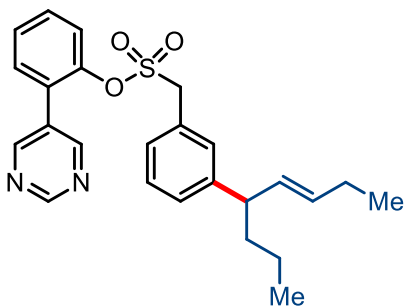
HRMS (*m/z*): [M + H]⁺ calcd for C₂₆H₂₈F₃N₂O₃S: 505.1767, found: 505.1762

(E)-2-(pyrimidin-5-yl)phenyl (3,4-dichloro-5-(oct-5-en-4-yl)phenyl)methanesulfonate (3w):

Pale-yellow oil; yield 69%; R_f = 0.35 (ethyl acetate/hexane = 1:4); ¹H NMR (500 MHz, CDCl₃) δ 9.24 (s, 1H), 8.84 (s, 2H), 7.47 – 7.43 (m, 2H), 7.42 – 7.39 (m, 1H), 7.35 (dd, J = 7.8, 1.5 Hz, 1H), 7.24 (d, J = 2.0 Hz, 1H), 7.11 (d, J = 2.0 Hz, 1H), 5.52 (dt, J = 15.0, 6.3 Hz, 1H), 5.39 (dd, J = 15.3, 7.7 Hz, 1H), 4.25 (s, 2H), 3.83 (q, J = 7.4 Hz, 1H), 2.02 – 1.95 (m, 2H), 1.63 – 1.56 (m, 2H), 1.35 – 1.28 (m, 1H), 1.24 – 1.16 (m, 1H), 0.92 (t, J = 7.4 Hz, 3H), 0.87 (t, J = 7.3 Hz, 3H).

¹³C NMR (126 MHz, CDCl₃) δ 156.6, 146.3, 145.8, 134.0, 133.8, 133.7, 132.7, 131.3, 131.1, 130.8, 130.2, 130.1, 129.7, 128.8, 128.7, 128.1, 125.9, 123.4, 56.7, 44.8, 37.5, 25.7, 20.5, 14.0, 13.8.

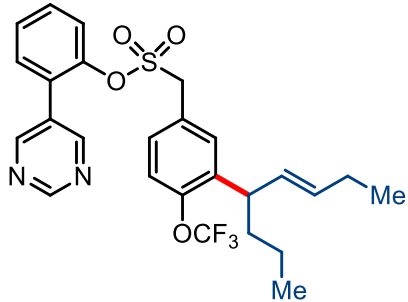
HRMS (*m/z*): [M + H]⁺ calcd for C₂₅H₂₇Cl₂N₂O₃S: 505.1114, found: 505.1110

(E)-2-(pyrimidin-5-yl)phenyl (3-(oct-5-en-4-yl)phenyl)methanesulfonate (3x):

Pale-yellow oil; yield 65%; R_f = 0.36 (ethyl acetate/hexane = 1:4); ¹H NMR (500 MHz, CDCl₃) δ 9.22 (s, 1H), 8.84 (s, 2H), 7.42 – 7.40 (m, 3H), 7.29 (t, J = 7.5 Hz, 1H), 7.24 – 7.16 (m, 2H), 7.16 – 7.09 (m, 2H), 5.50 – 5.42 (m, 2H), 4.31 (s, 2H), 3.19 (dd, J = 13.4, 6.6 Hz, 1H), 2.03 – 1.93 (m, 2H), 1.65 – 1.56 (m, 2H), 1.32 – 1.25 (m, 1H), 1.17 (ddd, J = 10.2, 8.7, 4.2 Hz, 1H), 0.93 (t, J = 7.5 Hz, 3H), 0.86 (t, J = 7.4 Hz, 3H).

¹³C NMR (126 MHz, CDCl₃) δ 157.8, 156.8, 146.8, 146.3, 132.5, 132.3, 131.1, 130.7, 130.2, 129.1, 128.8, 128.7, 128.4, 127.8, 126.5, 123.4, 57.9, 48.4, 38.3, 25.7, 20.7, 14.1, 13.9.

**(E)-2-(pyrimidin-5-yl)phenyl
(trifluoromethoxy)phenylmethanesulfonate (3y):**

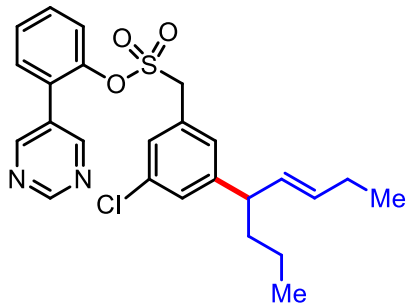


Pale-yellow oil; yield 64%; R_f = 0.32 (ethyl acetate/hexane = 1:4); ¹H NMR (400 MHz, CDCl₃) δ 9.23 (s, 1H), 8.85 (s, 2H), 7.42 (dd, J = 5.6, 2.3 Hz, 3H), 7.26 (s, 1H), 7.23 – 7.18 (m, 2H), 7.16 (dd, J = 8.5, 2.2 Hz, 1H), 5.50 – 5.36 (m, 2H), 4.30 (s, 2H), 3.68 – 3.58 (m, 1H), 2.01 – 1.95 (m, 2H), 1.63 – 1.51 (m, 2H), 1.35 – 1.27 (m, 1H), 1.20 – 1.12 (m, 1H), 0.91 (t, J = 7.4 Hz, 3H), 0.86 (t, J = 7.3 Hz, 3H).

¹³C NMR (101 MHz, CDCl₃) δ 157.9, 156.8, 147.9, 146.2, 139.2, 133.4, 131.5, 131.1 (d, J = 13.7 Hz), 130.7, 129.4, 128.8, 128.0, 125.3, 123.4 (q, J = 250 Hz), 57.2, 40.9, 37.7, 25.7, 20.5, 13.9, 13.8.

HRMS (*m/z*): [M + H]⁺ calcd for C₂₆H₂₈F₃N₂O₄S: 521.1716, found: 521.1714

(E)-2-(pyrimidin-5-yl)phenyl

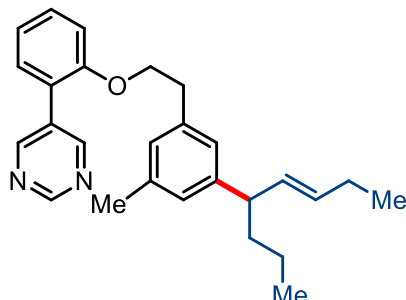


(3-chloro-5-(oct-5-en-4-yl)phenyl)methanesulfonate (3z):

Colorless oil; yield 51%; R_f = 0.35 (ethyl acetate/hexane = 1:4); ¹H NMR (500 MHz, CDCl₃) δ 9.23 (s, 1H), 8.81 (s, 2H), 7.51 – 7.38 (m, 3H), 7.38 – 7.34 (m, 1H), 7.24 (d, J = 1.9 Hz, 1H), 7.11 (d, J = 1.9 Hz, 1H), 5.53 (dt, J = 15.2, 6.3 Hz, 1H), 5.39 (dd, J = 15.3, 7.6 Hz, 1H), 4.24 (s, 2H), 3.83 (q, J = 7.4 Hz, 1H), 2.03 – 1.96 (m, 2H), 1.60 (d, J = 7.5 Hz, 2H), 1.35 – 1.31 (m, 1H), 1.20 (dd, J = 14.6, 7.3 Hz, 1H), 0.93 (t, J = 7.5 Hz, 3H), 0.89 (d, J = 7.3 Hz, 3H).

¹³C NMR (126 MHz, CDCl₃) δ 157.9, 156.7, 146.4, 145.9, 134.0, 133.9, 133.8, 132.1, 131.3, 130.8, 130.2, 129.7, 128.9, 128.8, 128.2, 125.9, 123.5, 56.8, 44.9, 37.6, 25.7, 20.6, 14.0, 13.8.

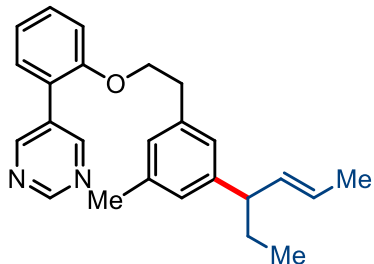
HRMS (*m/z*): [M + H]⁺ calcd for C₂₅H₂₈ClN₂O₃S: 471.1504, found: 471.1501.

(E)-5-(2-(3-methyl-5-(oct-5-en-4-yl)phenethoxy)phenyl)pyrimidine (5a):

Pale yellow oil; yield 86%; $R_f = 0.4$ (ethyl acetate/hexane = 1:4);
 ^1H NMR (500 MHz, CDCl_3) δ 9.17 (s, 1H), 8.90 (s, 2H), 7.38 (t, $J = 7.5$ Hz, 1H), 7.32 (d, $J = 7.4$ Hz, 1H), 7.07 (t, $J = 7.4$ Hz, 1H), 7.00 (d, $J = 8.3$ Hz, 1H), 6.86 (s, 1H), 6.80 (s, 2H), 5.55 – 5.33 (m, 2H), 4.21 (t, $J = 6.9$ Hz, 2H), 3.11 (dd, $J = 13.3, 6.6$ Hz, 1H), 2.99 (t, $J = 6.9$ Hz, 2H), 2.29 (s, 3H), 2.00 (dd, $J = 7.1, 4.5$ Hz, 2H), 1.59 (dd, $J = 14.7, 7.3$ Hz, 2H), 1.31 (s, 1H), 1.21 – 1.15 (m, 1H), 0.96 (t, $J = 7.4$ Hz, 3H), 0.87 (d, $J = 7.4$ Hz, 4H).

^{13}C NMR (126 MHz, CDCl_3) δ 157.0, 156.9, 156.0, 146.2, 138.2, 137.8, 133.1, 132.3, 131.7, 130.6, 130.4, 127.5, 126.6, 125.3, 123.6, 121.4, 112.3, 69.6, 48.6, 38.5, 35.8, 29.8, 25.7, 21.5, 20.8, 14.1, 14.0.

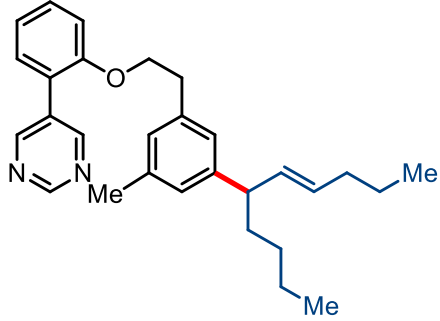
HRMS (m/z): [M + H]⁺ calcd for $\text{C}_{27}\text{H}_{33}\text{N}_2\text{O}$: 401.2587, found: 401.2584

(E)-5-(2-(3-(hex-4-en-3-yl)-5-methylphenethoxy)phenyl)pyrimidine (5b):

Colorless oil; yield 83%; $R_f = 0.38$ (ethyl acetate/hexane = 1:4);
 ^1H NMR (500 MHz, CDCl_3) δ 9.17 (s, 1H), 8.90 (s, 2H), 7.41 – 7.36 (m, 1H), 7.32 (dd, $J = 7.5, 1.4$ Hz, 1H), 7.07 (t, $J = 7.5$ Hz, 1H), 7.00 (d, $J = 8.3$ Hz, 1H), 6.84 (s, 1H), 6.80 (s, 1H), 6.78 (s, 1H), 5.56 – 5.36 (m, 2H), 4.20 (t, $J = 7.0$ Hz, 2H), 2.99 (t, $J = 6.9$ Hz, 3H), 2.28 (s, 3H), 1.68 – 1.60 (m, 5H), 0.82 (t, $J = 7.4$ Hz, 3H).

^{13}C NMR (126 MHz, CDCl_3) δ 157.0, 156.9, 155.9, 145.9, 138.2, 137.8, 135.2, 130.6, 130.4, 127.6, 126.6, 125.3, 124.7, 123.5, 121.3, 112.3, 69.5, 50.9, 35.8, 29.1, 21.5, 18.1, 12.4.

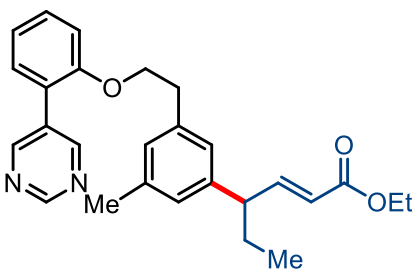
HRMS (m/z): [M + H]⁺ calcd for $\text{C}_{25}\text{H}_{29}\text{N}_2\text{O}$: 373.2274, found: 373.2271

(E)-5-(2-(3-(dec-6-en-5-yl)-5-methylphenethoxy)phenyl)pyrimidine (5c):

Colorless oil; yield 76%; $R_f = 0.42$ (ethyl acetate/hexane = 1:4); ^1H NMR (400 MHz, CDCl_3) δ 9.16 (s, 1H), 8.89 (s, 2H), 7.38 (td, $J = 8.3, 1.7$ Hz, 1H), 7.32 (dd, $J = 7.5, 1.6$ Hz, 1H), 7.07 (td, $J = 7.5, 0.8$ Hz, 1H), 6.99 (d, $J = 8.3$ Hz, 1H), 6.85 (s, 1H), 6.79 (s, 2H), 5.42 (qd, $J = 15.3, 7.0$ Hz, 2H), 4.20 (t, $J = 7.0$ Hz, 2H), 3.08 (q, $J = 7.5$ Hz, 1H), 2.98 (t, $J = 7.0$ Hz, 2H), 2.28 (s, 3H), 1.94 (dt, $J = 7.2, 4.6$ Hz, 2H), 1.57 (dd, $J = 6.8, 3.6$ Hz, 2H), 1.43 – 1.28 (m, 5H), 1.16 – 1.08 (m, 1H), 0.88 – 0.83 (m, 6H).

^{13}C NMR (101 MHz, CDCl_3) δ 157.0, 156.9, 156.0, 146.3, 138.2, 137.8, 134.3, 132.4, 130.6, 130.4, 130.0, 127.6, 126.6, 125.2, 123.6, 121.3, 112.3, 69.6, 48.9, 36.0, 35.8, 34.8, 22.8, 21.5, 14.2, 13.8.

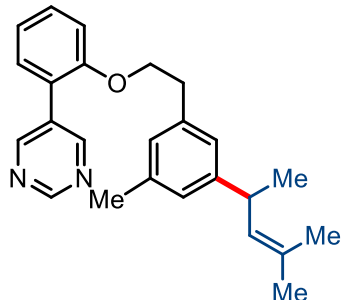
HRMS (m/z): [M + H]⁺ calcd for $\text{C}_{29}\text{H}_{37}\text{N}_2\text{O}$: 429.2900, found: 429.2905

(E)-ethyl 4-(3-methyl-5-(2-(pyrimidin-5-yl)phenoxy)ethyl)phenylhex-2-enoate (5d):

Colorless oil; yield 86%; $R_f = 0.28$ (ethyl acetate/hexane = 1:4); ^1H NMR (500 MHz, CDCl_3) δ 9.16 (s, 1H), 8.87 (s, 2H), 7.37 (t, $J = 7.8$ Hz, 1H), 7.30 (d, $J = 7.4$ Hz, 1H), 7.08 – 7.04 (m, 1H), 7.00 (dd, $J = 12.4, 7.9$ Hz, 2H), 6.83 (s, 2H), 6.77 (s, 1H), 5.78 (d, $J = 15.6$ Hz, 1H), 4.20 (t, $J = 6.7$ Hz, 2H), 4.15 (dd, $J = 14.5, 7.4$ Hz, 2H), 3.20 (q, $J = 7.5$ Hz, 1H), 2.98 (t, $J = 6.6$ Hz, 2H), 2.28 (s, 3H), 1.81 – 1.67 (m, 2H), 1.25 (t, $J = 7.1$ Hz, 3H), 0.85 (t, $J = 7.3$ Hz, 3H).

^{13}C NMR (126 MHz, CDCl_3) δ 166.8, 157.0, 156.9, 155.9, 151.8, 142.6, 138.6, 138.3, 132.3, 130.5, 130.4, 128.3, 126.8, 125.6, 123.5, 121.4, 120.8, 112.3, 69.4, 60.3, 50.2, 35.7, 27.9, 21.4, 14.3, 12.2.

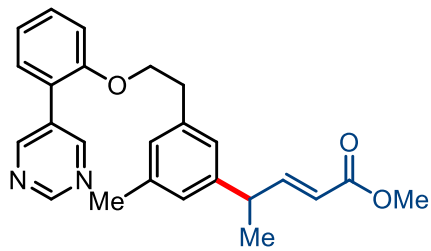
HRMS (m/z): [M + H]⁺ calcd for $\text{C}_{27}\text{H}_{31}\text{N}_2\text{O}_3$: 431.2329, found: 431.2329

5-(2-(3-Methyl-5-(4-methylpent-3-en-2-yl)phenethoxy)phenyl)pyrimidine (5e):

Colorless oil; yield 67%; $R_f = 0.32$ (ethyl acetate/hexane = 1:4); ^1H NMR (400 MHz, CDCl_3) δ 9.16 (s, 1H), 8.89 (s, 2H), 7.38 (td, $J = 8.3, 1.7$ Hz, 1H), 7.32 (dd, $J = 7.6, 1.7$ Hz, 1H), 7.07 (dd, $J = 7.8, 7.2$ Hz, 1H), 7.00 (d, $J = 8.3$ Hz, 1H), 6.90 (s, 1H), 6.84 (s, 1H), 6.79 (s, 1H), 5.26 – 5.19 (m, 1H), 4.20 (t, $J = 7.0$ Hz, 2H), 3.57 (dq, $J = 14.0, 7.0$ Hz, 1H), 2.99 (t, $J = 6.9$ Hz, 2H), 2.28 (s, 3H), 1.68 (d, $J = 0.9$ Hz, 3H), 1.66 (d, $J = 1.1$ Hz, 3H), 1.24 (d, $J = 7.0$ Hz, 3H).

^{13}C NMR (101 MHz, CDCl_3) δ 157.0, 156.9, 156.0, 147.7, 138.3, 137.8, 132.4, 130.6, 130.4, 130.3, 127.4, 126.1, 124.7, 123.5, 121.4, 112.3, 69.5, 38.2, 35.8, 25.9, 22.6, 21.5, 18.1.

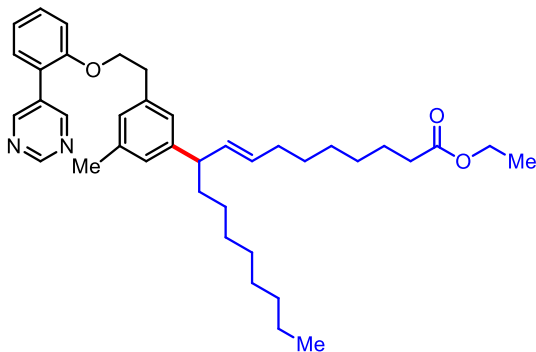
HRMS (m/z): [M + H]⁺ calcd for $\text{C}_{25}\text{H}_{29}\text{N}_2\text{O}$: 373.2274, found: 373.2273

(E)-methyl 4-(3-methyl-5-(2-(pyrimidin-5-yl)phenoxy)ethyl)phenyl)pent-2-enoate (5f):

Colorless oil; yield 83%; $R_f = 0.28$ (ethyl acetate/hexane = 1:4); ^1H NMR (400 MHz, CDCl_3) δ 9.16 (s, 1H), 8.86 (s, 2H), 7.38 (td, $J = 8.3, 1.7$ Hz, 1H), 7.30 (dd, $J = 7.5, 1.7$ Hz, 1H), 7.11 – 7.04 (m, 2H), 6.99 (d, $J = 8.3$ Hz, 1H), 6.84 (s, 2H), 6.78 (s, 1H), 5.80 (dd, $J = 15.7, 1.5$ Hz, 1H), 4.20 (t, $J = 6.7$ Hz, 2H), 3.71 (s, 3H), 3.58 – 3.48 (m, 1H), 2.98 (t, $J = 6.7$ Hz, 2H), 2.27 (s, 3H), 1.36 (d, $J = 7.0$ Hz, 3H).

^{13}C NMR (101 MHz, CDCl_3) δ 167.3, 157.0, 156.9, 155.9, 153.1, 143.6, 138.7, 138.4, 130.6, 130.4, 128.4, 126.4, 125.2, 123.5, 121.4, 119.7, 112.2, 69.4, 51.6, 42.0, 35.7, 21.4, 20.3.

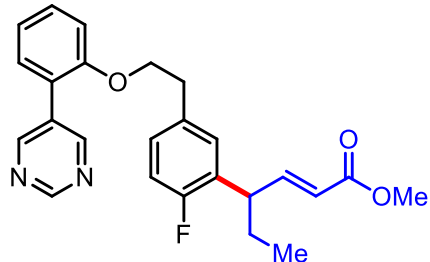
HRMS (m/z): [M + H]⁺ calcd for $\text{C}_{25}\text{H}_{27}\text{N}_2\text{O}_3$: 403.2016, found: 403.2014

(E)-Ethyl 10-(3-methyl-5-(2-(2-(pyrimidin-5-yl)phenoxy)ethyl)phenyl)octadec-8-enoate (5g):

Colorless oil; yield 86%; $R_f = 0.35$ (ethyl acetate/hexane = 1:4); ^1H NMR (500 MHz, CDCl_3) δ 9.16 (s, 1H), 8.89 (s, 2H), 7.40 – 7.36 (m, 1H), 7.32 (dd, $J = 7.5, 1.6$ Hz, 1H), 7.09 – 7.05 (m, 1H), 7.00 (d, $J = 8.3$ Hz, 1H), 6.84 (s, 1H), 6.79 (s, 2H), 5.51 – 5.33 (m, 2H), 4.20 (t, $J = 7.0$ Hz, 2H), 4.11 (q, $J = 7.1$ Hz, 2H), 3.07 (q, $J = 7.2$ Hz, 1H), 2.98 (t, $J = 7.0$ Hz, 2H), 2.31 – 2.24 (m, 6H), 1.96 (dd, $J = 13.7, 6.6$ Hz, 2H), 1.73 (s, 2H), 1.58 (d, $J = 6.9$ Hz, 4H), 1.28 – 1.19 (m, 19H), 0.86 (t, $J = 6.9$ Hz, 3H).

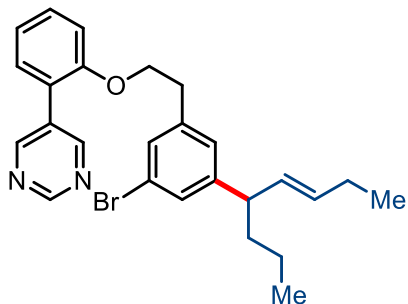
^{13}C NMR (126 MHz, CDCl_3) δ 174.0, 174.0, 157.0, 156.7, 156.0, 146.3, 138.2, 137.8, 134.2, 134.0, 130.6, 130.4, 130.3, 130.1, 127.6, 126.6, 125.2, 121.4, 112.3, 69.6, 60.3, 48.96, 48.95, 36.29, 36.26, 35.8, 34.5, 32.7, 32.6, 32.0, 29.7, 29.6, 29.5, 29.45, 29.4, 29.3, 29.29, 29.27, 29.1, 28.9, 27.8, 27.7, 25.1, 25.08, 22.8, 21.5, 14.4, 14.2.

HRMS (m/z): [M + H]⁺ calcd for $\text{C}_{39}\text{H}_{55}\text{N}_2\text{O}_3$: 599.4207, found: 599.4209.

(E)-methyl 4-(2-fluoro-5-(2-(2-(pyrimidin-5-yl)phenoxy)ethyl)phenyl)hex-2-enoate (5h):

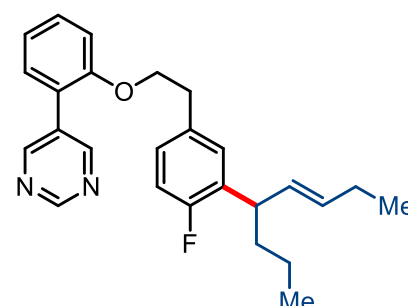
Colorless oil; yield 81%; $R_f = 0.25$ (ethyl acetate/hexane = 1:4); ^1H NMR (500 MHz, CDCl_3) δ 9.17 (s, 1H), 8.86 (s, 2H), 7.42 – 7.36 (m, 1H), 7.31 (d, $J = 7.5$ Hz, 1H), 7.11 – 7.01 (m, 2H), 6.96 (ddd, $J = 19.5, 11.5, 6.1$ Hz, 4H), 5.80 (d, $J = 15.6$ Hz, 1H), 4.18 (t, $J = 6.6$ Hz, 2H), 3.70 (s, 3H), 3.60 – 3.55 (m, 1H), 2.99 (t, $J = 6.5$ Hz, 2H), 1.84 – 1.75 (m, 1H), 1.75 – 1.65 (m, 1H), 0.86 (t, $J = 7.2$ Hz, 3H)

^{13}C NMR (126 MHz, CDCl_3) δ 167.1, 159.7 (d, $J = 245.7$ Hz), 156.9, 156.8, 155.8, 150.4, 134.1, 134.0, 130.57 (d, $J = 24.5$ Hz), 129.2 (d, $J = 9.8$ Hz), 128.9, 128.8, 121.6, 121.2, 115.8 (d, $J = 22.6$ Hz), 112.3, 69.3, 51.6, 43.4, 43.3, 35.2, 26.9, 12.2.

(E)-5-(2-(3-bromo-5-(oct-5-en-4-yl)phenethoxy)phenyl)pyrimidine (5i):

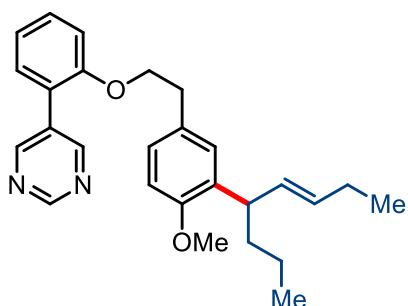
Colorless oil; yield 61%; $R_f = 0.4$ (ethyl acetate/hexane = 1:4); ¹H NMR (400 MHz, CDCl₃) δ 9.17 (s, 1H), 8.88 (s, 2H), 7.41 – 7.36 (m, 1H), 7.32 (dd, $J = 7.6, 1.7$ Hz, 1H), 7.16 (t, $J = 1.5$ Hz, 1H), 7.11 – 7.06 (m, 2H), 6.99 (d, $J = 7.9$ Hz, 1H), 6.89 (s, 1H), 5.50 – 5.35 (m, 2H), 4.19 (t, $J = 6.8$ Hz, 2H), 3.09 (q, $J = 7.3$ Hz, 1H), 2.98 (t, $J = 6.7$ Hz, 2H), 2.04 – 1.96 (m, 2H), 1.60 – 1.51 (m, 2H), 1.34 – 1.27 (m, 1H), 1.16 (ddd, $J = 9.2, 6.9, 2.6$ Hz, 1H), 0.95 (d, $J = 7.4$ Hz, 3H), 0.86 (d, $J = 7.4$ Hz, 3H).

¹³C NMR (101 MHz, CDCl₃) δ 157.1, 157.0, 156.9, 156.0, 148.5, 140.1, 132.5, 132.2, 130.6, 130.5, 129.5, 128.8, 127.2, 123.7, 122.6, 121.6, 112.3, 69.1, 48.4, 38.3, 35.5, 25.7, 20.7, 14.1, 13.9.

(E)-5-(2-(4-fluoro-3-(oct-5-en-4-yl)phenethoxy)phenyl)pyrimidine (5j):

Colorless oil; yield 64%; $R_f = 0.42$ (ethyl acetate/hexane = 1:4); ¹H NMR (500 MHz, CDCl₃) δ 9.16 (s, 1H), 8.87 (s, 2H), 7.41 – 7.36 (m, 1H), 7.32 (dd, $J = 7.5, 1.4$ Hz, 1H), 7.08 (t, $J = 7.4$ Hz, 1H), 6.98 (dd, $J = 10.4, 4.9$ Hz, 2H), 6.93 – 6.86 (m, 2H), 5.55 – 5.42 (m, 2H), 4.19 (t, $J = 6.8$ Hz, 2H), 3.47 (dd, $J = 8.6, 5.6$ Hz, 1H), 2.99 (t, $J = 6.8$ Hz, 2H), 1.99 (qd, $J = 7.3, 4.4$ Hz, 2H), 1.64 – 1.54 (m, 2H), 1.30 (dd, $J = 8.6, 4.3$ Hz, 1H), 1.18 (ddd, $J = 9.4, 9.0, 3.5$ Hz, 1H), 0.94 (t, $J = 7.5$ Hz, 3H), 0.87 (t, $J = 7.2$ Hz, 3H).

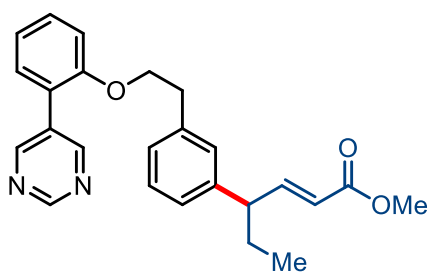
¹³C NMR (126 MHz, CDCl₃) δ 160.6 (d, $J = 244.4$ Hz), 157.0, 155.9, 133.6, 133.5, 132.7, 132.6, 132.5, 132.2, 131.3, 130.5 (d, $J = 17.1$ Hz), 129.1 (d, $J = 5.4$ Hz), 127.8, 127.7, 123.6, 121.5, 115.5 (d, $J = 22.6$ Hz), 112.3, 69.5, 41.8, 37.5, 35.2, 25.6, 20.8, 14.1, 13.9.

(E)-5-(2-(4-methoxy-3-(oct-5-en-4-yl)phenethoxy)phenyl)pyrimidine (5k):

Colorless oil; yield 81%; $R_f = 0.38$ (ethyl acetate/hexane = 1:4);
 ^1H NMR (400 MHz, CDCl_3) δ 9.16 (s, 1H), 8.90 (s, 2H), 7.38 (ddd, $J = 8.3, 7.5, 1.7$ Hz, 1H), 7.32 (dd, $J = 7.6, 1.7$ Hz, 1H), 7.07 (td, $J = 7.5, 1.0$ Hz, 1H), 6.99 (dd, $J = 8.3, 0.7$ Hz, 1H), 6.94 (dd, $J = 11.3, 2.2$ Hz, 2H), 6.76 (d, $J = 8.1$ Hz, 1H), 5.56 – 5.39 (m, 2H), 4.18 (t, $J = 7.0$ Hz, 2H), 3.79 (s, 3H), 3.62 (q, $J = 7.4$ Hz, 1H), 2.97 (t, $J = 7.1$ Hz, 2H), 2.03 – 1.94 (m, 2H), 1.58 – 1.51 (m, 2H), 1.35 – 1.28 (m, 1H), 1.17 (ddd, $J = 13.4, 6.8, 2.0$ Hz, 1H), 0.94 (t, $J = 7.4$ Hz, 3H), 0.86 (t, $J = 7.3$ Hz, 3H).

^{13}C NMR (101 MHz, CDCl_3) δ 156.0, 156.9, 155.0, 155.8, 134.5, 132.4, 132.3, 131.8, 130.6, 130.4, 129.7, 128.3, 127.2, 123.5, 121.4, 112.4, 111.0, 69.8, 55.8, 41.1, 37.7, 35.2, 25.7, 20.8, 14.2, 14.1.

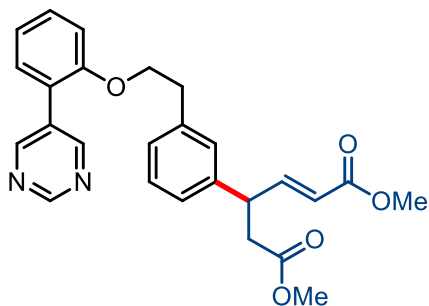
HRMS (m/z): [M + H]⁺ calcd for $\text{C}_{27}\text{H}_{33}\text{N}_2\text{O}_2$: 417.2537, found: 417.2536

(E)-methyl 4-(3-(2-(pyrimidin-5-yl)phenoxy)ethyl)phenyl)hex-2-enoate (5l):

Colorless oil; yield 76%; $R_f = 0.3$ (ethyl acetate/hexane = 1:4);
 ^1H NMR (500 MHz, CDCl_3) δ 9.17 (s, 1H), 8.85 (s, 2H), 7.38 (t, $J = 7.8$ Hz, 1H), 7.31 (d, $J = 7.4$ Hz, 1H), 7.23 (t, $J = 7.5$ Hz, 1H), 7.09 – 6.95 (m, 6H), 5.79 (d, $J = 15.6$ Hz, 1H), 4.21 (t, $J = 6.7$ Hz, 2H), 3.70 (s, 3H), 3.25 (q, $J = 7.5$ Hz, 1H), 3.02 (t, $J = 6.7$ Hz, 2H), 1.75 (ddd, $J = 18.4, 13.8, 6.5$ Hz, 2H), 0.85 (t, $J = 7.3$ Hz, 3H).

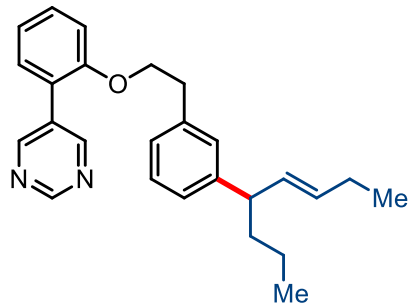
^{13}C NMR (126 MHz, CDCl_3) δ 167.2, 157.0, 156.9, 155.9, 152.1, 142.6, 138.5, 130.6, 130.5, 128.9, 128.6, 127.5, 126.0, 123.6, 121.5, 120.6, 112.3, 69.3, 51.6, 50.3, 35.8, 28.0, 12.2.

HRMS (m/z): [M + H]⁺ calcd for $\text{C}_{25}\text{H}_{27}\text{N}_2\text{O}_3$: 403.2016, found: 403.2021

(E)-dimethyl 4-(3-(2-(2-(pyrimidin-5-yl)phenoxy)ethyl)phenyl)hex-2-enedioate (5m):

Colorless oil; yield 75%; $R_f = 0.25$ (ethyl acetate/hexane = 1:4);
 ^1H NMR (400 MHz, CDCl_3) δ 9.16 (s, 1H), 8.81 (s, 2H), 7.41 – 7.35 (m, 1H), 7.30 (dd, $J = 7.6, 1.6$ Hz, 1H), 7.24 (t, $J = 7.6$ Hz, 1H), 7.13 – 7.02 (m, 4H), 7.00 (t, $J = 6.7$ Hz, 2H), 5.81 (dd, $J = 15.7, 1.4$ Hz, 1H), 4.21 (t, $J = 6.6$ Hz, 2H), 3.99 (q, $J = 7.2$ Hz, 1H), 3.69 (s, 3H), 3.61 (s, 3H), 3.01 (t, $J = 6.6$ Hz, 2H), 2.85 – 2.70 (m, 2H).

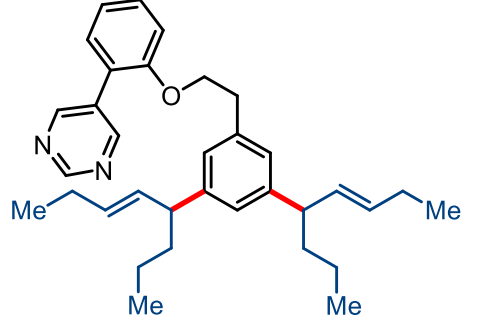
^{13}C NMR (101 MHz, CDCl_3) δ 171.7, 166.9, 157.0, 155.8, 149.7, 140.9, 138.8, 132.2, 130.6, 130.4, 129.2, 128.4, 128.1, 127.9, 125.9, 123.6, 121.5, 121.2, 112.3, 69.2, 51.9, 51.7, 44.1, 39.3, 35.8.

(E)-5-(2-(3-(oct-5-en-4-yl)phenethoxy)phenyl)pyrimidine (5n):

Colorless oil; yield 63%; $R_f = 0.42$ (ethyl acetate/hexane = 1:4); ^1H NMR (400 MHz, CDCl_3) δ 9.17 (s, 1H), 8.88 (s, 2H), 7.41 – 7.35 (m, 1H), 7.31 (dd, $J = 7.5, 1.6$ Hz, 1H), 7.21 (t, $J = 7.7$ Hz, 1H), 7.10 – 7.03 (m, 2H), 6.99 (t, $J = 8.1$ Hz, 3H), 5.53 – 5.37 (m, 2H), 4.22 (t, $J = 6.9$ Hz, 2H), 3.14 (dd, $J = 14.2, 7.1$ Hz, 1H), 3.03 (t, $J = 6.9$ Hz, 2H), 1.99 (qd, $J = 7.4, 4.6$ Hz, 2H), 1.64 – 1.53 (m, 2H), 1.31 (dd, $J = 13.7, 6.2$ Hz, 1H), 1.22 – 1.13 (m, 1H), 0.95 (t, $J = 7.4$ Hz, 3H), 0.87 (t, $J = 7.3$ Hz, 3H).

^{13}C NMR (101 MHz, CDCl_3) δ 157.0, 156.9, 155.9, 146.3, 137.9, 133.0, 131.8, 130.6, 130.5, 128.6, 128.3, 126.7, 125.8, 123.6, 121.4, 112.3, 69.5, 48.6, 38.5, 35.9, 25.7, 20.8, 14.2, 14.0.

HRMS (m/z): [M + H]⁺ calcd for $\text{C}_{26}\text{H}_{31}\text{N}_2\text{O}$: 387.2430, found: 387.2437

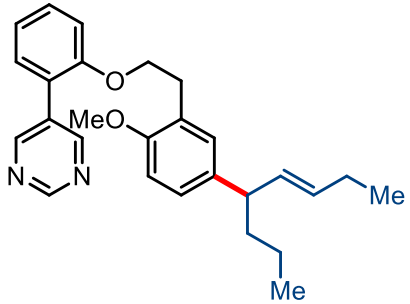
5-(2-((E)-oct-5-en-4-yl)-5-((S,E)-oct-5-en-4-yl)phenethoxy)phenyl)pyrimidine (5n'):

Colorless oil; yield 18%; $R_f = 0.5$ (ethyl acetate/hexane = 1:4); ^1H NMR (400 MHz, CDCl_3) δ 9.16 (s, 1H), 8.93 (s, 2H), 7.42 – 7.35 (m, 1H), 7.33 (dd, $J = 7.5, 1.6$ Hz, 1H), 7.07 (td, $J = 7.5, 0.8$ Hz, 1H), 7.00 (d, $J = 8.0$ Hz, 1H), 6.85 (s, 1H), 6.81 (s, 2H), 5.52 – 5.38 (m, 4H), 4.20 (t, $J = 7.2$ Hz, 2H), 3.12 (dd, $J = 13.8, 6.9$ Hz, 2H), 3.01 (t, $J = 7.2$ Hz, 2H), 2.00 (qd, $J = 7.4, 4.8$ Hz, 4H), 1.58 (dd, $J = 15.0, 7.4$ Hz, 4H), 1.30 – 1.23 (m, 2H), 1.19 – 1.14 (m, 2H), 0.95 (t, $J = 7.4$ Hz, 6H), 0.87 (t, $J = 7.3$ Hz, 6H).

^{13}C NMR (101 MHz, CDCl_3) δ 157.0, 156.0, 146.2, 137.6, 133.1, 133.12, 131.7, 130.6, 130.4, 125.8, 125.2, 123.5, 121.4, 112.4, 69.7, 48.7, 38.6, 38.5, 35.9, 25.7, 20.8, 14.2, 14.0.

(E)-5-(2-(2-methoxy-5-(oct-5-en-4-yl)phenethoxy)phenyl)pyrimidine (5o):

Colorless oil; yield 77%; $R_f = 0.45$ (ethyl acetate/hexane = 1:4); ^1H NMR (500 MHz, CDCl_3) δ

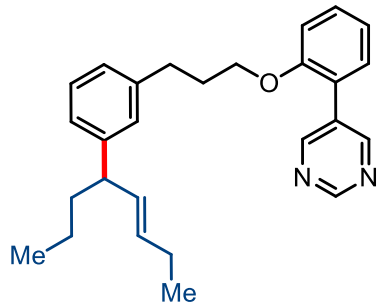


9.16 (s, 1H), 8.90 (s, 2H), 7.41 – 7.36 (m, 1H), 7.32 (dd, $J = 7.4, 1.4$ Hz, 1H), 7.09 – 7.00 (m, 3H), 6.93 (d, $J = 2.0$ Hz, 1H), 6.79 (d, $J = 8.4$ Hz, 1H), 5.49 – 5.36 (m, 2H), 4.21 (t, $J = 7.2$ Hz, 2H), 3.80 (s, 3H), 3.16 – 3.08 (m, 1H), 3.06 (t, $J = 7.3$ Hz, 2H), 1.98 (ddd, $J = 14.7, 7.3, 4.4$ Hz, 2H), 1.56 (ddd, $J = 13.3, 8.9, 6.0$ Hz, 2H), 1.25 – 1.13 (m, 2H), 0.94 (t, $J = 7.4$ Hz, 3H), 0.87 (t, $J = 7.4$ Hz, 3H).

0.87 (t, $J = 7.4$ Hz, 3H).

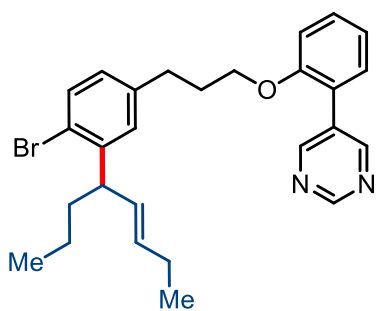
^{13}C NMR (126 MHz, CDCl_3) δ 157.0, 156.9, 156.1, 155.9, 137.9, 133.3, 132.4, 131.5, 130.5, 130.3, 130.2, 126.7, 125.7, 123.4, 121.2, 112.4, 110.3, 68.0, 55.4, 47.7, 38.5, 30.8, 25.7, 20.8, 14.1, 14.0.

HRMS (m/z): [M + Na]⁺ calcd for $\text{C}_{27}\text{H}_{32}\text{N}_2\text{NaO}_2$: 439.2356, found: 439.2351

(E)-5-(2-(3-(3-(oct-5-en-4-yl)phenyl)propoxy)phenyl)pyrimidine (5p):

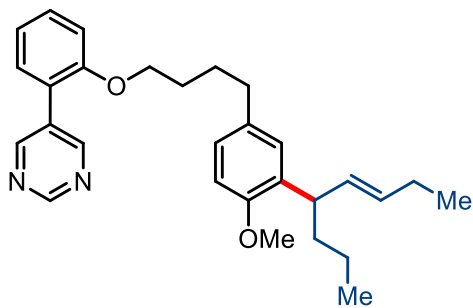
Colorless oil; yield 67%; $R_f = 0.5$ (ethyl acetate/hexane = 1:4); ^1H NMR (400 MHz, CDCl_3) δ 9.17 (s, 1H), 8.98 – 8.95 (m, 2H), 7.40 – 7.32 (m, 2H), 7.18 (dd, $J = 9.4, 5.7$ Hz, 1H), 7.08 (dd, $J = 8.1, 7.2$ Hz, 2H), 6.93 (d, $J = 6.0$ Hz, 3H), 5.54 – 5.40 (m, 2H), 4.00 (t, $J = 6.1$ Hz, 2H), 3.20 – 3.06 (m, 1H), 2.72 – 2.64 (m, 2H), 2.11 – 2.03 (m, 2H), 1.99 (ddd, $J = 12.2, 7.5, 4.1$ Hz, 2H), 1.59 (dd, $J = 15.7, 7.9$ Hz, 2H), 1.25 – 1.08 (m, 2H), 0.95 (td, $J = 7.4, 3.2$ Hz, 3H), 0.88 – 0.85 (m, 3H).

^{13}C NMR (101 MHz, CDCl_3) δ 157.0, 156.1, 146.0, 143.5, 141.1, 138.5, 133.2, 133.1, 132.4, 131.7, 131.6, 130.6, 130.4, 128.5, 128.4, 127.9, 127.7, 126.0, 125.3, 123.6, 121.4, 112.4, 67.5, 48.7, 38.5, 32.3, 30.8, 25.7, 20.8, 14.1, 14.0.

(E)-5-(2-(3-(4-bromo-3-(oct-5-en-4-yl)phenyl)propoxy)phenyl)pyrimidine (5q):

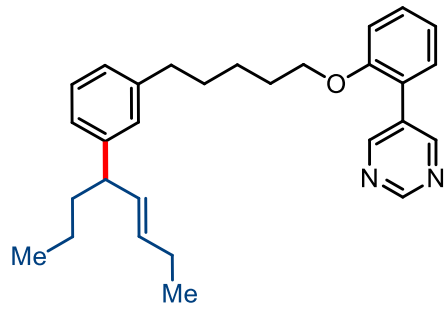
Colorless oil; yield 71%; $R_f = 0.48$ (ethyl acetate/hexane = 1:4); ^1H NMR (400 MHz, CDCl_3) δ 9.17 (s, 1H), 8.96 (s, 2H), 7.42 – 7.33 (m, 3H), 7.08 (ddd, $J = 8.3, 6.5, 2.7$ Hz, 1H), 6.96 (d, $J = 8.3$ Hz, 1H), 6.93 (d, $J = 2.1$ Hz, 1H), 6.79 (dd, $J = 8.1, 2.2$ Hz, 1H), 5.50 (dt, $J = 15.3, 6.0$ Hz, 1H), 5.40 (dd, $J = 15.3, 7.4$ Hz, 1H), 3.97 (t, $J = 6.2$ Hz, 2H), 3.72 (q, $J = 7.4$ Hz, 1H), 2.63 (t, $J = 7.5$ Hz, 2H), 2.10 – 1.95 (m, 4H), 1.56 (dd, $J = 15.2, 7.6$ Hz, 2H), 1.35 – 1.29 (m, 1H), 1.20 – 1.13 (m, 1H), 0.94 (t, $J = 7.5$ Hz, 3H), 0.87 (t, $J = 7.3$ Hz, 3H).

^{13}C NMR (101 MHz, CDCl_3) δ 157.0, 156.9, 156.0, 144.6, 140.5, 132.9, 132.8, 132.4, 131.5, 131.4, 130.7, 130.4, 128.6, 127.5, 123.6, 122.2, 121.5, 112.4, 67.2, 46.5, 37.9, 31.8, 30.6, 25.7, 22.2, 22.1, 20.6, 14.1, 13.9.

(E)-5-(2-(4-(4-methoxy-3-(oct-5-en-4-yl)phenyl)butoxy)phenyl)pyrimidine (5r):

Colorless oil; yield 72%; $R_f = 0.5$ (ethyl acetate/hexane = 1:4); ^1H NMR (400 MHz, CDCl_3) δ 9.15 (s, 1H), 8.94 (s, 2H), 7.42 – 7.36 (m, 1H), 7.33 (dd, $J = 7.5, 1.6$ Hz, 1H), 7.07 (t, $J = 7.2$ Hz, 1H), 6.99 (d, $J = 8.3$ Hz, 1H), 6.96 – 6.86 (m, 2H), 6.76 (d, $J = 8.5$ Hz, 1H), 5.63 – 5.38 (m, 2H), 4.01 (t, $J = 6.3$ Hz, 2H), 3.78 (s, 3H), 3.70 – 3.57 (m, 1H), 2.56 (t, $J = 7.4$ Hz, 2H), 2.06 – 1.91 (m, 2H), 1.77 (dd, $J = 13.6, 6.9$ Hz, 2H), 1.71 – 1.66 (m, 2H), 1.62 – 1.56 (m, 2H), 1.34 – 1.30 (m, 1H), 1.21 – 1.16 (m, 1H), 0.95 (t, $J = 7.5$ Hz, 3H), 0.87 (t, $J = 7.3$ Hz, 3H).

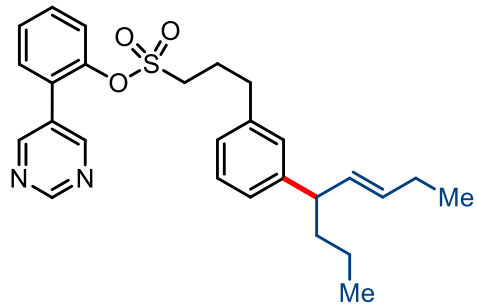
^{13}C NMR (101 MHz, CDCl_3) δ 157.0, 156.9, 156.2, 155.3, 134.1, 134.0, 132.6, 132.4, 131.6, 130.6, 130.4, 127.9, 126.3, 123.6, 121.3, 112.4, 111.0, 68.5, 55.8, 41.1, 37.8, 34.8, 29.8, 28.8, 28.0, 25.8, 20.9, 14.2, 14.1.

(E)-5-(2-((5-(3-(oct-5-en-4-yl)phenyl)pentyl)oxy)phenyl)pyrimidine (5s):

Colorless oil; yield 63%; $R_f = 0.52$ (ethyl acetate/hexane = 1:4); ^1H NMR (500 MHz, CDCl_3) δ 9.15 (s, 1H), 8.93 (s, 2H), 7.39 (t, $J = 7.7$ Hz, 1H), 7.33 (d, $J = 7.4$ Hz, 1H), 7.18 (t, $J = 7.8$ Hz, 1H), 7.08 (d, $J = 8.1$ Hz, 2H), 6.98 (dd, $J = 19.8, 7.0$ Hz, 3H), 5.59 – 5.33 (m, 2H), 4.00 (t, $J = 6.5$ Hz, 2H), 3.15 (q, $J = 7.3$ Hz, 1H), 2.56 (dd, $J = 15.9, 8.2$ Hz, 2H), 2.07 – 1.95 (m, 2H), 1.77 (d, $J = 6.3$ Hz, 2H), 1.68 (d, $J = 9.9$ Hz, 2H), 1.62 (d, $J = 7.4$ Hz, 2H), 1.48 – 1.38 (m, 2H), 1.21 (dd, $J = 14.8, 7.5$ Hz, 2H), 0.96 (t, $J = 7.4$ Hz, 3H), 0.88 (t, $J = 7.3$ Hz, 3H).

^{13}C NMR (126 MHz, CDCl_3) δ 157.0, 156.3, 145.8, 143.2, 142.5, 139.9, 133.2, 132.4, 131.7, 130.6, 130.4, 128.4, 127.8, 127.5, 125.9, 124.9, 121.3, 112.5, 68.6, 48.7, 48.3, 38.6, 36.0, 35.5, 31.2, 29.1, 25.7, 20.8, 14.1, 14.0.

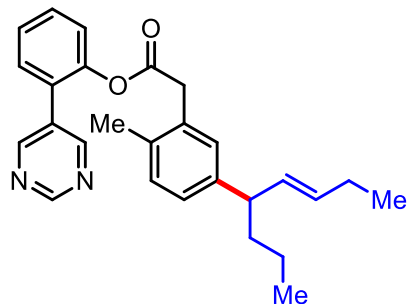
HRMS (m/z): $[\text{M} + \text{H}]^+$ calcd for $\text{C}_{29}\text{H}_{37}\text{N}_2\text{O}$: 429.2900, found: 429.2901

(E)-2-(pyrimidin-5-yl)phenyl 3-(3-(oct-5-en-4-yl)phenyl)propane-1-sulfonate (3aa):

Colorless oil; yield 61%; $R_f = 0.4$ (ethyl acetate/hexane = 1:4); ^1H NMR (500 MHz, CDCl_3) δ 9.21 (s, 1H), 8.87 (s, 2H), 7.49 – 7.39 (m, 4H), 7.22 (t, $J = 7.5$ Hz, 1H), 7.15 – 6.98 (m, 2H), 6.93 (s, 1H), 5.57 – 5.40 (m, 2H), 3.16 (dd, $J = 13.8, 6.8$ Hz, 1H), 3.08 – 2.98 (m, 2H), 2.64 (dd, $J = 16.0, 8.4$ Hz, 2H), 2.11 – 1.94 (m, 4H), 1.71 – 1.64 (m, 2H), 1.39 – 1.29 (m, 1H), 1.21 – 1.11 (m, 1H), 0.95 (t, $J = 7.3$ Hz, 3H), 0.88 (t, $J = 7.2$ Hz, 3H).

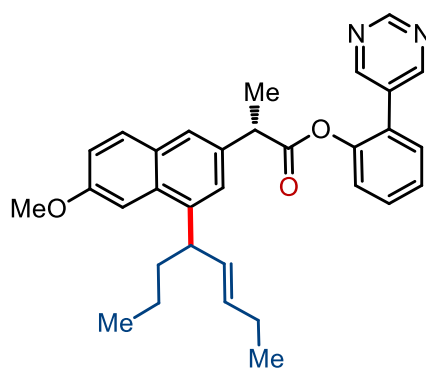
^{13}C NMR (126 MHz, CDCl_3) δ 157.9, 156.9, 146.5, 146.0, 139.4, 133.0, 131.9, 131.2, 130.8, 128.8, 128.5, 128.0, 127.9, 127.8, 125.9, 125.8, 123.6, 50.9, 48.6, 38.5, 33.9, 25.7, 24.9, 20.8, 14.1, 14.0.

HRMS (m/z): [M + H]⁺ calcd for $\text{C}_{27}\text{H}_{33}\text{N}_2\text{O}_3\text{S}$: 465.2206, found: 465.2206

(E)-2-(pyrimidin-5-yl)phenyl 2-(2-methyl-5-(oct-5-en-4-yl)phenyl)acetate (7a): Pale yellow

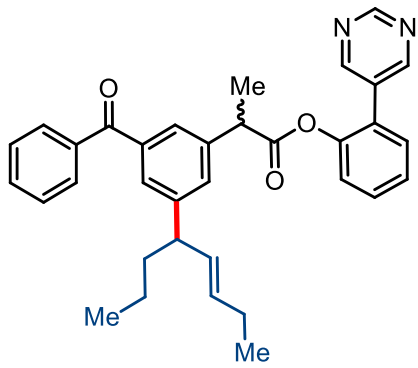
oil; yield 52%; $R_f = 0.32$ (ethyl acetate/hexane = 1:4); ^1H NMR (500 MHz, CDCl_3) δ 9.18 (s, 1H), 8.74 (s, 2H), 7.46 (dt, $J = 8.2, 4.7$ Hz, 1H), 7.37 (d, $J = 4.4$ Hz, 2H), 7.18 (d, $J = 8.0$ Hz, 1H), 7.08 (d, $J = 7.8$ Hz, 1H), 7.02 (dd, $J = 7.8, 1.5$ Hz, 1H), 6.95 (s, 1H), 5.47 (dd, $J = 8.8, 5.6$ Hz, 2H), 3.69 (s, 2H), 3.14 (q, $J = 7.1$ Hz, 1H), 2.12 (s, 3H), 2.00 (dd, $J = 7.3, 5.1$ Hz, 2H), 1.61 (d, $J = 7.6$ Hz, 2H), 1.30 (d, $J = 6.4$ Hz, 1H), 1.21 – 1.17 (m, 1H), 0.95 (d, $J = 7.4$ Hz, 3H), 0.88 (d, $J = 7.4$ Hz, 3H).

^{13}C NMR (101 MHz, CDCl_3) δ 169.7, 157.7, 156.5, 134.1, 133.1, 131.8, 131.5, 131.3, 130.7, 130.6, 130.5, 129.6, 128.0, 127.0, 123.3, 48.1, 39.2, 38.4, 25.7, 20.8, 19.1, 14.2, 14.0.

2-(Pyrimidin-5-yl)phenyl**2-(6-methoxy-4-(E)-oct-5-en-4-yl)naphthalen-2-ylpropanoate**

(7b): Pale yellow oil; yield 65%; R_f = 0.4 (ethyl acetate/hexane = 1:4); 1:1 d.r.; ¹H NMR (500 MHz, CDCl₃) δ 8.91 (s, 1H), 8.65 (s, 2H), 7.87 (s, 1H), 7.68 (d, J = 8.3 Hz, 1H), 7.46 – 7.39 (m, 1H), 7.37 – 7.31 (m, 2H), 7.26 (s, 1H), 7.12 – 7.05 (m, 2H), 7.00 (s, 1H), 5.62 – 5.50 (m, 2H), 4.01 – 3.95 (m, 1H), 3.93 (s, 4H), 2.03 – 1.96 (m, 2H), 1.78 (d, J = 5.6 Hz, 2H), 1.52 (d, J = 6.8 Hz, 3H), 1.41 (dd, J = 15.2, 6.5 Hz, 1H), 1.33 (d, J = 6.8 Hz, 1H), 0.92 (dd, J = 14.4, 7.5 Hz, 6H).

¹³C NMR (101 MHz, CDCl₃) δ 172.9, 157.6, 156.3, 148.2, 143.8, 134.8, 133.9, 132.8, 132.7, 132.3, 130.6, 130.3, 128.6, 128.1, 127.7, 126.8, 125.5, 125.3, 123.2, 122.3, 117.3, 103.9, 55.3, 45.8, 42.9, 38.2, 25.8, 20.9, 18.5, 14.3, 14.0.

2-(Pyrimidin-5-yl)phenyl 2-(3-benzoyl-5-((E)-oct-5-en-4-yl)phenyl)propanoate (7c): Pale

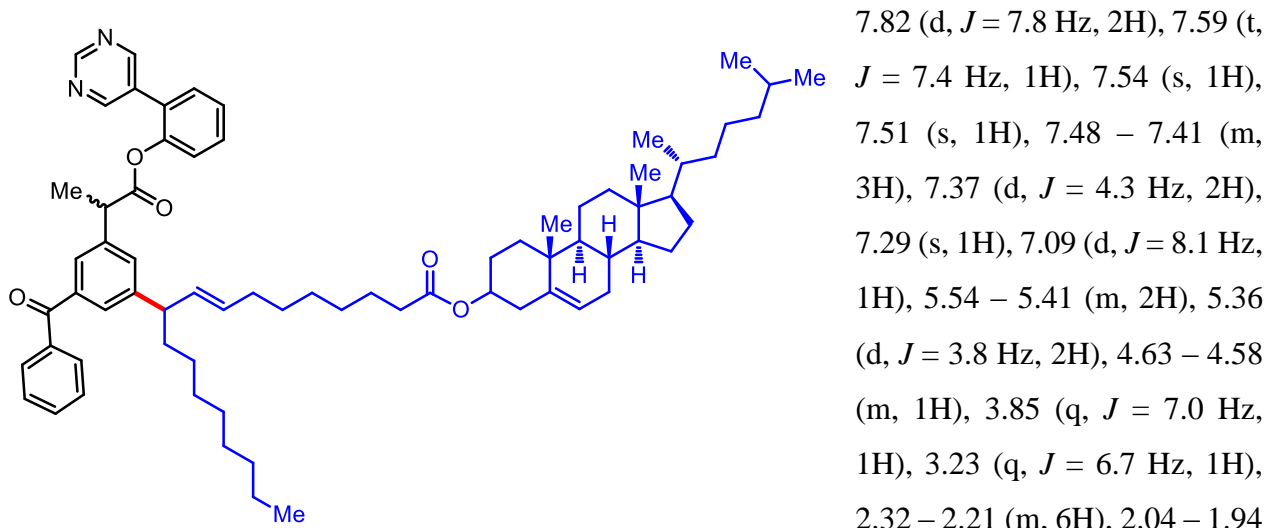
yellow oil; yield 67%; R_f = 0.38 (ethyl acetate/hexane = 1:4); 8:1 d.r.; ¹H NMR (400 MHz, CDCl₃) δ 9.13 (s, 1H), 8.73 (s, 2H), 7.83 (d, J = 8.0 Hz, 2H), 7.60 (t, J = 7.4 Hz, 1H), 7.55 (s, 1H), 7.53 – 7.43 (m, 4H), 7.37 (d, J = 4.3 Hz, 2H), 7.29 (d, J = 1.1 Hz, 1H), 7.10 (d, J = 8.0 Hz, 1H), 5.48 (dd, J = 20.7, 5.2 Hz, 2H), 3.86 (q, J = 7.0 Hz, 1H), 3.31 – 3.21 (m, 1H), 2.08 – 1.97 (m, 2H), 1.67 – 1.62 (m, 2H), 1.47 (d, J = 7.1 Hz, 3H), 1.34 (dd, J = 13.8, 7.2 Hz, 1H), 1.20 (dd, J = 14.8, 7.3 Hz, 1H), 0.96 (t, J = 7.5 Hz, 3H), 0.89 (t, J = 7.3 Hz, 3H).

¹³C NMR (101 MHz, CDCl₃) δ 196.6, 172.4, 156.4, 148.1, 146.9, 146.8, 139.5, 138.3, 137.8, 132.7, 132.6, 132.2, 132.1, 130.9, 130.6, 130.4, 130.2, 128.7, 128.4, 128.0, 127.0, 126.9, 126.8,

123.1, 48.4, 45.5, 45.4, 38.3, 25.7, 20.8, 18.4, 14.0.

HRMS (*m/z*): [M + Na]⁺ calcd for C₃₄H₃₄KN₂O₃: 557.2201, found: 557.2208

(10E)-10,13-dimethyl-17-6-methylheptan-2-yl)-2,3,4,7,8,9,10,11,12,13,14,15,16,17-tetradecahydro-1H-cyclopenta[a]phenanthren-3-yl 10-(3-benzoyl-5-(1-oxo-1-(2-(pyrimidin-5-yl)phenoxy)propan-2-yl)phenyl)octadec-8-enoate (7d): Pale yellow oil; yield 73%; $R_f = 0.5$ (ethyl acetate/hexane = 1:4); 9:1 d.r.; ^1H NMR (500 MHz, CDCl_3) δ 9.11 (s, 1H), 8.70 (s, 2H),

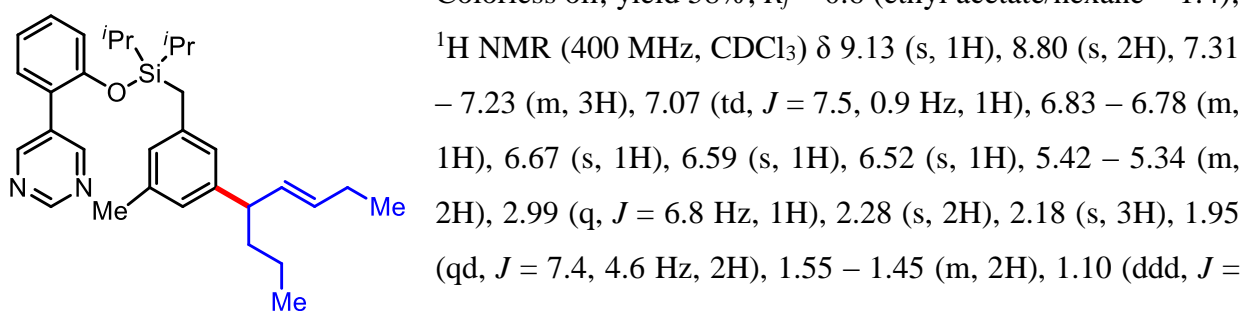


(m, 6H), 1.89 – 1.79 (m, 5H), 1.64 – 1.43 (m, 20H), 1.18 – 1.05 (m, 14H), 1.01 – 0.97 (m, 6H), 0.91 (d, $J = 6.5$ Hz, 5H), 0.85 (dd, $J = 6.5, 4.4$ Hz, 12H).

^{13}C NMR (126 MHz, CDCl_3) δ 196.6, 173.3, 172.3, 157.7, 156.4, 148.1, 146.8, 139.8, 139.5, 138.3, 137.8, 132.6, 131.3, 130.9, 130.6, 130.3, 128.7, 128.4, 128.0, 127.0, 126.9, 123.1, 122.7, 73.8, 56.8, 56.3, 50.2, 48.7, 45.5, 42.4, 39.8, 39.6, 38.3, 37.1, 36.7, 36.3, 36.1, 35.9, 34.8, 32.6, 32.2, 32.1, 31.9, 29.7, 29.3, 28.3, 28.1, 27.9, 25.1, 24.4, 23.9, 23.0, 22.6, 21.1, 19.4, 18.8, 18.4, 14.2, 11.9.

(E)-5-((diisopropyl(3-methyl-5-(oct-5-en-4-yl)benzyl)silyloxy)phenyl)pyrimidine (9a):

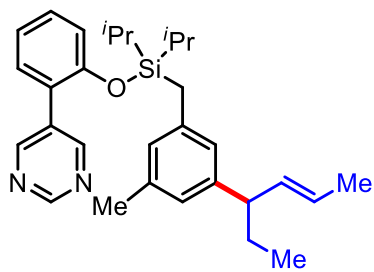
Colorless oil; yield 58%; $R_f = 0.6$ (ethyl acetate/hexane = 1:4);



16.0, 11.2, 4.1 Hz, 4H), 0.92 – 0.86 (m, 15H), 0.83 (t, J = 7.3 Hz, 3H).

^{13}C NMR (101 MHz, CDCl_3) δ 157.0, 153.1, 145.7, 137.9, 137.7, 133.3, 132.9, 131.3, 130.5, 130.3, 127.2, 125.7, 125.1, 124.9, 121.9, 119.6, 48.5, 38.4, 25.7, 21.5, 21.1, 20.8, 17.4, 14.1, 13.9, 12.94, 12.91.

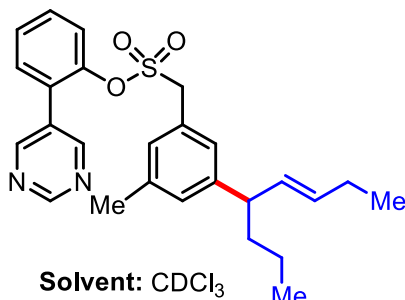
(E)-5-((2-(((3-(hex-4-en-3-yl)-5-methylbenzyl)diisopropylsilyl)oxy)phenyl)pyrimidine (9b):



Colorless oil; yield 63%; R_f = 0.6 (ethyl acetate/hexane = 1:4); ^1H NMR (400 MHz, CDCl_3) δ 9.13 (s, 1H), 8.79 (s, 2H), 7.30 – 7.24 (m, 2H), 7.08 (td, J = 7.5, 1.0 Hz, 1H), 6.84 – 6.80 (m, 1H), 6.67 (s, 1H), 6.58 (s, 1H), 6.53 (s, 2H), 5.47 – 5.31 (m, 2H), 2.87 (q, J = 7.3 Hz, 1H), 2.29 (s, 2H), 2.18 (s, 3H), 1.60 (d, J = 5.9 Hz, 3H), 1.57 – 1.50 (m, 2H), 1.13 – 1.06 (m, 2H), 0.93 – 0.88 (m, 12H), 0.76 (t, J = 7.3 Hz, 3H).

^{13}C NMR (101 MHz, CDCl_3) δ 157.0, 153.1, 145.5, 137.9, 137.7, 135.4, 132.9, 130.6, 130.4, 127.3, 125.7, 125.2, 124.9, 124.4, 121.9, 119.7, 50.7, 28.9, 21.5, 21.1, 18.1, 17.4, 12.9, 12.4.

(E)-2-(pyrimidin-5-yl)phenyl (3-methyl-5-(oct-5-en-4-yl)phenyl)methanesulfonate (3a; with cis-4-octene): Colorless oil; yield 78% (*meta*:others = 10:1); ^1H NMR (400 MHz, CDCl_3) δ 9.22



(s, 1H), 8.85 (s, 2H), 7.40 (t, J = 2.8 Hz, 3H), 7.25 – 7.22 (m, 1H), 7.02 (s, 1H), 6.94 (s, 2H), 5.48 – 5.44 (m, 2H), 4.26 (s, 2H), 3.18 – 3.10 (m, 1H), 2.32 (s, 3H), 2.01 – 1.95 (m, 2H), 1.59 (dt, J = 8.5, 4.1 Hz, 2H), 1.34 – 1.27 (m, 1H), 1.17 (ddd, J = 10.1, 8.5, 4.1 Hz, 1H), 0.93 (d, J = 7.5 Hz, 3H), 0.85 (d, J = 7.4 Hz, 3H).

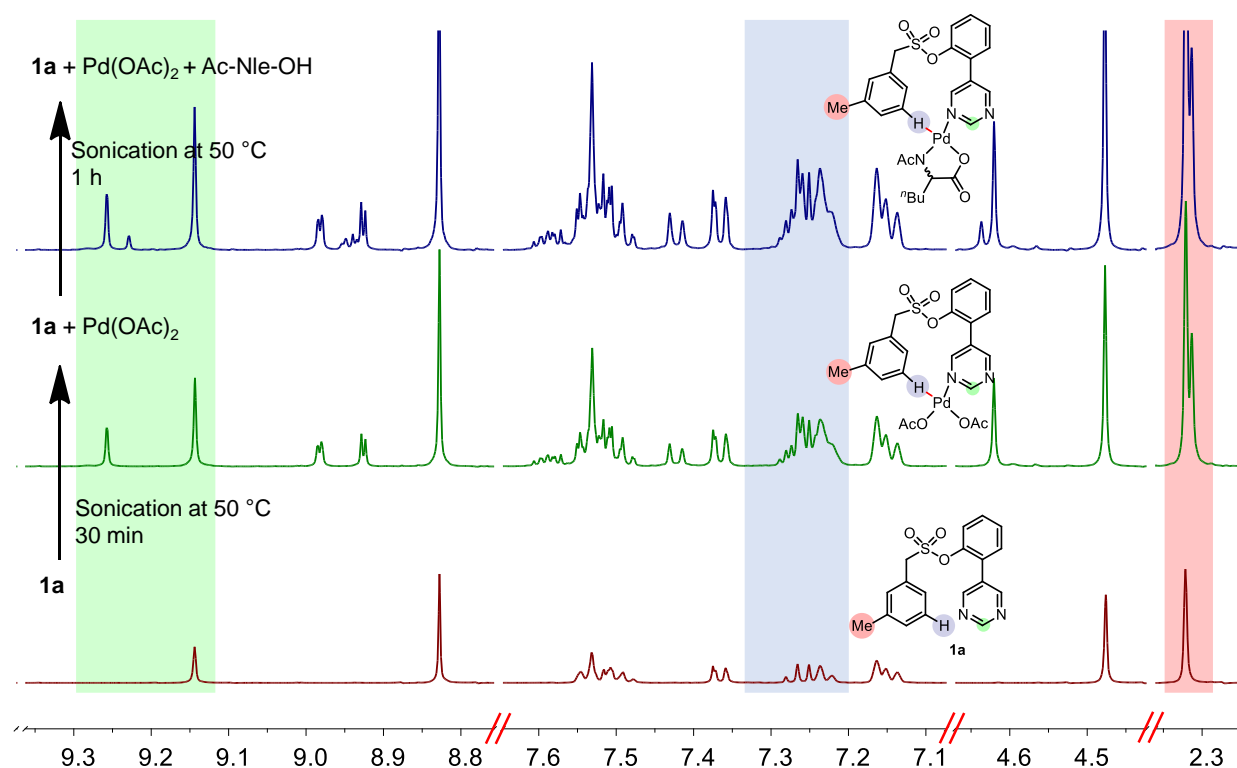
with *cis*-4-octene

^{13}C NMR (101 MHz, CDCl_3) δ 157.9, 156.8, 146.7, 146.4, 138.9, 132.6, 132.2, 131.1, 130.7, 129.6, 129.1, 128.7, 127.8, 127.2, 126.3, 123.4, 57.9, 48.4, 38.4, 25.7, 21.4, 20.7, 14.1, 14.0.

2.7. Mechanistic studies

2.7.1. NMR spectroscopic studies: Interaction between $\text{Pd}(\text{OAc})_2$ and arene, further effect on addition of *N*-acetyl norleucine were determined by ^1H NMR spectroscopy. Samples were prepared as follow:

- 1) Compound **1a** (0.025 mmol, 8 mg) was weighted and transfer to a NMR tube, followed by 500 μL of CD_3CN .
- 2) 20 mol% of $\text{Pd}(\text{OAc})_2$ was added to the same NMR tube and sonicated for 30 min at 50 $^\circ\text{C}$.
- 3) 30 mol% of Ac-Nle-OH was added to the above NMR tube and sonicated for 1 h at 50 $^\circ\text{C}$.



^1H NMR experiments revealed the indispensable role of Pd-catalyst and the ligand in this transformation. In the presence of $\text{Pd}(\text{OAc})_2$ and Ac-Nle-OH, a prominent chemical shift of **1a** suggested strong interactions with catalyst and ligand (highlighted in color shade), likely through the pyrimidine-N, which eventually leads to C–H activation.

2.7.2. Kinetic experiments:

Kinetic studies were carried out under standard reaction conditions with 2-(pyrimidin-5-yl)phenyl m-tolylmethanesulfonate (0.05 mmol scale) and *trans*-4-octene. Set of parallel reactions were carried out in a 10 mL reaction tubes separately and quenched at different time points. After cooling down to room temperature, 1 equiv. of 1,3,5-trimethoxy benzene (TMB) was added to each reaction tubes. The reaction mixtures were filtered through short celite pad using ethyl acetate as the eluent. The filtrate was then treated with aqueous ammonia solution (28-30%) to remove Cu(II) from the reaction mixtures. The organic layer was then separated and dried under reduced pressure. Yield of the product in each reaction was determined by ^1H NMR spectroscopy using TMB as an internal standard. All the reactions were repeated twice and the average yield was taken to plot the graph against time (minute).

Comparison of reaction rate with different aliphatic internal olefins:

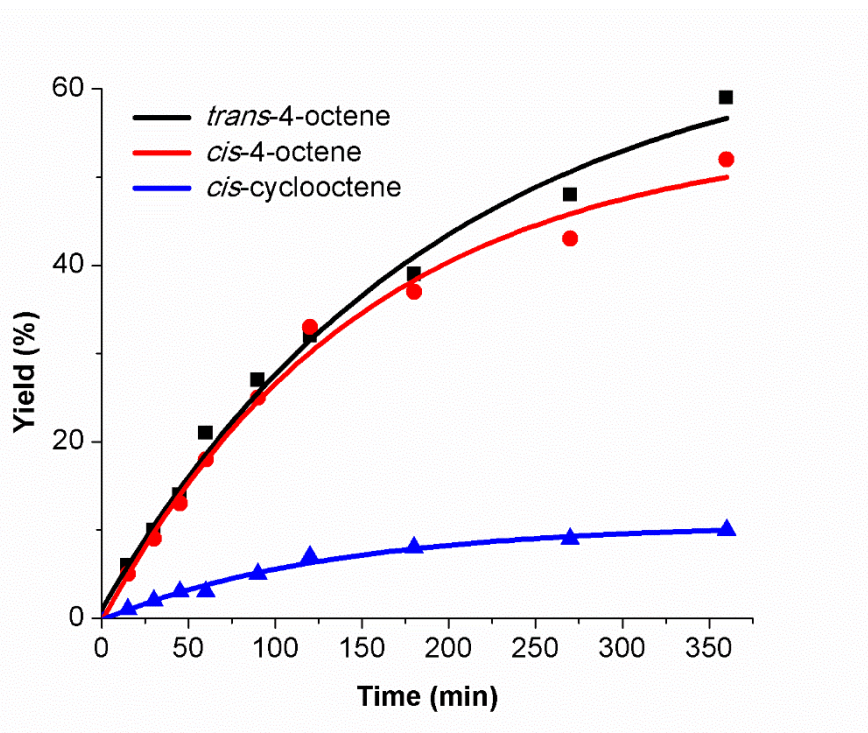


Figure S6. Kinetic comparison of different aliphatic internal olefins

Kinetic dependence study of different reaction components

In addition to the standard reaction condition, kinetics studies of reactions without CuF_2 , ligand and Ag_2CO_3 were also performed in a stepwise control experiment.

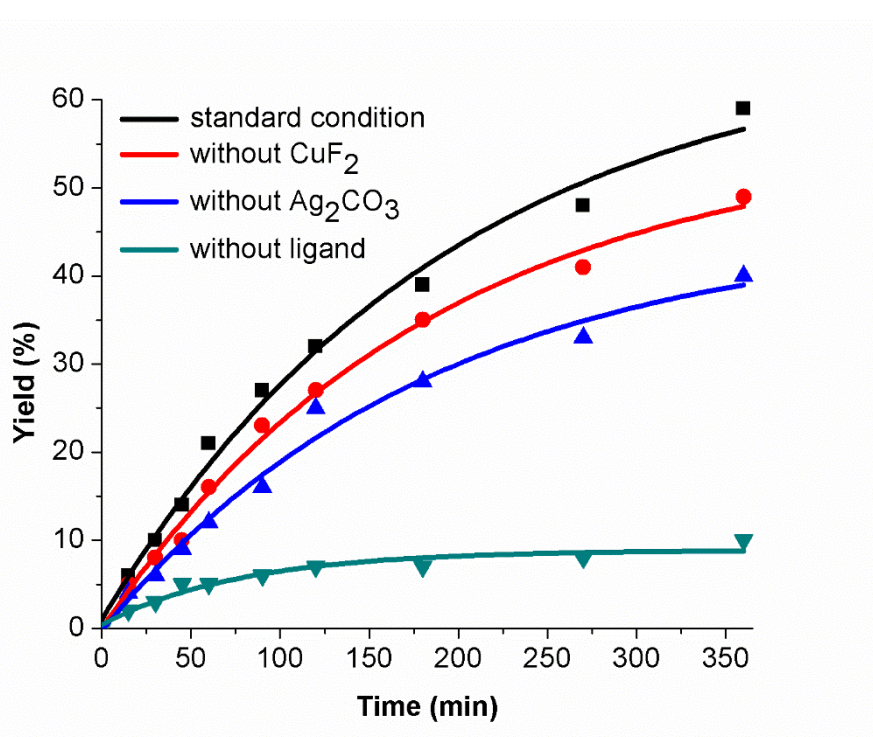
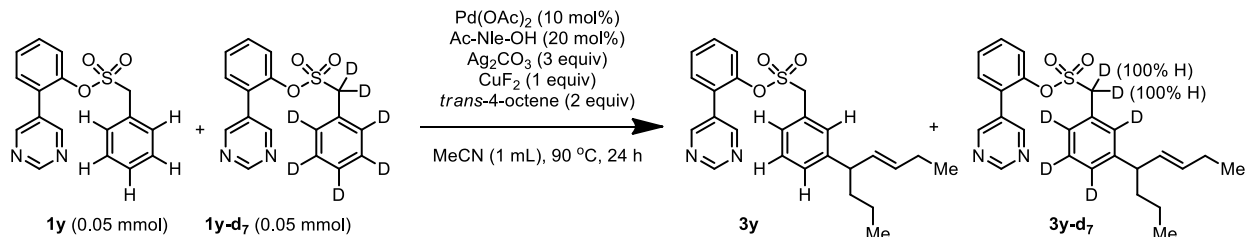


Figure S7. Kinetic dependence of reaction components

P_H/P_D determination:



An oven dried reaction tube was charged with magnetic stirring bar, 0.05 mmol of each **1y** and **1y-d₇**, 10 mol% Pd(OAc)₂, 20 mol% Ac-Nle-OH, 3 equiv Ag₂CO₃, 1 equiv CuF₂ and 2 equiv trans-4-octene. Then 1 mL of MeCN was added and the reaction mixture was vigorously stirred at 90 °C for 24 h. After completion of reaction, the mixture was diluted with ethyl acetate and filtered through celite. Filtrate was concentrated under reduced pressure and then the crude reaction mixture was subjected to preparative column chromatography (10% ethyl acetate/pet ether mixture was used as an eluent) to afford allylated product.

*Under optimized reaction condition, 100% H/D exchange were observed in benzylic –CD₂ of **3y-d₇**.*

$P_H/P_D = 1.08$

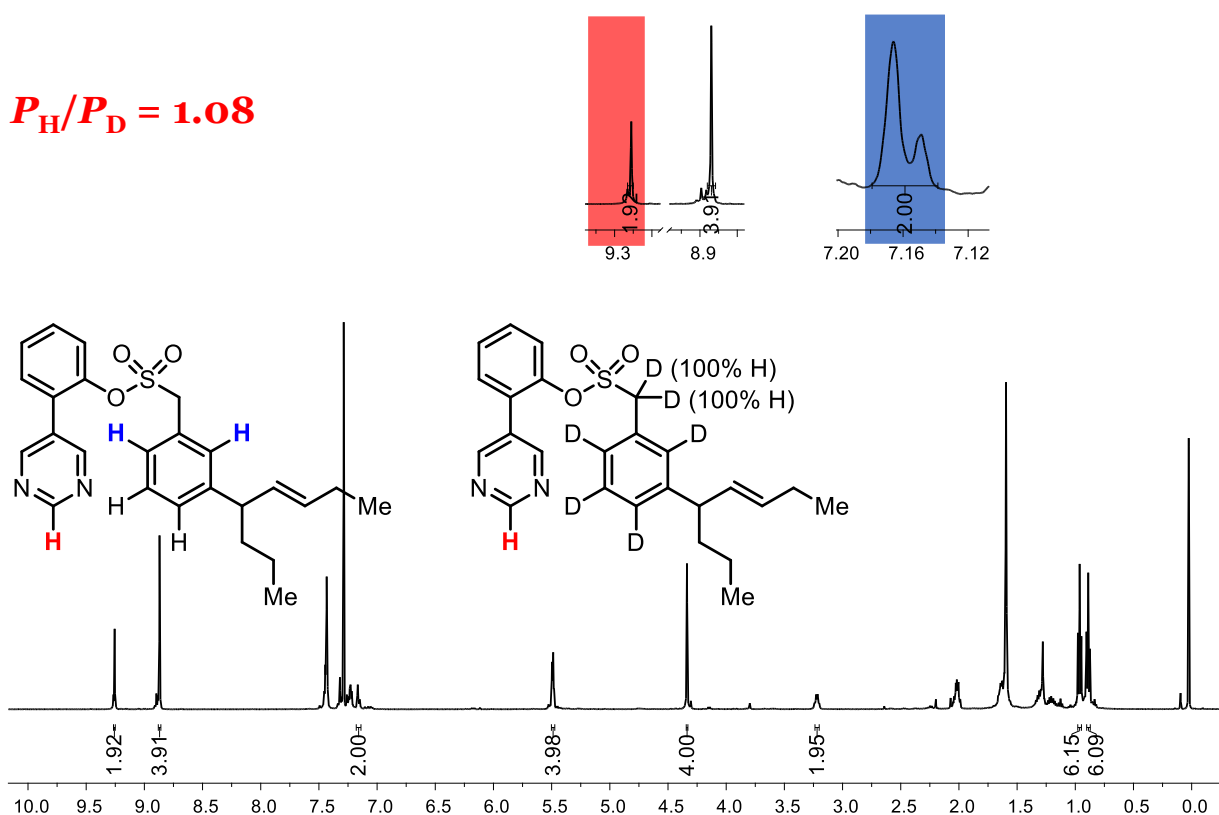
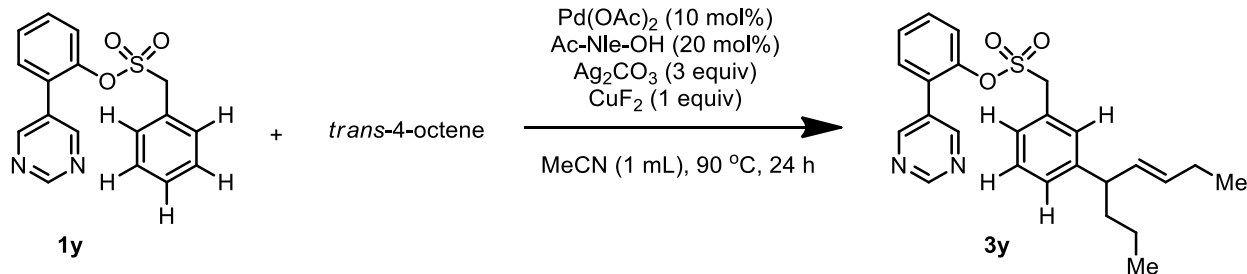


Figure S8. ^1H NMR spectrum of **(3y + 3y-d₇)**.

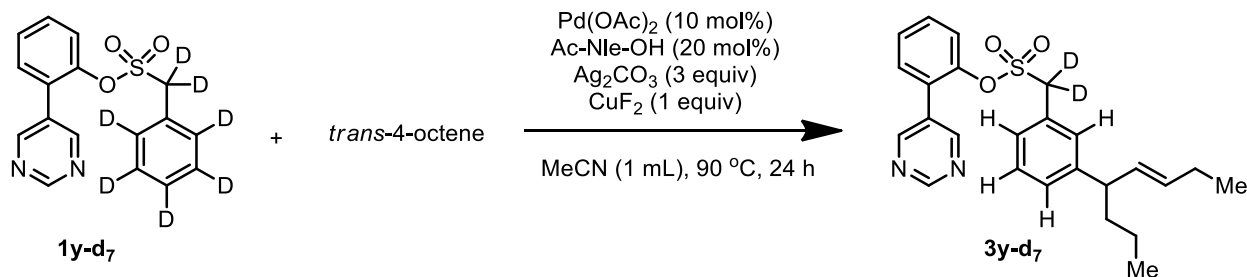
k_H/k_D determination:

As mentioned in the manuscript, for **1y** both the *meta*- positions are open, formation of *mono*- and *di*-allylated products are observed. Therefore, we decided to study the conversion of starting materials as opposed to yield of the products for the kinetic studies. k_H/k_D value was determined by following initial slope methods (yields below 30%).



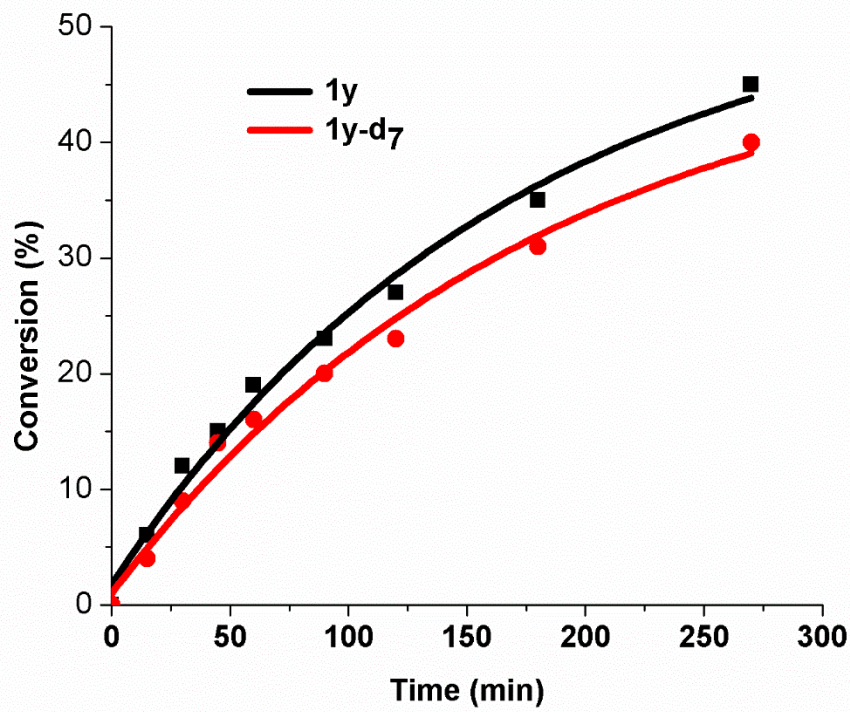
Run	1y (mmol)	Trans-4-octene 2a (mmol)	Pd(OAc) ₂ (mmol)	Ac-Nle-OH (mmol)	Ag ₂ CO ₃ (mmol)	CuF ₂ (mmol)
4 and 5	0.1	0.2	0.01	0.02	0.3	0.1

Entry	Time	Run 4	Run 5	Average
		Conversion (%)	Conversion (%)	Conversion (%)
1	0	0	0	0
2	15	5	7	6
3	30	11	13	12
4	45	16	14	15
5	60	19	19	19
6	90	21	25	23
7	120	26	28	27
8	180	33	37	35
9	270	44	46	45



Run	1y-d7 (mmol)	Trans-4-octene 2a (mmol)	Pd(OAc) ₂ (mmol)	Ac-Nle-OH (mmol)	Ag ₂ CO ₃ (mmol)	CuF ₂ (mmol)
6 and 7	0.1	0.2	0.01	0.02	0.3	0.1

Entry	Time	Run 6	Run 7	Average
		Conversion (%)	Conversion (%)	Conversion (%)
1	0	0	0	0
2	15	4	4	4
3	30	9	9	9
4	45	15	13	14
5	60	17	15	16
6	90	20	20	20
7	120	22	24	23
8	180	30	32	31
9	270	40	40	40

**Figure S9.** Determination of kinetic isotope effectNow, Rate = $k \cdot [1y]^x [2a]^y$

For run (4 and 5), initial rate = Rate (4 and 5)

So, Rate = $k_H \cdot [1y]^x [2a]^y$

or, $0.241 \text{ (mmol-1.min-1)} = k_H \cdot [0.1]^x [0.2]^y$

For run (6 and 7), initial rate = Rate (6 and 7)

So, Rate = $k_D \cdot [1\mathbf{y-d}_7]^x [2\mathbf{a}]^y$

or, $0.204 \text{ (mmol-1.min-1)} = k_D \cdot [0.1]^x [0.2]^y$

So, $k_H / k_D = \text{Rate (4 and 5) / Rate (6 and 7)}$

or, $k_H / k_D = 0.241 \text{ (mmol-1.min-1)} / 0.204 \text{ (mmol-1.min-1)}$

or, $\mathbf{k_H / k_D = 1.18}$

2.7.3. Mass spectrometric studies:

Compound **1a** (0.025 mmol, 8 mg), 25 mol% of Pd(OAc)₂, 50 mol% of N-Ac-Nle-OH were weighted and transfer to a 5 mL glass vial, followed by 1 mL of CH₃CN and sonicated for 30 min at 50 °C. Upon completion of sonication, mixture was filtered through celite and then ESI-MS was recorded with the filtrate.

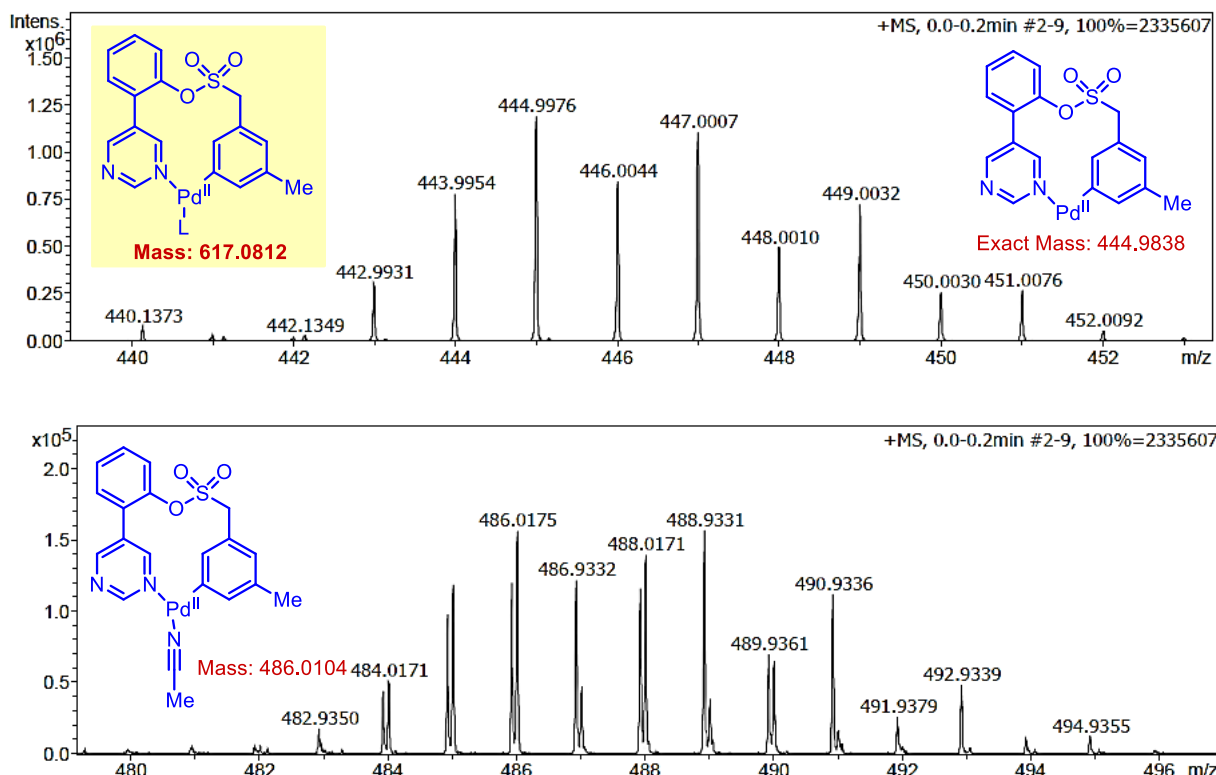


Figure S10. ESI-MS spectra of **1a**-Pd complex.

2.7.4. X-ray crystallography study:

Compound **1a** (0.025 mmol, 8 mg), 25 mol% of Pd(OAc)₂, 50 mol% of N-Ac-Nle-OH were weighted and transfer to a 5 mL glass vial, followed by 1 mL of CH₃CN and sonicated for 30 min at 50 °C. Upon completion of sonication, the mixture was filtered through celite and then solvent was removed under reduced pressure. The solid residue was subjected for crystallization.

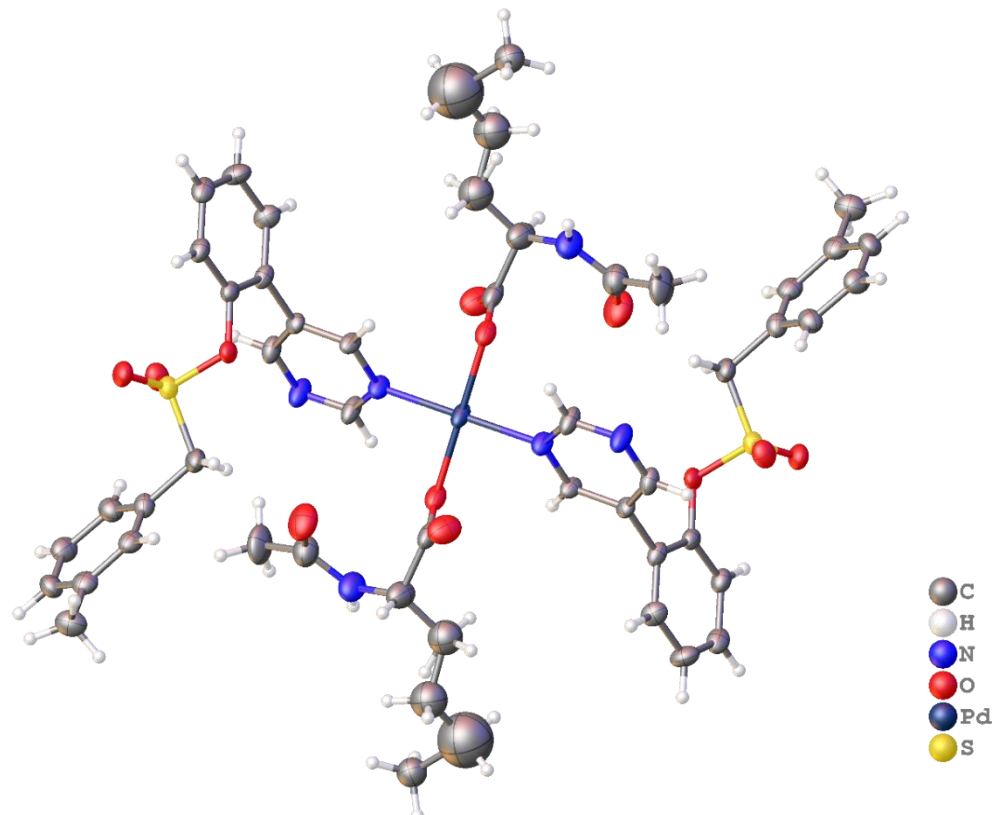


Figure S11. X-ray crystal structure of **1a**-Pd-ligand (Ac-Nle-OH) complex (CCDC **1894286**).

Crystallographic data:

Bond precision: C-C = 0.0092 Å

Wavelength=0.71073

Cell: a=6.0700(2)

b=12.6058(6)

c=35.2471(13)

Alpha = 90

beta = 94.058(3)

gamma = 90

Temperature: 150 K

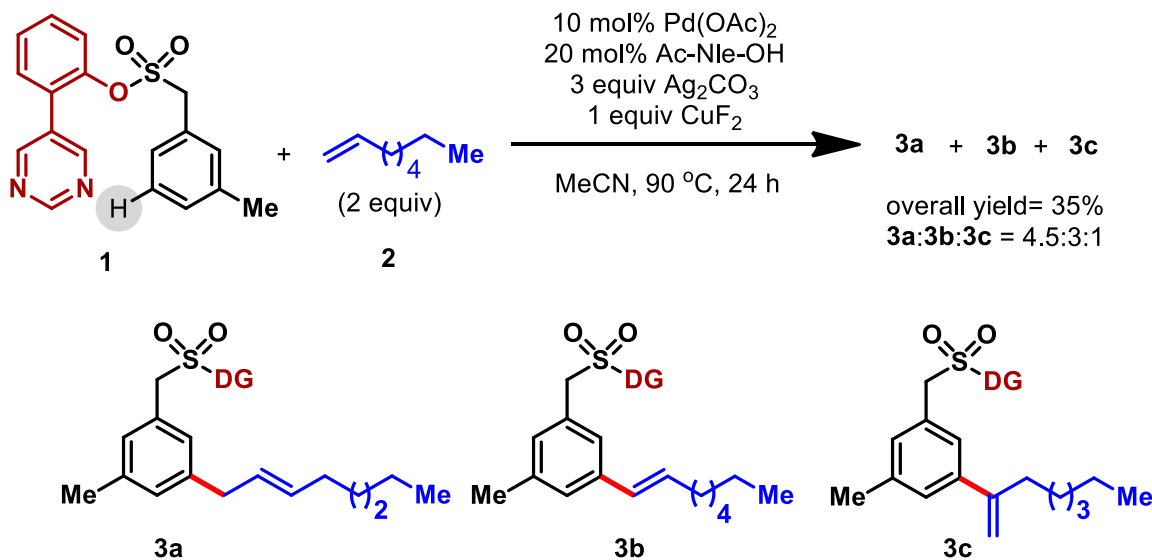
Calculated

Reported

Volume	2690.25(18)	2690.25(18)
Space group	P 21/c	P 1 21/c 1
h,k,lmax	7,14,41	7,14,41
R (reflections)= 0.0695(3554)		wR2 (reflections)= 0.2361(4740)

2.8. General procedure for palladium catalyzed *meta*-selective C–H allylation with terminal olefin

To an oven-dried screw cap reaction tube charged with a magnetic stir-bar was added 2-(pyrimidin-5-yl)phenyl m-tolylmethanesulfonate **1a** (0.2 mmol, 1 equiv), Pd(OAc)₂ (10 mol%), N-acetyl norleucine (20 mol%), Ag₂CO₃ (3 equiv) and CuF₂ (1 equiv). 1-Octene (2 equiv) was added with a micro litter pipette and 2 mL acetonitrile was added with a disposable laboratory syringe under aerobic condition. The tube was placed in a preheated oil bath at 90 °C and the reaction mixture was stirred for 24 h. The reaction mixture was then cooled to room temperature and filtered through a celite pad with ethyl acetate. The filtrate was concentrated and the crude compound was purified by column chromatography using silica gel (100-200 mesh size) and petroleum ether / ethyl acetate as an eluent to afford the alkenylated compound in 35% yield. ¹H NMR of the compound reveled the mixture of positional isomers in 4.5:3:1 ratio.



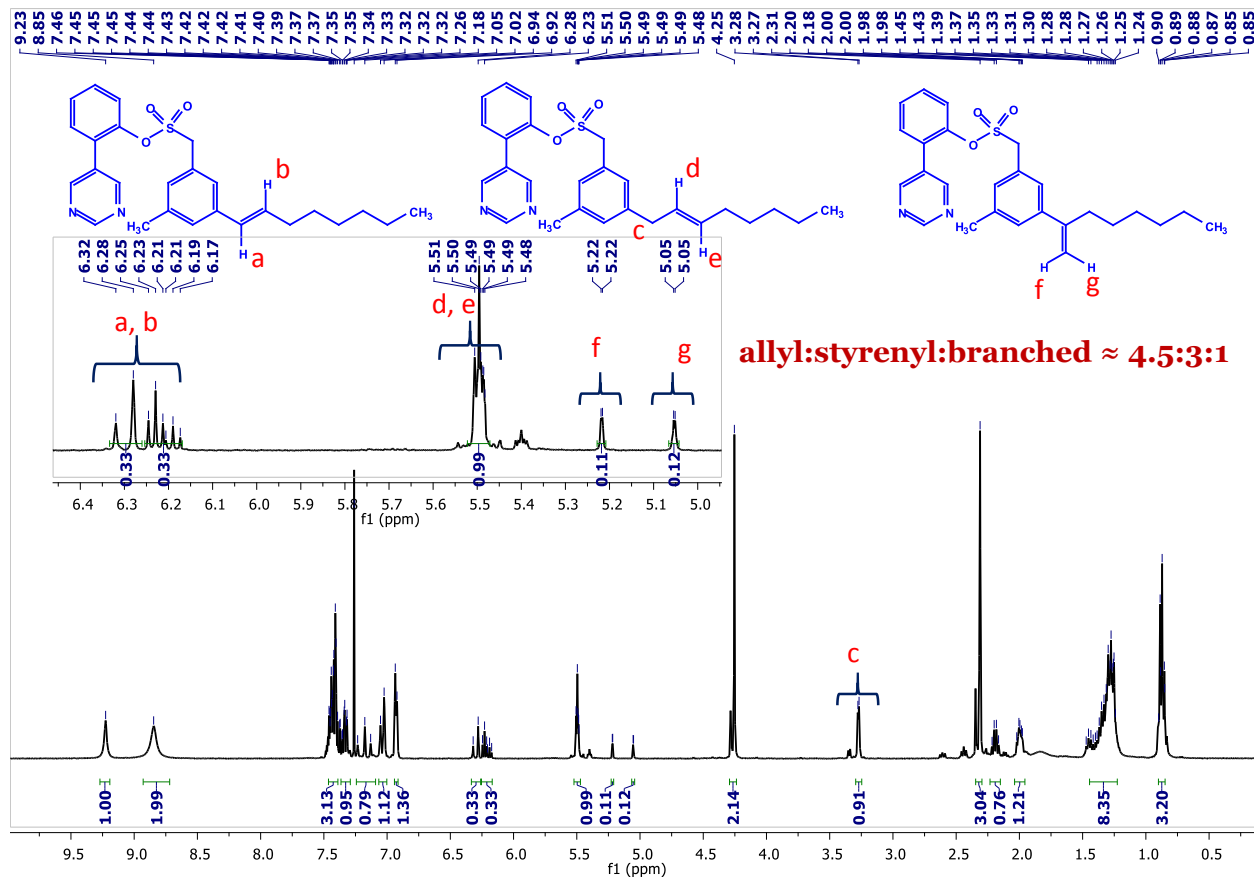


Figure S12. ¹H NMR of the product mixture from the reaction of **1a** with 1-octene under optimized reaction conditions.

2.9. Computational Methods

Density functional theory (DFT) calculations were performed with *Gaussian 16* rev. A.03.¹ Geometry optimisations were carried out using recently developed global-hybrid meta-NGA (nonseparable gradient approximation) MN15 functional² with a mixed Karlsruhe-family basis set of triple- ζ valence def2-TZVPPD (where ‘D’ indicates diffuse basis functions) for Pd³ atom and def2-SVP^{4,5} for all other atoms (BS1). This functional was chosen as it performs much better than many other functionals in predicting transition metal reaction barrier heights.² Previously, Pd(II)-catalysed C-C bond formations have been studied using other functionals including meta-GGA TPSS and range-separated ω B97X-D functionals.^{6,7} MN15 has been shown to give better agreement in geometry predictions of both transition metal complex and organic molecules than many other functionals including ω B97X-D and TPSS.² Minima and transition structures on the potential energy surface (PES) were confirmed as such by harmonic frequency analysis, showing respectively zero and one imaginary frequency, at the same level of theory. Single point (SP) corrections were performed separately with either MN15 or ω B97X-D⁸ functional and def2-QZVPP⁴ basis set for all atoms. The SMD continuum solvation model⁹ was carried out to include the effect of acetonitrile solvent on the computed Gibbs energy profile. Gibbs energies were evaluated at 363.15 K, using a quasi-RRHO treatment of vibrational entropies.^{10,11} Vibrational entropies of frequencies below 100 cm⁻¹ were obtained according to a free rotor description, using a smooth damping function to interpolate between the two limiting descriptions. The free energies were further corrected using standard concentration of 1 mol/L, which were used in solvation calculations. SMD(acetonitrile)- ω B97X-D/def2-QZVPP//MN15/BS1 Gibbs energies were given with SMD(acetonitrile)-MN15/def2-QZVPP//MN15/BS1 Gibbs energies given in brackets throughout. All values are quoted in kcal mol⁻¹.

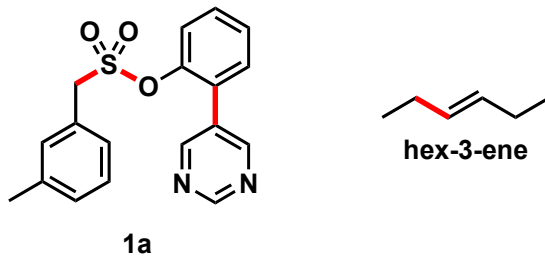
The .wfn files for NCIPILOT were generated at MN15/DGDZVP^{14,15} level of theory. Noncovalent interaction (NCI) indices calculated with NCIPILOT were visualised at gradient isosurface value of $s = 0.5$ au. These are coloured according to the sign of (λ_2) over the range of -0.1 (blue = attractive) to +0.1 (red = repulsive). All molecular structures and molecular orbitals were visualized using *PyMOL* software.¹⁶ Dihedral scans were done in gas phase using MN15/def2-SVP and the energies were taken without further corrections.

Geometries of all optimized structures (in .xyz format with their associated energy in Hartrees) are included in a separate folder named *structures_xyz* with an associated README file. All these data have been deposited with this Supporting Information and uploaded to zenodo.org (DOI: 10.5281/zenodo.2775841).

All Python scripts used for data analysis have been made available - <https://github.com/bobbypaton> - under a creative commons CC-BY license.

2.9.1 Conformational considerations for starting materials

The starting materials for computational modelling, sulfonyl arene, **1a**, and *trans*-hex-3-ene, were first conformationally sampled. The possible rotamers for sulfonyl arene, **1a**, were generated by systematically varying a combination of key dihedral angles shown in red (Scheme S1) and optimising the structures. The crystal structure of *trans*-hex-3-ene was obtained as a starting point for structure optimisation; additional rotamers were generated by varying the given dihedral angle in red (Scheme S1) and doing structural optimisations. The lowest energy conformers for each starting material were used for subsequent calculations.



Scheme S1. Rotamers were generated by varying the dihedral angles in red in conformational sampling of the most stable conformer used for reaction modelling.

2.9.2 C–H activation in the presence of ligand

The amino acid ligand, *N*-Ac-norleucine, lowered the C–H activation barrier by forming a 5-membered palladacycle as shown in the main text (**ts-1'** at 20.0^\ddagger (20.8^\ddagger) kcal mol $^{-1}$). Other possible arrangements of this ligand were found to have higher activation barriers than **ts-1'** (Figure S13).

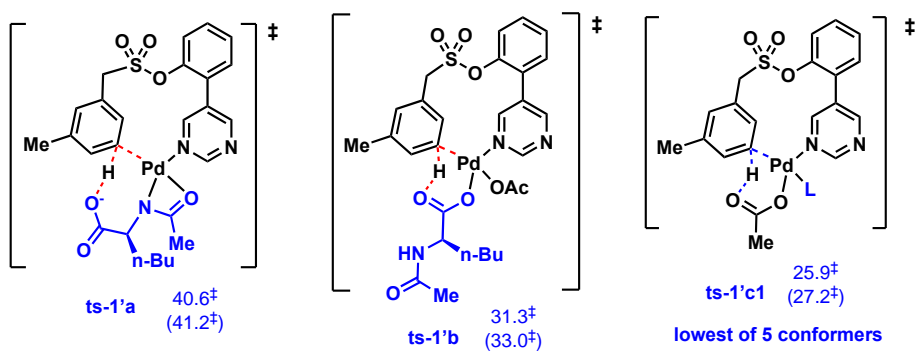


Figure S13. Possible arrangements of ligand for C–H activation step. Gibbs energies are given in kcal mol^{-1} .

2.9.3 Exact identity of the ligand in 1,2-migratory insertion TDTs

The intermediate after MPAA ligand-assisted C–H activation (**int-2'**) has the resulting ligand in imidic acid form. The subsequent 1,2-migratory insertion TS leading from here (**ts-3'a** at 41.7 kcal mol^{-1} , Figure S14) has a much higher barrier than its tautomeric form (**ts-3'b** at 27.1 kcal mol^{-1} , Figure S14). The coordination by acetate (**ts-3** at 23.2 kcal mol^{-1} , Figure S14) has the lowest barrier amongst these three possibilities. We anticipated that **ts-3** and **ts-3'b** would be rather close in energy, since they both coordinate to Pd-centre in a monodentate fashion (Figure S14), where the Pd–N interactions would dominate over other possible non-covalent interactions (NCIs) in the side chains. Although the amino acid side chain could provide better NCIs than the methyl group in acetate, it could also give rise to potentially more steric hinderance.

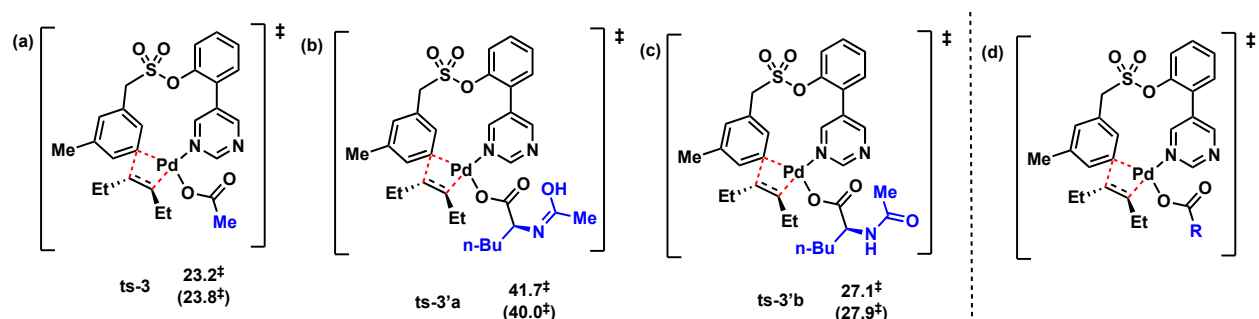


Figure S14. TDTs with either acetate (a) or amino acid in tautomeric forms (b and c) as the monodentate ligand. These can be thought of having the structure in (d) where the R-groups vary. Gibbs energies are given in kcal mol^{-1} .

In the computational study of similar systems where amino acid ligands were used for the C–H activation step, the amino acid (a.a.) was retained as a monodentate ligand for all subsequent steps.^{17,18} We envisioned that the acetate ligand and the a.a. ligand would have similar effects in 1,2-migratory insertion step and replacing the a.a. ligand with acetate would not affect the energy profile too much (Note that the main role of the a.a. ligand is in the C–H activation step). Conformational searches were thus performed for the 1,2-migratory insertion step above with either acetate or amino acid as the monodentate coordinating ligand. A total of 6 TSs were found for acetate ligand and 11 TSs for the a.a. ligand (these structures are given in folder *3_ligand_identity_in_TDTS* accompanying this ESI). All these are higher than C–H activation barrier, as expected since this step was overall rate-determining and C–H activation is reversible as measured by kinetic isotopic effect experimentally. Although the lowest barrier TSs were those with the a.a. ligand, these are really close in barrier to those of the lowest TS with acetate ligand (within 2 kcal mol⁻¹). For modelling purposes, it is sufficient to use acetate instead of the full a.a. ligand since the conclusion of the mechanism will remain the same.

2.9.4 Relative stabilities of **int-5** and **int-7** and β -hydride elimination TSs

We found, via intrinsic reaction coordinates (IRC) analyses, that **int-5** eventually lead to the product formation via direct β -hydride elimination (**ts-5**, Figure 5 main text) forming a metal-bonded Pd(II) hydride, whereas **int-7** underwent acetate-assisted β -hydride elimination (**ts-7**) with much lower activation barrier. **Int-7** was much more stable than **int-5** since in the latter, the acetate group was near the 14-membered palladacycle ring, giving rise to unfavourable interactions with the arene, as shown in the NCI plot (circled in green) in Figure S15. Alternative TSs for β -hydride elimination following each of these intermediates were given in Figure S16. Note that **ts-7'**, having the Pd-coordinating acetate-O atom forming 3-membered ring in the TS is much less favoured than **ts-7**, which has the non-coordinating acetate-O atom forming 5-membered ring.

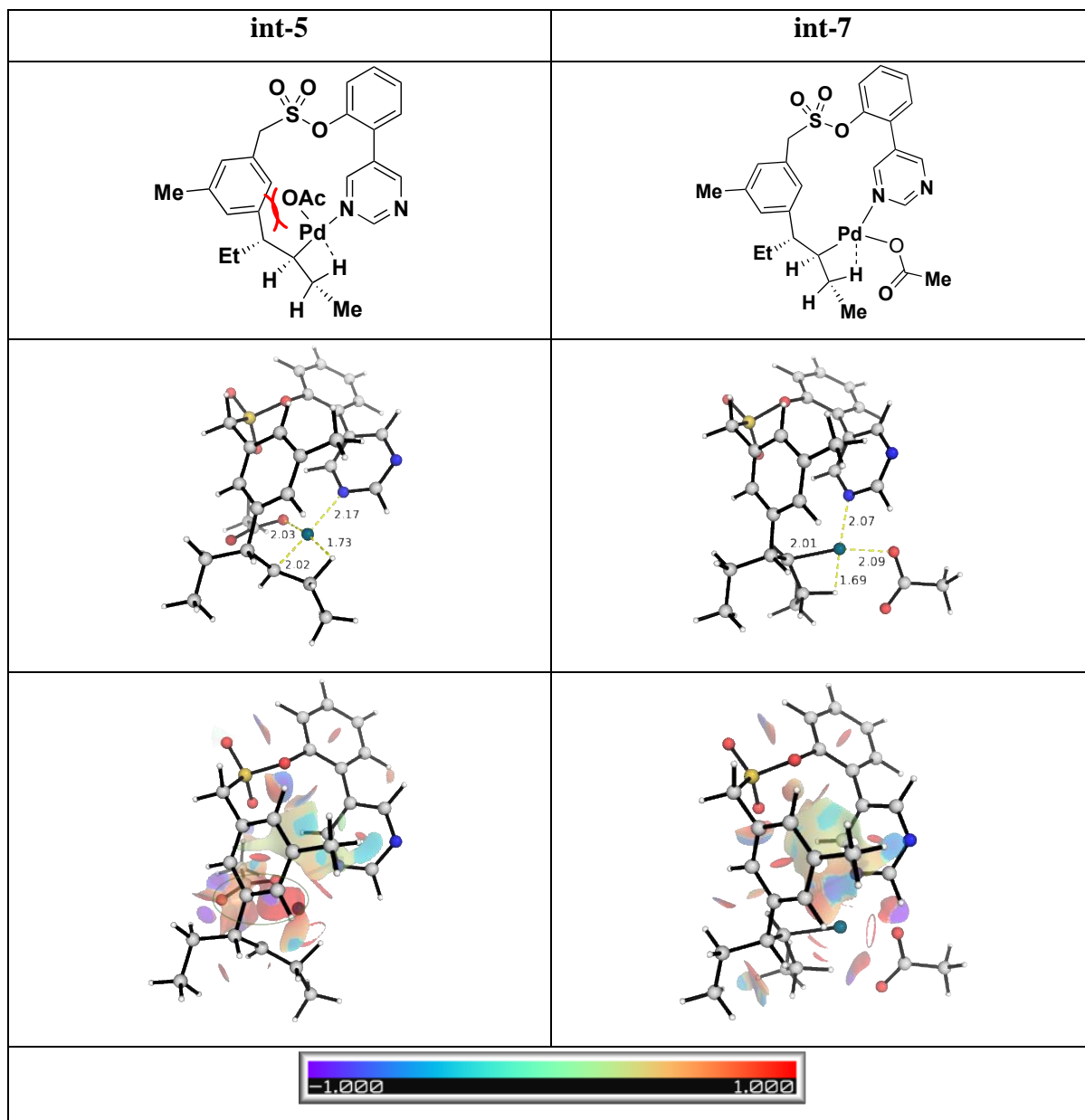


Figure S15. Relative stabilities of **int-5** and **int-7** and their NCI plots to indicate the sterics present.

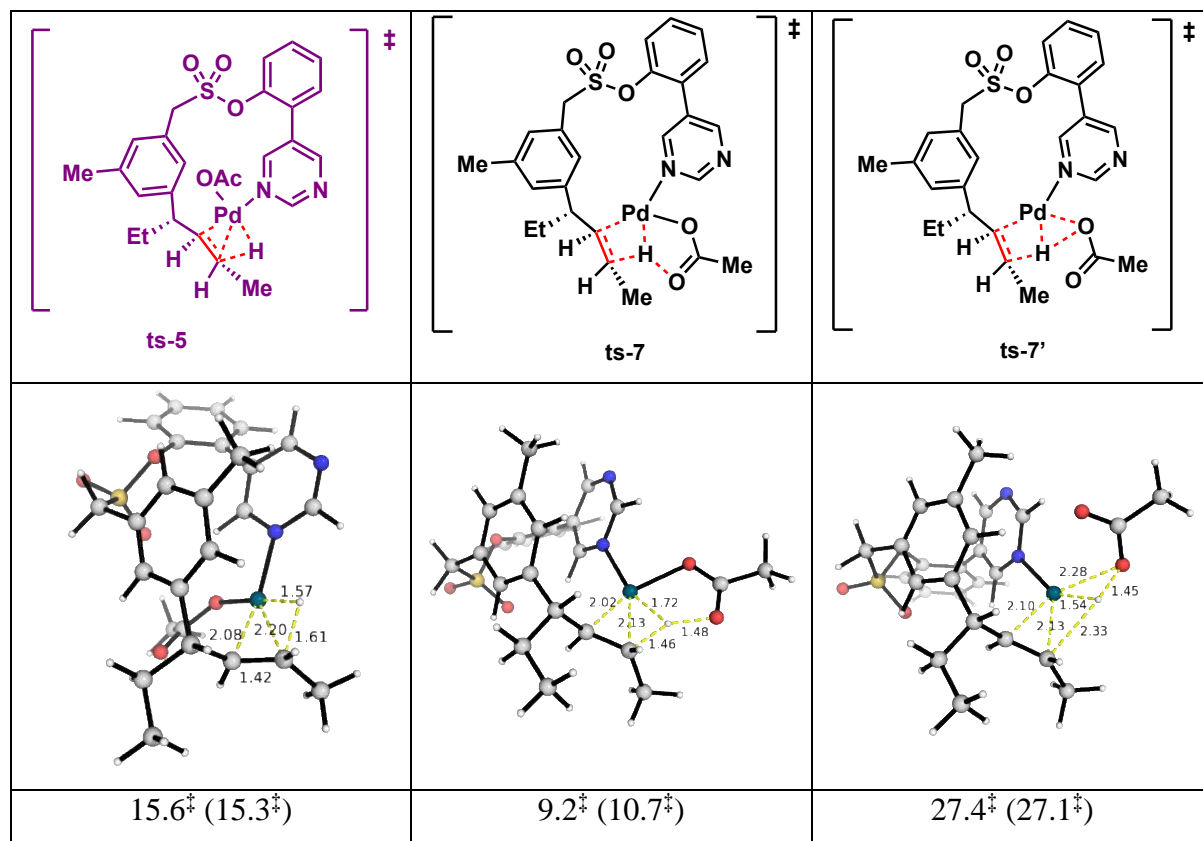
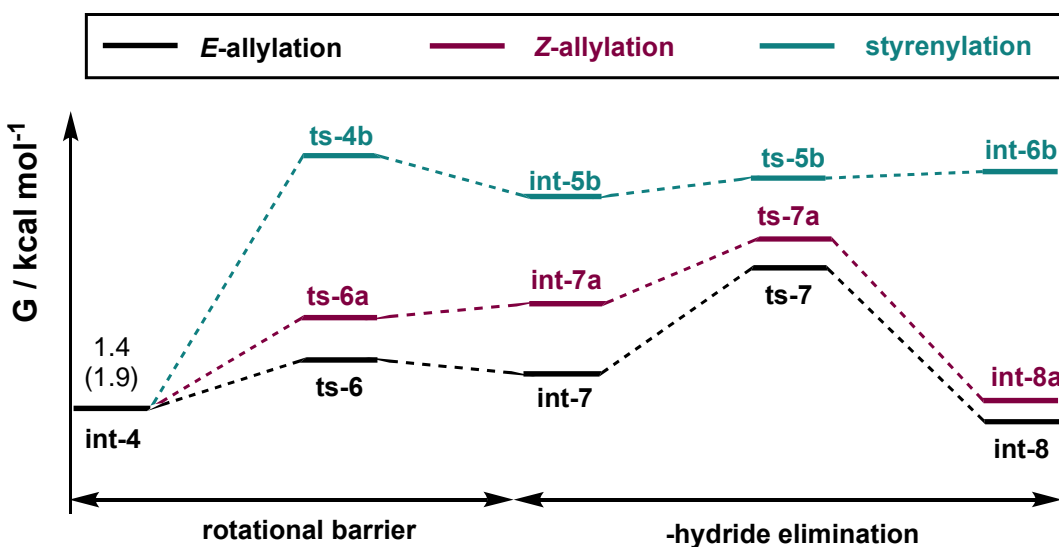


Figure S16. Alternative TSs for β -hydride elimination step to form the final product.

2.9.5 Product selectivity studies for *trans*-hexene substrate

The formations of both *E*- and *Z*-allylated products proceed via ligand-assisted β -hydride elimination whereas styrenylation proceeds via direct β -hydride elimination due to unfavourable arrangement of the acetate ligand. Styrenylation involves unfavourable palladacycle ring strain such that its direct β -hydride elimination proceeds via the displacement of the directing group pyrimidinyl-N atom by the acetate ligand that subsequently binds via bidentate mode (**ts-5b**, 19.2 kcal mol⁻¹) rather than via the intact palladacycle with the acetate ligand bound in a monodentate fashion (**ts-5b-c2**) (Figure S17). As a result, to form the styrenyl product the rotational barrier became the overall regio-determining step and this required a very high barrier as the palladacycle experienced huge strain when H_s was brought to interact agostically with Pd(II) centre (Figure S18(ii)).



Reaction product	direct β -H elimination				ligand-promoted β -H elimination				Overall barrier ^a
	ts-4x	int-5x	ts-5x	int-6x	ts-6x	int-7x	ts-7x	int-8x	
E-allyl (x=nil)	15.0 [‡] (14.9 [‡])	12.4 (12.7)	15.6 [‡] (15.3 [‡])	8.5 (8.4)	4.3 [‡] (4.7 [‡])	3.8 (6.0)	9.2 [‡] (10.7 [‡])	-0.4 (-0.3)	7.8 (8.8)
Z-allyl (x=a)	16.8 [‡] (16.5 [‡])	14.7 (15.1)	17.6 [‡] (17.6 [‡])	9.6 (10.0)	5.9 [‡] (6.4 [‡])	7.0 (8.9)	11.3 [‡] (12.7 [‡])	0.7 (0.6)	9.9 (10.8)
styrenyl (x=b)	21.0^{‡, b} (21.8[‡])	17.9 (18.7)	19.2 ^{‡, c} (19.2 [‡])	20.4 (18.3)	21.0^{‡, b} (21.8[‡])	3.9 (4.7)	48.5 [‡] (48.3 [‡])	10.5 (8.3)	19.6 (19.9)

^a We take the lowest value of the two. Both *E*- and *Z*-allylation preferred acetate-promoted β -hydride elimination, whereas styrenylation preferred direct β -hydride elimination via Pd(II) hydride complex.

^b Rotational TS for styrenylation are the same regardless of whether β -hydride elimination occurs directly or via ligand involvement. The prerequisite is to bring the H_s atom to interact agostically with Pd(II)-centre.

^c The TS where the directing group got displaced (**ts-5b**) has a lower activation barrier than the one where it remains coordinated (**ts-5b-c2**) since the former released the unfavourable strain in the palladacycle.

Table S10. Gibbs energies for selectivity studies for *trans*-hexene. TDTs values are given in bold.

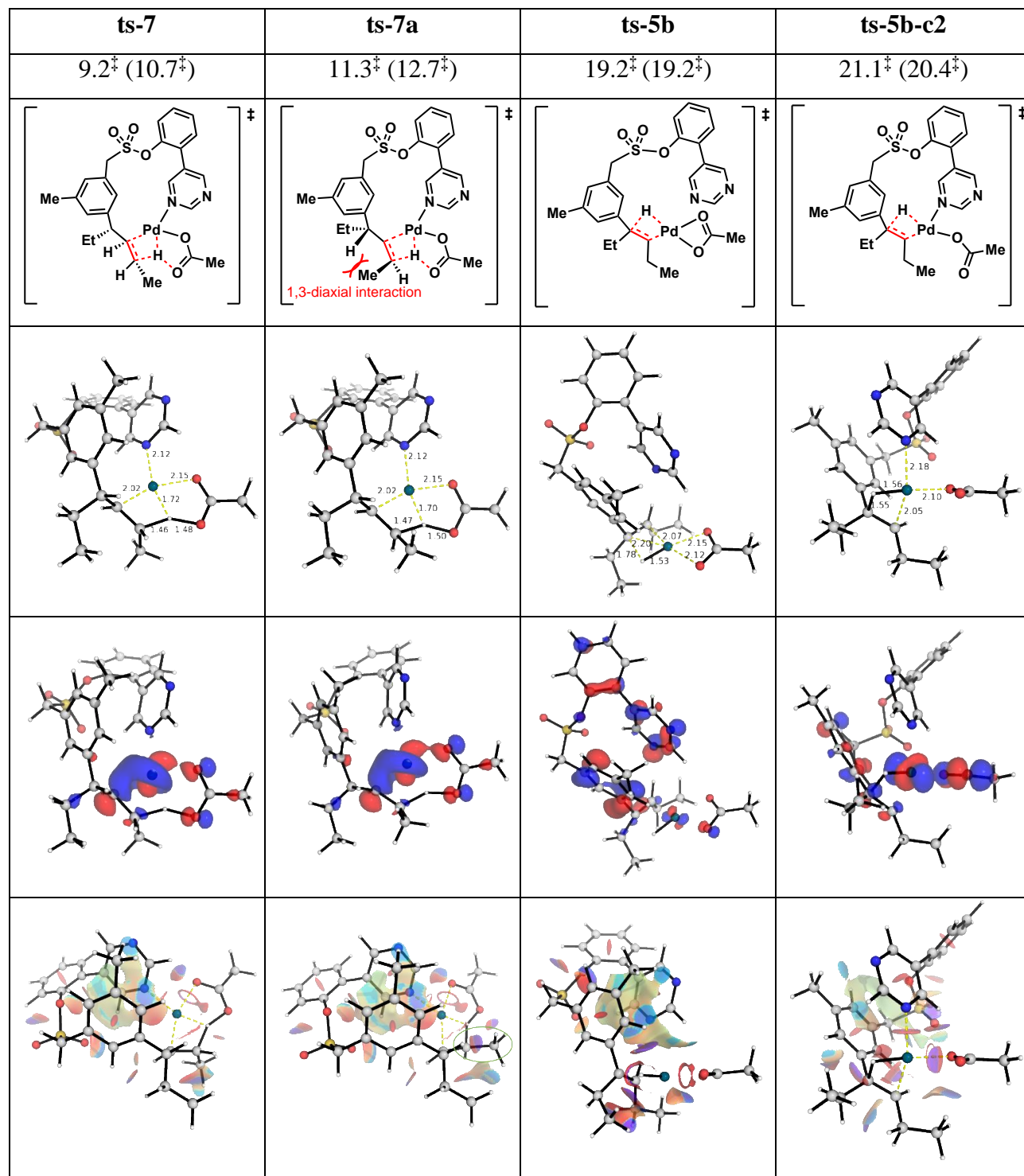


Figure S17. Product selectivity studies. The β -hydride elimination TSs for each product formation is given, with their HOMOs (isosurface value of 0.05) and NCI plots.

The dihedral angle scans allow us to compare the rotational barriers required to form allyl- vs styrenyl-product since the rotational barrier for the latter is regio-determining. We can see that styrenylation has a hugely disfavoured ring strain when the required H atom (H_s in Figure S18(ii)) is brought to interact agostically with Pd(II) centre – a prerequisite for the subsequent β -hydride elimination. Note that as discussed in the main text, the allylation involved steps that did not impose any strain on the 14-m palladacycle whereas the styrenylation severely distorted the palladacycle giving rise to hugely unfavourable ring strains.

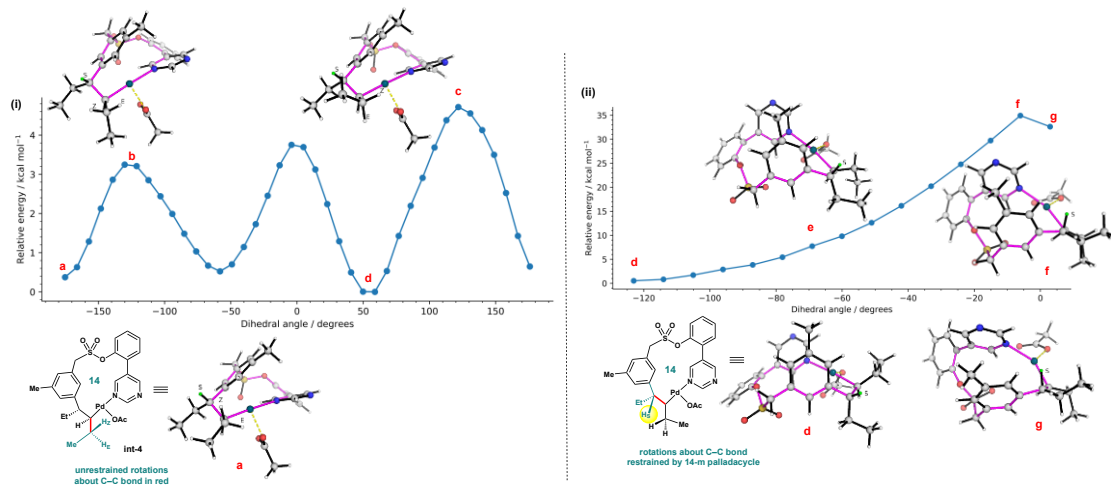
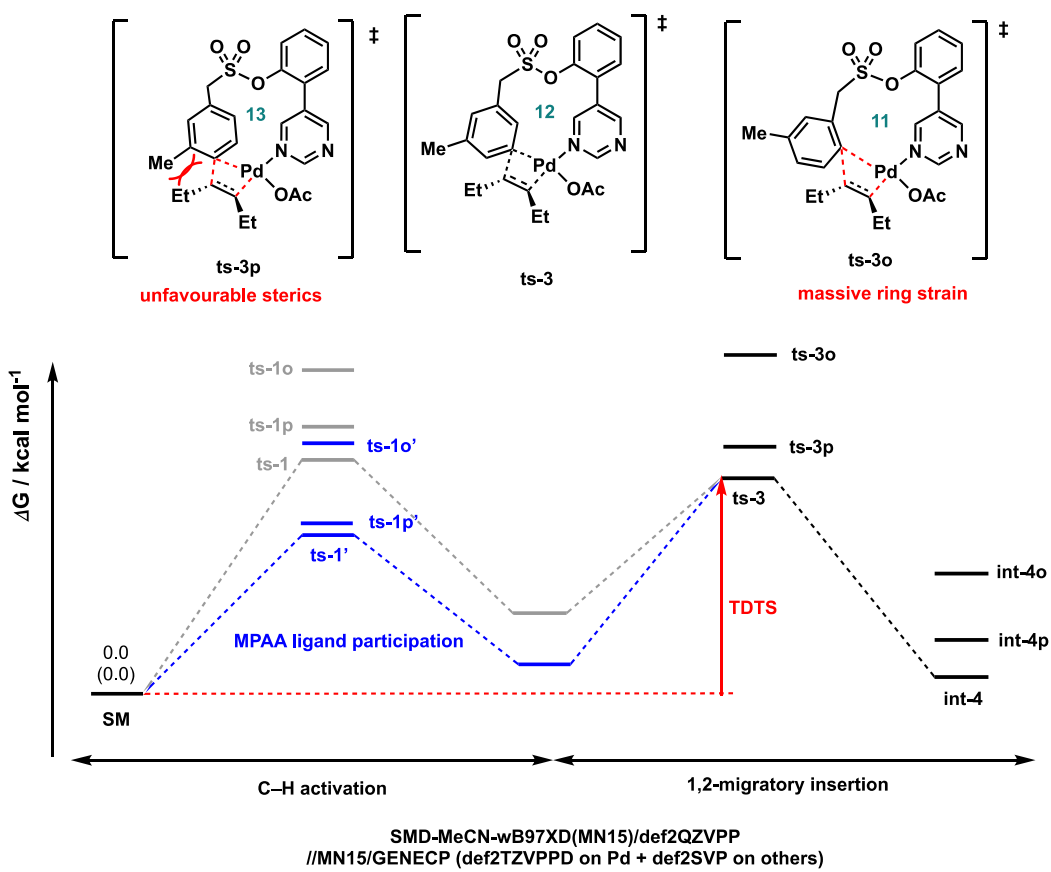


Figure S18. Dihedral angle scan (about C–C bond in red) for rotational barrier for the formation of (i) *E*-/*Z*-allylated products and (ii) styrenyl product for *trans*-hexene substrate. Note the different energy scales used. In (ii), note the position of styrenyl proton (H_s , labelled *S* in green), which is restrained in a position away from Pd(II)-centre by the conformationally rigid ring (outlined in purple).

2.9.6 Arene site-selectivity (HOMO, NCI plots and isodesmic studies)

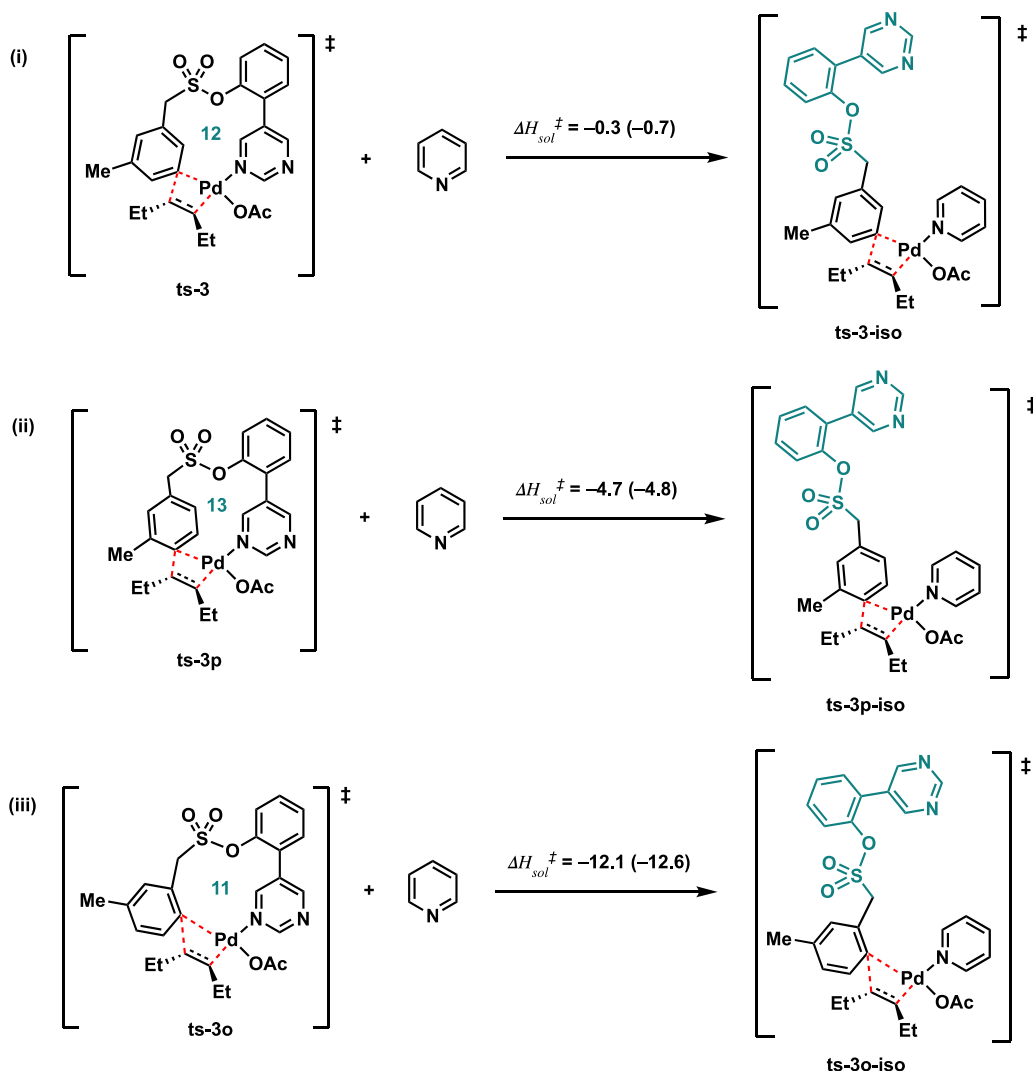
The *ortho-/para*-positions on the arene for potential activation were compared to *meta*-activation. The C–H activation and 1,2-migratory insertion steps were studied. The comparative energies for the key steps were given in Table S11. For the turnover frequency determining step, *para*-insertion (**ts-3p**) was 3.9 kcal mol⁻¹ higher in activation barrier than *meta*-insertion (**ts-3**), translating to 1 in 222 selectivity; *ortho*-insertion (**ts-3o**) was 12.7 kcal mol⁻¹ higher than ts-3, making *ortho*-insertion uncompetitive (1 in 40 million). These agreed well with observed selectivities which can be traced to unfavorable sterics involved in *ortho*- and *para*-addition (Figure S19).



Allylation site	ts-1x	ts-1x'	ts-3x	int-4x
<i>meta-</i> (x=nil)	26.7 [‡] (28.2 [‡])	20.0 [‡] (20.8 [‡])	23.2[‡] (23.8[‡])	1.4 (1.9)
<i>ortho-</i> (x=o)	35.8 [‡] (34.9 [‡])	28.7 [‡] (29.2 [‡])	37.0[‡] (35.5[‡])	19.2 (18.2)
<i>para-</i> (x=p)	28.6 [‡] (28.6 [‡])	20.5 [‡] (20.0 [‡])	28.2[‡] (26.7[‡])	8.4 (8.2)

Table S11| Arene site-selectivity studies. MPAA ligands lowered C–H activation in all cases such that 1,2- migratory insertion (ts-3x) becomes the TDTS whose barriers are given in bold.

In addition to the stereoelectronic effects associated with arene site selectivity, the ring strain energies in these TSs were calculated from the reaction enthalpy of the isodesmic reaction^{19,20} shown in Scheme S2. Specifically, a hypothetical pyridine ligand was used for TS searches to release the ring strain where the directing group (DG) got uncoordinated. The starting conformation for the DG (highlighted in green, Scheme S2) in all 3 cases was made the same in a linear form for subsequent TS searches. The enthalpies of the reactions were further corrected with SMD solvation model: $\Delta H_{sol}^{\ddagger} = \Delta H_{gas}^{\ddagger} - \Delta E_{gas}^{\ddagger} + \Delta E_{sol}^{\ddagger}$. The calculations showed that the *meta*-insertion TDTS had the lowest ring strain at 0.3 kcal mol⁻¹, followed by *para*-insertion TDTS, with 4.7 kcal mol⁻¹; *ortho*-insertion TDTS had the largest ring strain at 12.1 kcal mol⁻¹. These values are in excellent quantitative agreement with the selectivity studies (Table S11, where *para*-TDTS is about 4 kcal mol⁻¹ and *ortho*-TDTS is about 12 kcal mol⁻¹ higher than *meta*-TDTS).



Scheme S2. Computed ring strain energies by study of isodesmic reaction where a hypothetical pyridine ligand is involved. Enthalpies quoted are corrected with solvent effect and in kcal mol^{-1} .

The HOMOs for insertion TDTSSs for *meta-/ortho-/para*-activation were plotted in Figure S19 Top. These show similar electron distributions, suggesting that electronic factors are less important in the selectivity of arene site activation. NCI plots (Figure S19 Bottom) show that **ts-3p** was sterically disfavoured when the methyl-group on the ring came close to the alkene being added whereas in **ts-3o**, the excessive ring strain made this TS highly strained (the directing group got twisted out of shape), giving rise to unfavourably high activation barrier. The possibility of addition to the other *ortho*-site would bring the methyl-group into close proximity of the alkene being added, further increasing the activation strain and was thus not considered.

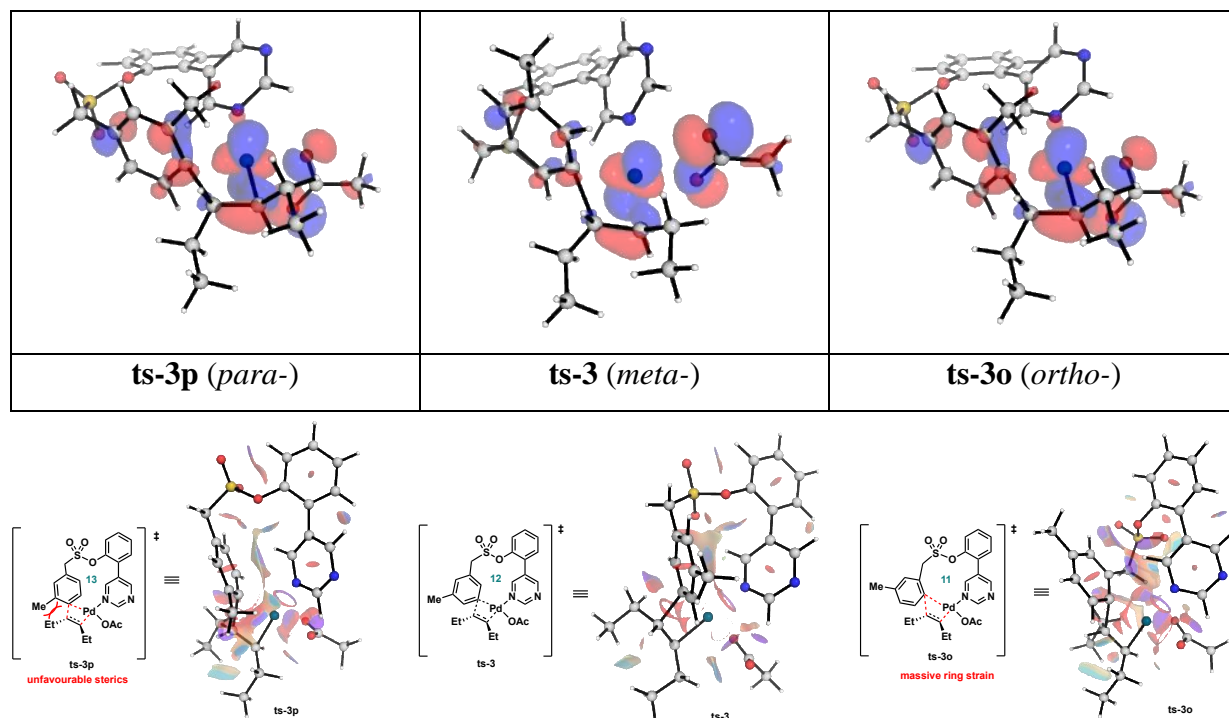
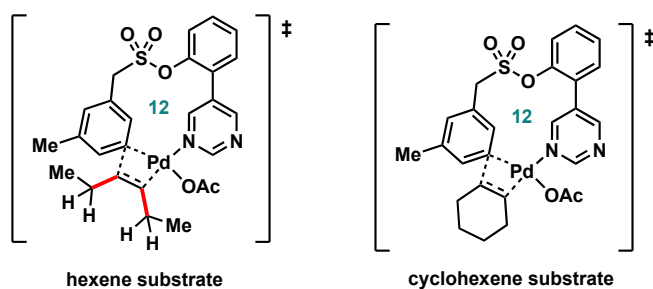


Figure S19. Insertion TSs from *para*-, *meta*- and *ortho*-activated complexes. Top: HOMOs at an isovalue of 0.04. Bottom: NCI plots.

2.9.7 General conformational sampling of TDTSSs (1,2-migratory insertion step)

Once a TS was found, the structure was used as starting guesses for searching TS conformers. The palladacycle ring was frozen and rotamers along C–C bonds in red (Scheme S3) were generated for TS conformational searches. Altogether, 9 TSs were found for each orientation of alkene (18 TSs for each of *trans*-hexene and *cis*-hexene) and 4 TSs were found for each orientation of cyclohexene (8 TSs altogether). The optimized TS structures and their relative energy barriers with respect to the lowest barrier TS for *trans*-hexene substrate ($\Delta\Delta G^\ddagger$) were shown in Figure S20.



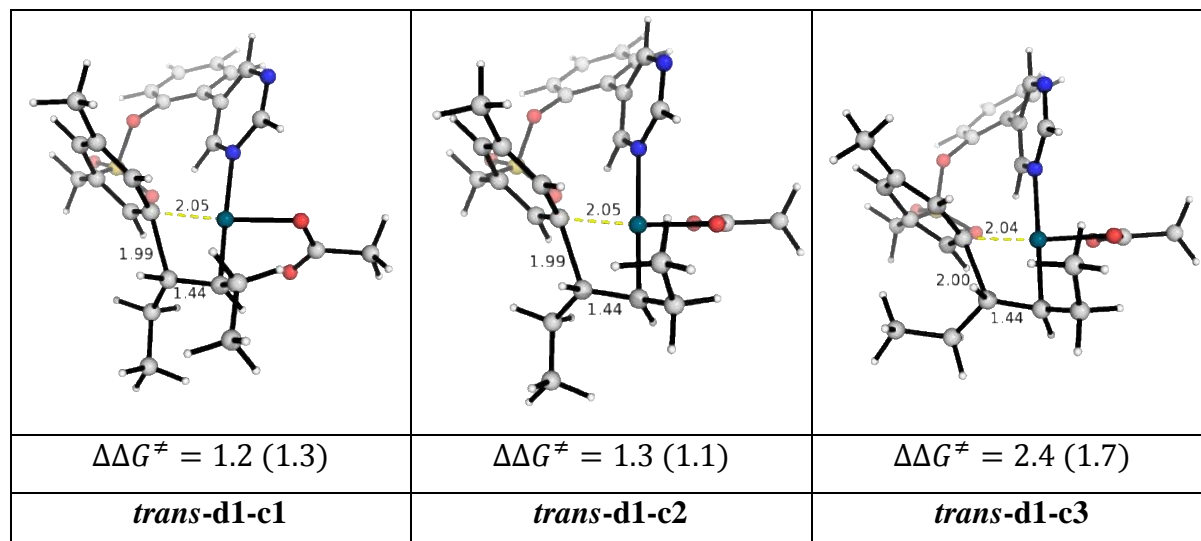
Scheme S4. Rotamers were generated by varying the dihedral angles in red in conformational sampling of the 1,2-migratory insertion TDTSSs for *trans*- and *cis*-hexene substrates; for cyclohexene substrate, the buckling of the half-chair in different orientations were considered.

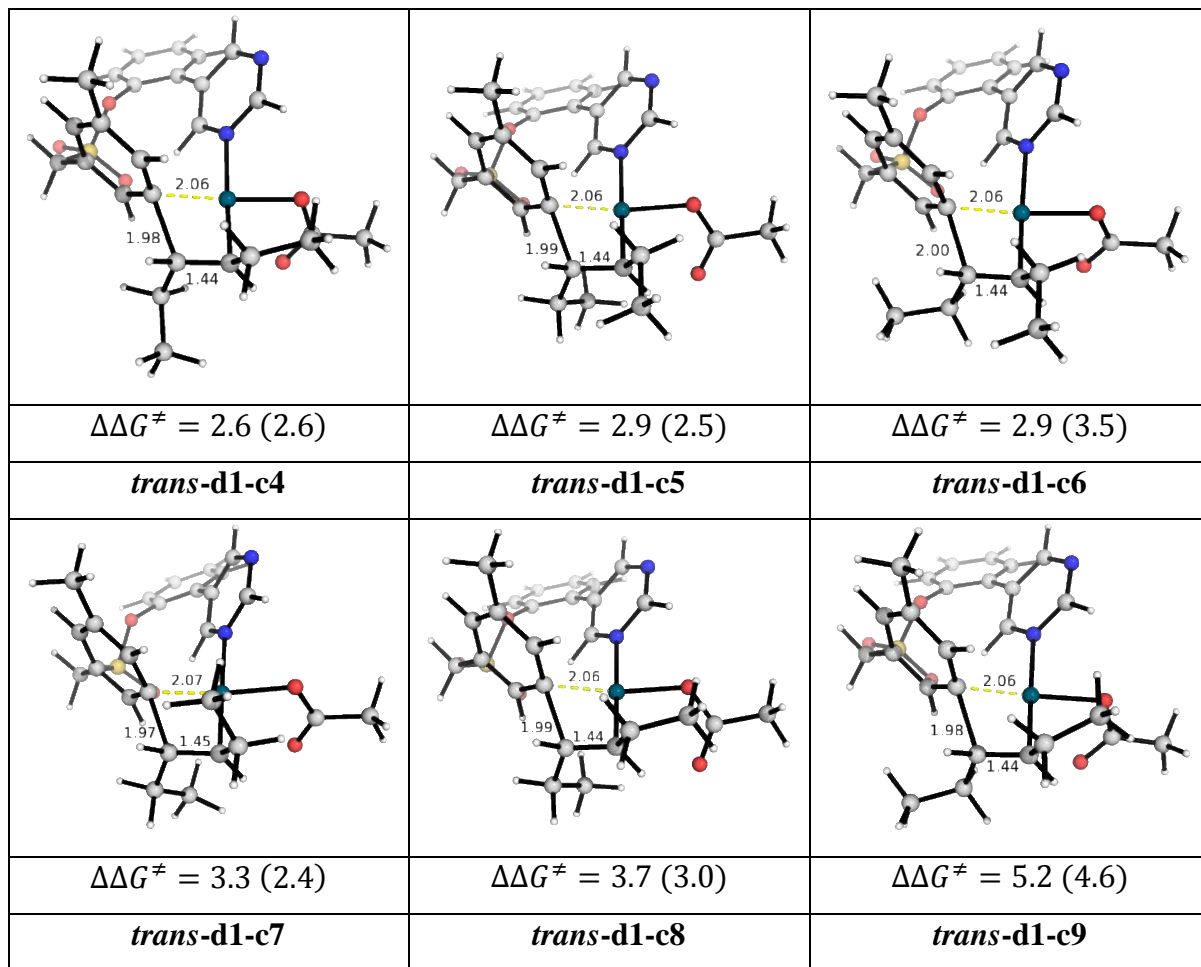
Boltzmann weighting and selectivity

All TDTSS conformers were used for Boltzmann weighting to give selectivity ratio. Standard procedures for Boltzmann weighting were applied (see, for example, Equation (2) of ref.²¹ and SI of ref.²²); specifically, the selectivity between two products A and B were calculated *via*

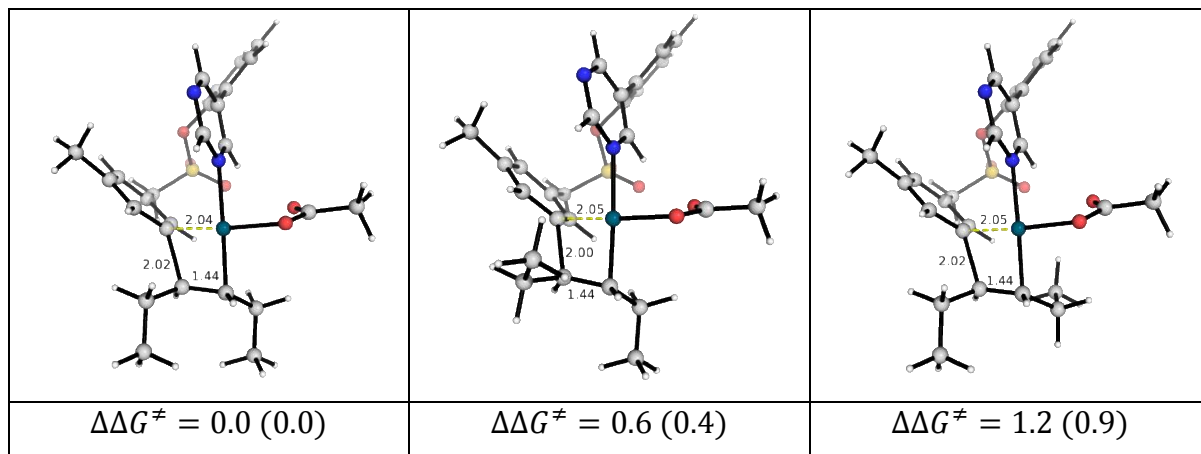
$$\frac{[A]}{[B]} = \frac{\sum_{i \in \text{all confs}, A}^N e^{-\Delta\Delta G_{0i,A}^\ddagger / RT}}{\sum_{j \in \text{all confs}, B}^N e^{-\Delta\Delta G_{0j,B}^\ddagger / RT}} \quad (1)$$

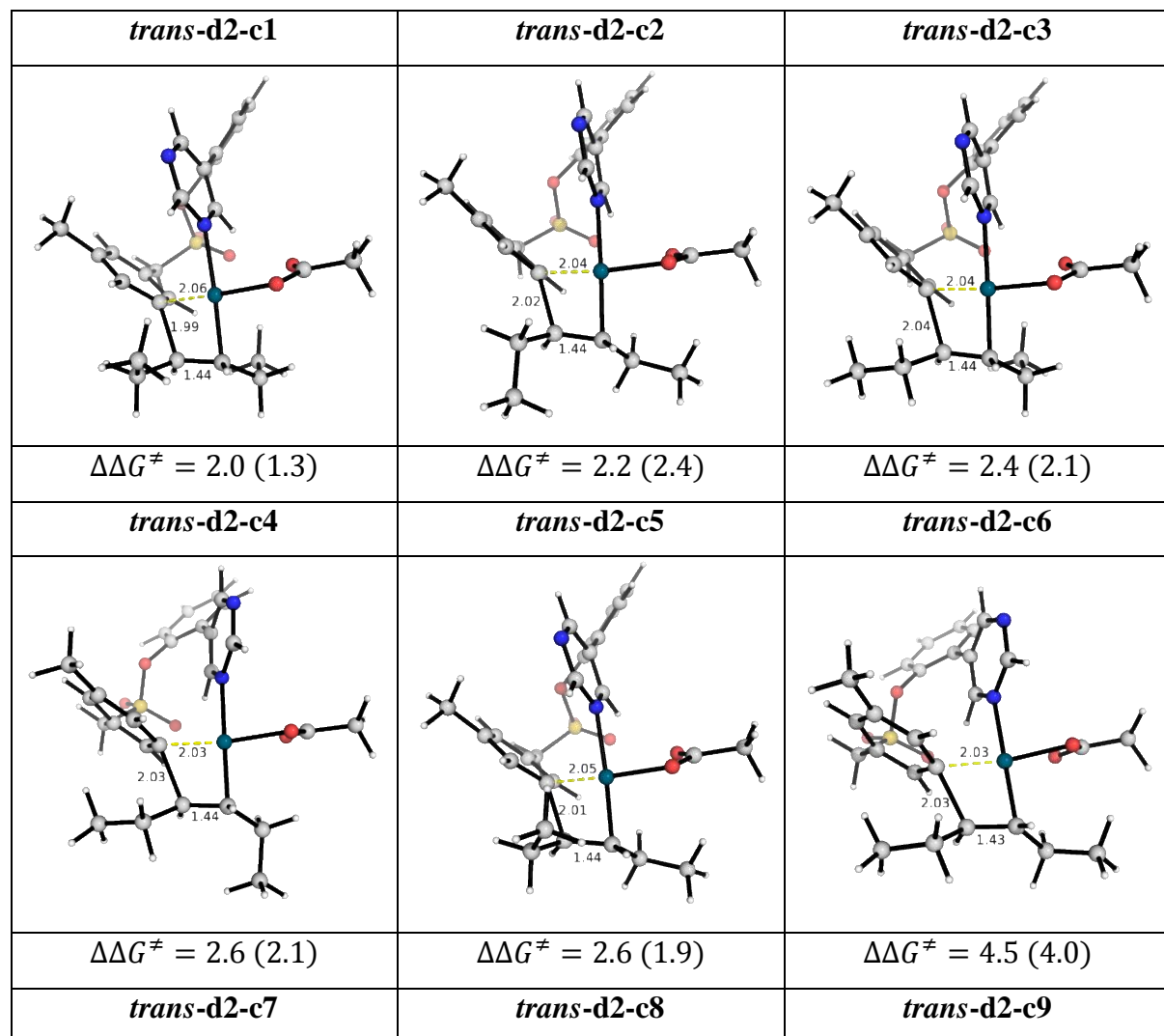
where $\Delta\Delta G_{0i,X}^\ddagger = \Delta G_{i,X}^\ddagger - \Delta G_{0,X}^\ddagger$ is the energy difference between the i^{th} conformer of product X ($X = A, B$) and the lowest energy conformer of all products, state 0.



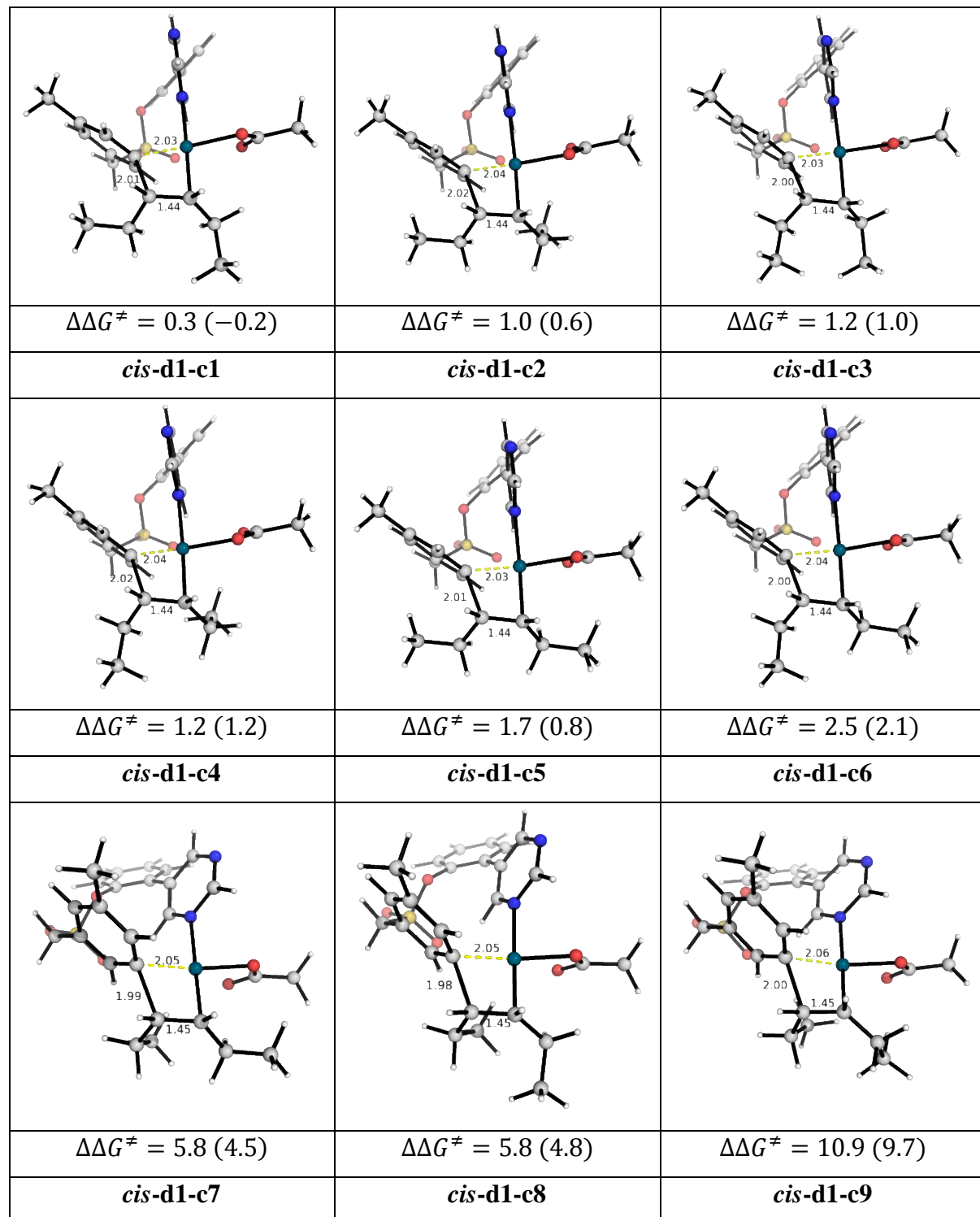


(a) Conformers for 1,2-migratory insertion TDTs for diastereomer 1 (d1) formation from *trans*-hexene.

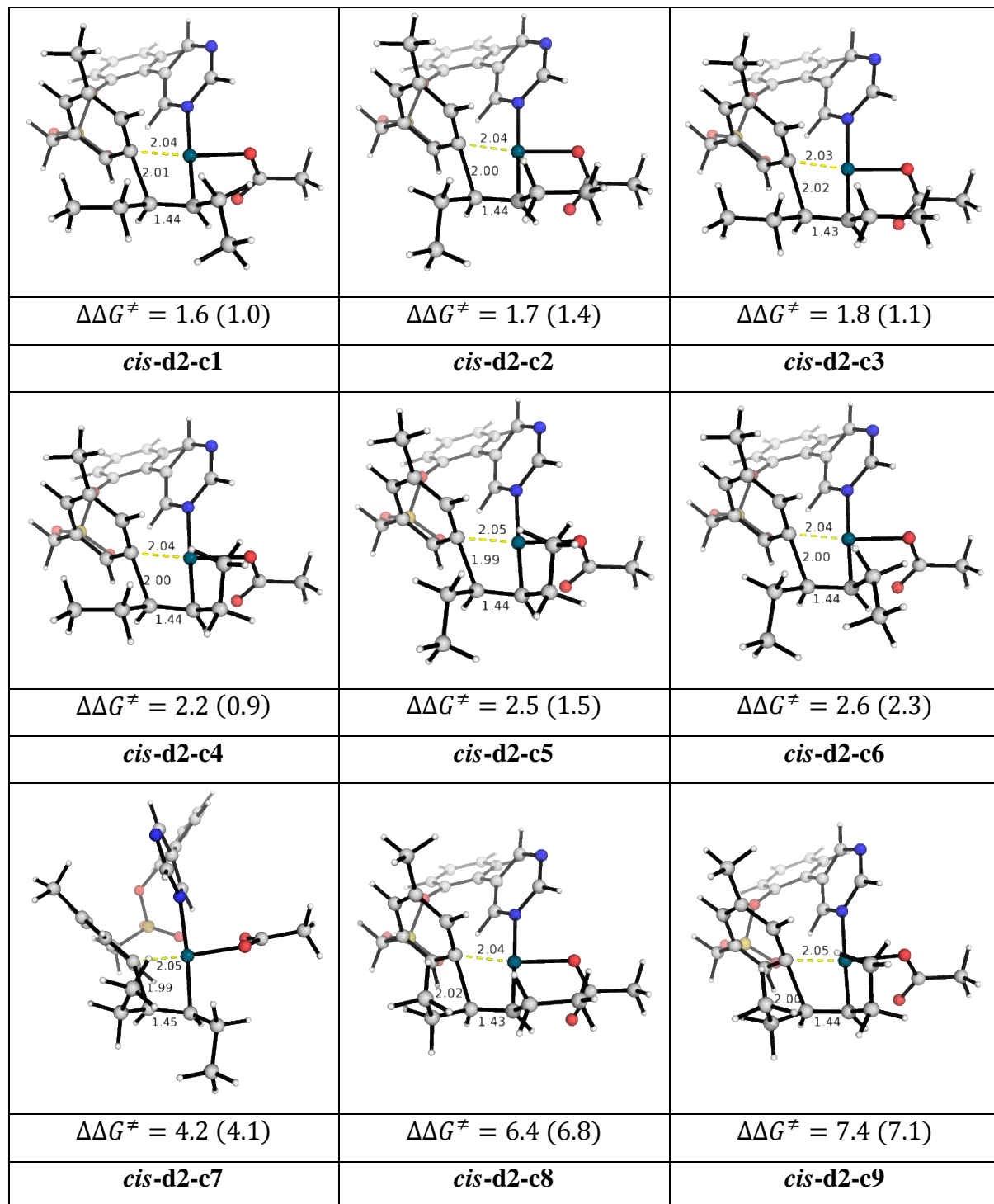




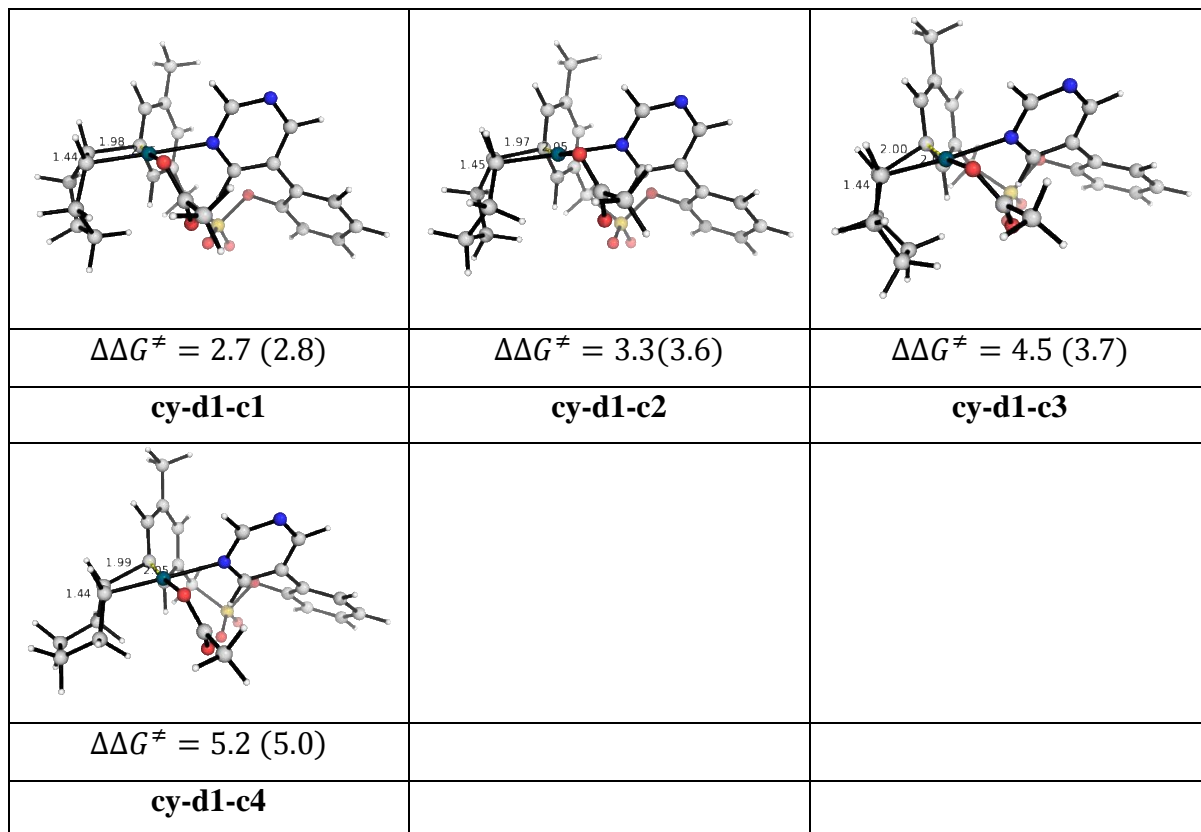
(b) Conformers for 1,2-migratory insertion TDTs for diastereomer 2 (d2) formation from *trans*-hexene.



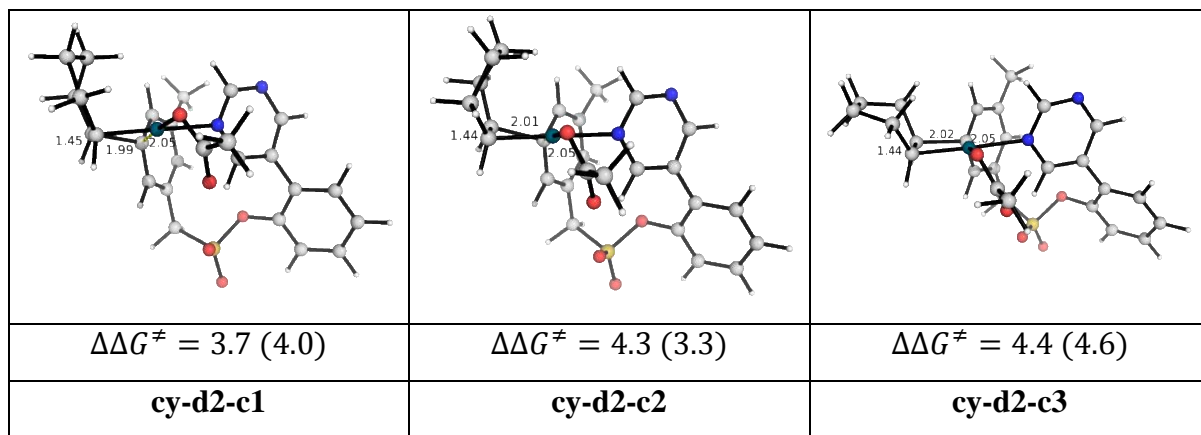
(c) Conformers for 1,2-migratory insertion TDTs for diastereomer 1 (d1) formation from *cis*-hexene.

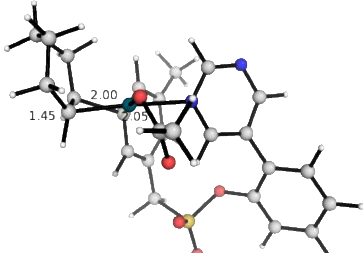


(d) Conformers for 1,2-migratory insertion TDTs for diastereomer 2 (d2) formation from *cis*-hexene.



(e) Conformers for 1,2-migratory insertion TDTs for diastereomer 1 (d1) formation from cyclohexene (cy).



		
$\Delta\Delta G^\ddagger = 4.4 \text{ (4.8)}$		
cy-d2-c4		

(f) Conformers for 1,2-migratory insertion TDTs for diastereomer 2 (d2) formation from cyclohexene (cy).

Figure S20. Optimized TS geometries for 1,2-migratory insertion TDTs step for *trans*-hexne (a and b), *cis*-hexene (c and d) and cyclohexene (e and f). All TSs were taken relative to the same minima (*trans*-d2-c1). Relative $\Delta\Delta G^\ddagger$ values are in kcal mol⁻¹. Bond lengths are given in Angstroms.

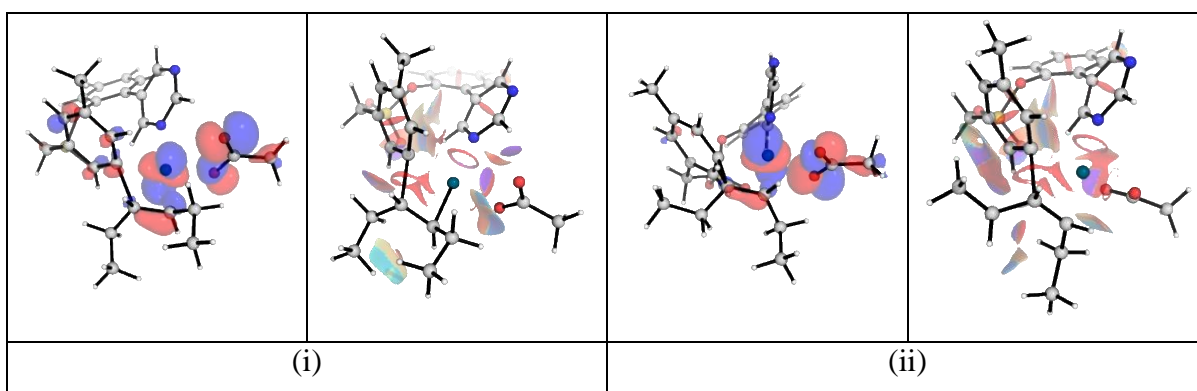
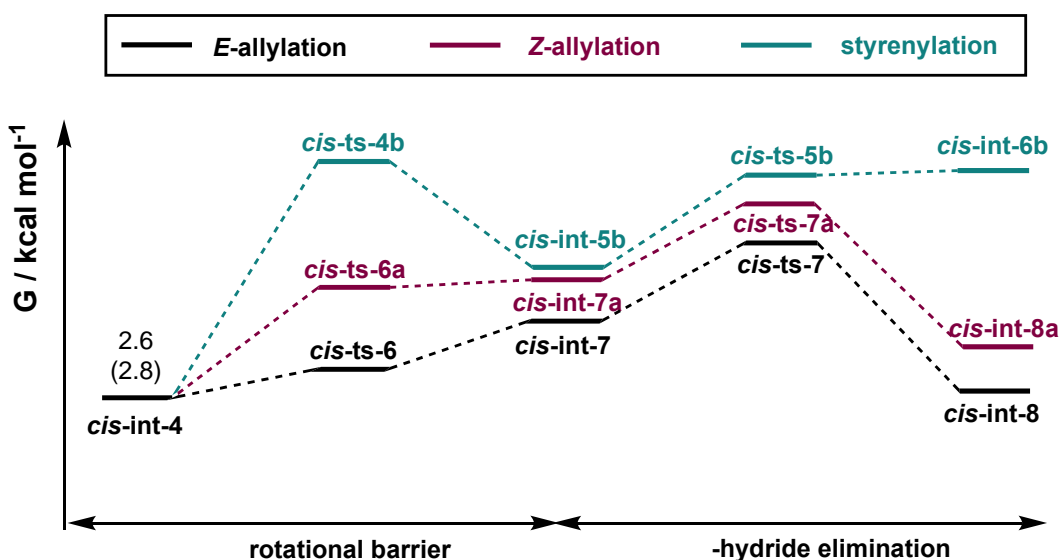


Figure S21. HOMO (isosurface value of 0.04) and NCI plots for the 1,2-migrator insertion TDTs lowest barrier conformer for (i) *trans*-hexene and (ii) *cis*-hexene. The comparisons show that stereoelectronics are rather similar, suggesting similar reactivities.

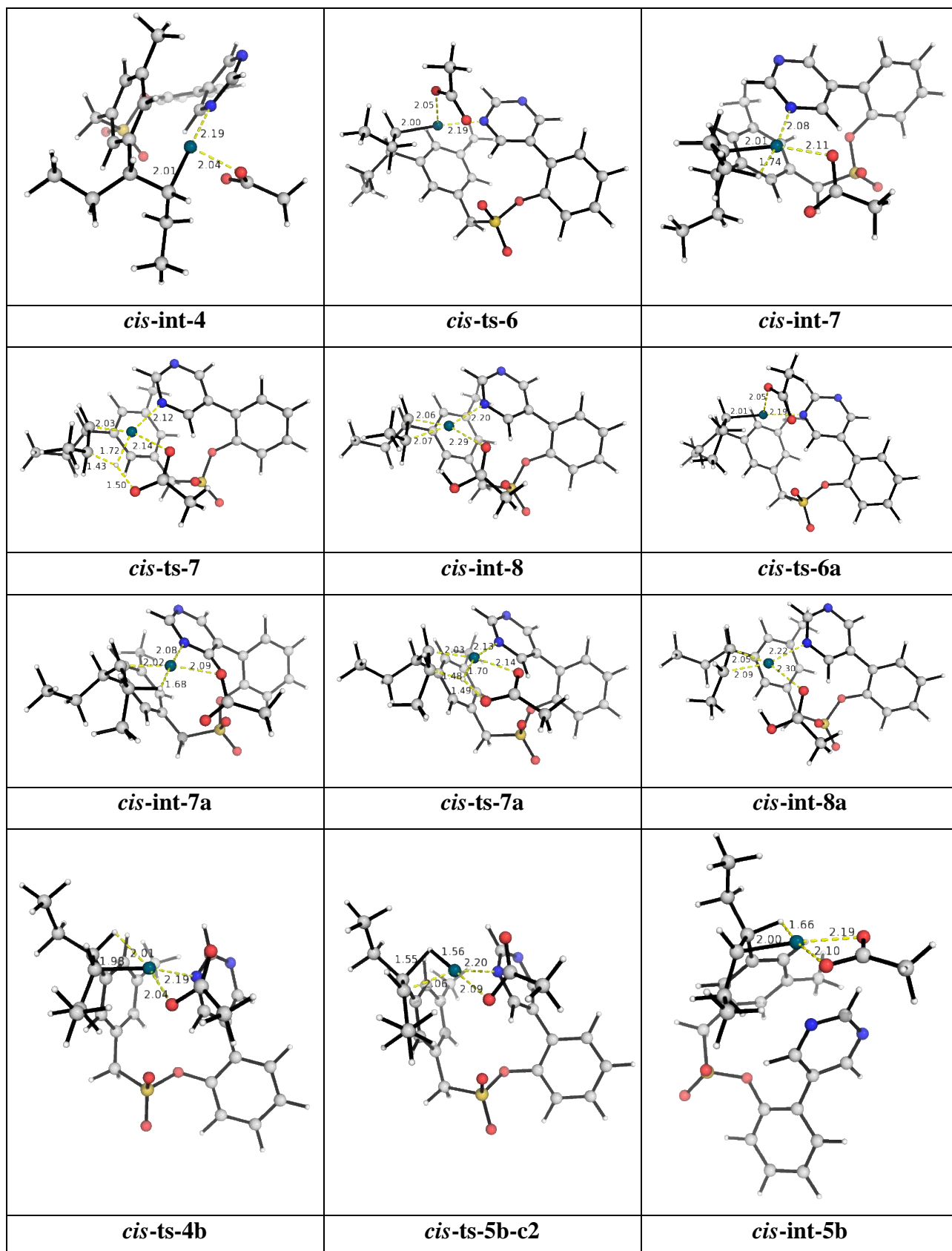
2.9.8 Product selectivity studies for *cis*-hexene substrate

Following from results using *trans*-hexene (section 2.9.5), the lowest pathways for *cis*-hexene product selectivity were studied and the key TS structures shown. Here again, for styrenylation, the TS where the DG got displaced (*cis*-ts-5b at 16.1^\ddagger (15.3^\ddagger) kcal mol $^{-1}$) has a lower activation barrier than the one where it remained coordinated (*cis*-ts-5b-c2 at 23.1^\ddagger (22.5^\ddagger) kcal mol $^{-1}$) since the former released the unfavourable strain in the palladacycle (Figure S22).



Reaction product	direct β -H elimination				ligand-promoted β -H elimination				Overall barrier
	<i>cis</i> -ts-4x	<i>cis</i> -int-5x	<i>cis</i> -ts-5x	<i>cis</i> -int-6x	<i>cis</i> -ts-6x	<i>cis</i> -int-7x	<i>cis</i> -ts-7x	<i>cis</i> -int-8x	
E-allyl (x=nil)	—	—	—	—	4.9^\ddagger (5.1^\ddagger)	10.8 (10.5)	13.8[‡] (14.9[‡])	3.5 (3.0)	11.2 (12.1)
Z-allyl (x=a)	—	—	—	—	10.7^\ddagger (11.4^\ddagger)	11.7 (13.3)	17.4[‡] (18.6[‡])	7.1 (6.4)	14.8 (15.8)
styrenyl (x=b)	20.8[‡] (22.2[‡])	11.7 (12.3)	16.1[‡] (15.3[‡])	17.1 (14.8)	—	—	—	—	18.2 (19.4)

Table S11. Gibbs energies for selectivity studies for *cis*-hexene. TDTs values are given in bold.



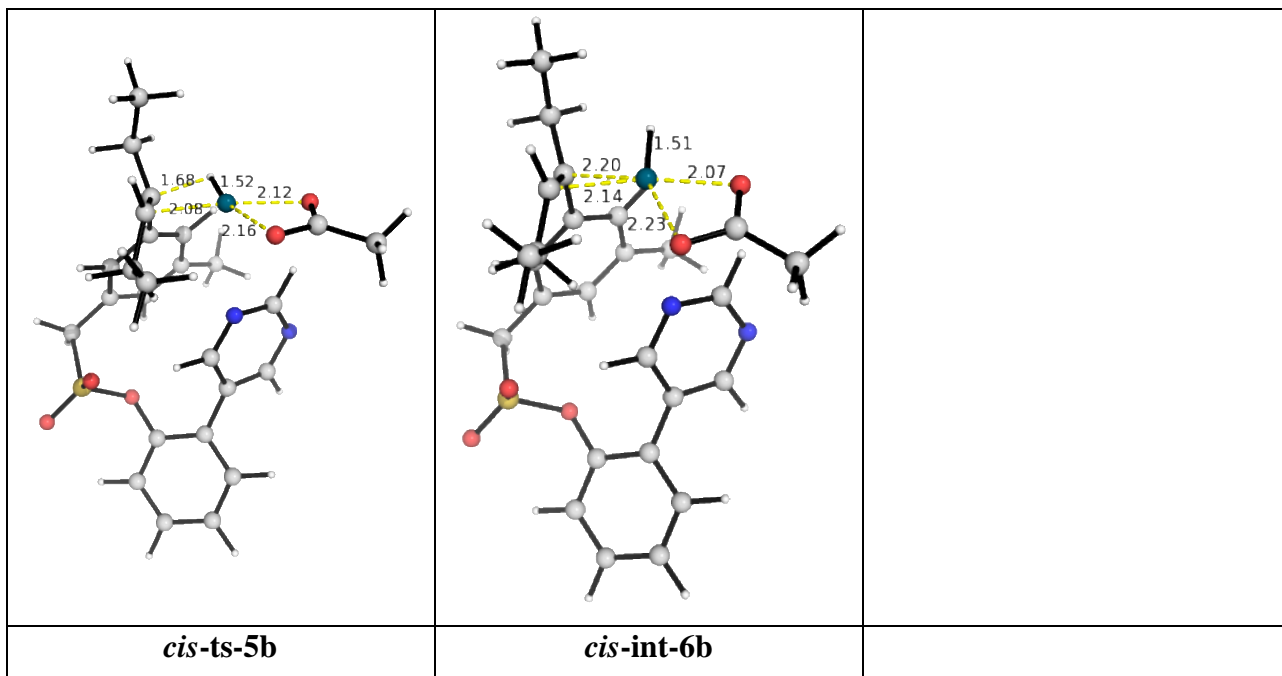


Figure S22. Optimised TS structures for selectivity studies using *cis*-hexene substrate.

HOMOs for ligand-assisted β -H elimination for both allylation using *cis*-hexene substrate (Figure S23) are similar to each other and similar to those for *trans*-hexene (Figure S17), where a σ^*_{CC} bond is broken and a π_{CC} bond is formed as the deprotonation occurred. The differences in the *E*-/*Z*-allylation stereoselectivity could arise due to the slightly less favourable NCIs in *Z*-allylation (Figure S23).

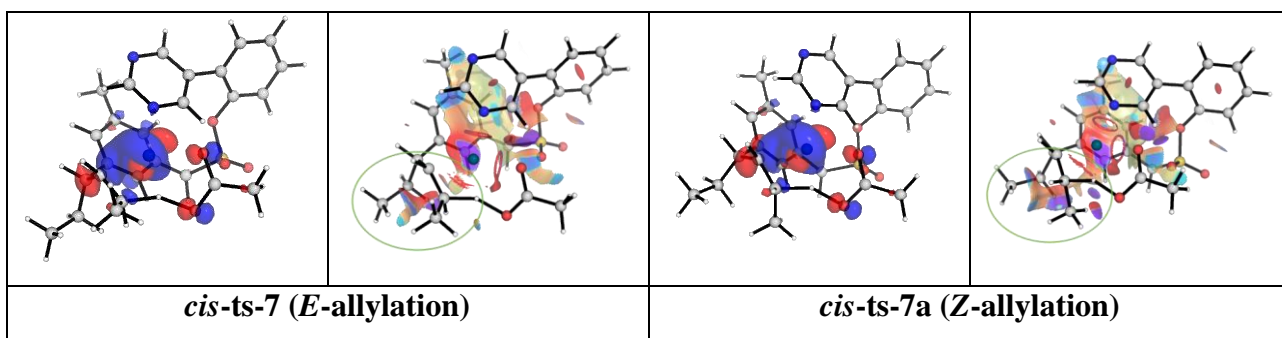


Figure S23. HOMOs (isosurface value 0.05) and NCI plots for *E*- vs *Z*-allylated product selectivity for *cis*-hexene substrate.

Although for allylation, the ligand-assisted β -H elimination is the r.d.s. for product selectivity, the rotational barrier to bring the H_s atom to interact agostically with Pd(II) centre before direct β -H elimination is the r.d.s. for styrenylation. A comparison between such rotations by the dihedral angle scans along key C–C bonds can be instructive (Figure S24).

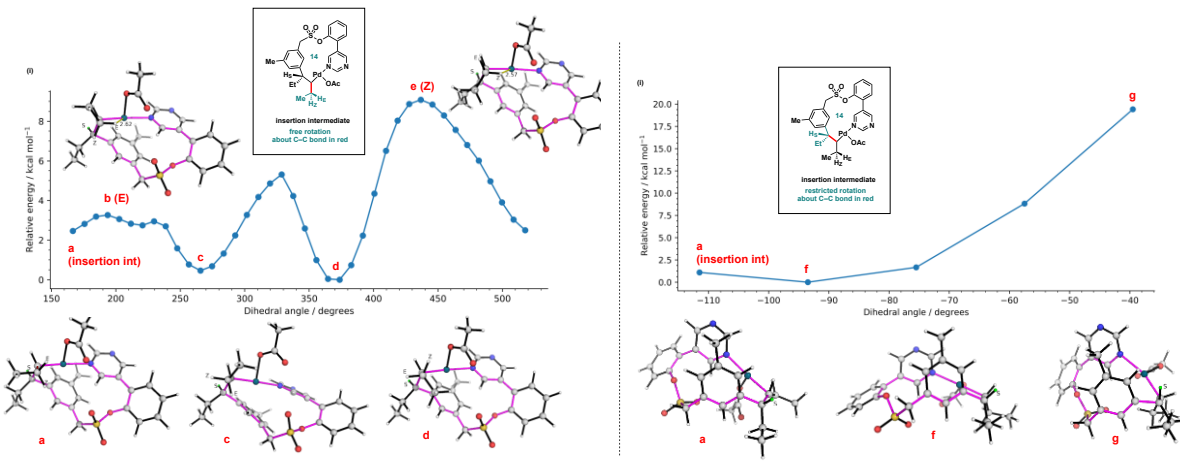


Figure S24. Dihedral angle scan (about C–C bond in red) for rotational barrier for the formation of (i) *E*-/*Z*-allylated products and (ii) styrenyl product for *cis*-hexene substrate. Note the different energy scales used. In (ii), the position of styrenyl proton (H_s , labelled *S* in green) is restrained away from Pd(II)-centre by the conformationally rigid ring (outlined in purple).

2.9.9 Product selectivity studies for cyclohexene substrate

Initial dihedral angle scans were performed about the key C–C bonds to locate rotational barriers bringing the H atom (for subsequent β -H elimination) to interact agostically with Pd(II)-centre (Figure S25). Only rotational barriers for *Z*-allylation could be located; both *E*-allylation and styrenylation had rotational barriers that were about 30 kcal mol⁻¹ higher than for *Z*-allylation; these arise due to unfavourable ring distortions imposed by the rigid cyclohexyl ring fused to the rigid palladacycle in the insertion intermediate. The overall Gibbs energy profile for cyclohexene substrate were shown in Figure S26. Given that the subsequent ligand-assisted β -H elimination for *Z*-allylation (**cy-ts-7a**) was 6.3 kcal mol⁻¹ higher than the rotational barrier (**cy-ts-6a**), we estimate

that the barriers for both *E*-allylation and styrenylation are at least ~20 kcal mol⁻¹ higher than *Z*-allylation (**cy-ts-7a**), thus being disfavoured by 1 in a trillion. Therefore, if at all, only *Z*-allylated product can be formed using cyclohexene substrate.

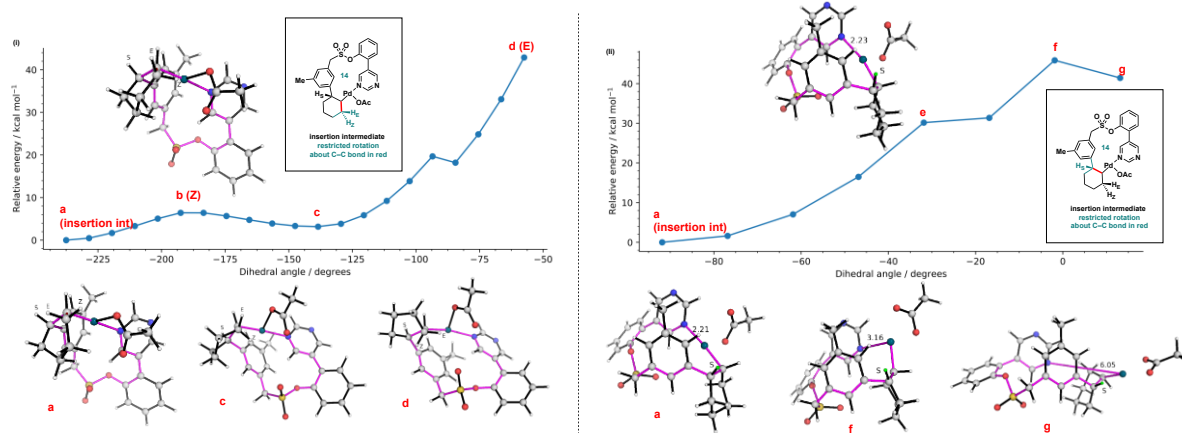


Figure S25. Dihedral angle scan (about C–C bond in red) for rotational barrier for the formation of (i) *E*/*Z*-allylated products and (ii) styrenyl product for cyclohexene substrate.

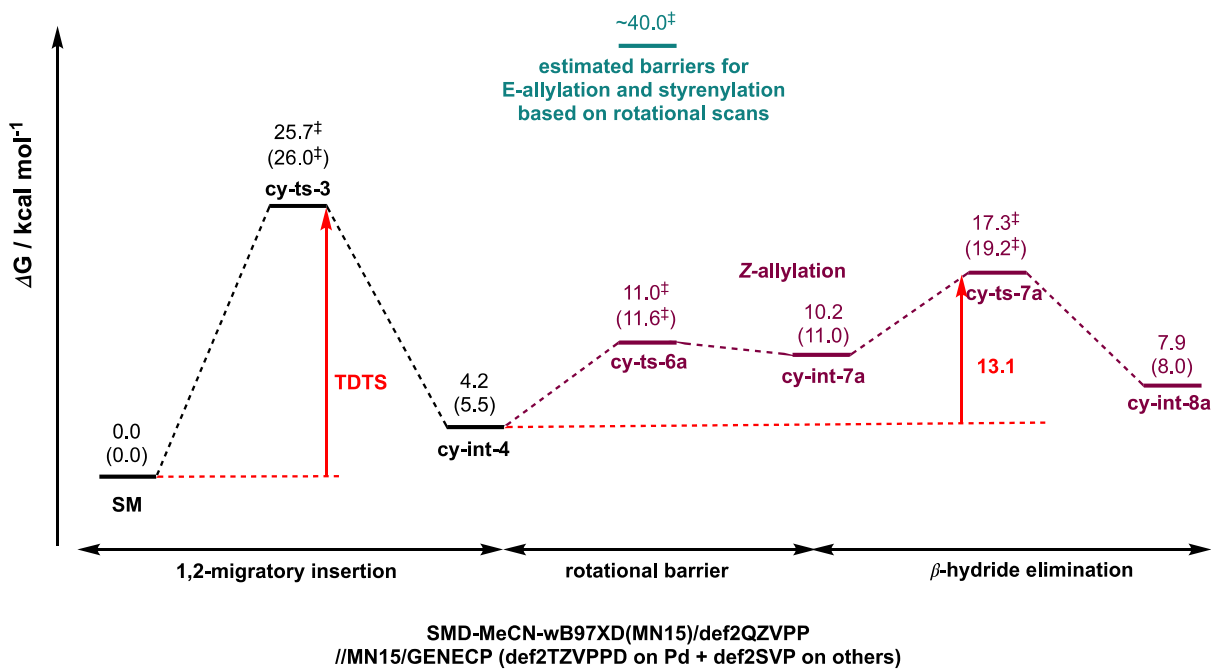


Figure S26. Gibbs free energy profile for *Z*-allylation using cyclohexene substrate. **cy-ts-3** is the same as **cy-d1-c1** as in Figure S20(e).

2.9.10 Absolute energies, zero-point energies

Absolute values (in Hartrees) for SCF energy, zero-point vibrational energy (ZPE), enthalpy and quasi-harmonic Gibbs free energy (at 363K) for optimised structures are given below. For harmonic frequency analysis, a plus (+) sign indicates that the lowest frequency of the optimised energy minimal structures is positive, and single negative frequency for each transition state is included. Single point corrections in SMD acetonitrile using ω B97X-D and MN15 functionals are also included. Each sub-heading corresponds to a subfolder inside the *structures_xyz* folder where all optimised structural coordinates are given in .xyz format, along with the corresponding (gas-phase) energy, *E*.

Structure	E/au	ZPE/a u	H/au	qh-G/au	Im.Freq/ cm ⁻¹	SP ω B97X-D (MeCN)	SP MN15 (MeCN)
0. Starting materials:							
arene	-	0.3115	-	-	-	-	-
1a	1426.522 9	09	1426.180 7	1426.269	+	1429.0622721 6	1428.691971 5
trans-	-	0.1651	-	-	-	-	-
hexen	235.3139 9	1	235.1364 5	235.1857 7	+	-235.88622142 -235.7628220	-235.7628220
cis-	-	0.1654	-	-	-	-	-
hexen	235.3122 6	29	235.1344 6	235.1835 2	+	-235.88455969 -235.7610397	-235.7610397
cyclo-	-	0.1463	-	-	-	-	-
hexen	234.1283 2	25	233.9727 3	234.0146 6	+	-234.68105898 -234.5687484	-234.5687484

HOA	-	0.0621	-	-	-	-	-	-
c	228.6445	97	228.5750	228.6124	+/-	-229.13726389	-229.0706003	
	3		2	2				

N-

acetyl	-	0.2314	-	-	-	-	-	-
-	593.1581	35	592.9054	592.9754	+/-	-594.47065223	-594.2582931	
norle	9		8	6				
ucine								

Pd(OAc)₂	-	0.1043	-	-	-	-	-	-
	583.8099	26	583.6901	583.7484	+/-	-585.03620367	-584.6482919	
	3		2	8				

Pd₃(OAc)₆	-	0.3178	-	-	-	-	-	-
	1751.587	68	1751.221	1751.347	+/-	1755.2153780	1754.047381	
	3		8	2		1		6

1. meta-allylation:								
----------------------------	--	--	--	--	--	--	--	--

int-1	-	0.4173	-	-	-	-	-	-
	2010.361	36	2009.896	2010.018	+/-	2014.1207433	2013.362453	
			6	7		0		1

ts-1	-	0.4119	-	-	-	-	-	-
	2010.336	75	2009.877	2009.998	-	2014.0948740	2013.332751	
	1		4	9	1136.100	8		5

int-2	-	0.4172	-	-	-	-	-	-
	2010.351	56	2009.886	2010.010	+/-	2014.1104499	2013.350665	
	5		8	3		7		7

int-1'	2146.206	0.5229	-	2145.631	-	2145.763	+	2150.3058485	-2149.465115
	8	38		5				4	
ts-1'	2146.190	0.5178	-	2145.621	2145.751	1275.114	-	2150.2850861	-2149.445114
	9	66		2	8	7		0	
int-2'	2146.215	0.5236	-	2145.639	-	2145.771	+	2150.3093651	-2149.472983
	2	42		2				5	
int-3	2017.031	0.5210	-	2016.458	2016.590	+	-	2020.8726358	2020.056335
	4	84			4			8	5
ts-3	2017.015	0.5202	-	2016.443	2016.574	-	-	2020.8571594	-2020.04
	3	4		9	2	281.0309		6	
int-4	2017.054	0.5225	-	2016.481	2016.610	+	-	2020.8951539	-2020.078034
	6	03			2			7	
ts-4	2017.039	0.5205	-	2016.468	2016.595	-95.8045	-	2020.8725658	-2020.056365
	5	7		5	9			1	
int-5	2017.042	0.5207	-	2016.470	2016.599	+	-	2020.8761334	-2020.059231
	4	22		5	5			5	

ts-5	2017.037	0.5184	-	2016.468	2016.596	-	534.1546	-	2020.8694761	-2020.053557
	6	43		4	3			2		
int-6	2017.048	0.5198	-	2016.477	2016.606	-	+	-	2020.8814551	-2020.065211
	7	9		5	8			4		
int-7	2017.047	0.5209	-	2016.475	2016.605	-	+	-	2020.8896222	-2020.069785
	9	31		9	3			6		
ts-7	-	0.5169	-	2016.475	2016.603	-	960.7952	-	2020.8775839	-2020.058839
	2017.043	19		4	8			4		
int-8	2017.065	0.5214	-	2016.492	2016.622	-	+	-	2020.8959791	-2020.079392
	1	65			8			2		
ts-7'	2017.016	0.5163	-	2016.448	-	2016.579	-	-	2020.8468038	-2020.030891
	5	98		5		975.0604		1		

2. Regioselectivity (Z-allylation vs styrenylation):

ts-4a	2017.037	0.5211	-	2016.465	2016.592	-	-77.2317	-	2020.8707224	-2020.05477
	2	16		9	7			4		
int-5a	2017.039	0.5211	-	2016.466	2016.595	-	+	-	2020.8730736	-2020.056043
	1	07		9	6			1		

ts-5a	2017.033	0.5184	-	2016.464	2016.592	-	2020.8663071	-2020.049971
	9	58		8	6	516.2140	8	
int-6a	2017.045	0.5199	-	2016.474	2016.603	+	2020.8797064	-2020.062662
	6	94		3	6		2	
ts-7a	2017.040	0.5172	-	2016.472	2016.600	-	2020.8747277	-2020.056175
	3	41		5	6	912.4642	9	
ts-4b	2017.019	0.5206	-	2016.448	2016.576	-49.4039	2020.8627730	-2020.045129
	5	51		3	3		3	
int-5b	2017.023	0.5203	-	2016.451	2016.581	+	2020.8663448	-2020.04869
	8			3	2		6	
ts-5b	2017.023	0.5175	-	2016.454	2016.585	-	2020.8604659	-2020.044136
	3	49		2	2	244.3729	9	
int-6b	2017.027	0.5189	-	2016.456	2016.587	+	2020.8603052	-2020.047355
	2	73		4	4		0	
ts-7b	2016.985	0.5138	-	2016.419	2016.549	-1493.046	2020.8110423	-2019.995037
	3	83		9	9	9	8	

3. Ligand identity in TDTS:

ts-3-	-	2017.015	0.5202	2016.443	2016.574	281.0309	-2020.85716
Ac-c1	35	4	89	18	0		-2020.03997
ts-3-	-	2017.012	0.5200	2016.441	2016.571	286.4834	-2020.85668
Ac-c2	91	6	55	93	0		-2020.03961
ts-3-	-	2017.010	0.5201	2016.439	2016.570	284.0324	-2020.85518
Ac-c3	98	7	44	63	0		-2020.03759
ts-3-	-	2017.012	0.5201	2016.441	2016.571	305.7022	-2020.85540
Ac-c4	57	3	08	53	0		-2020.03868
ts-3-	-	2017.002	0.5201	2016.430	2016.560	296.0877	-2020.85451
Ac-c5	08	5	87	47	0		-2020.03664
ts-3-	-	2017.002	0.5201	2016.431	2016.560	295.2832	-2020.85081
Ac-c6	34	1	16	56	0		-2020.03394
ts3' _b -aa-c1	-	2381.537	0.6894	-	-	-	-
	3	22		2380.782	2380.942	284.2484	2386.1978885
ts3' _b -aa-c2	-	2381.537	0.6895	-	-	-	-
	8	07		2380.783	2380.940	283.7738	2386.1972974
				2	7	2	2

ts3' _b	-	0.6891	-	-	-	-	-
-aa-c3	2381.532 2	98	2380.777 5	-2380.9	283.7067	2386.1955226 0	-2385.2316
ts3' _b	-	0.6895	-	-	-	-	-
-aa-c4	2381.535 5	09	2380.780 7	-2380.94	281.9868	2386.1959698 2	-2385.2323
ts3' _b	-	0.6892	-	-	-	-	-
-aa-c5	2381.532 1	92	2380.777 4	2380.936 9	304.8330	2386.1946542 6	-2385.2314
ts3' _b	-	0.6893	-	-	-	-	-
-aa-c6	2381.535 7	62	2380.781 2	-2380.9	269.5971	2386.1950421 6	-2385.2323
ts3' _b	-	0.6894	-	-	-	-	-
-aa-c7	2381.531 3	85	2380.776 5	-2380.9	281.9394	2386.1943224 0	-2385.23
ts3' _b	-	0.6896	-	-	-	-	-
-aa-c8	2381.535 2	71	2380.780 3	2380.938 6	303.3393	2386.1923800 4	-2385.2307
ts3' _b	-	0.6898	-	-	-	-	-
-aa-c9	2381.531 5	67	2380.776 6	2380.934 6	298.0564	2386.1915142 5	-2385.2285
ts3' _b	-	0.6896	-	-	-	-	-
-aa-	2381.539 c10	94 8	2380.785 2	2380.942 1	273.9343	2386.1922180 4	-2385.2285

ts3'_b	-	0.6898	-	-	-	-	-	-
-aa-	2381.538	9	2380.783	2380.939	-	2386.1899442	-	-2385.2285
c11			3	5	301.0522	8		

ts3'_b	-	0.6897	-	-	-	-	-	-
-aa-	2381.537	51	2380.782	2380.939	-	2386.1901799	-	-2385.2268
c12	3		5	7	281.9361	8		

3. Ligand non-participation in C–H activation and insertion:

ts-1'a	2146.150	0.5181	-	-	-	-	-	-
		13	2145.580	2145.711	-	2150.2517966	-	-2149.412069
	6		5	9	436.6324	3		

ts-1'b	2374.853	0.5819	-	-	-	-	-	-
		88	2374.211	2374.360	1144.373	2379.4260737	2378.518059	
	4		4	9	3	3	2	

ts-1'c1	2374.859	0.5813	-	-	-	-	-	-
		02	2374.217	2374.366	1121.517	2379.4343307	2378.527017	
	1		3	4	4	9	9	9

ts-1'c2	2374.862	0.5816	-	-	-	-	-	-
		18	2374.220	2374.368	1158.865	2379.4322103	2378.524855	
	2		2	8	0	7	8	8

ts-1'c3	2374.864	0.5818	-	-	-	-	-	-
		42	2374.222	2374.370	1167.889	2379.4311132	2378.523873	
	4		3	6	9	8	8	6

ts-1'c4	2374.857	0.5818	-	-	-	-	-	-
		3	2374.215	2374.363	1158.697	2379.4280753	2378.519836	
			1	1	9	6	6	5

ts-1'c5	-	2374.839	0.5817	-	2374.198	2374.345	1119.736	2379.4117375	2378.504226
	9	15		2	5		2	3	6

4. Arene site selectivity (*ortho*- vs *para*-):

ts-1o	-	2010.327	0.4123	-	2009.868	2009.989	1136.403	2014.0809551	2013.322784
	2	35		4	4		8	2	8

ts-1o-c2	-	2010.326	0.4127	-	2009.867	2009.987	-	2014.0754951	2013.317891
	4	28		5	3		974.1986	4	6

ts-1o'	-	2146.191	0.5181	-	2145.621	2145.753	1079.014	2150.2836752	-2149.445889
	6	62		7	1		6	5	

ts-3o	-	2017.002	0.5204	-	2016.430	2016.560	-	2020.8357802	-2020.021731
	5	45		9	9		330.9693	2	

int-4o	-	2017.037	0.5230	-	2016.463	2016.591	+	2020.8678039	-2020.052957
	3	08		3	9			5	

ts-1p	-	2010.335	0.4121	-	2009.877	2009.998	1147.996	2014.0921925	2013.332518
	9	69		2	4		6	9	6

ts-1p-c2	-	2010.337	0.4123	-	2009.878	2009.999	1129.467	2014.0909101	2013.332141
	3	06		7	2		5	4	8

ts-1p'	2146.181	0.5182	-	2145.611	2145.742	-	744.9454	-	2150.2710257	-2149.431512
			9		2	5			2	
	4									
ts-3p	2017.011	0.5207	-	2016.439	2016.568	-	-293.7	-	2020.8506834	-2020.036795
			13		9	8			1	
	5									
int-4p	2017.046	0.5229	-	2016.472	2016.601	-	+	-	2020.8846075	-2020.068617
			73		5	4			0	
	4									

5. Boltzmann sampling for 1,2-migratory**insertion:**

trans-d1-c1	2017.012	0.5201	-	2016.441	2016.571	-	305.7022	-	2020.8554024	-2020.038678
			25		1	5			9	
	6									
trans-d1-c2	2017.014	0.5201	-	2016.442	2016.572	-	293.1491	-	2020.8556619	-2020.039368
			58		8	8			3	
	2									
trans-d1-c3	2017.012	0.5198	-	2016.441	2016.571	-	277.2951	-	2020.8532857	2020.037741
			17		2	6			9	
	3									
trans-d1-c4	2017.012	0.5200	-	2016.441	2016.571	-	-316.8	-	2020.8530009	-2020.036383
			1		2	8			1	
	6									

<i>trans-</i> d1-c5	-	2017.014 9	0.5204 54	-	2016.443 4	2016.572 8	-316.9	2020.8539279 1	-2020.037906
<i>trans-</i> d1-c6	-	2017.008 5	0.5197 82	-	2016.437 3	-	2016.568 317.3912	2020.8522987 7	-2020.034701
<i>trans-</i> d1-c7	-	2017.014 4	0.5205 09	-	2016.442 8	2016.572 5	-	2020.8530853 6	-2020.037854
<i>trans-</i> d1-c8	-	2017.016 8	0.5208 16	-	2016.445 3	2016.573 6	-	2020.8536826 7	-2020.038209
<i>trans-</i> d1-c9	-	2017.009 5	0.5198 96	-	2016.438 3	2016.568 5	-	2020.8490570 4	-2020.033366
<i>trans-</i> d2-c1	-	2017.014 1	0.5196 63	-	2016.443 1	2016.573 3	-	-2020.85718	-2020.040593
<i>trans-</i> d2-c2	-	2017.014 9	0.5196 12	-	2016.444 7	2016.573 7	-	-2020.856582	-2020.040347
<i>trans-</i> d2-c3	-	2017.017 3	0.5202 44	-	2016.446 288.8986	2016.575 6	-	2020.8566662	-2020.040614

<i>trans-</i> d2-c4	-	2017.017 8	0.5203 81	-	2016.446 5	-	2016.575 304.4657	-	-2020.855951	-2020.040502
<i>trans-</i> d2-c5	-	2017.012 8	0.5198 58	-	2016.441 6	-	2016.571 4	-	-2020.8542	-2020.037271
<i>trans-</i> d2-c6	-	2017.014 6	0.5198 44	-	2016.443 6	-	2016.572 9	-	-2020.854195	-2020.038113
<i>trans-</i> d2-c7	-	2017.011 1	0.5198 6	-	2016.44 -2016.44	-	2016.570 1	-	2020.8531970 9	-2020.037409
<i>trans-</i> d2-c8	-	2017.014 7	0.5197 73	-	2016.443 8	-	2016.573 303.2176	-	-2020.853935	-2020.038479
<i>trans-</i> d2-c9	-	2017.010 5	0.5201 14	-	2016.439 3	-	2016.568 8	-	2020.8509175 9	-2020.035064
<i>cis-</i> d1-c1	-	2017.011 4	0.5197 7	-	2016.440 3	-	2016.570 6	-	2020.8545480 9	-2020.038653
<i>cis-</i> d1-c2	-	2017.014 3	0.5202 43	-	2016.443 3	-	2016.572 289.5588	-	2020.8546081 5	-2020.038579

<i>cis-</i> d1-c3	-	2017.009	0.5198	-	2016.438	2016.568	-	305.4801	-	2020.8529871	-2020.036652
		4	8		1	6			9		
<i>cis-</i> d1-c4	-	2017.012	0.5202	-	2016.441	-	-	296.5738	-	2020.8540071	-2020.037311
		8	44		4	2016.571			6		
<i>cis-</i> d1-c5	-	2017.013	0.5200	-	2016.442	2016.571	-	287.1232	-	2020.8534278	-2020.038021
		2	84		1	3			3		
<i>cis-</i> d1-c6	-	2017.012	0.5201	-	2016.441	2016.568	-	295.7306	-	2020.8532794	-2020.037221
		64	8		8	8			5		
<i>cis-</i> d1-c7	-	2017.012	0.5207	-	2016.440	2016.568	-	300.2449	-	2020.8480517	-2020.033502
		87	5		9				7		
<i>cis-</i> d1-c8	-	2017.010	0.5208	-	2016.438	2016.567	-	308.1908	-	2020.8478232	-2020.03263
		3	06		6	4			8		
<i>cis-</i> d1-c9	-	2017.005	0.5211	-	2016.433	2016.561	-	314.0032	-	2020.8401955	-2020.025393
		1	4		3	8			6		
<i>cis-</i> d2-c1	-	2017.010	0.5201	-	2016.438	2016.569	-	298.4609	-	2020.8528853	-2020.037075
		3	14		9	1			9		

<i>cis-</i> d2-c2	-	2017.010 9	0.5204 54	-	2016.439 3	2016.569 1	-	300.5416 6	2020.8532499	-2020.03695
<i>cis-</i> d2-c3	-	2017.012 4	0.5204 31	-	2016.441 1	2016.570 2	-	287.7811 4	2020.8536031	-2020.038019
<i>cis-</i> d2-c4	-	2017.011 7	0.5201 84	-	2016.440 4	2016.570 2	-	300.4347 6	2020.8521707	-2020.037598
<i>cis-</i> d2-c5	-	2017.010 1	0.5203 28	-	2016.438 6	2016.568 7	-	309.4578 3	2020.8515561	-2020.036441
<i>cis-</i> d2-c6	-	2017.007 9	0.5202 58	-	2016.436 4	2016.566 7	-	313.6194 3	2020.8512690	-2020.034999
<i>cis-</i> d2-c7	-	2017.008 2	0.5203 27	-	2016.436 8	2016.565 7	-	-296.732 2	2020.8498942	-2020.033341
<i>cis-</i> d2-c8	-	2017.003 6	0.5207 16	-	2016.431 9	2016.561 5	-	311.8461 5	2020.8461443	-2020.028735
<i>cis-</i> d2-c9	-	2017.002 8	0.5206 98	-	2016.431 1	2016.560 6	-	316.5124 0	2020.8444883	-2020.028321

cy-d1-c1	-	2015.824	0.5009	-	2015.275	2015.399	-	309.5106	-	2019.6462757	-2018.840491
	5		39		2	7			0		
cy-d1-c2	-	2015.823	0.5013	-	2015.273	-	2015.398	-	314.2776	-	2019.6457994
	3		42		7					2	-2018.839852
cy-d1-c3	-	2015.826	0.5012	-	2015.277	2015.400	-	-	301.2641	-	2019.6445767
	6		53		1	6				2	-2018.840282
cy-d1-c4	-	2015.821	0.5013	-	2015.271	2015.395	-	-	292.1391	-	2019.6428992
	07		07		2	6				9	-2018.83771
cy-d2-c1	-	2015.823	0.5009	-	2015.274	2015.397	-	-304.458	-	2019.6457031	-2018.839656
	6		56		4	8				0	
cy-d2-c2	-	2015.825	0.5009	-	2015.276	2015.399	-	-291.53	-	2019.6448124	-2018.840874
	2		5			3				2	
cy-d2-c3	-	2015.819	0.5008	-	2015.269	2015.394	-	-	276.5101	-	2019.6439305
	3		87		8	1				1	-2018.838106
cy-d2-c4	-	2015.822	0.5010	-	2015.273	2015.396	-	-	303.1028	-	2019.644799
	5		28		3	5					2018.838686
											55

6. Isodesmic studies:

pyridine	-	0.0894	-	-	-	+	-248.30904588	-248.2228936
ne	247.7627	73	247.6659	247.7041				
	6		6	1				
ts-3-iso	-	0.6108	-	-	-	-	-	-
	2264.788	71	2264.117	2264.267	325.2881		2269.1677108	-2268.26553
	5		5	2			1	
ts-3o-iso	-	0.6118	-	-	-	-	-	-
	2264.803	69	2264.132	2264.277	285.3699		2269.1666541	-2268.26716
	6		7	6			2	
ts-3p-iso	-	0.6116	-	-	-	-	-	-
	2264.794	33	2264.123	2264.270	310.8723		2269.1700187	-2268.27014
	2		8				6	
7. cis-hexene product selectivity:								
cis-int-4	-	0.5222	-	-	-	-	-	-
	2017.049	86	2016.475	2016.605		+	2020.8908183	-2020.074007
	1		5	0			1	
cis-ts-6	-	0.5221	-	-	-	-	-	-
	2017.047	16	2016.475	2016.602	-56.3933		2020.8881911	-2020.071351
	7		3	6			8	
cis-int-7	-	0.5218	-	-	-	-	-	-
	2017.045	79	2016.473	2016.600		+	-2020.878591	-2020.062478
	8		3	9				
cis-ts-7	-	0.5176	-	-	-	-	-	-
	2017.04	15	2016.472	2016.598	894.6881		2020.8699586	-2020.051674
			1	9			6	

<i>cis</i> -int-8	-	2017.065 2	0.5221 18	-	2016.491 8	-	2016.621 1	+	-	2020.8893887 0	-	2020.073698 04
<i>cis</i> -ts-6a	-	2017.038 5	0.5224 31	-	2016.465 9	-	2016.593 1	-99.8893	-	2020.8792089 8	-	-2020.061699
<i>cis</i> -int-7a	-	2017.039 4	0.5218 02	-	2016.467	-	2016.594 5	+	-	2020.8770836 8	-	-2020.058029
<i>cis</i> -ts-7a	-	2017.034 6	0.5180 17	-	2016.466 5	-	2016.592 8	978.8647	-	2020.8649285 9	-	-2020.046586
<i>cis</i> -int-8a	-	2017.060 4	0.5228 8	-	2016.486 6	-	2016.614 9	+	-	2020.8851595 8	-	-2020.069733
<i>cis</i> -ts-4b	-	2017.016 3	0.5205 14	-	2016.445	-	2016.573 9	-82.2613	-	2020.8602446 6	-	-2020.041432
<i>cis</i> -int-5b	-	2017.034 2	0.5203 72	-	2016.462 2	-	2016.593 0	+	-	2020.8734714 1	-	-2020.056019
<i>cis</i> -ts-5b	-	2017.029	0.5178 17	-	2016.459 9	-	2016.589 8	366.9912	-	2020.8643520 8	-	-2020.049118

<i>cis</i> - int-6b	-	2017.031 8	0.5189 39	-	2016.461 1	2016.591 8	-	+	2020.8635495 5	-2020.05077
------------------------	---	---------------	--------------	---	---------------	---------------	---	---	-------------------	-------------

<i>cis-ts-</i> 5b-c2	-	2017.015 8	0.5180 3	-	2016.446 8	2016.575 6	-	-	2020.8542316 6	-2020.038656
--------------------------------	---	---------------	-------------	---	---------------	---------------	---	---	-------------------	--------------

8. cyclohexene product selectivity:

<i>cy-</i> int-4	-	2015.863 9	0.5032 7	-	2015.312 3	2015.435 8	-	+	2019.6837660 1	-2018.876402
---------------------	---	---------------	-------------	---	---------------	---------------	---	---	-------------------	--------------

<i>cy-ts-</i> 6a	-	2015.859 1	0.5033 92	-	2015.308 4	2015.429 7	-	-88.5455	2019.6741799 0	-2018.868046
----------------------------	---	---------------	--------------	---	---------------	---------------	---	-----------------	-------------------	--------------

<i>cy-</i> int-7a	-	2015.859 1	0.5025 39	-	2015.308 4	2015.431 1	-	+	2019.6741475 5	-2018.867609
----------------------	---	---------------	--------------	---	---------------	---------------	---	---	-------------------	--------------

<i>cy-ts-</i> 7a	-	2015.847 7	0.4985 27	-	2015.301 7	2015.422 7	-	1032.925 6	2019.6597835 8	-2018.851573
----------------------------	---	---------------	--------------	---	---------------	---------------	---	----------------------	-------------------	--------------

<i>cy-</i> int-8a	-	2015.871 7	0.5032 44	-	2015.320 1	2015.443 5	-	+	2019.6780552 2	-2018.872553
----------------------	---	---------------	--------------	---	---------------	---------------	---	---	-------------------	--------------

2.9.11 Optimized geometries

Geometries of all optimized structures (in .xyz format with their associated energy in Hartrees) are included in a separate folder named *structures_xyz* with an associated README file. All these data have been deposited with this Supporting Information and uploaded to zenodo.org (DOI: 10.5281/zenodo.2775841).

3. References:

Full reference for ref (1):

Gaussian 16, Revision A.01, Frisch, M. J.; Trucks, G. W.; Schlegel, H. B.; Scuseria, G. E.; Robb, M. A.; Cheeseman, J. R.; Scalmani, G.; Barone, V.; Mennucci, B.; Petersson, G. A.; Nakatsuji, H.; Caricato, M.; Li, X.; Hratchian, H. P.; Izmaylov, A. F.; Bloino, J.; Zheng, G.; Sonnenberg, J. L.; Hada, M.; Ehara, M.; Toyota, K.; Fukuda, R.; Hasegawa, J.; Ishida, M.; Nakajima, T.; Honda, Y.; Kitao, O.; Nakai, H.; Vreven, T.; Montgomery Jr., J. A.; Peralta, J. E.; Ogliaro, F.; Bearpark, M.; Heyd, J. J.; Brothers, E.; Kudin, K. N.; Staroverov, V. N.; Kobayashi, R.; Normand, J.; Raghavachari, K.; Rendell, A.; Burant, J. C.; Iyengar, S. S.; Tomasi, J.; Cossi, M.; Rega, N.; Millam, J. M.; Klene, M.; Knox, J. E.; Cross, J. B.; Bakken, V.; Adamo, C.; Jaramillo, J.; Gomperts, R.; Stratmann, R. E.; Yazyev, O.; Austin, A. J.; Cammi, R.; Pomelli, C.; Ochterski, J. W.; Martin, R. L.; Morokuma, K.; Zakrzewski, V. G.; Voth, G. A.; Salvador, P.; Dannenberg, J. J.; Dapprich, S.; Daniels, A. D.; Farkas, Ö.; Foresman, J. B.; Ortiz, J. V.; Cioslowski, J.; Fox, D. J. Gaussian, Inc., Wallingford CT, 2016.

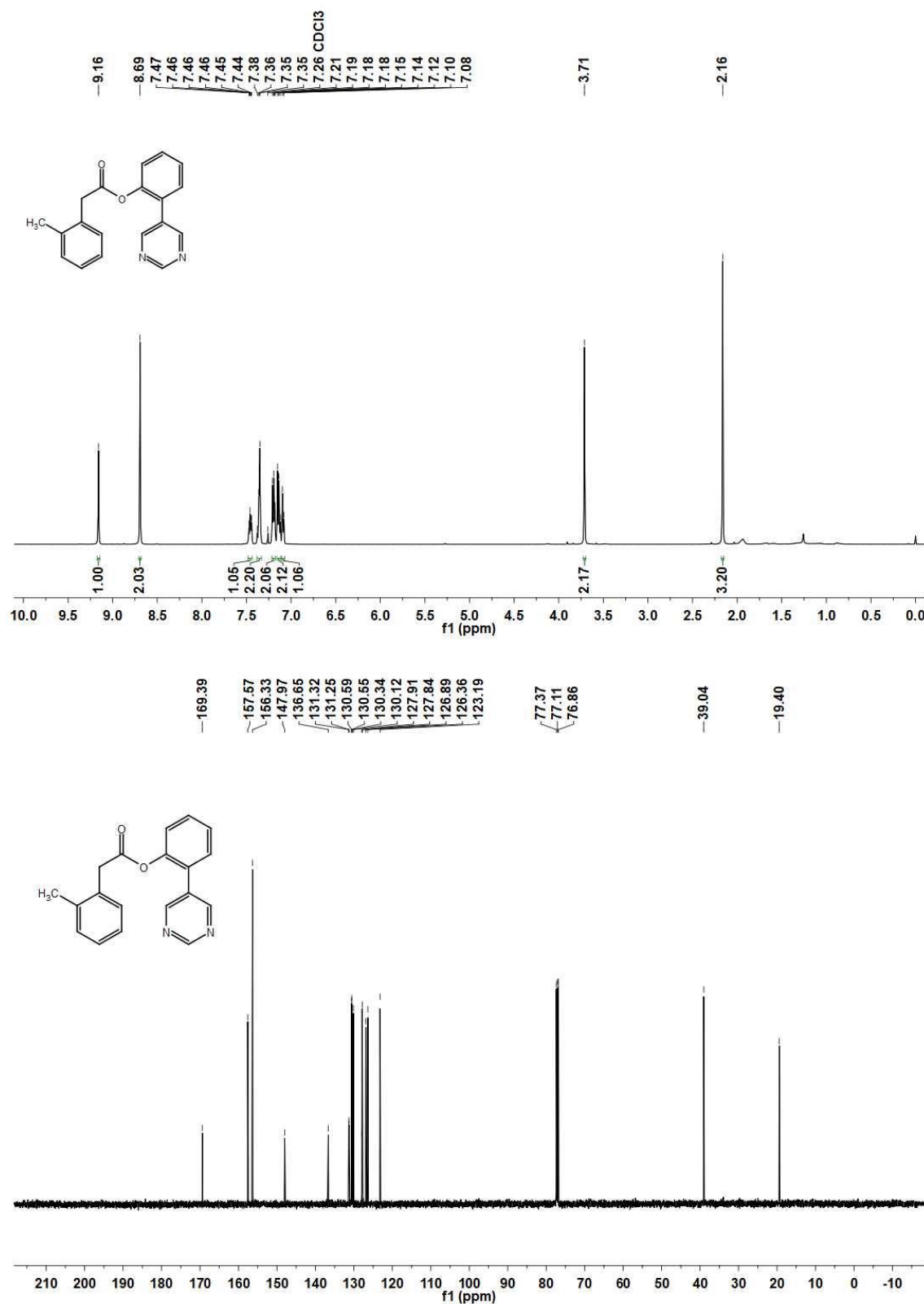
- (1) Frisch, M. J.; Trucks, G. W.; Schlegel, H. B.; Scuseria, G. E.; Robb, M. A.; Cheeseman, J. R.; Scalmani, G.; Barone, V.; Mennucci, B.; Petersson, G. A.; et al. Gaussian 16, Revision A.01. 2016.
- (2) Yu, H. S.; He, X.; Li, S. L.; Truhlar, D. G. MN15: A Kohn–Sham Global-Hybrid Exchange–Correlation Density Functional with Broad Accuracy for Multi-Reference and Single-Reference Systems and Noncovalent Interactions. *Chem. Sci.* **2016**, 7 (8), 5032–5051.

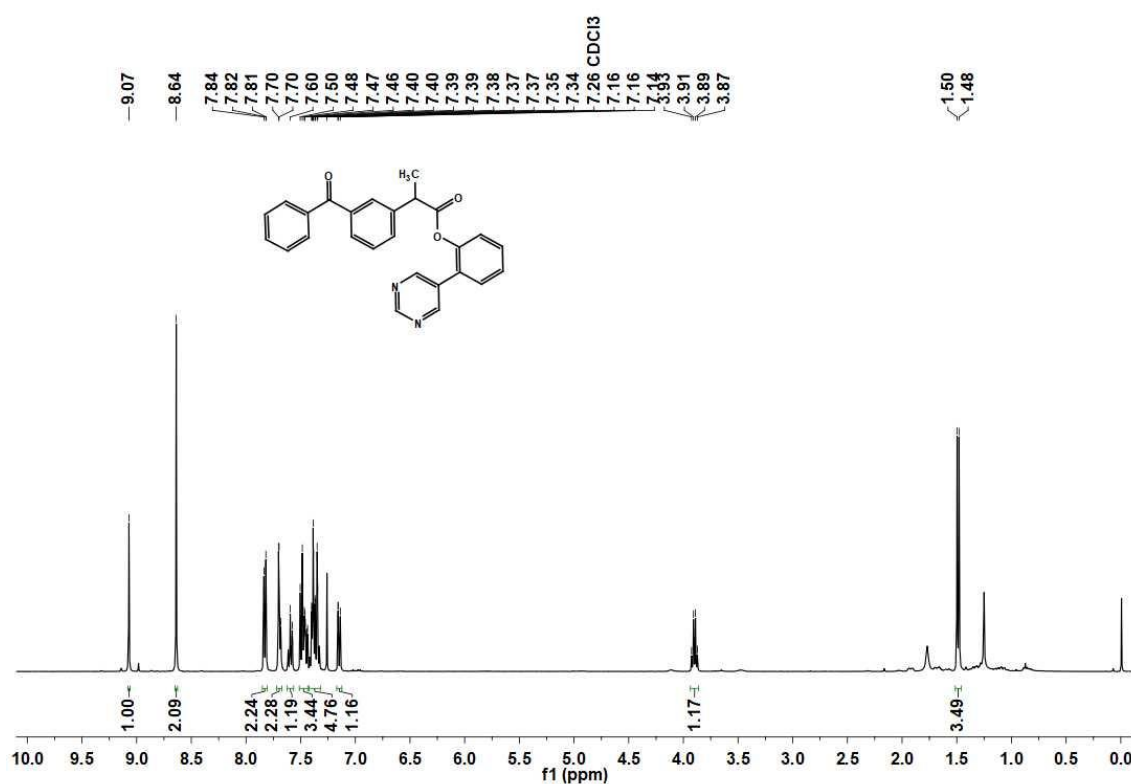
- (3) Andrae, D.; Häußermann, U.; Dolg, M.; Stoll, H.; Preuß, H. Energy-Adjustedab Initio Pseudopotentials for the Second and Third Row Transition Elements. *Theor. Chim. Acta* **1990**, 77 (2), 123–141.
- (4) Weigend, F.; Ahlrichs, R. Balanced Basis Sets of Split Valence{,} Triple Zeta Valence and Quadruple Zeta Valence Quality for H to Rn: Design and Assessment of Accuracy. *Phys. Chem. Chem. Phys.* **2005**, 7 (18), 3297–3305.
- (5) Weigend, F. Accurate Coulomb-Fitting Basis Sets for H to Rn. *Phys. Chem. Chem. Phys.* **2006**, 8 (9), 1057–1065.
- (6) Mekareeya, A.; Walker, P. R.; Couce-Rios, A.; Campbell, C. D.; Steven, A.; Paton, R. S.; Anderson, E. A.; Ross Walker, P.; Couce-Rios, A.; Campbell, C. D.; et al. Mechanistic Insight into Palladium-Catalyzed Cycloisomerization: A Combined Experimental and Theoretical Study. *J. Am. Chem. Soc.* **2017**, 139 (29), 10104–10114.
- (7) Deb, A.; Hazra, A.; Peng, Q.; Paton, R. S.; Maiti, D. Detailed Mechanistic Studies on Palladium-Catalyzed Selective C–H Olefination with Aliphatic Alkenes: A Significant Influence of Proton Shuttling. *J. Am. Chem. Soc.* **2017**, 139 (2), 763–775.
- (8) Chai, J.-D.; Head-Gordon, M. Long-Range Corrected Hybrid Density Functionals with Damped Atom-Atom Dispersion Corrections. *Phys. Chem. Chem. Phys.* **2008**, 10 (44), 6615–6620.
- (9) Marenich, A. V; Cramer, C. J.; Truhlar, D. G. Universal Solvation Model Based on Solute Electron Density and on a Continuum Model of the Solvent Defined by the Bulk Dielectric Constant and Atomic Surface Tensions. *J. Phys. Chem. B* **2009**, 113 (18), 6378–6396.
- (10) Grimme, S. Supramolecular Binding Thermodynamics by Dispersion-Corrected Density Functional Theory. *Chem. – A Eur. J.* **2012**, 18 (32), 9955–9964.
- (11) Funes-Ardoiz, I.; Paton, R. S. GoodVibes v1.0.1 <http://doi.org/10.5281/zenodo.56091>.
- (12) E. D. Glendening, A. E. Reed, J. E. Carpenter, and F. W. NBO Version 3.1.,
- (13) Contreras-García, J.; Johnson, E. R.; Keinan, S.; Chaudret, R.; Piquemal, J.-P.; Beratan,

- D. N.; Yang, W. NCIPLOT: A Program for Plotting Noncovalent Interaction Regions. *J. Chem. Theory Comput.* **2011**, *7* (3), 625–632.
- (14) Sosa, C.; Andzelm, J.; Elkin, B. C.; Wimmer, E.; Dobbs, K. D.; Dixon, D. A. A Local Density Functional Study of the Structure and Vibrational Frequencies of Molecular Transition-Metal Compounds. *J. Phys. Chem.* **1992**, *96* (16), 6630–6636.
- (15) Godbout, N.; Salahub, D. R.; Andzelm, J.; Wimmer, E. Optimization of Gaussian-Type Basis Sets for Local Spin Density Functional Calculations. Part I. Boron through Neon, Optimization Technique and Validation. *Can. J. Chem.* **1992**, *70* (2), 560–571.
- (16) Schrödinger, LLC. *The {PyMOL} Molecular Graphics Development Component, Version~1.8*; 2015.
- (17) Maji, A.; Guin, S.; Feng, S.; Dahiya, A.; Singh, V. K.; Liu, P.; Maiti, D. Experimental and Computational Exploration of Para-Selective Silylation with a Hydrogen-Bonded Template. *Angew. Chemie - Int. Ed.* **2017**, *56* (47), 14903–14907.
- (18) Maji, A.; Dahiya, A.; Lu, G.; Bhattacharya, T.; Brochetta, M.; Zanoni, G.; Liu, P.; Maiti, D. H-Bonded Reusable Template Assisted Para-Selective Ketonisation Using Soft Electrophilic Vinyl Ethers. *Nat. Commun.* **2018**, *9* (1).
- (19) Wheeler, S. E.; Houk, K. N.; Schleyer, P. V. R.; Allen, W. D. A Hierarchy of Homodesmotic Reactions for Thermochemistry. *J. Am. Chem. Soc.* **2009**, *131* (7), 2547–2560.
- (20) Wheeler, S. E. Homodesmotic Reactions for Thermochemistry. *Wiley Interdisciplinary Reviews: Computational Molecular Science*. 2012, pp 204–220.
- (21) Peng, Q.; Duarte, F.; Paton, R. S. Computing Organic Stereoselectivity - from Concepts to Quantitative Calculations and Predictions. *Chem. Soc. Rev.* **2016**, *45* (22), 6093–6107.
- (22) Fang, L.; Saint-Denis, T. G.; Taylor, B. L. H.; Ahlquist, S.; Hong, K.; Liu, S.; Han, L.; Houk, K. N.; Yu, J. Q. Experimental and Computational Development of a Conformationally Flexible Template for the Meta-C-H Functionalization of Benzoic Acids. *J. Am. Chem. Soc.* **2017**, *139* (31), 10702–10714.

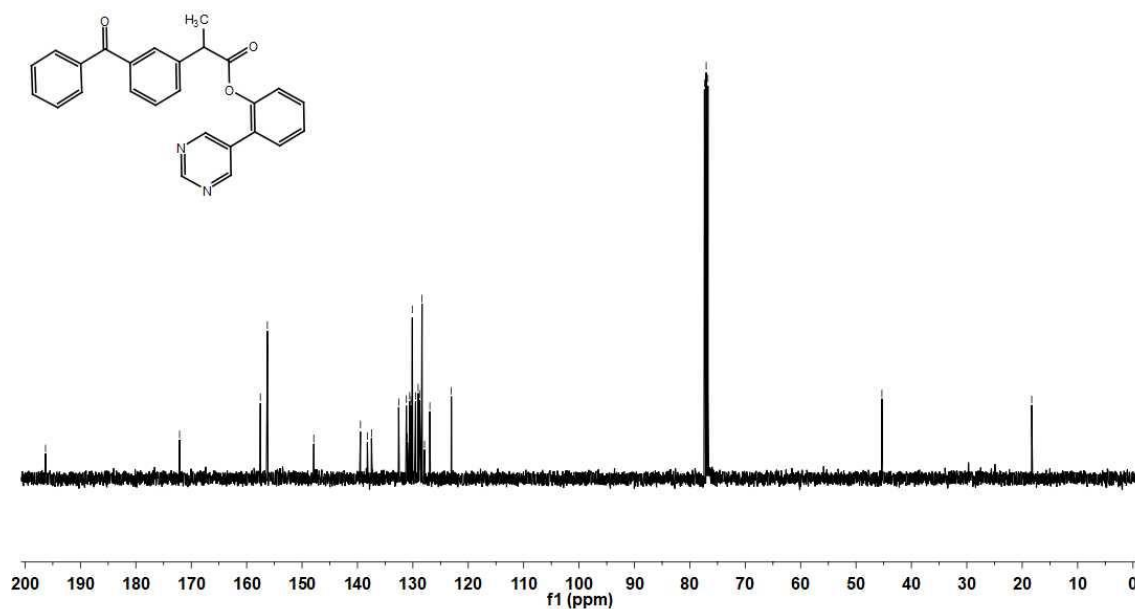
4. Author Contributions

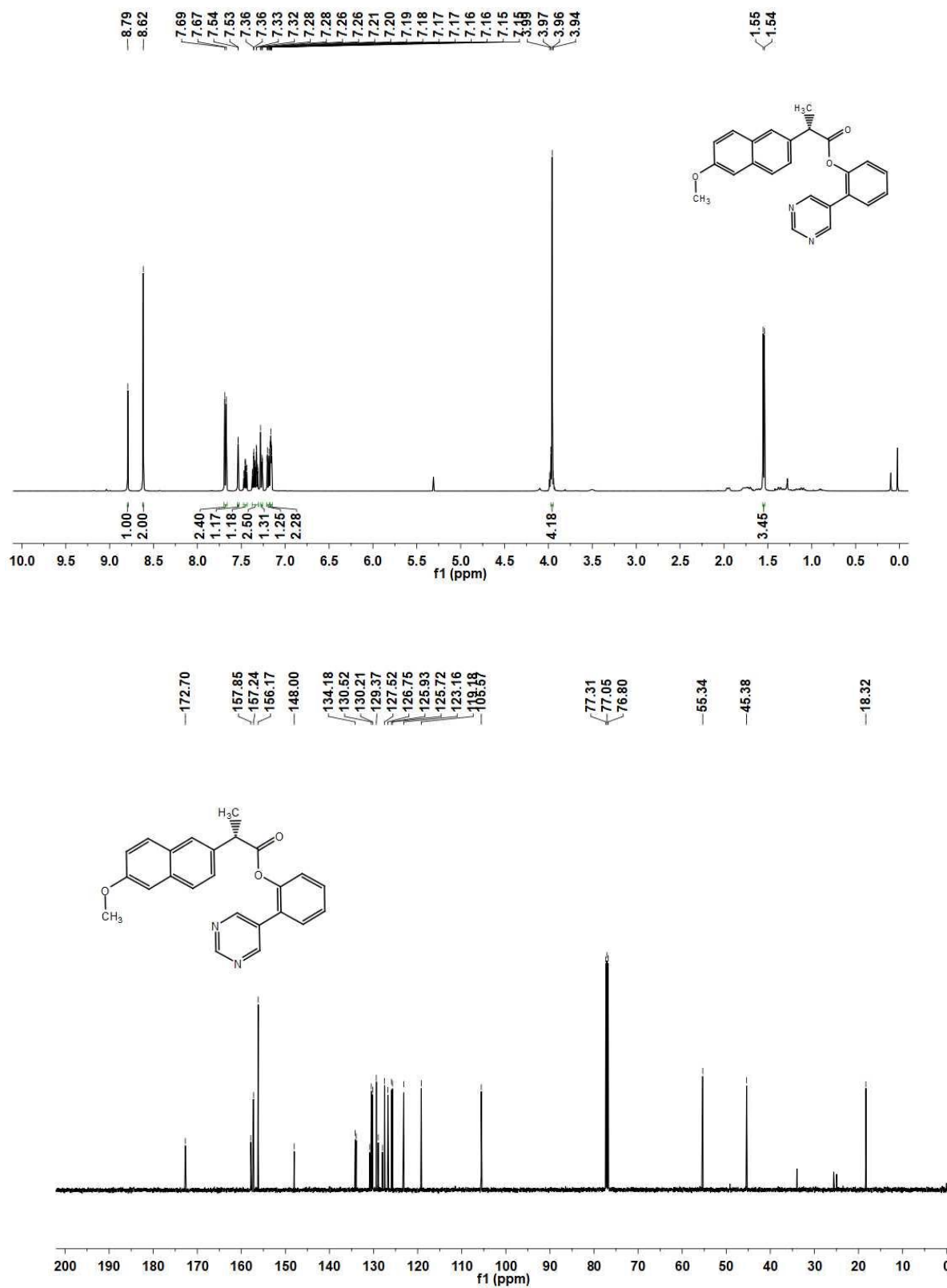
T.K.A. and R.M. conceived and developed the palladium catalyzed *meta*-selective C–H allylation. T.K.A. and R.M. optimized the reaction conditions. TKA, M.S.S., S.M. and N.P. prepared the starting materials and identified the substrates scope. TKA and M.S. conducted the mechanistic investigations. X.Z. designed and performed the computational studies. R.S.P supervised the computational studies. D.M. supervised the project. T.K.A. and X.Z. wrote the manuscript with input from R.S.P. and D.M. All authors read and commented on the manuscript.

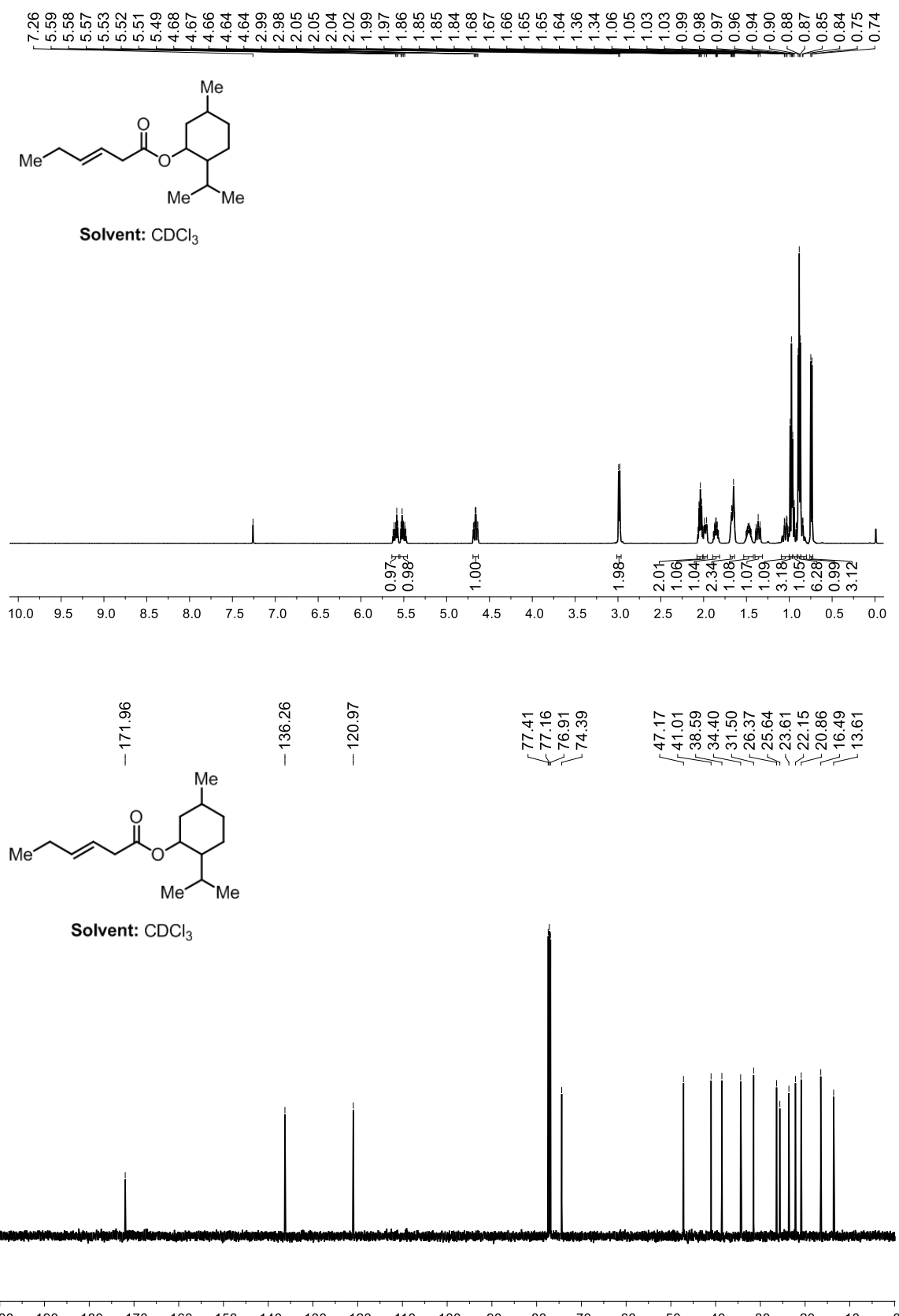
5. NMR spectra of starting materials

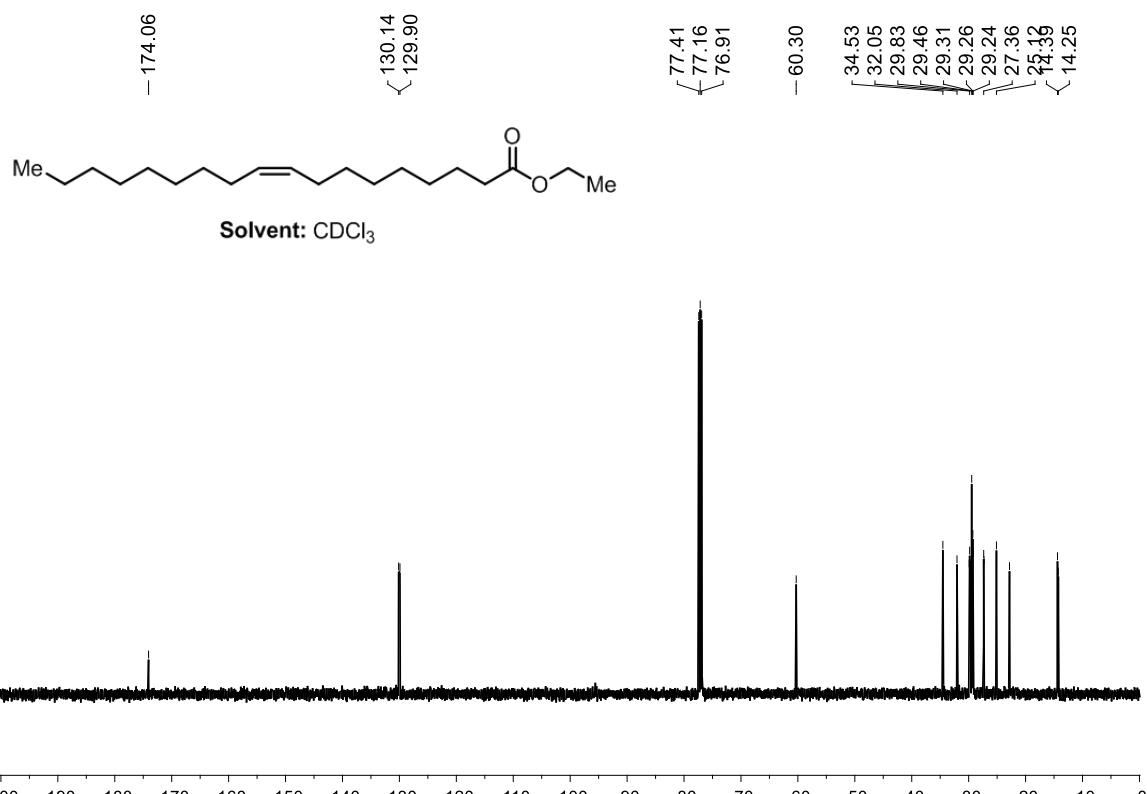
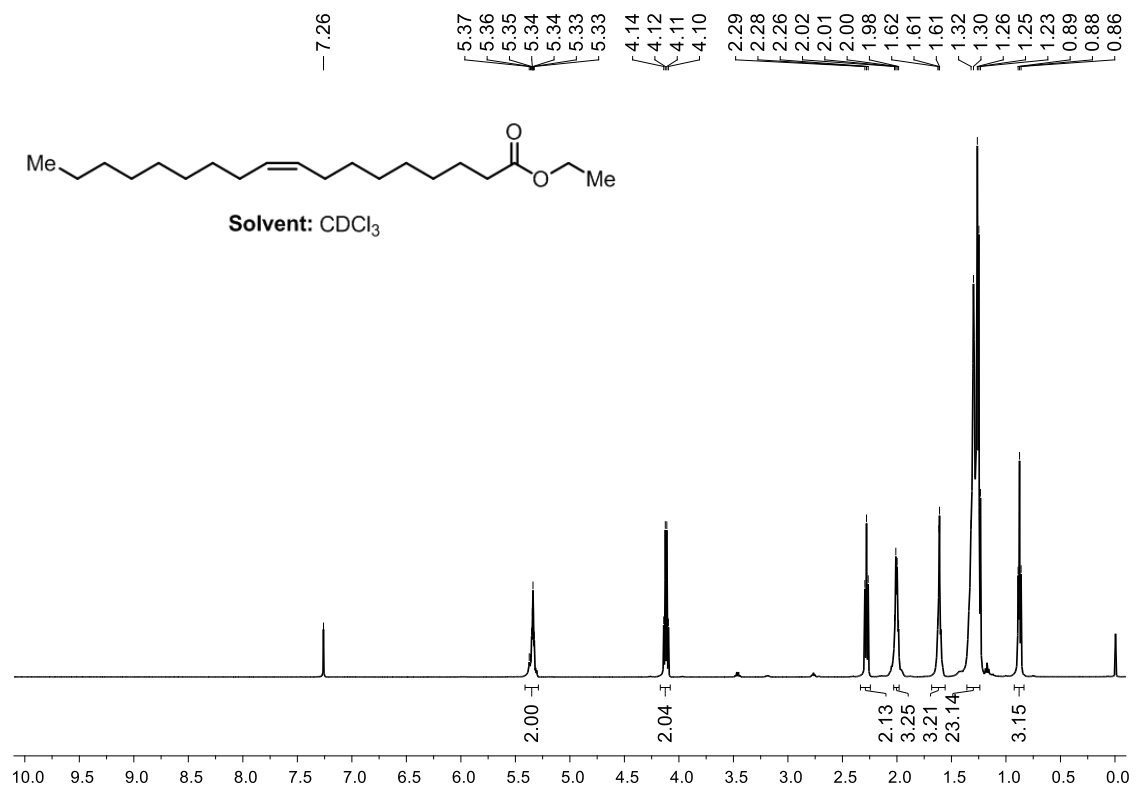


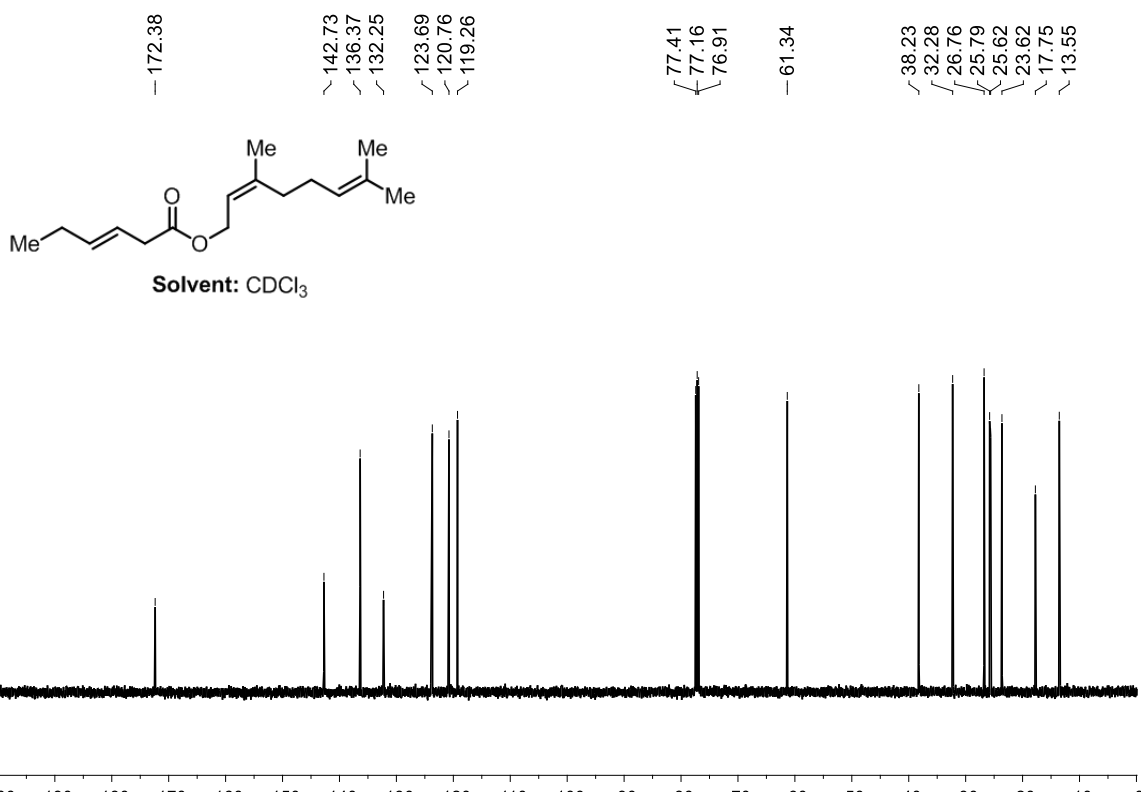
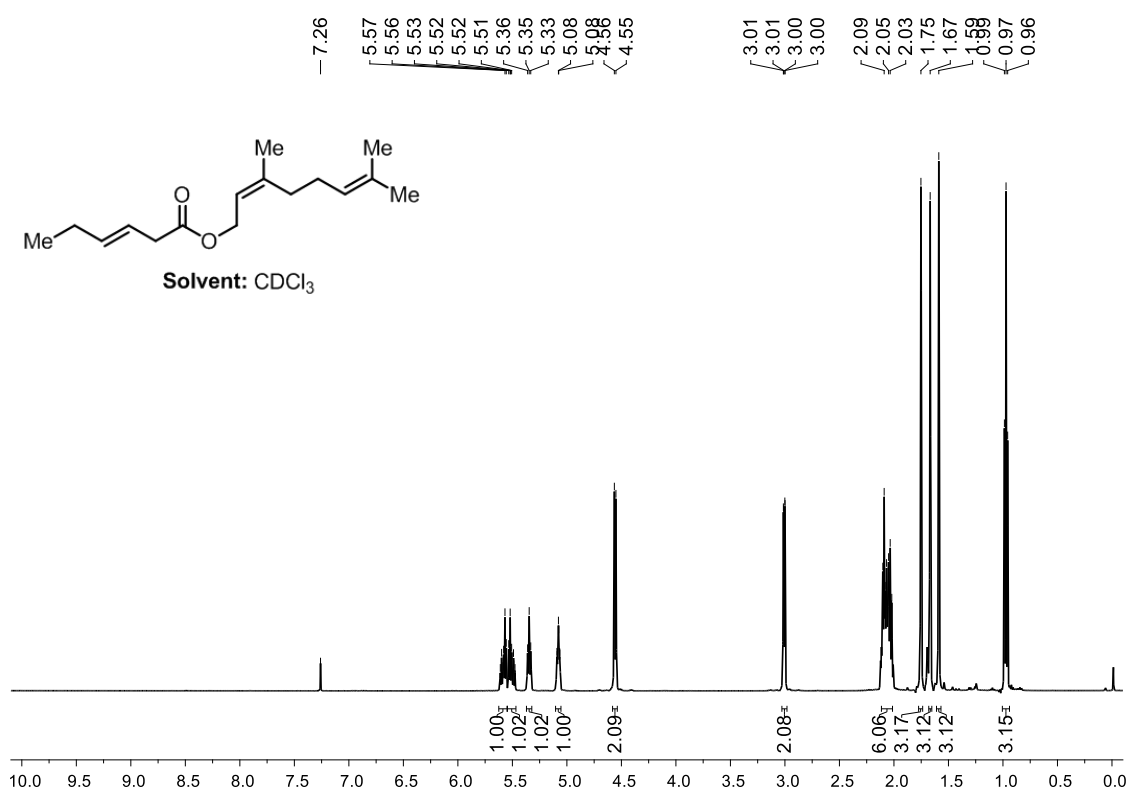
Chemical shifts (δ): 196.31, 172.11, 157.53, 156.26, 147.88, 139.46, 138.21, 137.46, 132.55, 131.17, 131.00, 130.58, 130.34, 130.10, 129.51, 129.04, 128.79, 128.35, 127.89, 126.93, 123.05, 77.36, 77.05, 76.73, 45.33, 18.28.

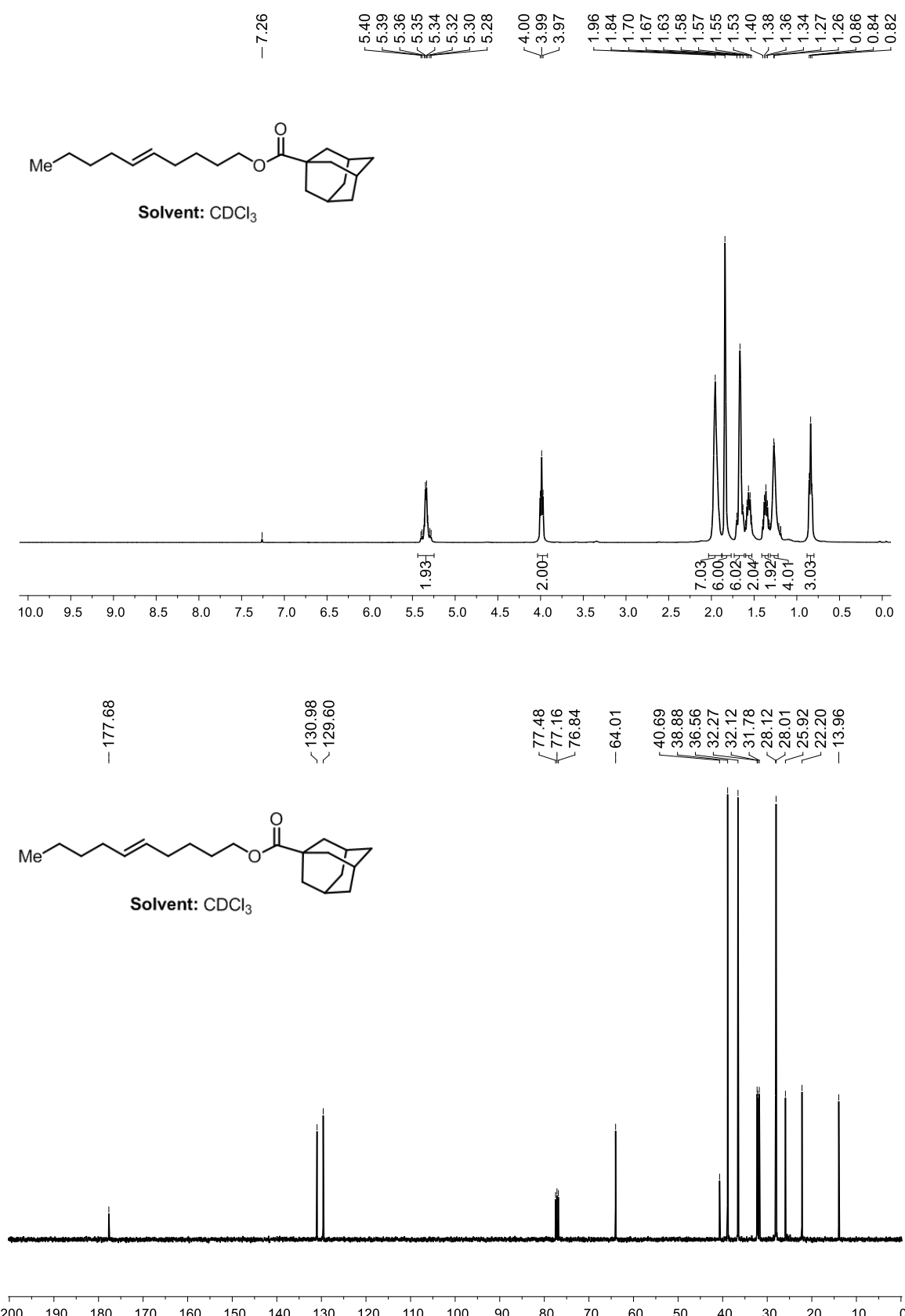


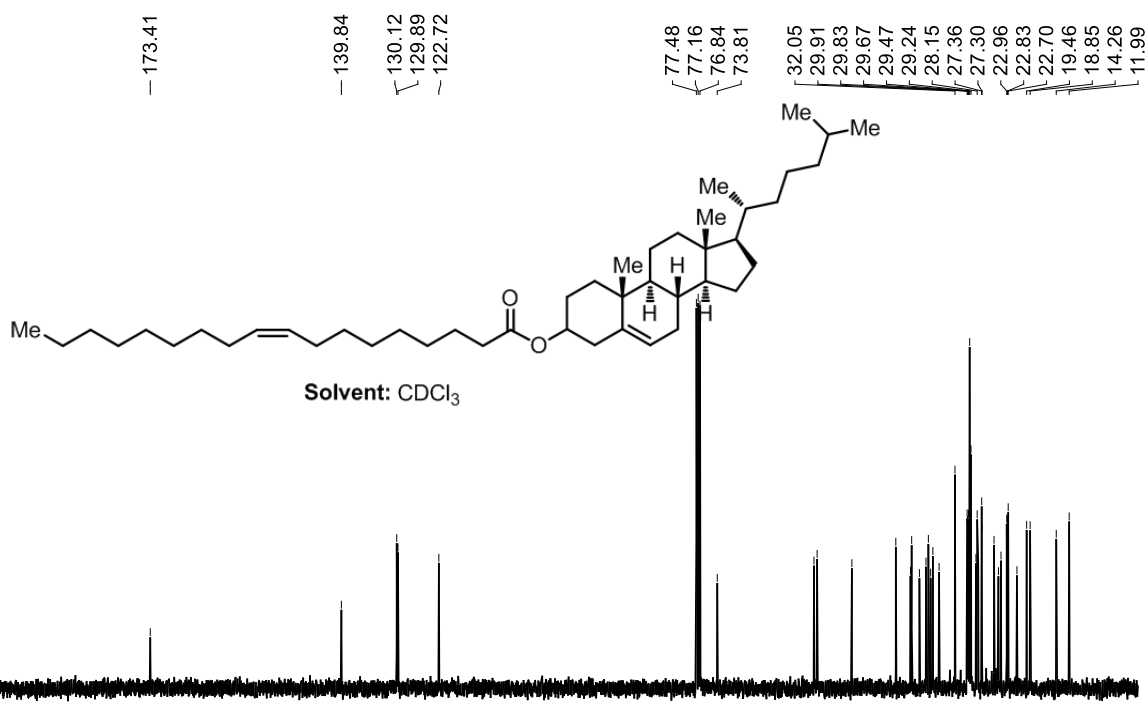
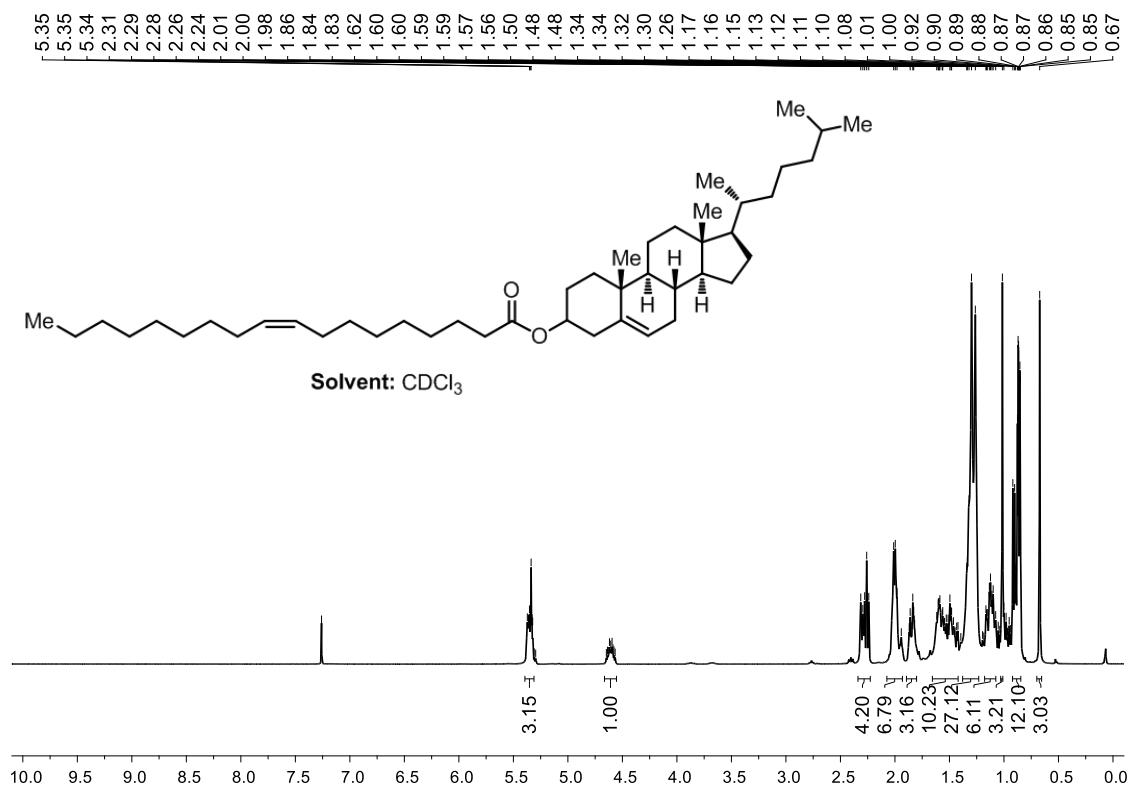


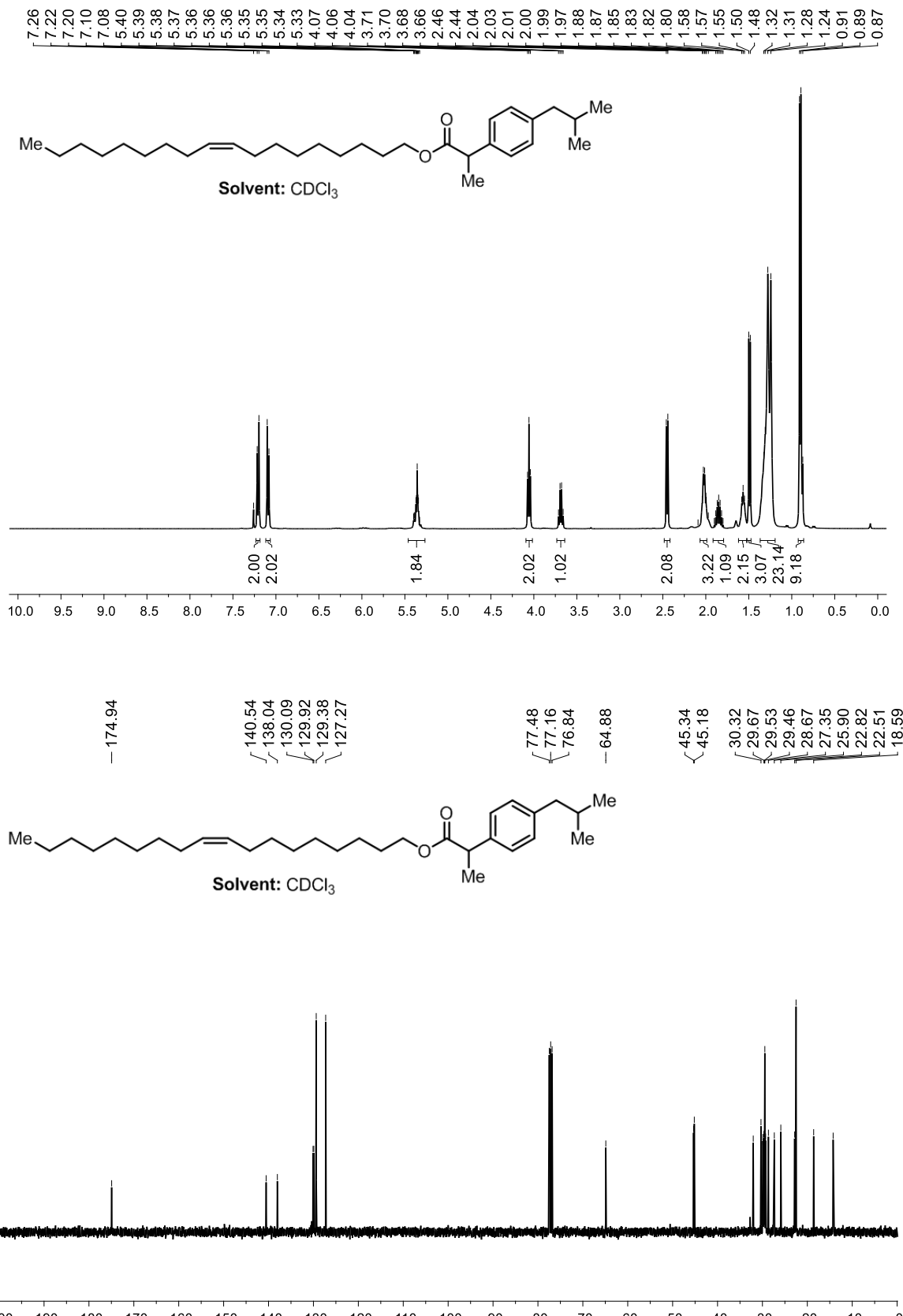


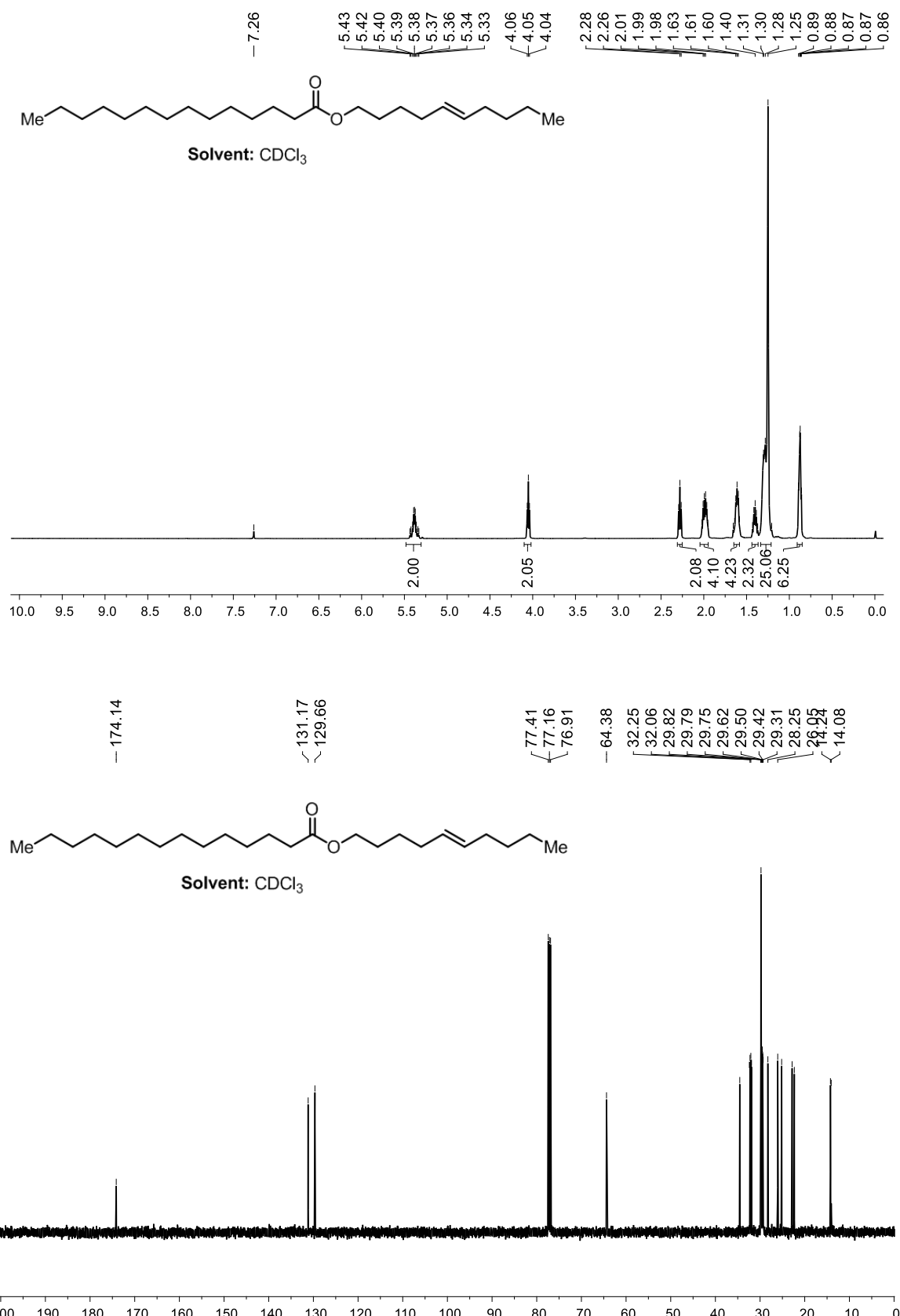












NMR spectra of allylated compounds

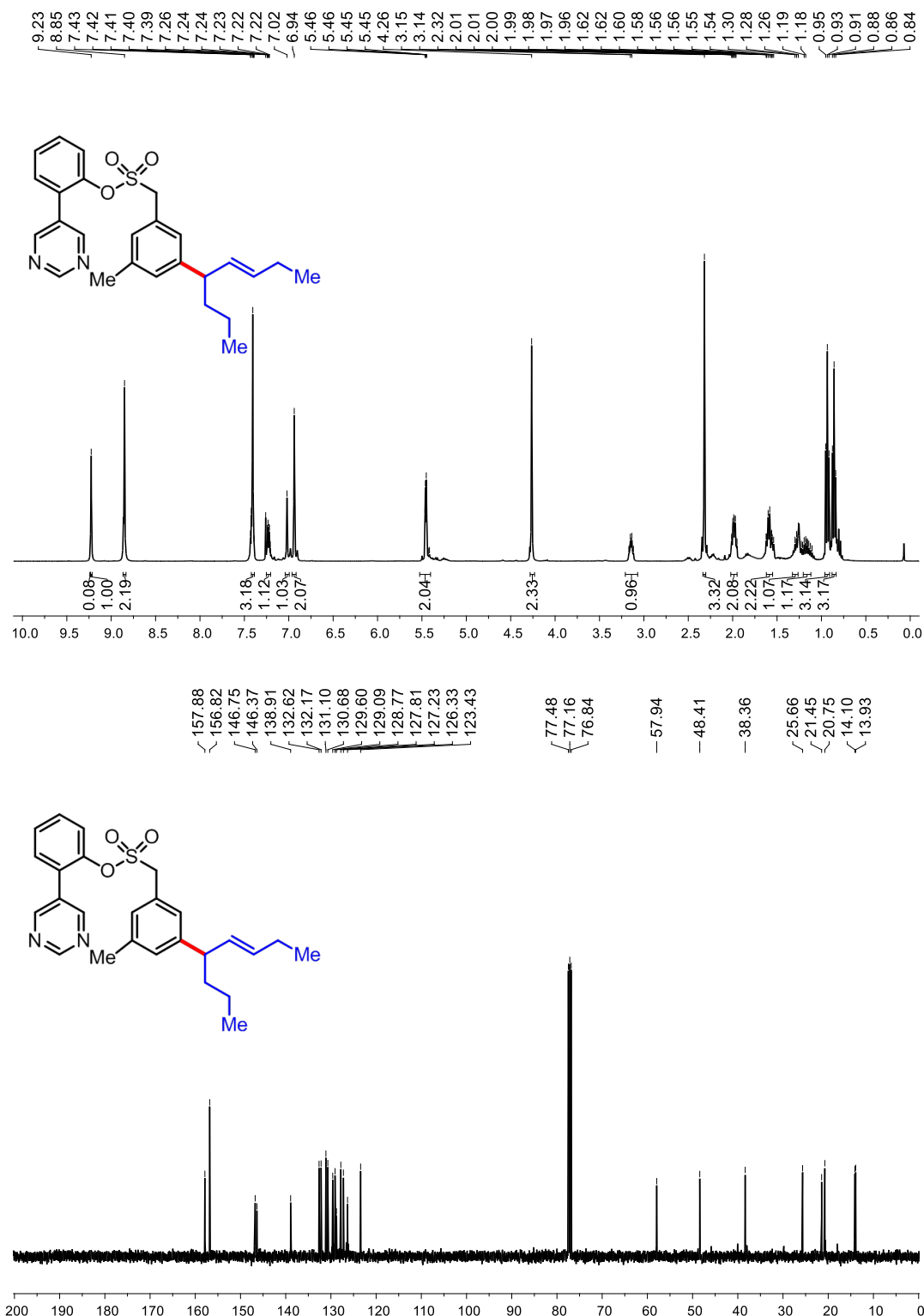
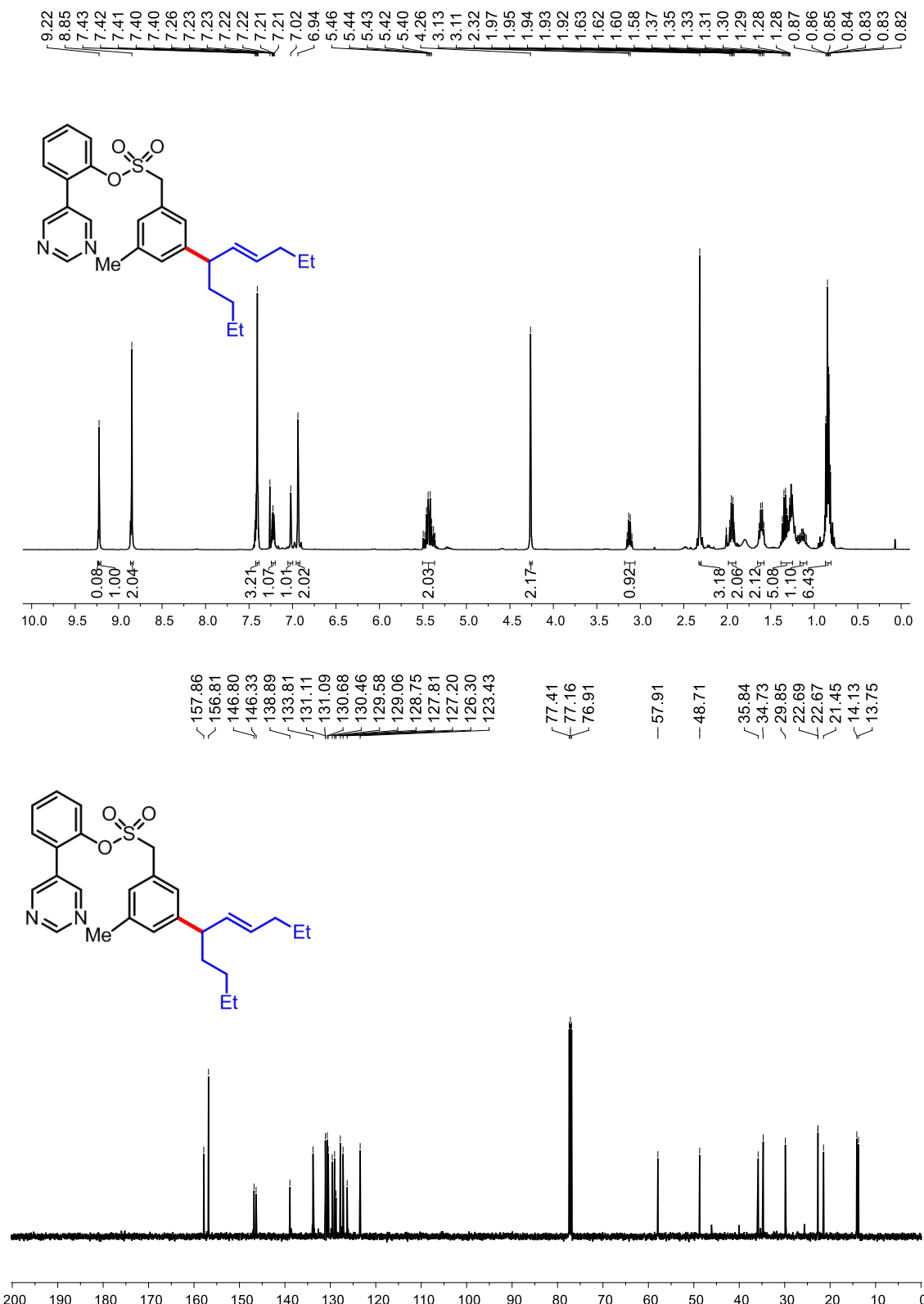
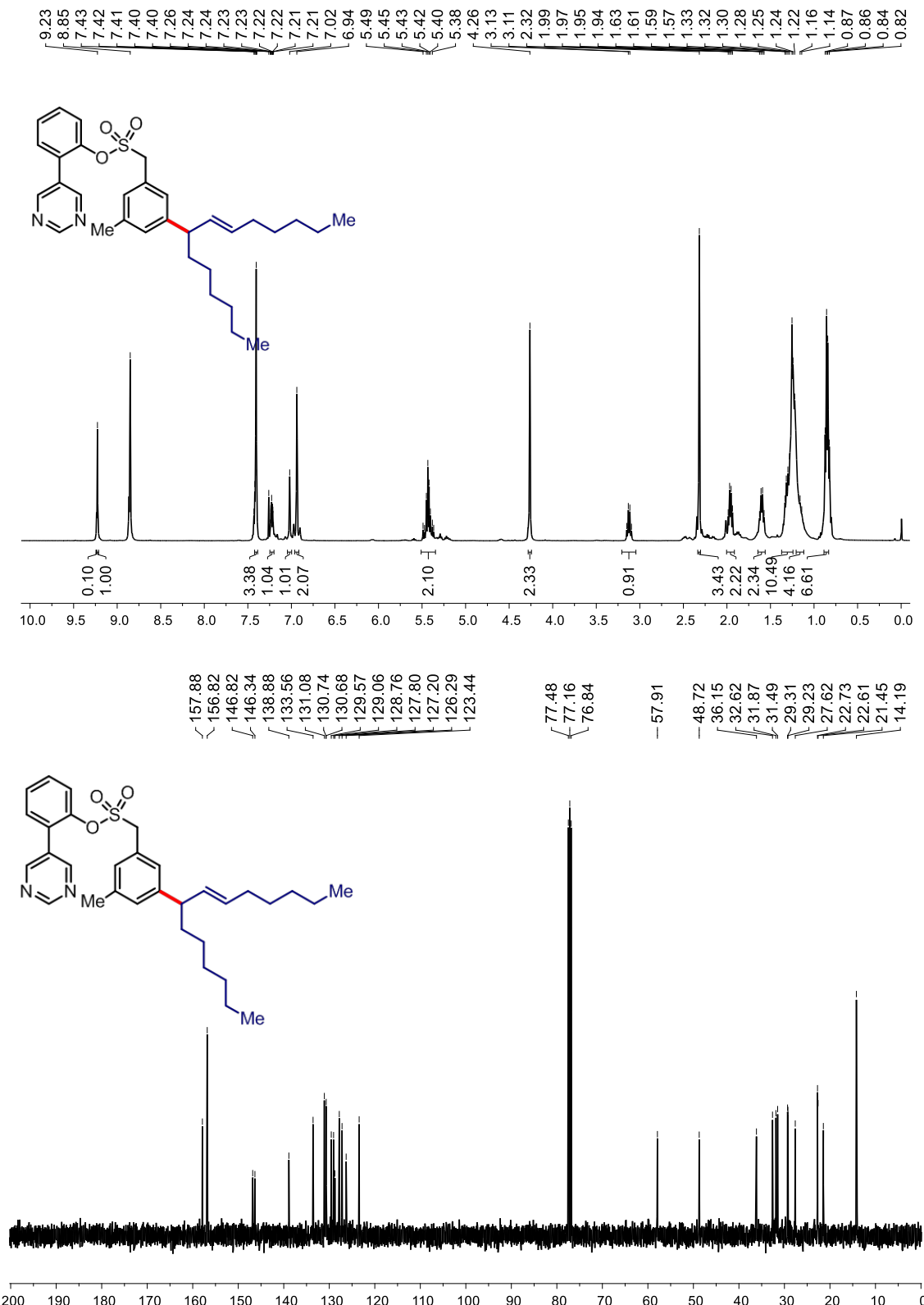


Figure S27. ^1H (top) and ^{13}C (bottom) NMR of **3a**

**Figure S28.** ¹H (top) and ¹³C (bottom) NMR of **3b**

**Figure S29.** ¹H (top) and ¹³C (bottom) NMR of 3c

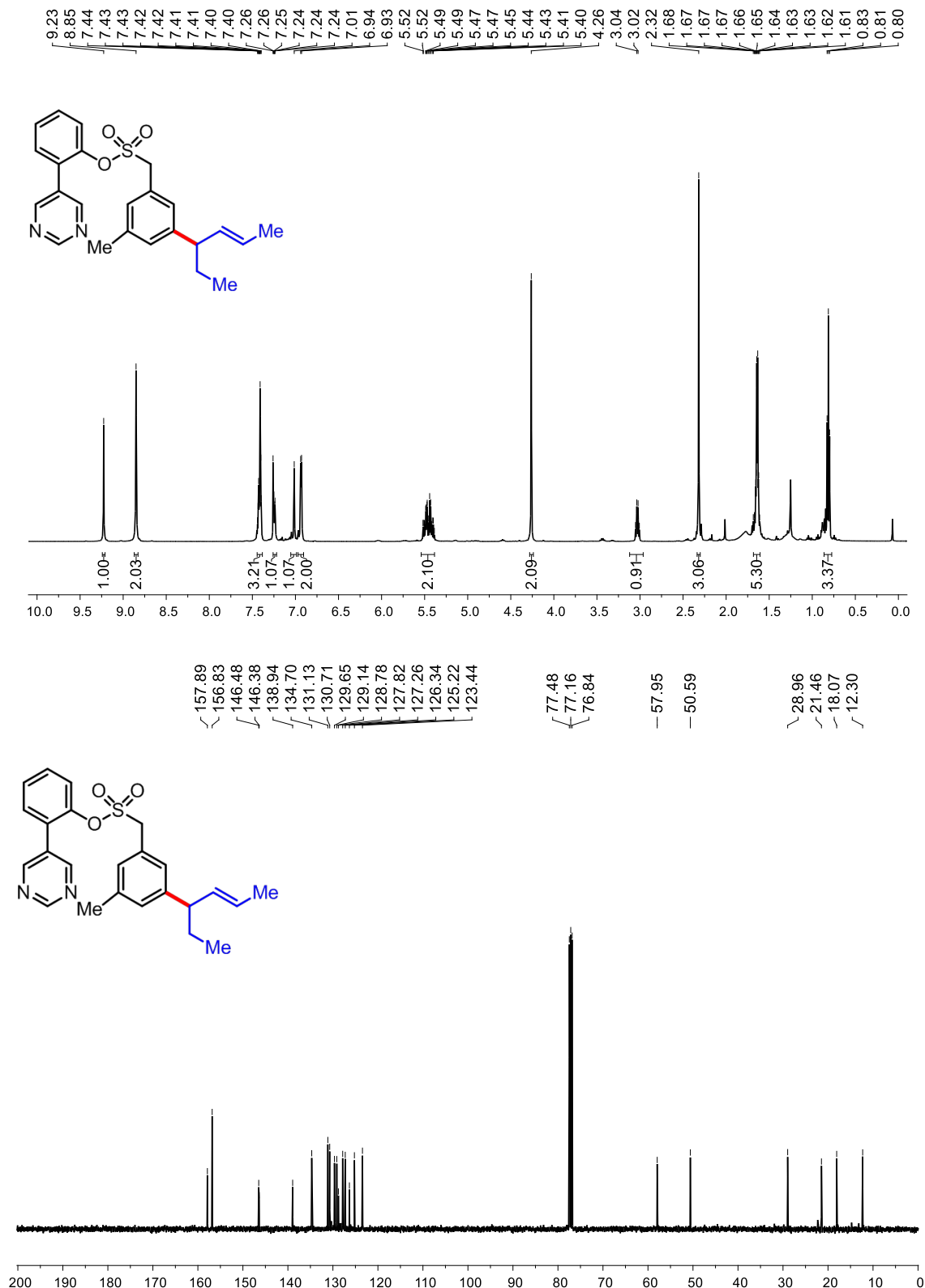


Figure S30. ¹H (top) and ¹³C (bottom) NMR of 3d

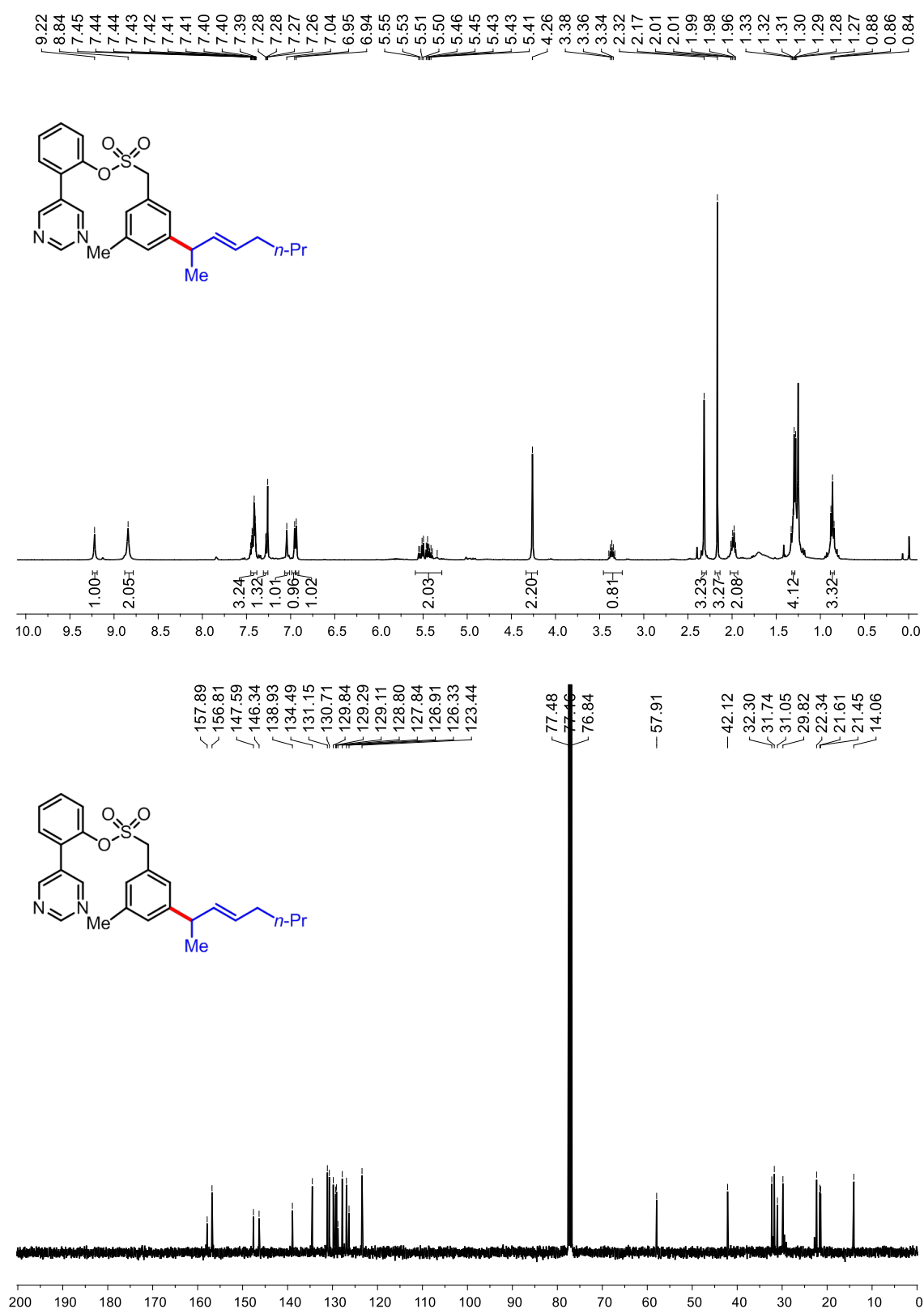


Figure S31. ^1H (top) and ^{13}C (bottom) NMR of **3e**

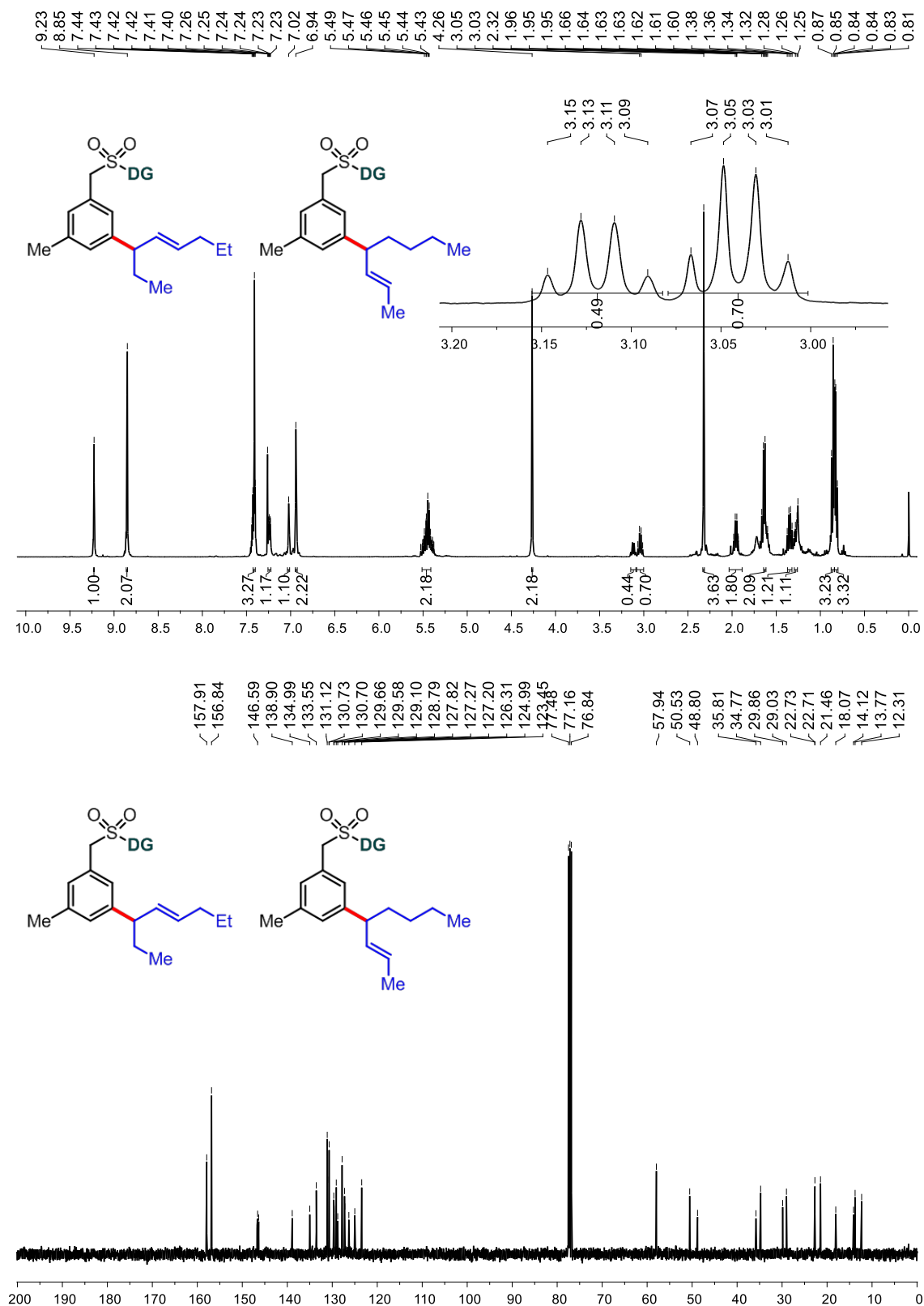
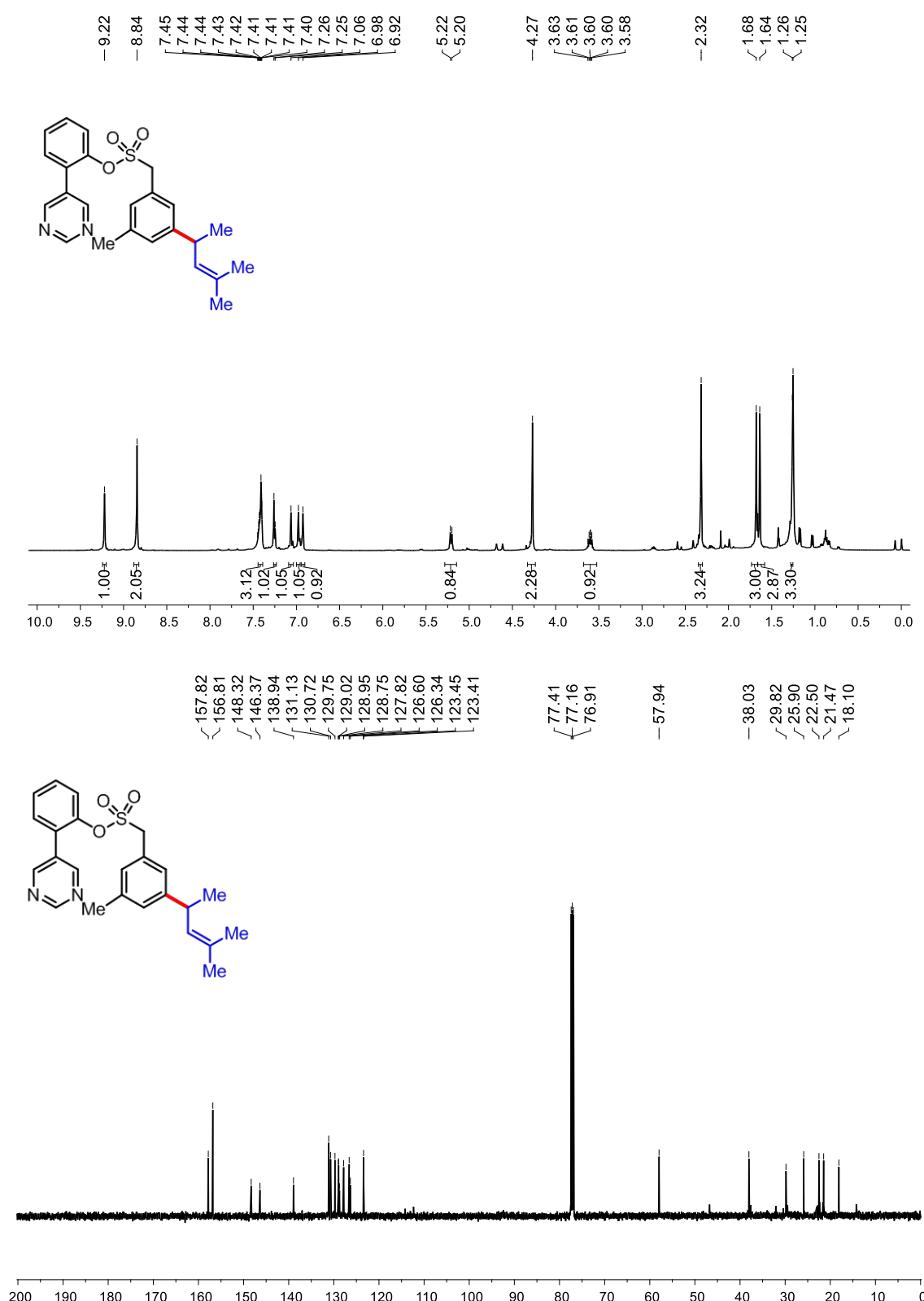


Figure S32. ^1H (top) and ^{13}C (bottom) NMR of **3f**

**Figure S33.** ¹H (top) and ¹³C (bottom) NMR of **3g**

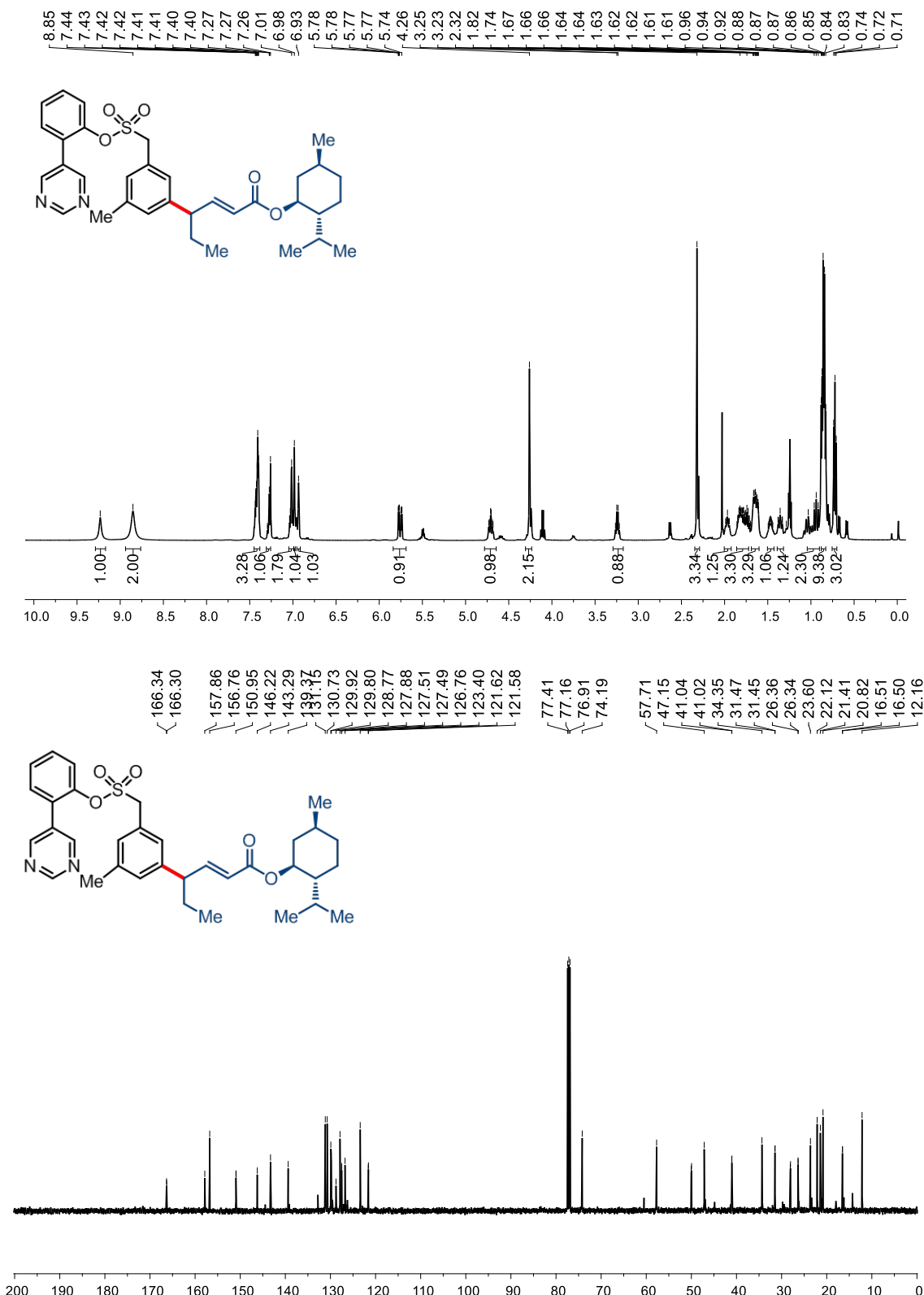


Figure S34. ^1H (top) and ^{13}C (bottom) NMR of **3h**

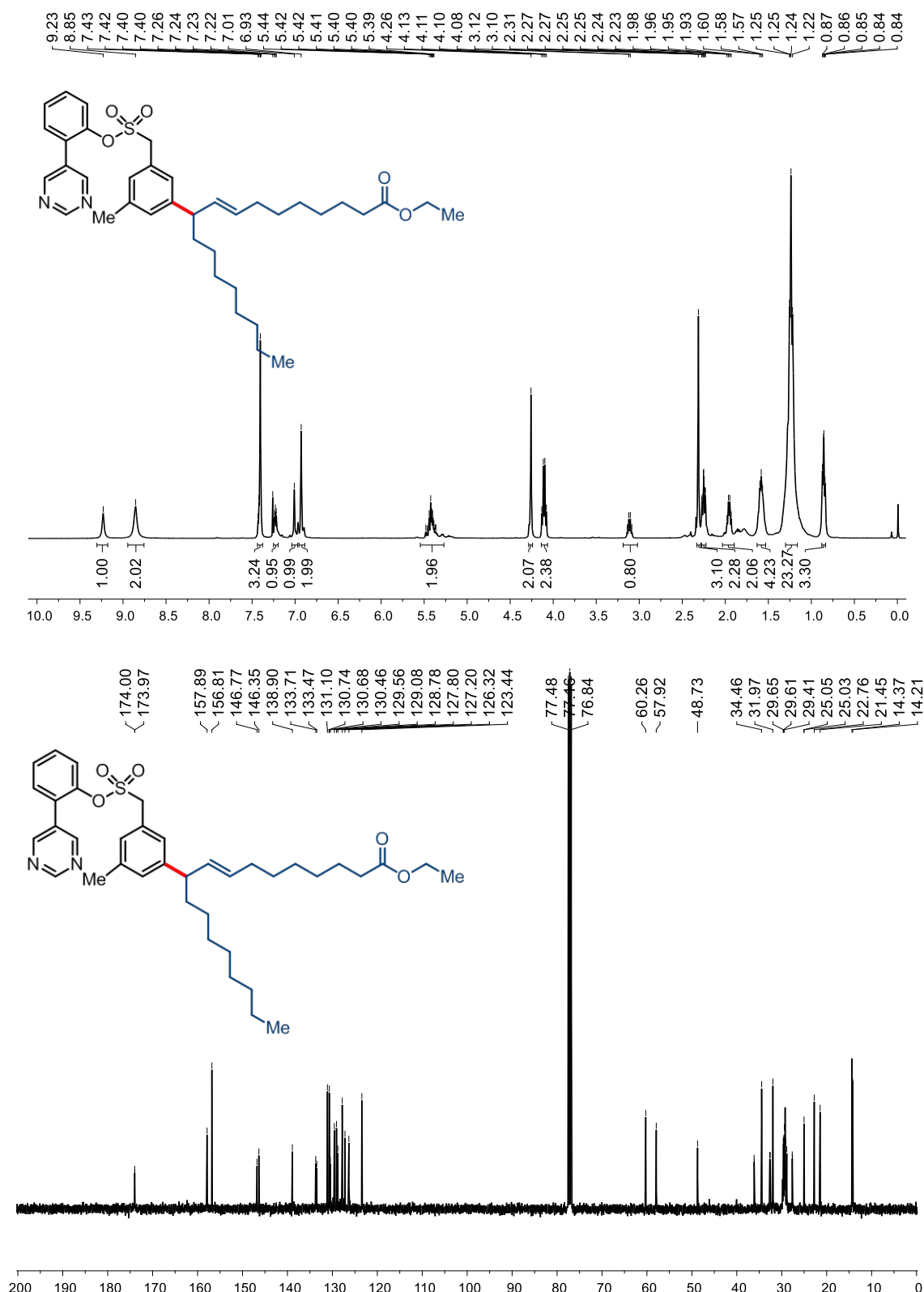


Figure S35. ¹H (top) and ¹³C (bottom) NMR of **3i**

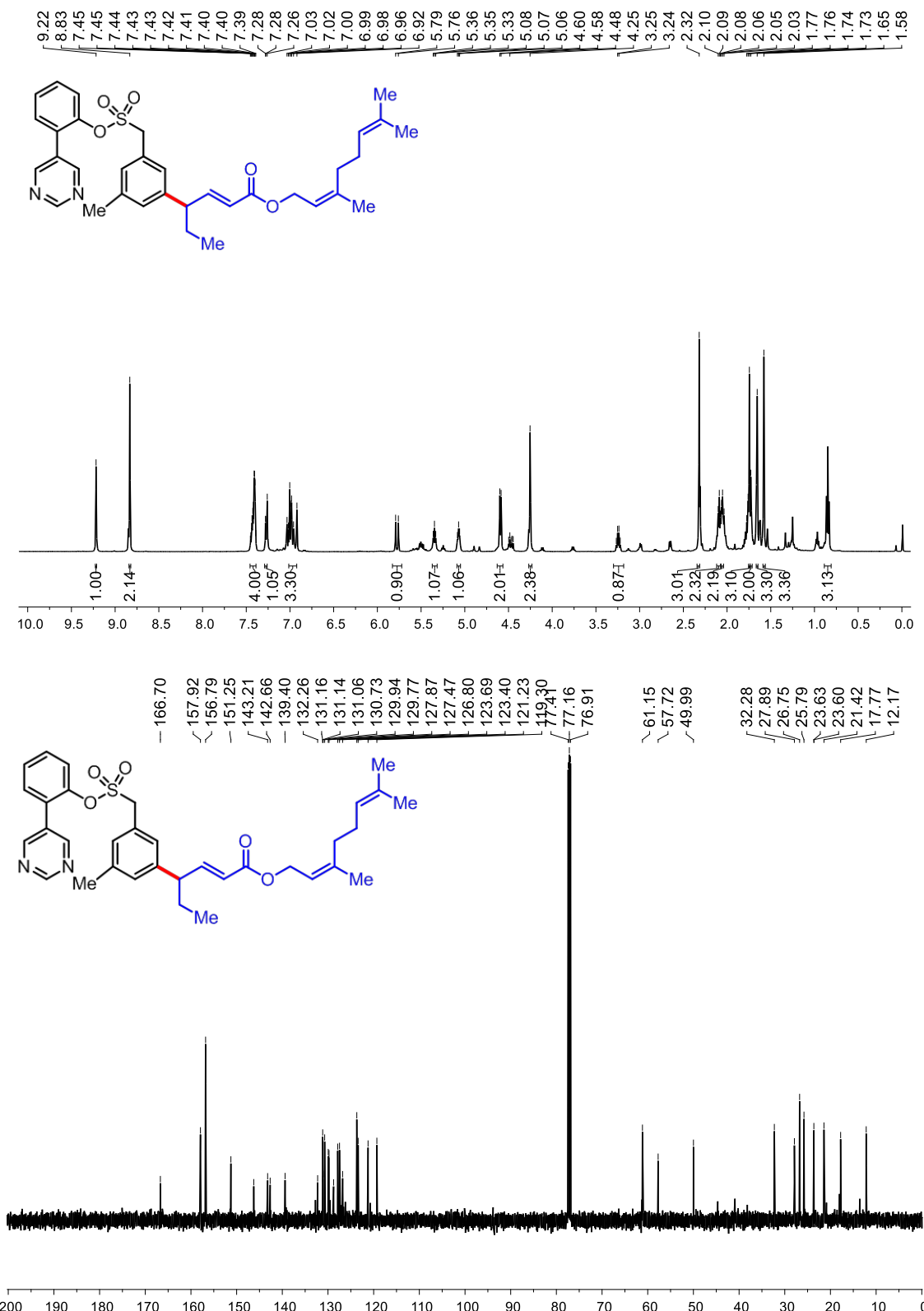


Figure S36. ^1H (top) and ^{13}C (bottom) NMR of **3j**

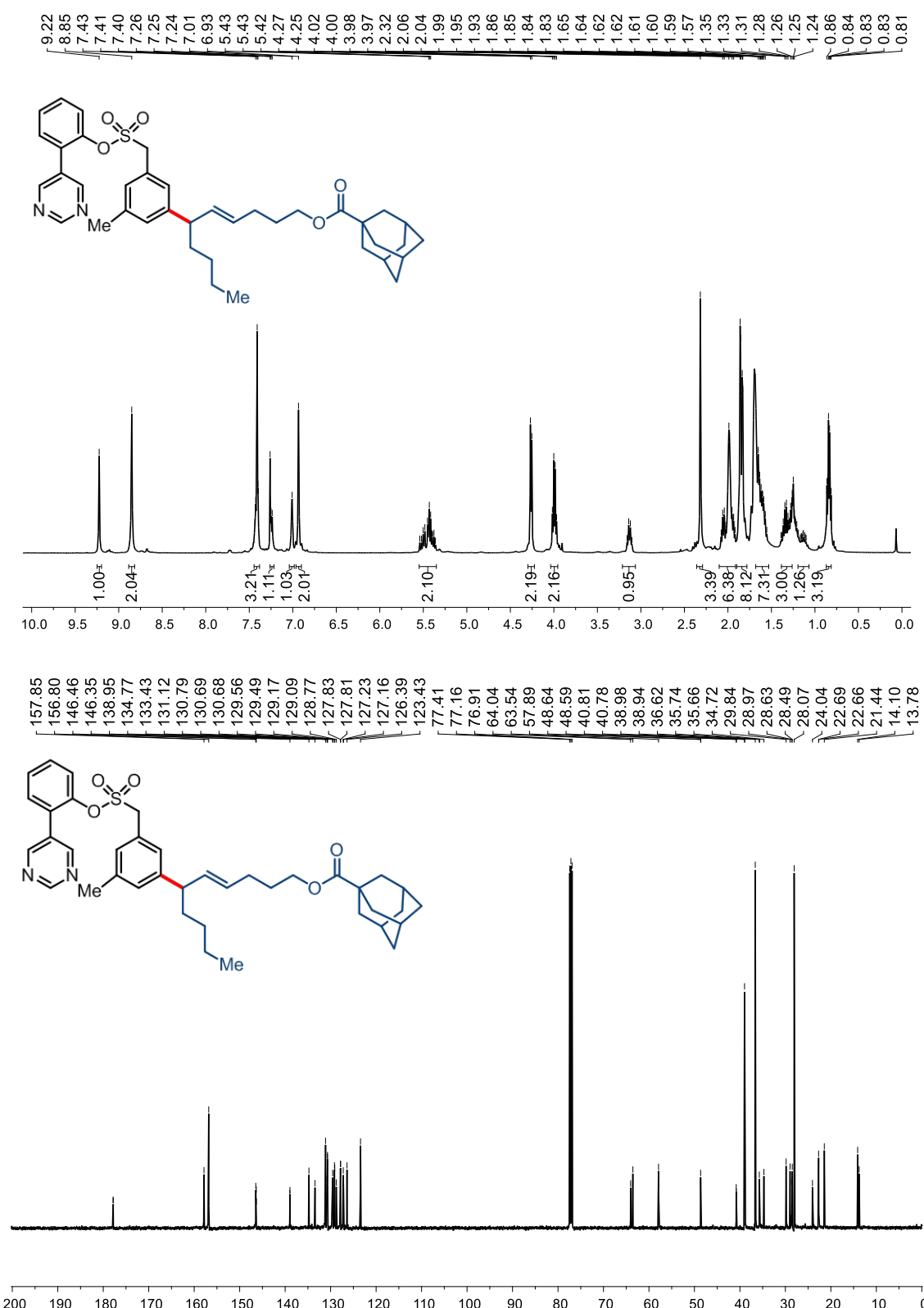


Figure S37. ^1H (top) and ^{13}C (bottom) NMR of **3k**

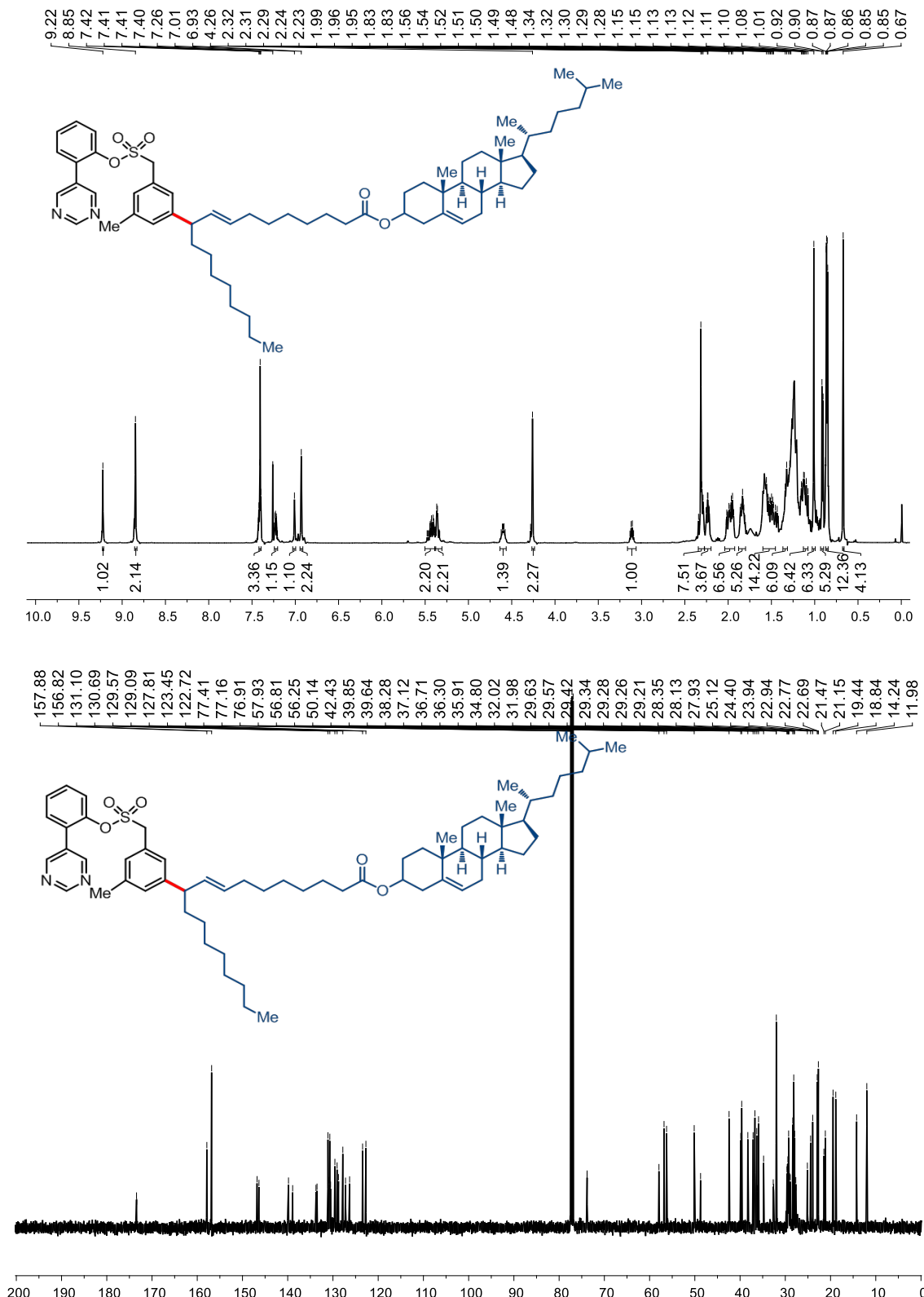
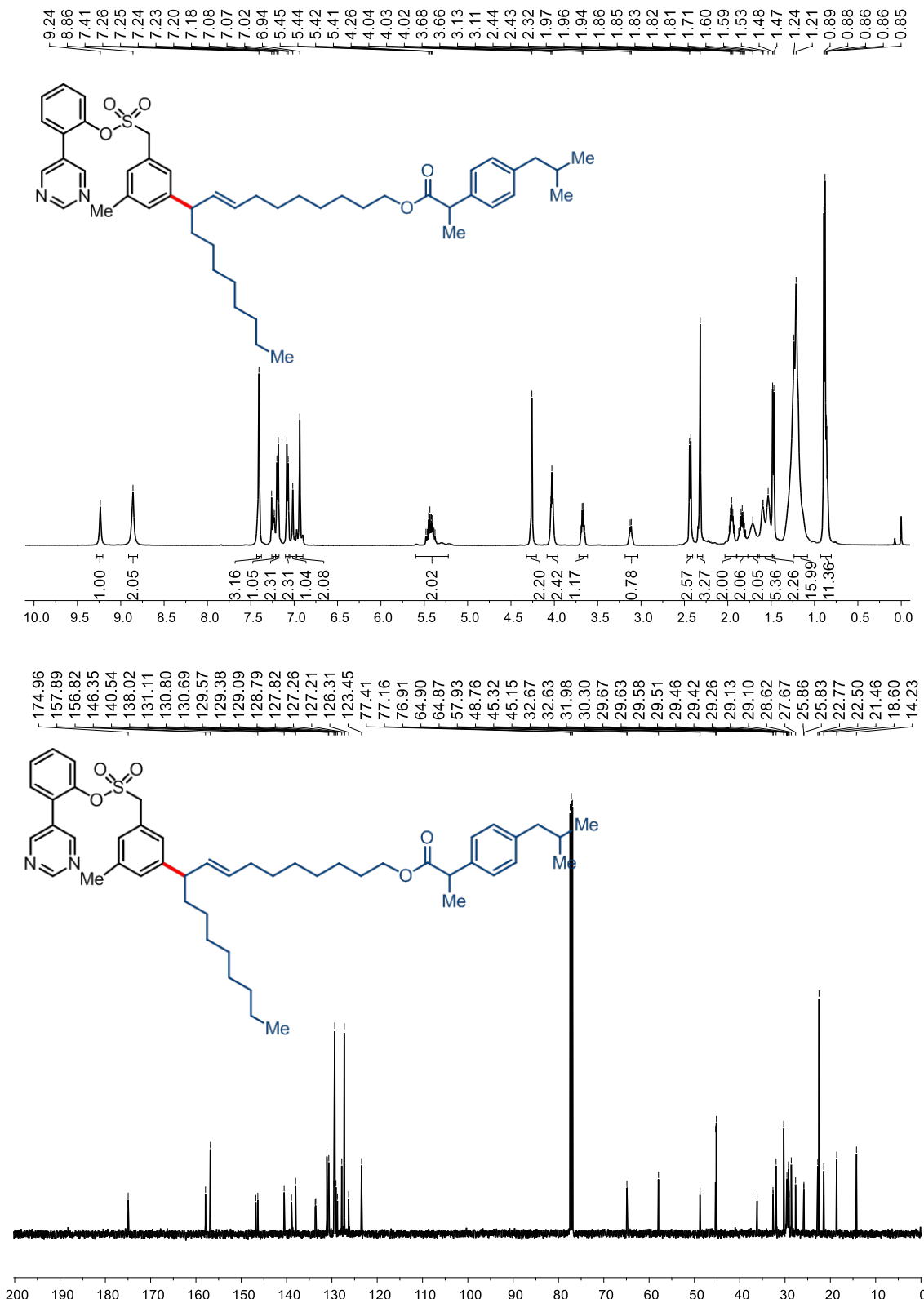


Figure S38. ^1H (top) and ^{13}C (bottom) NMR of **3l**

**Figure S39.** ¹H (top) and ¹³C (bottom) NMR of **3m**

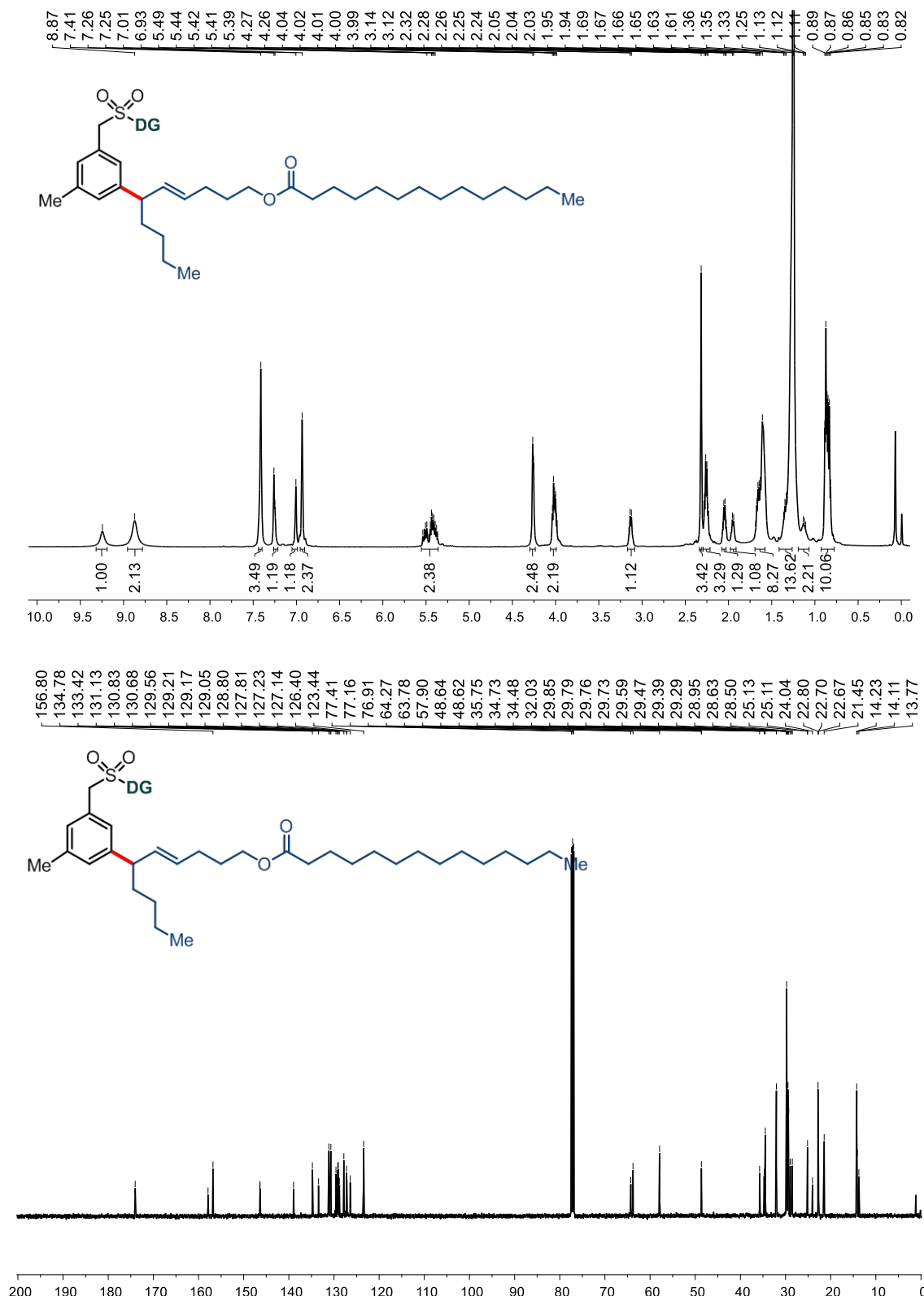


Figure 40. ¹H (top) and ¹³C (bottom) NMR of **3n**

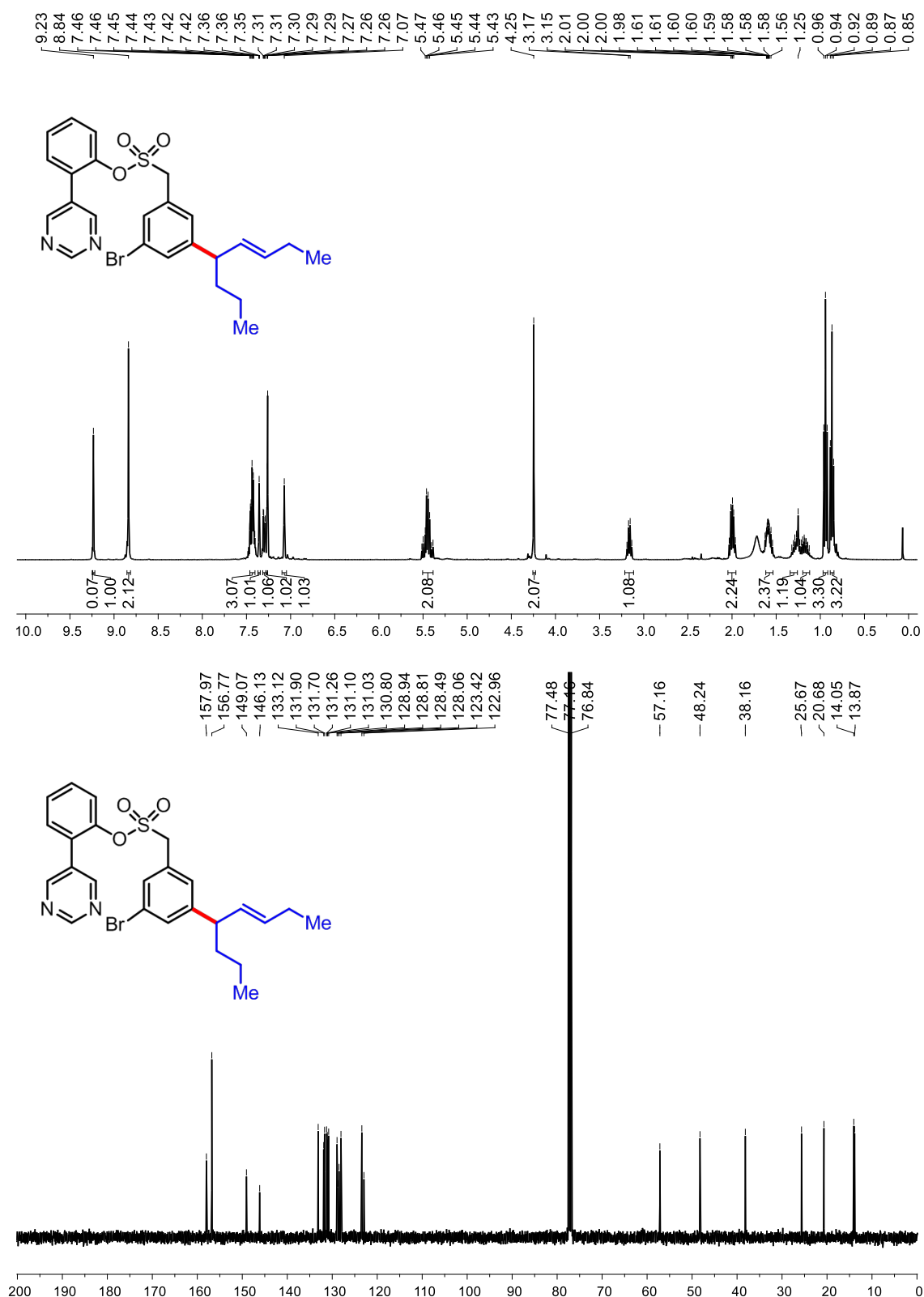
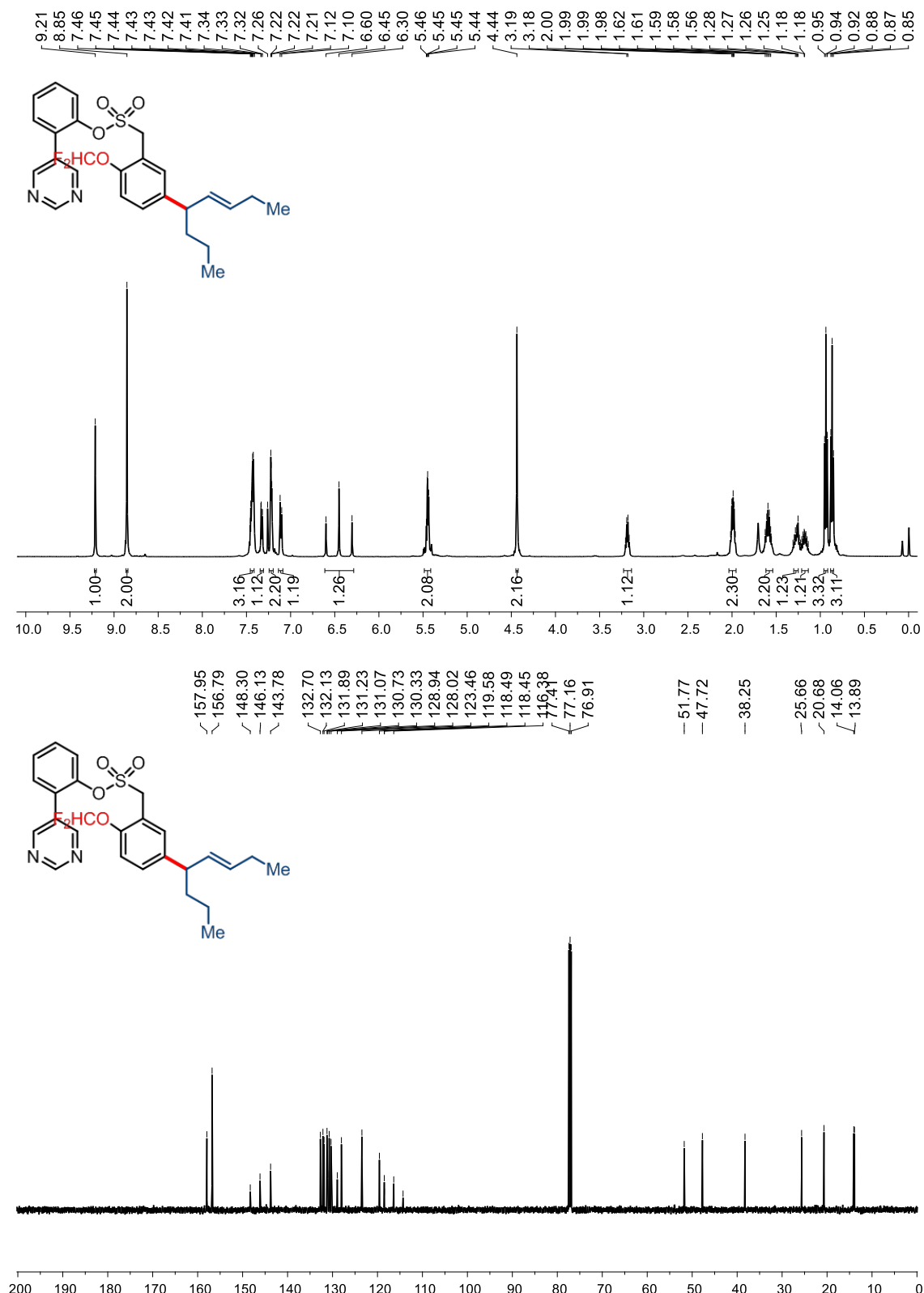


Figure S41. ¹H (top) and ¹³C (bottom) NMR of 3o

**Figure S42.** ¹H (top) and ¹³C (bottom) NMR of 3p

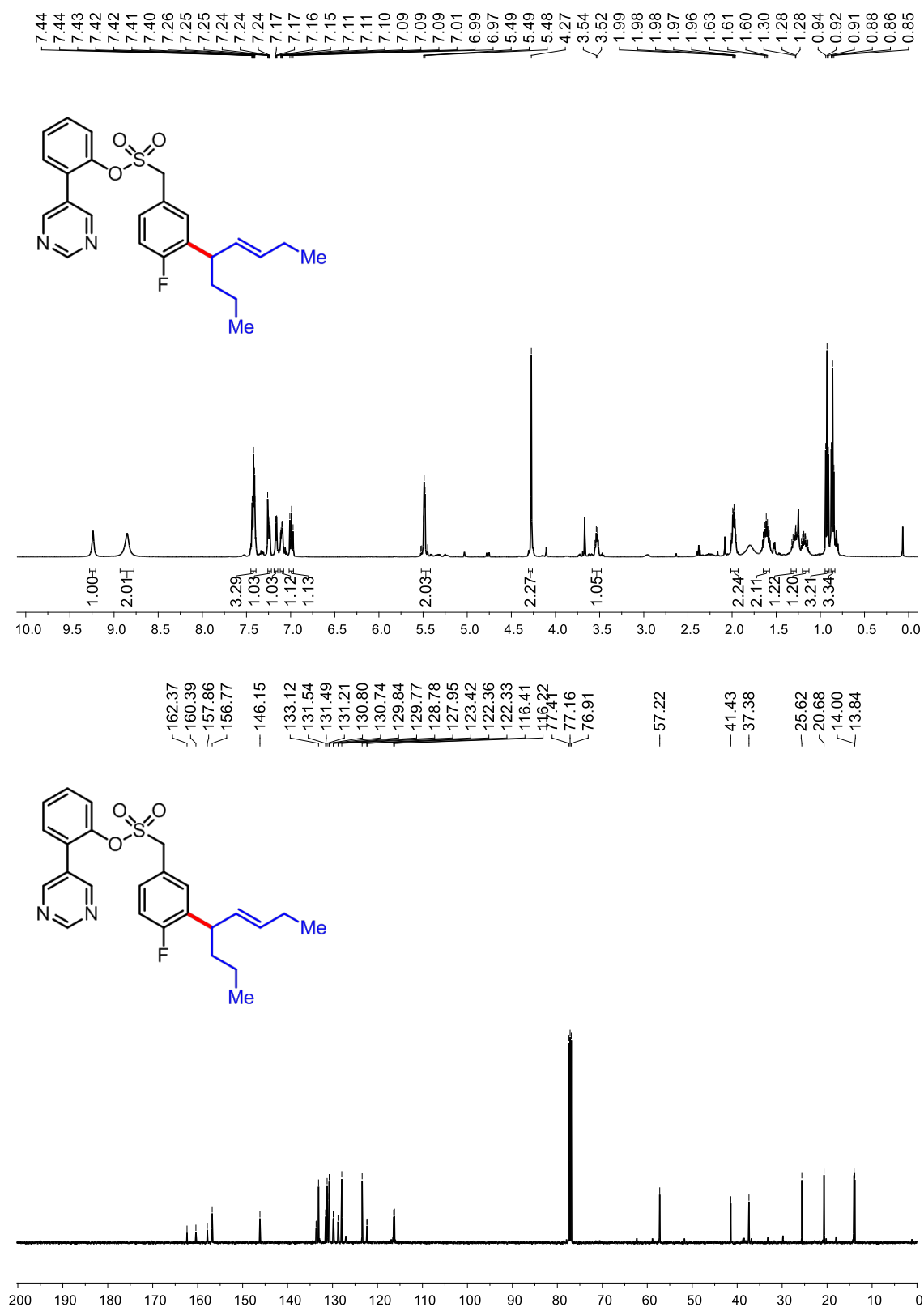
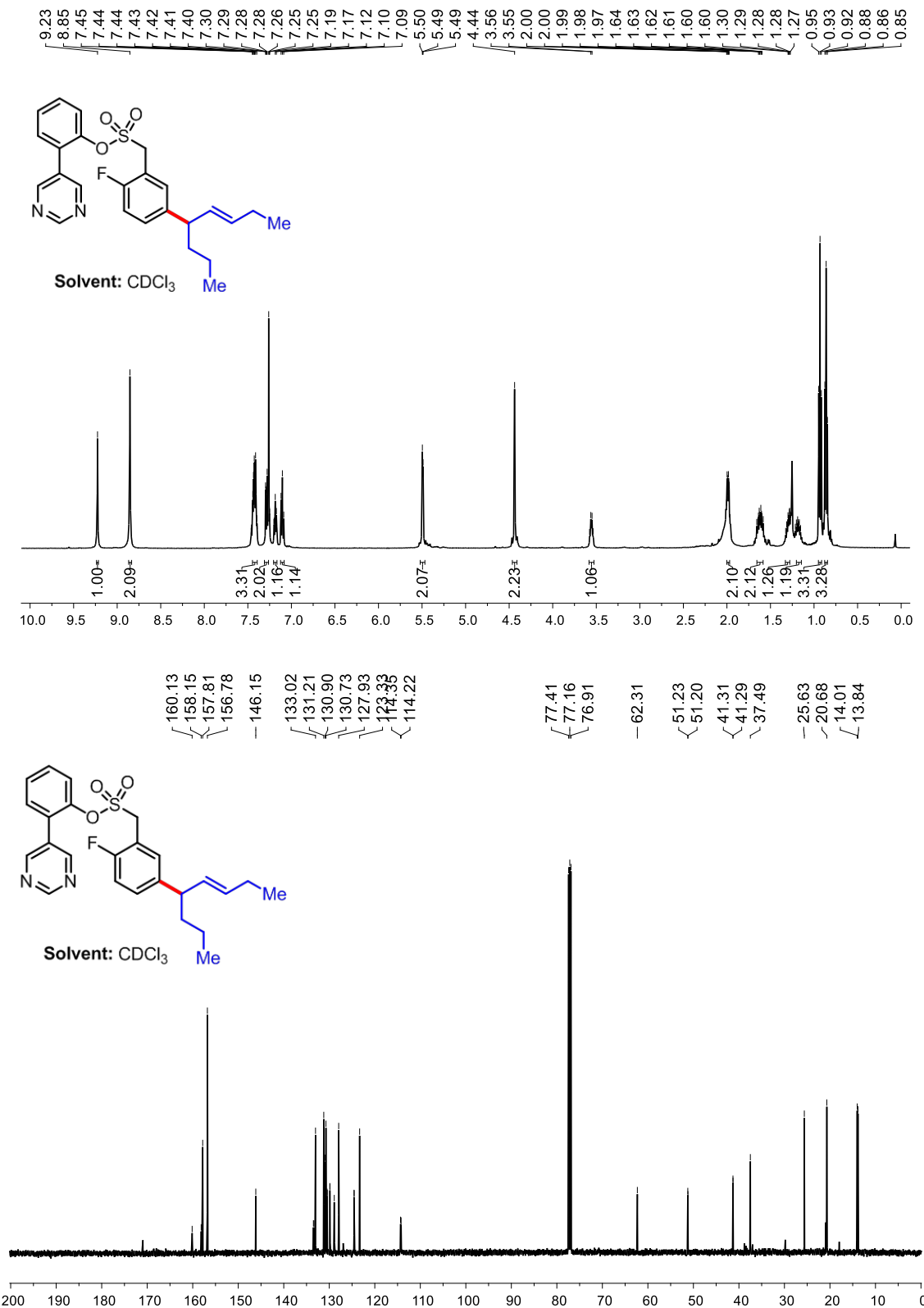


Figure S43. ¹H (top) and ¹³C (bottom) NMR of 3q

**Figure S44.** ^1H (top) and ^{13}C (bottom) NMR of **3r**

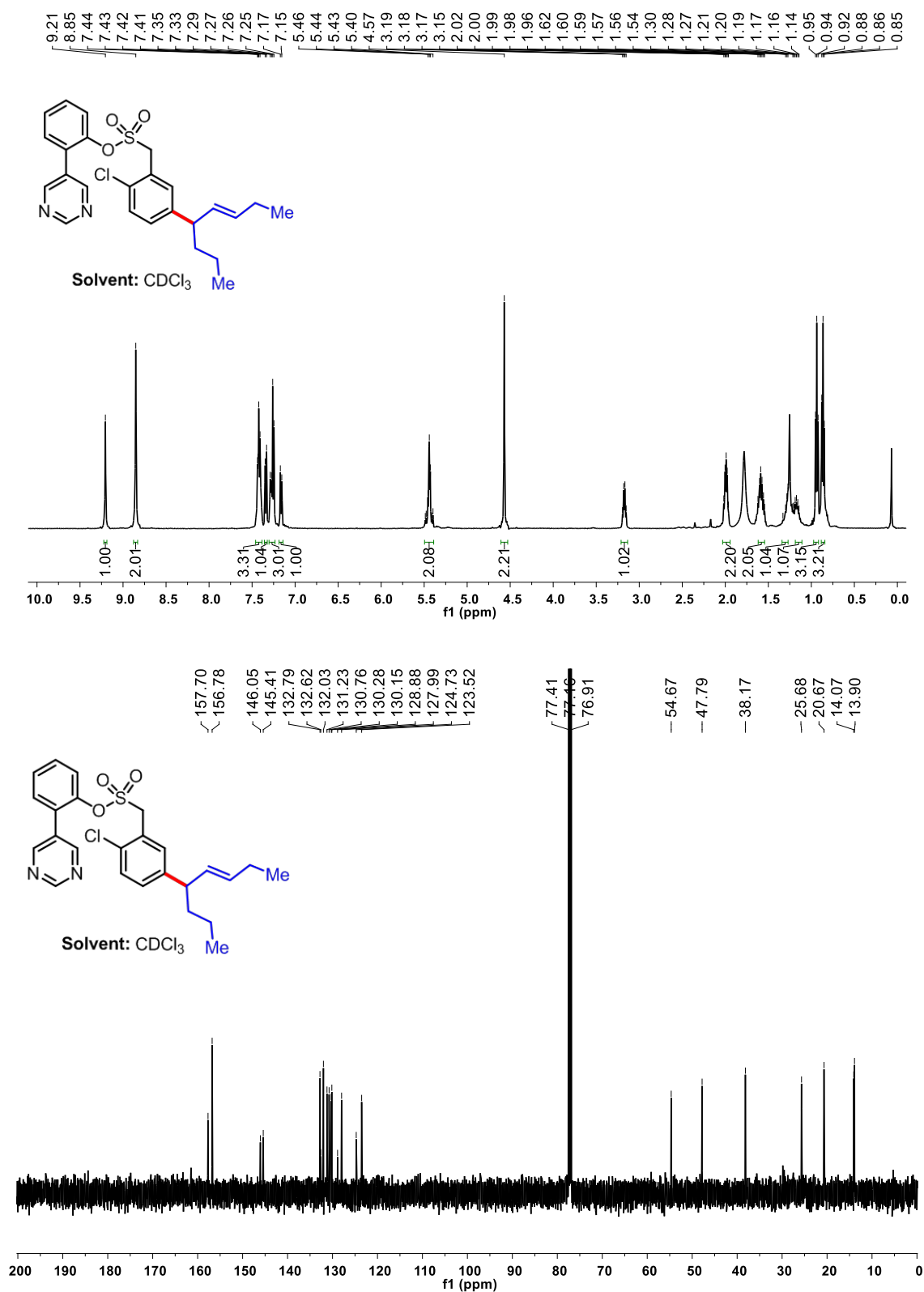
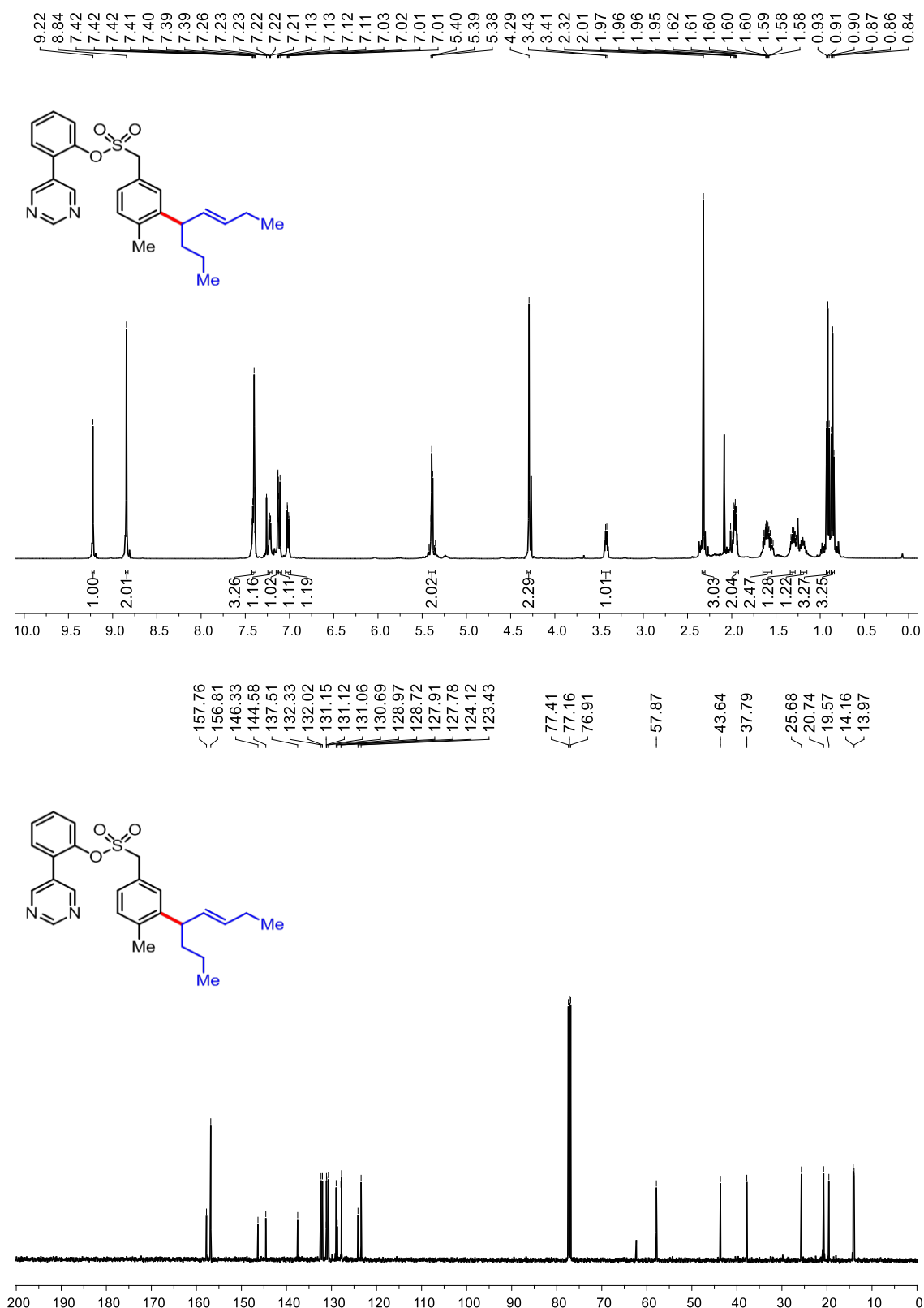


Figure S45. ¹H (top) and ¹³C (bottom) NMR of 3s

**Figure S46.** ¹H (top) and ¹³C (bottom) NMR of 3t

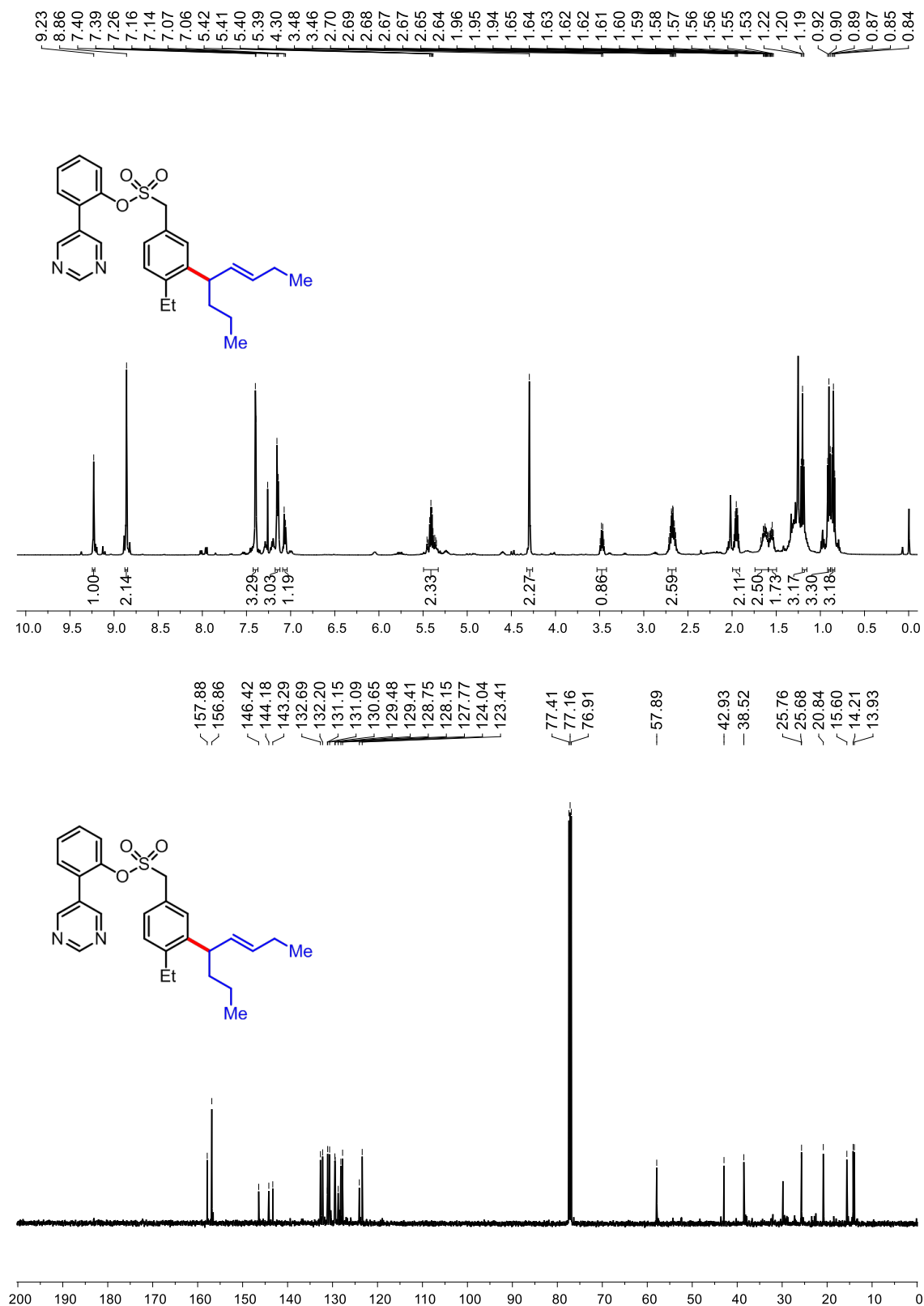
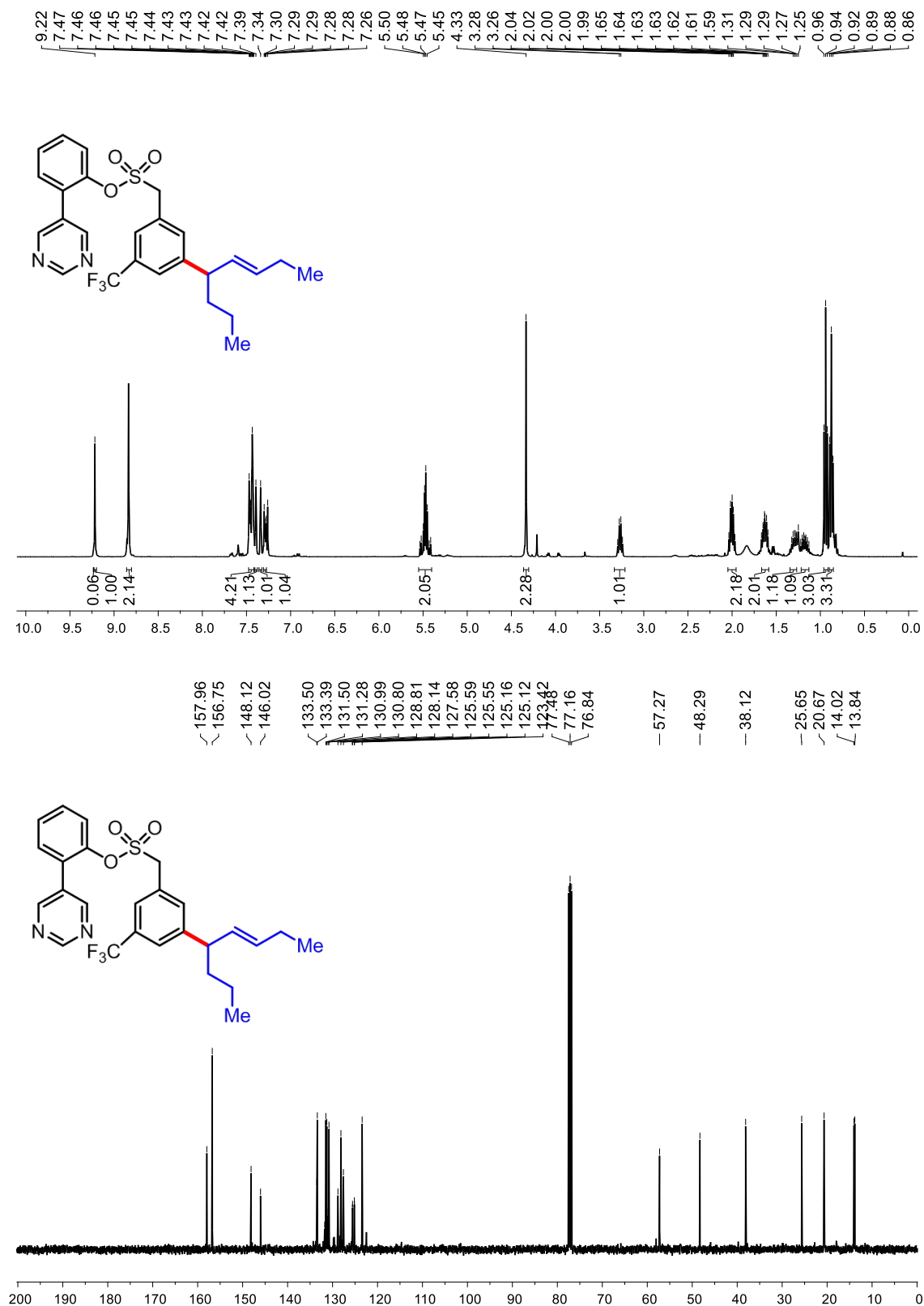


Figure S47. ^1H (top) and ^{13}C (bottom) NMR of **3u**

**Figure S48.** ¹H (top) and ¹³C (bottom) NMR of **3v**

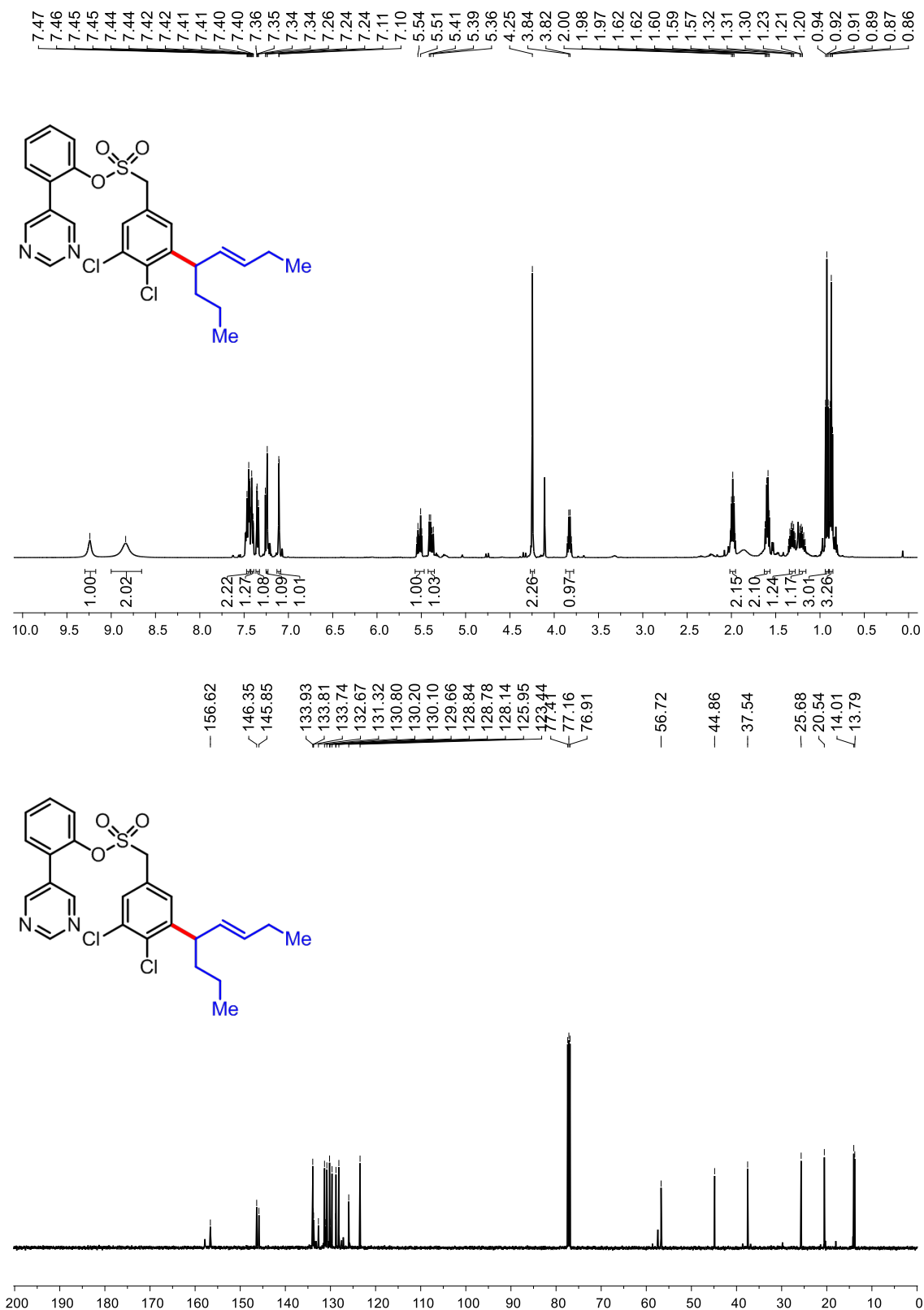


Figure S49. ^1H (top) and ^{13}C (bottom) NMR of **3w**

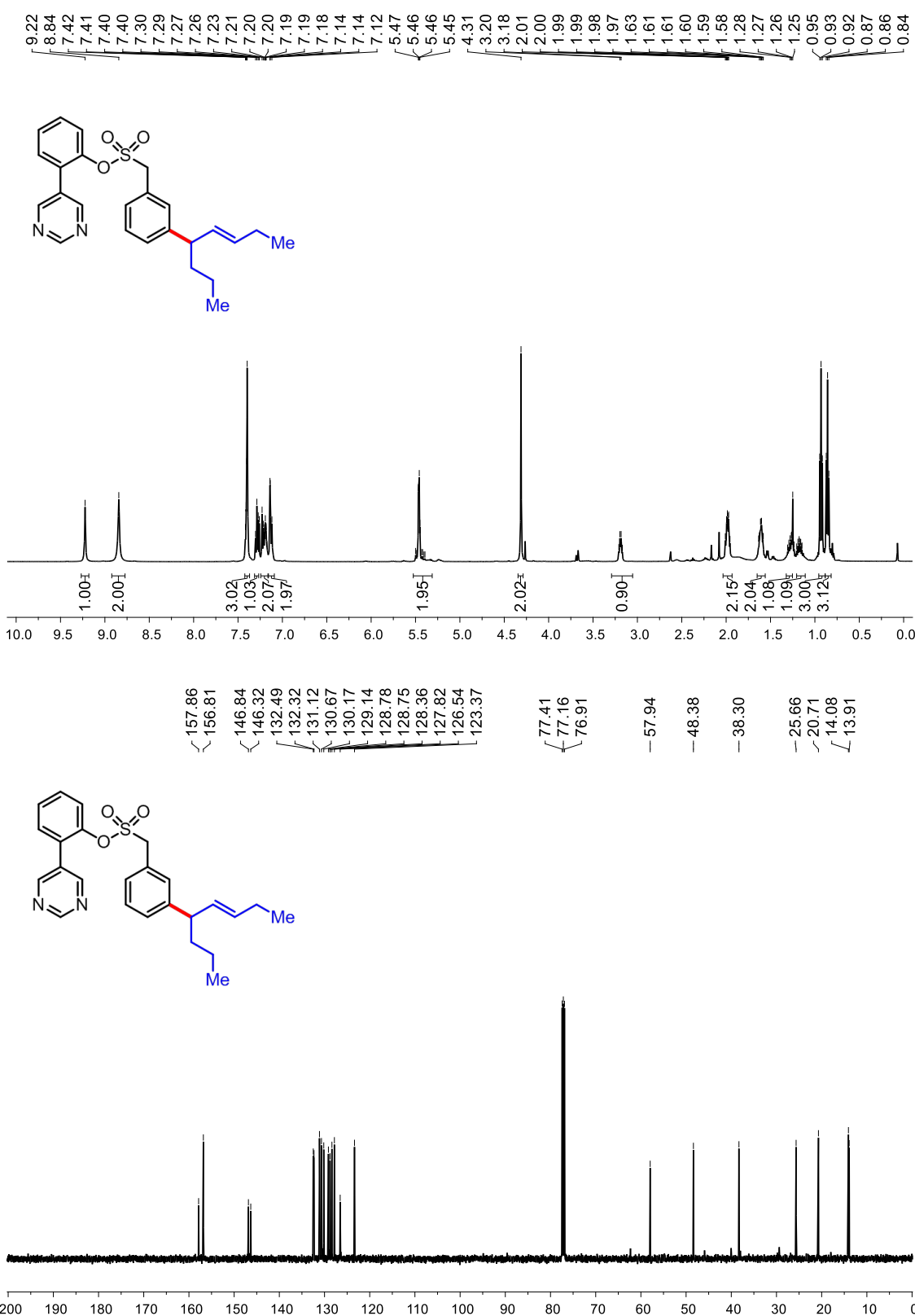


Figure S50. ^1H (top) and ^{13}C (bottom) NMR of **3x**

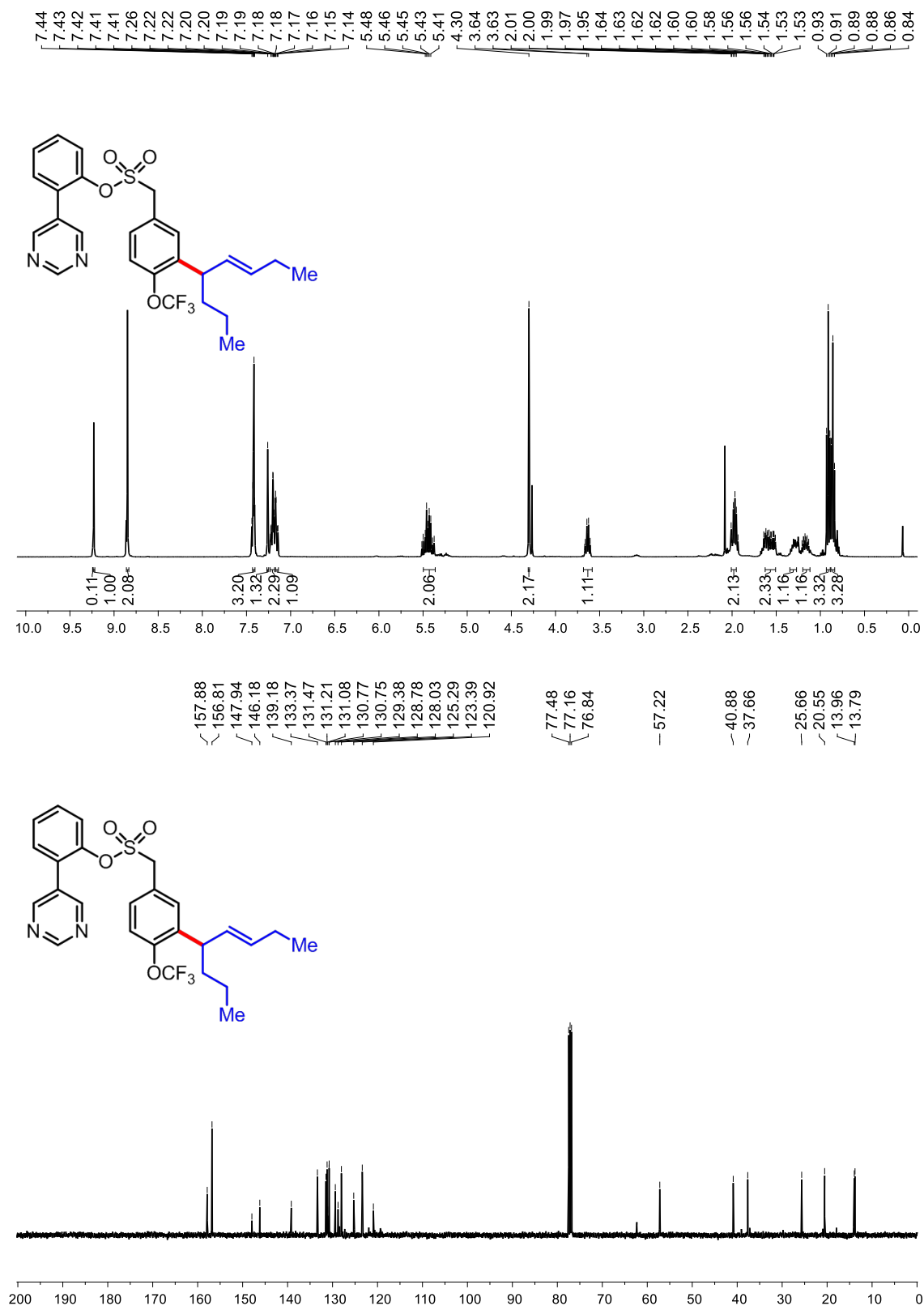


Figure S51. ¹H (top) and ¹³C (bottom) NMR of 3y

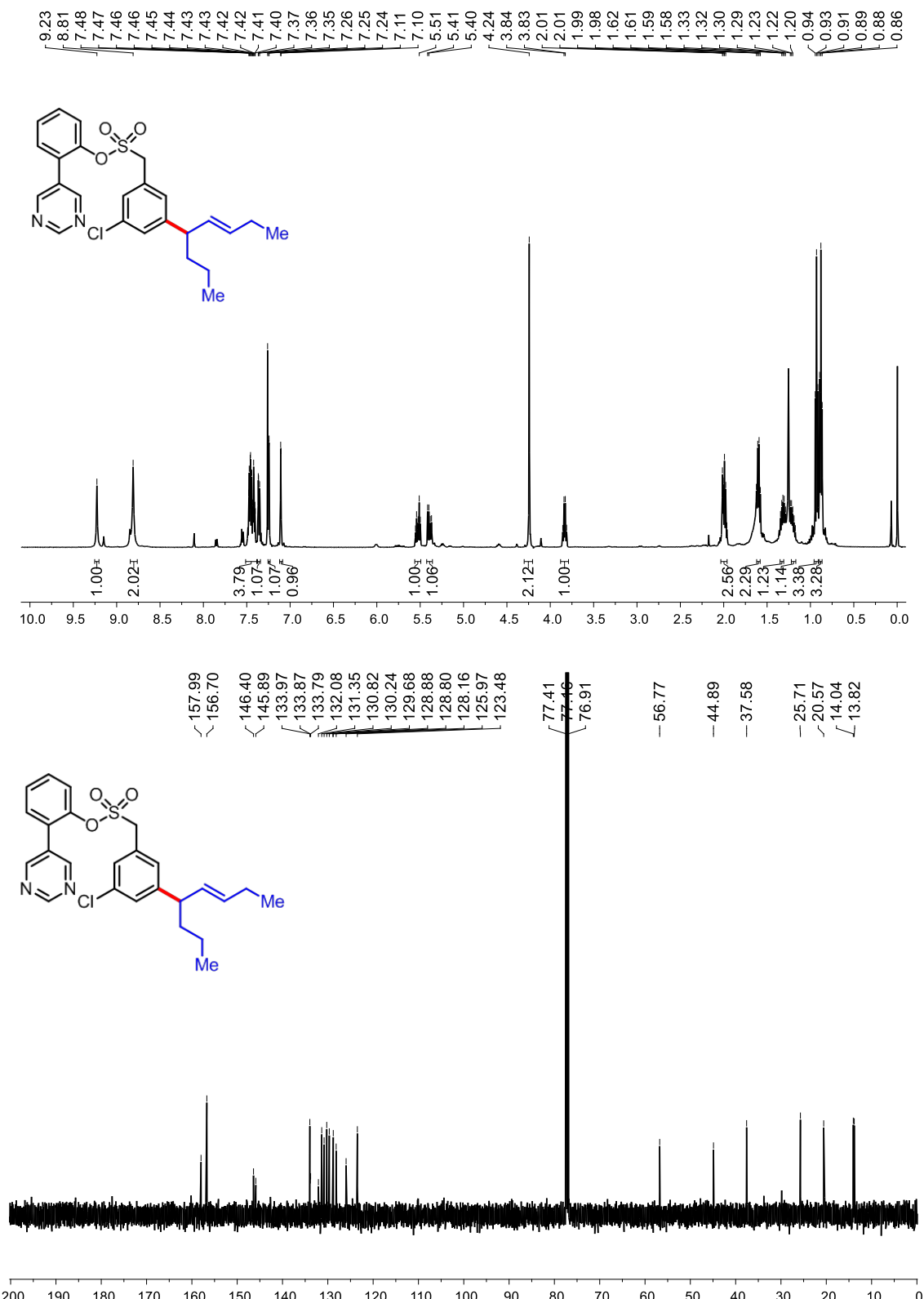


Figure S52. ^1H (top) and ^{13}C (bottom) NMR of **3z**

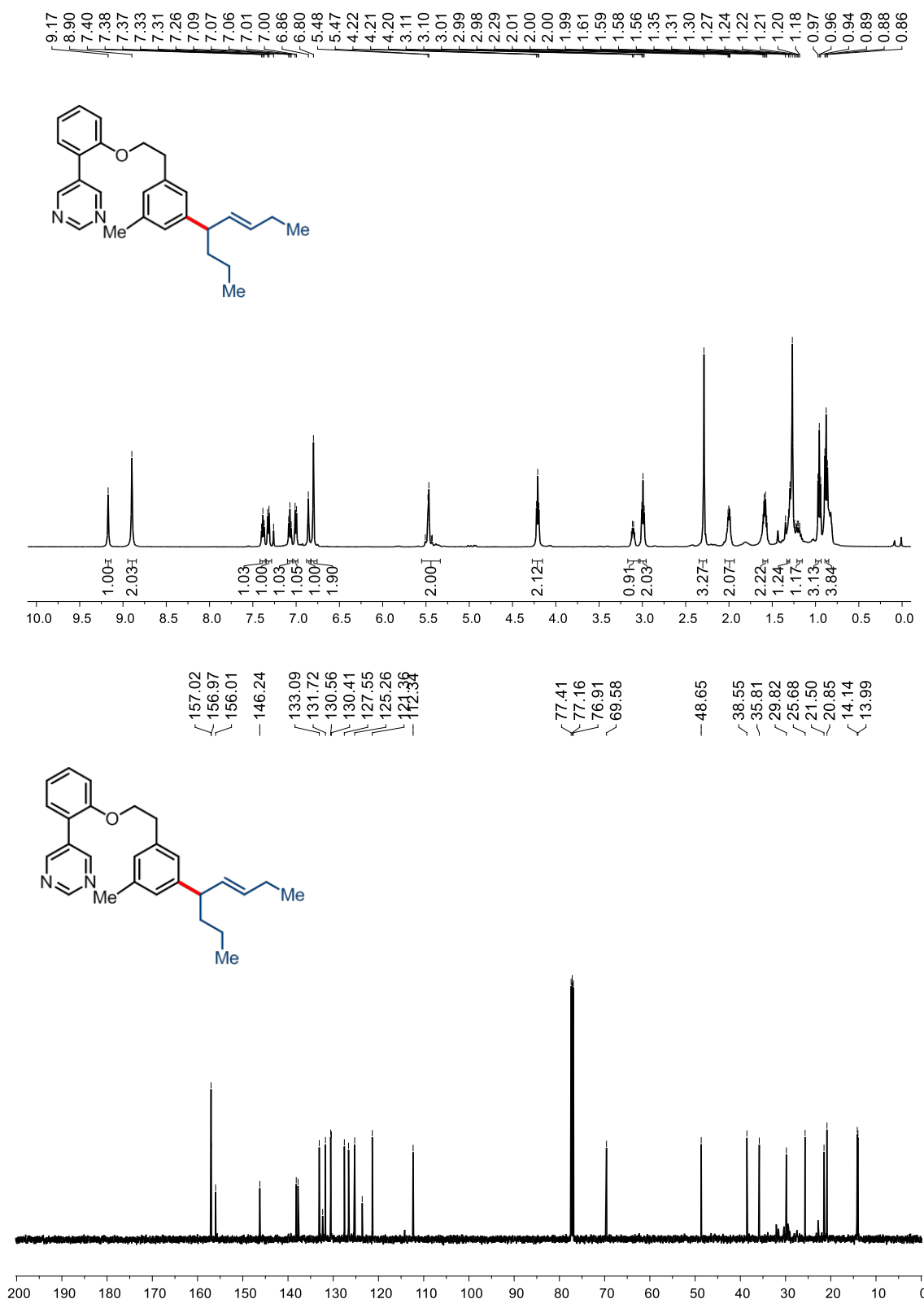
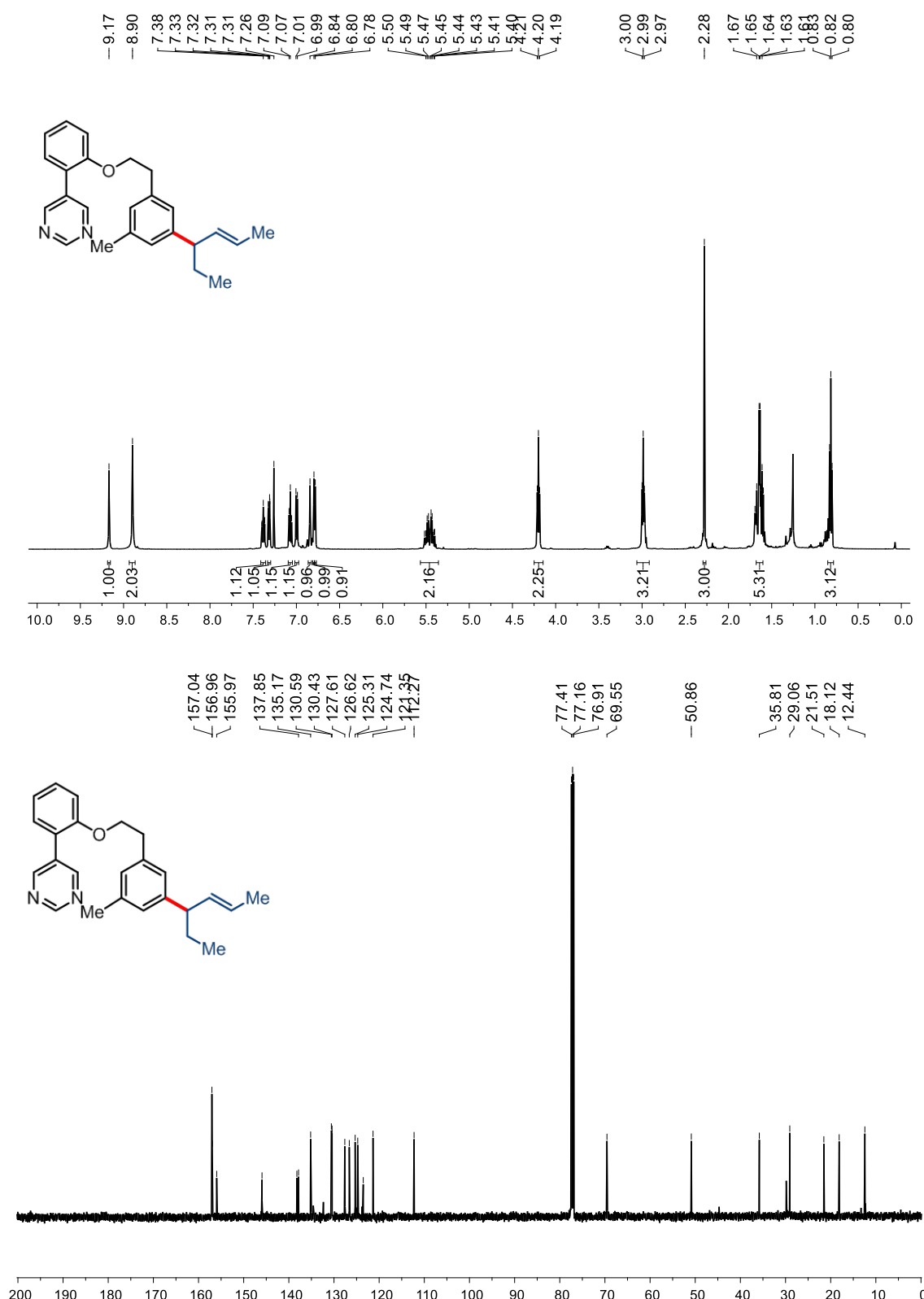


Figure S53. ¹H (top) and ¹³C (bottom) NMR of **5a**

**Figure S54.** ^1H (top) and ^{13}C (bottom) NMR of **5b**

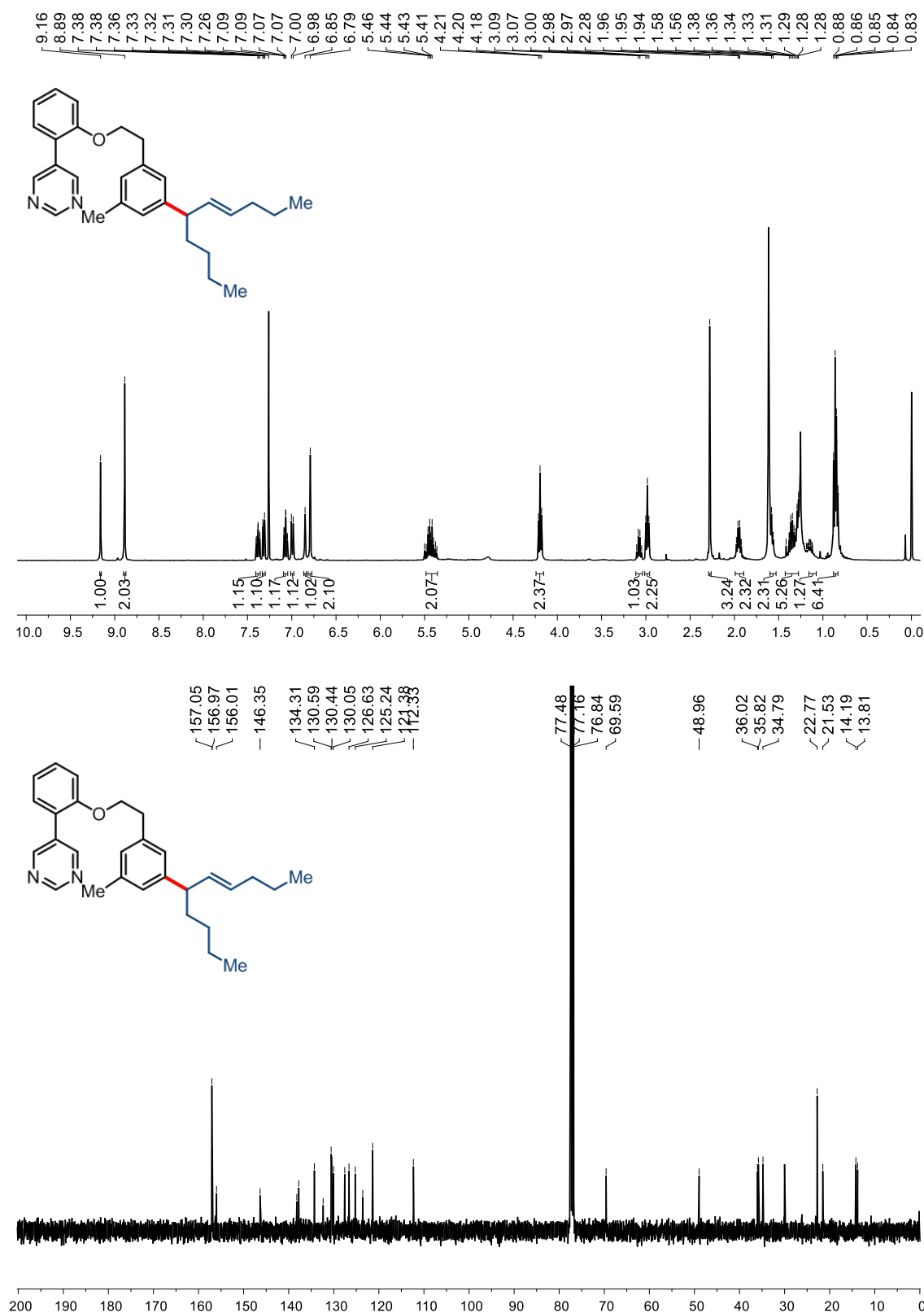


Figure S55. ¹H (top) and ¹³C (bottom) NMR of **5c**

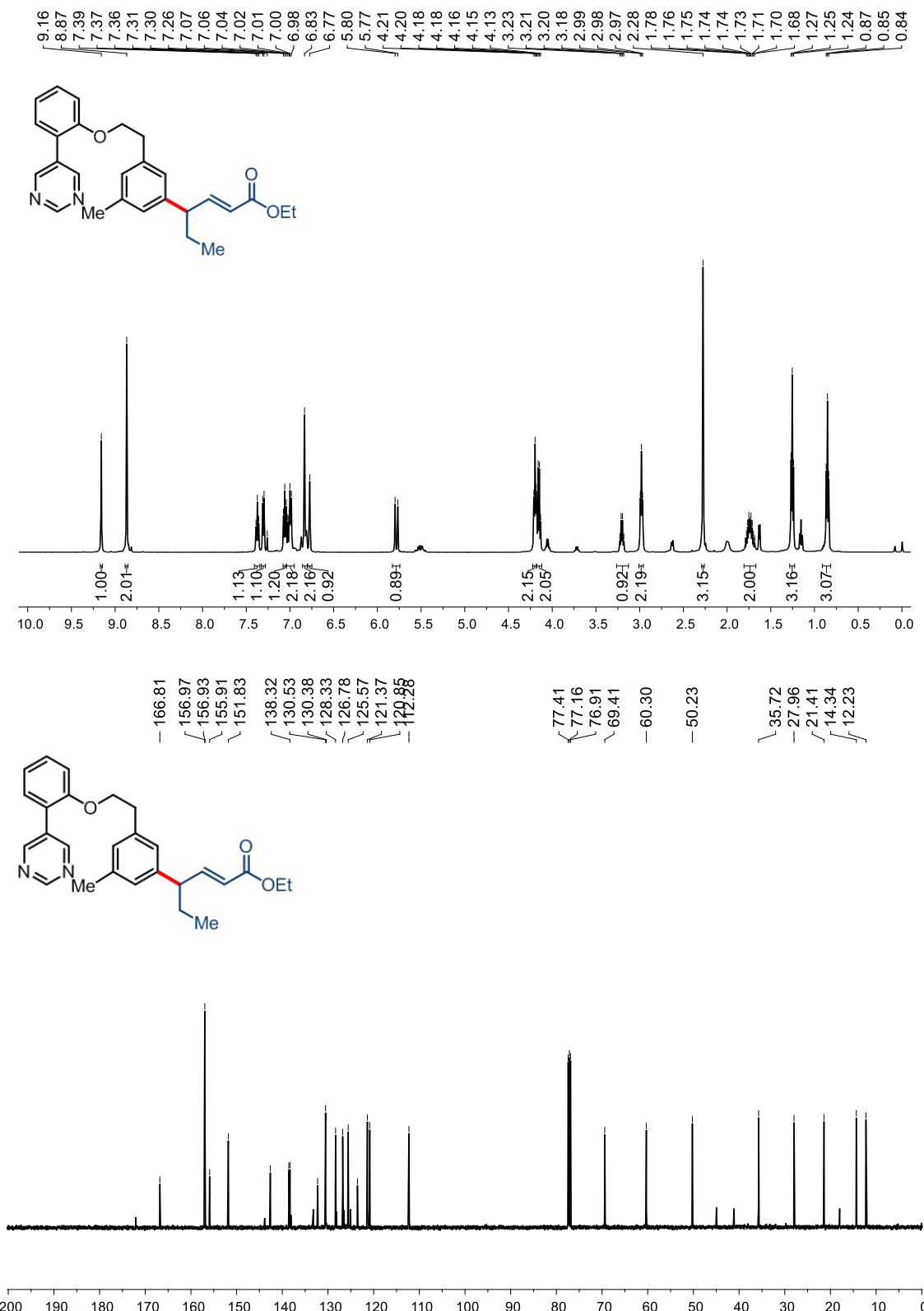
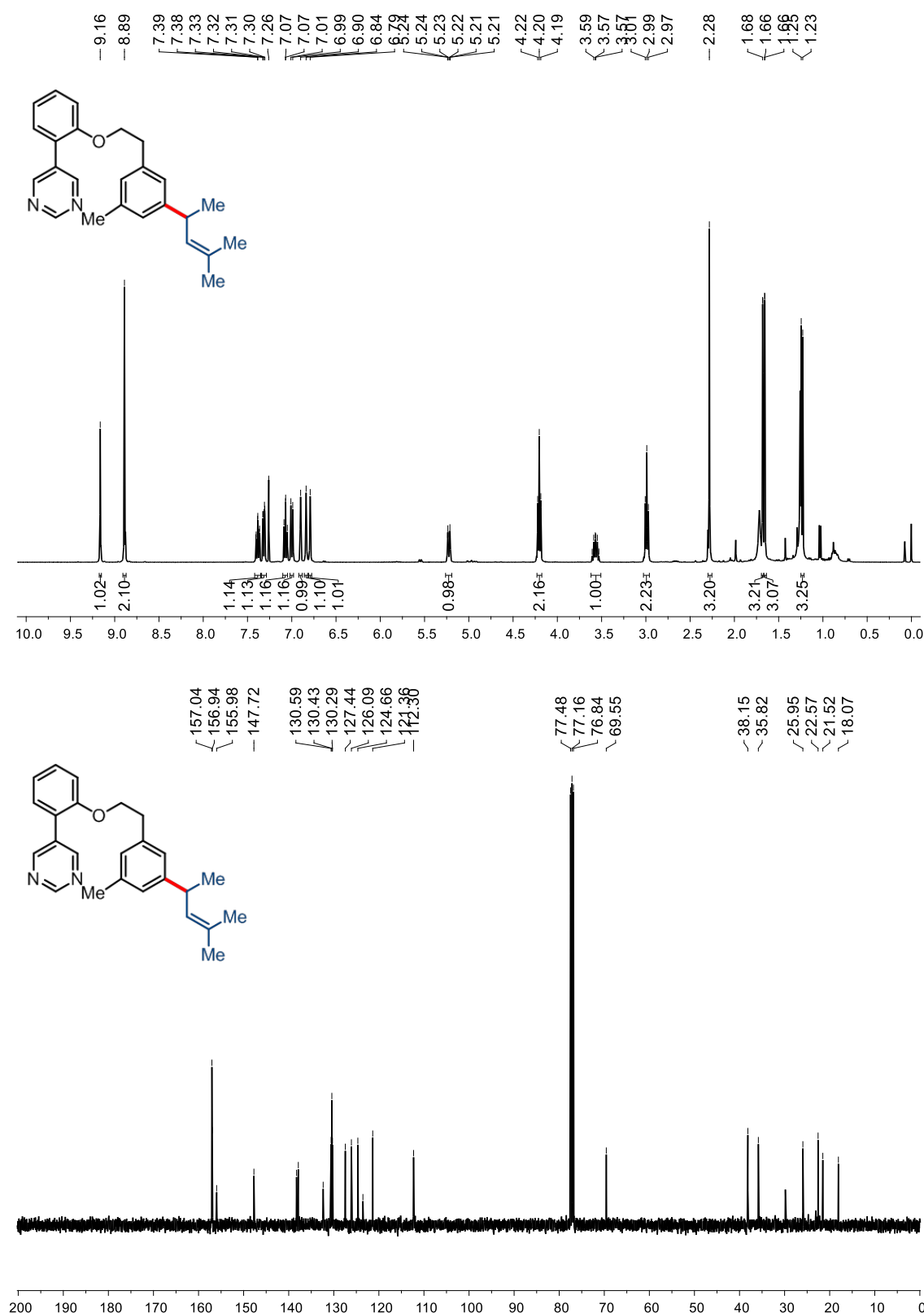


Figure S56. ^1H (top) and ^{13}C (bottom) NMR of **5d**

**Figure S57.** ^1H (top) and ^{13}C (bottom) NMR of **5e**

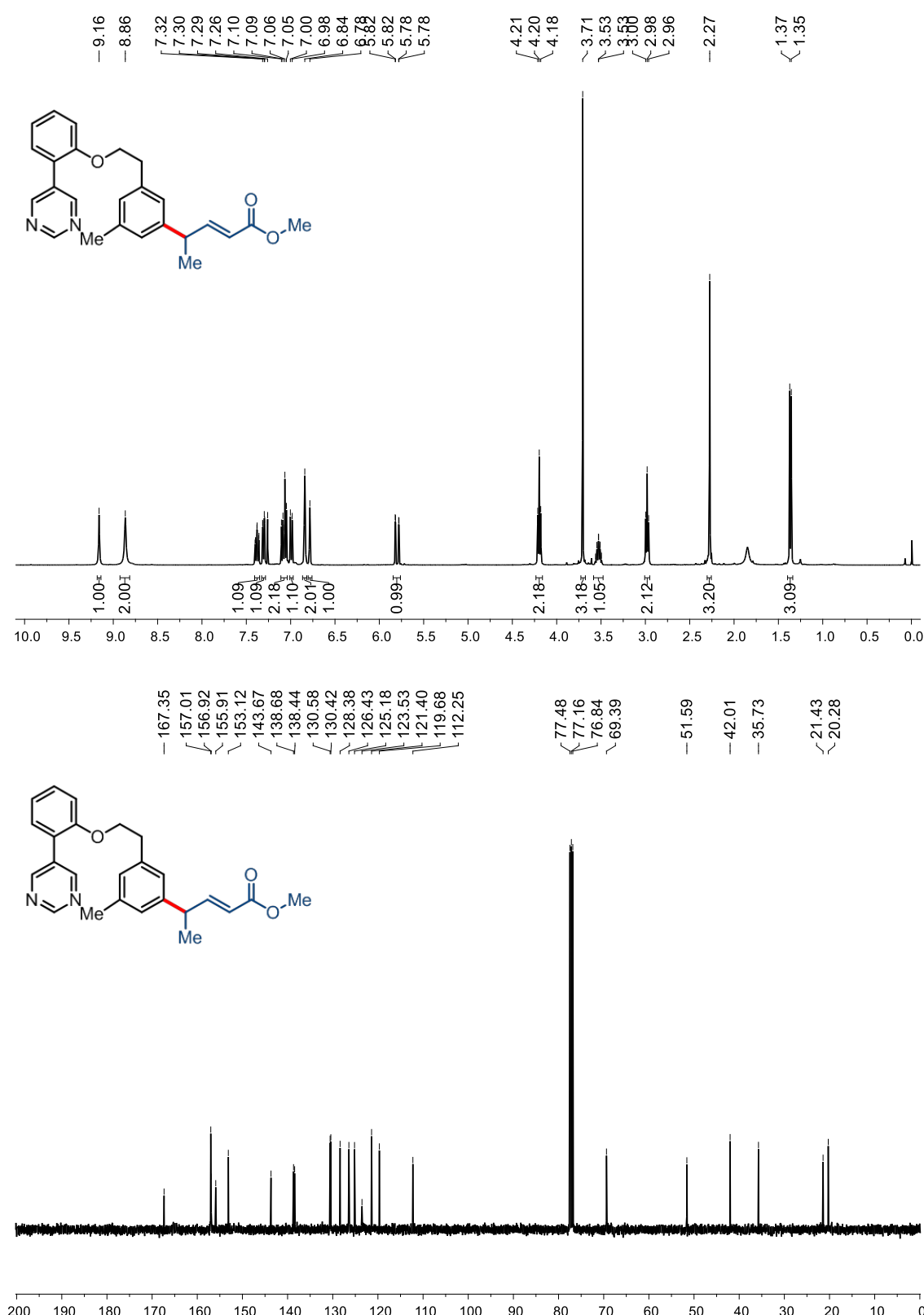


Figure S58. ^1H (top) and ^{13}C (bottom) NMR of **5f**

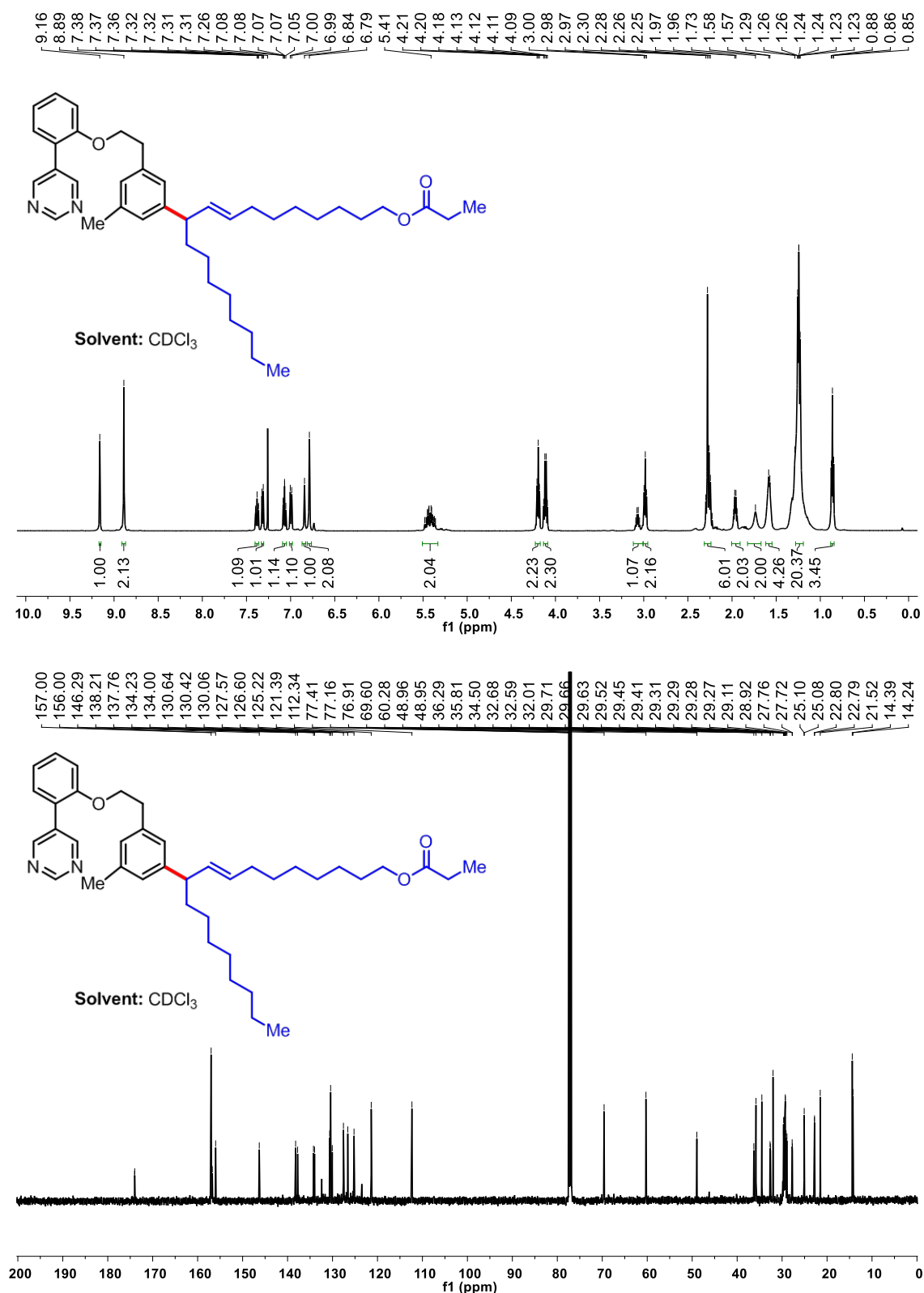


Figure S59. ^1H (top) and ^{13}C (bottom) NMR of **5g**

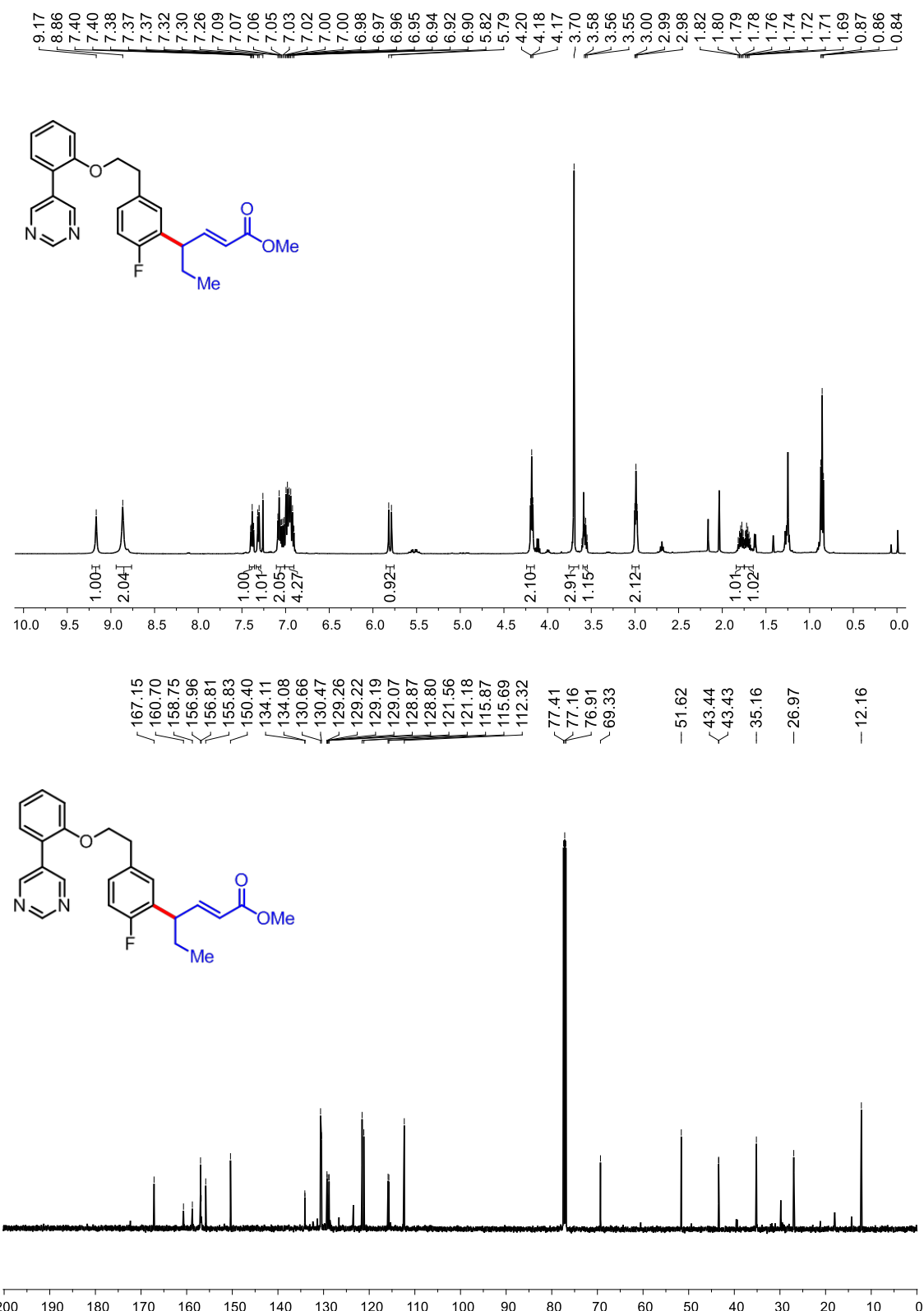


Figure S60. ^1H (top) and ^{13}C (bottom) NMR of **5h**

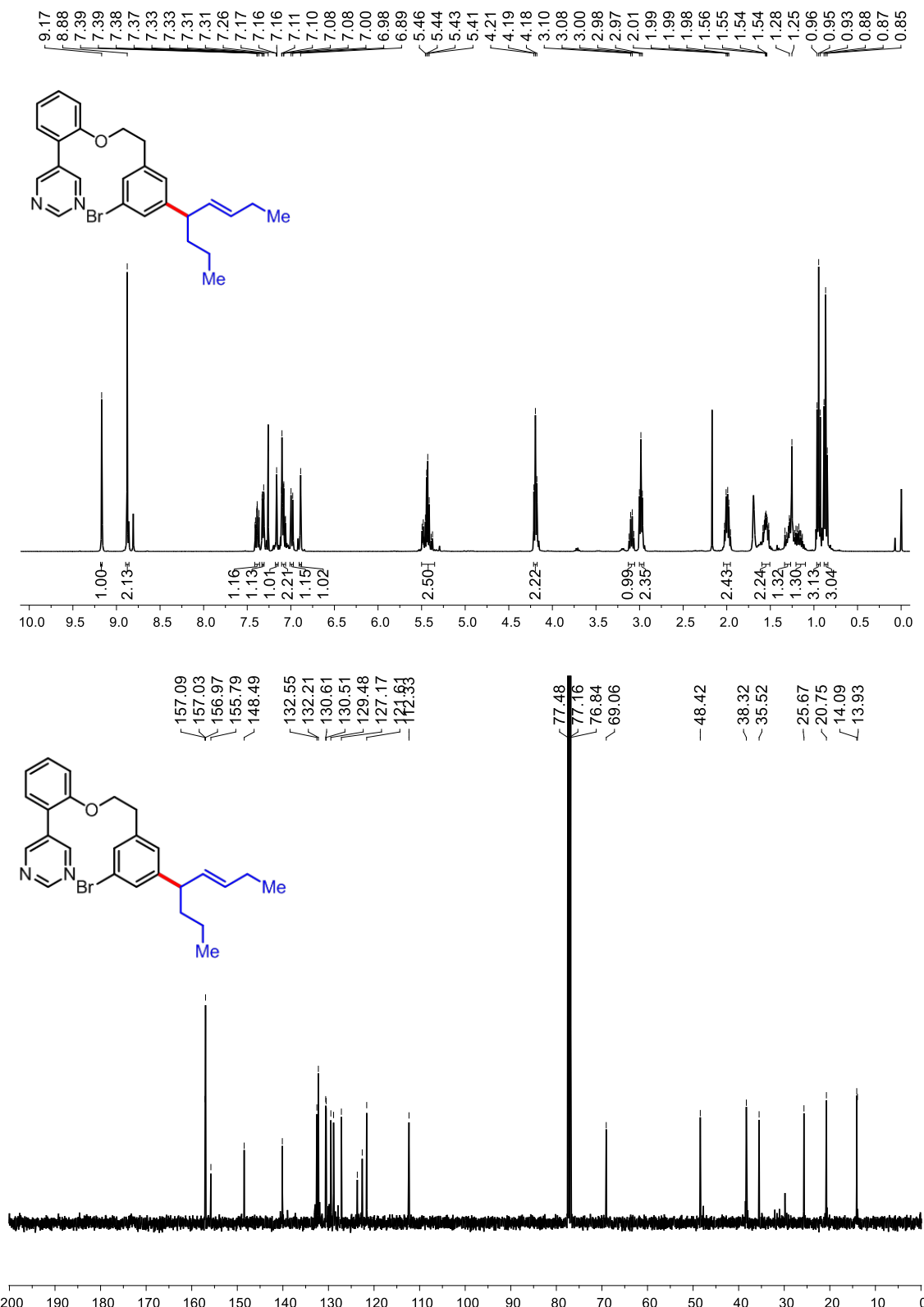


Figure S61. ^1H (top) and ^{13}C (bottom) NMR of **5i**

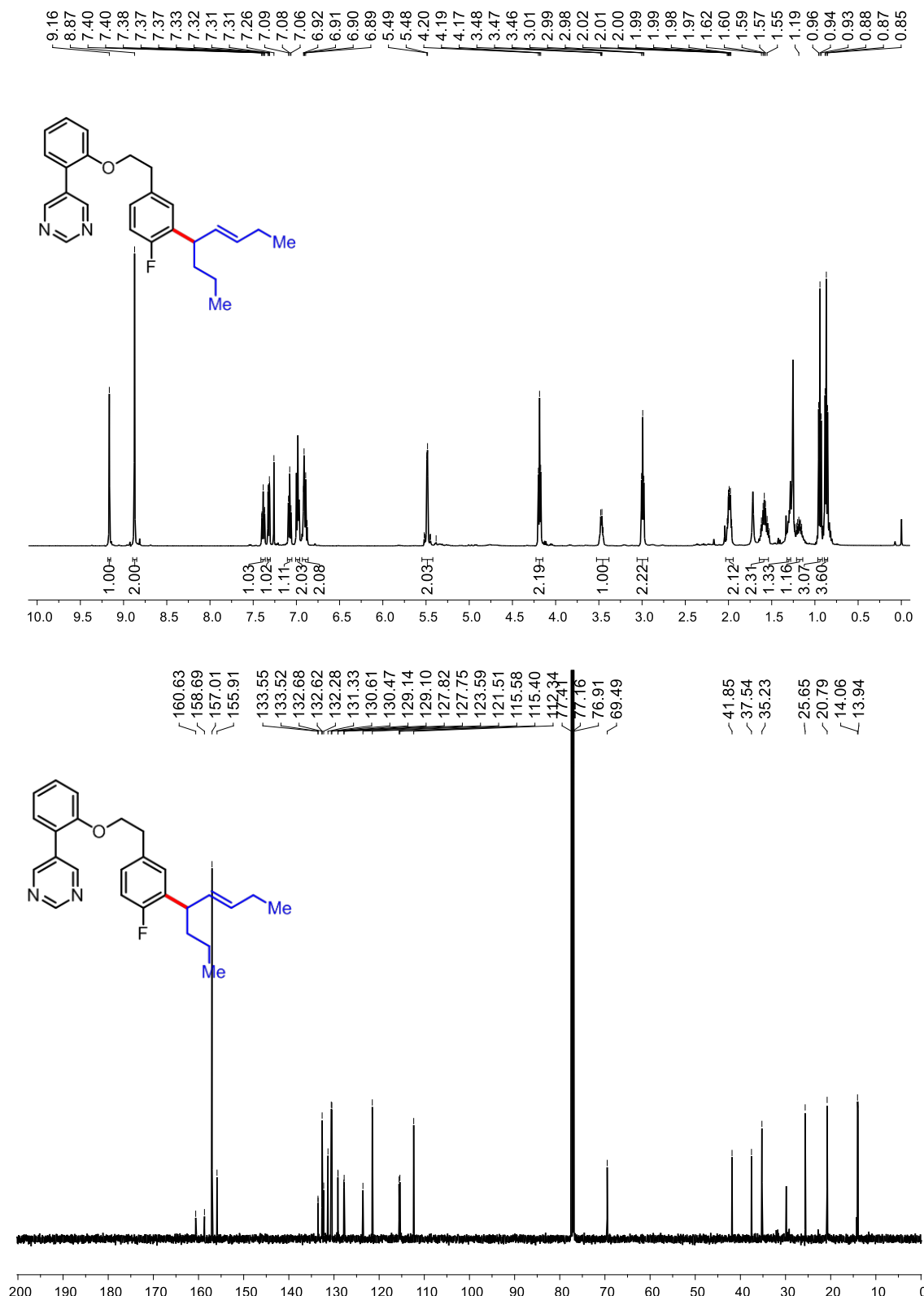


Figure S62. ^1H (top) and ^{13}C (bottom) NMR of **5j**

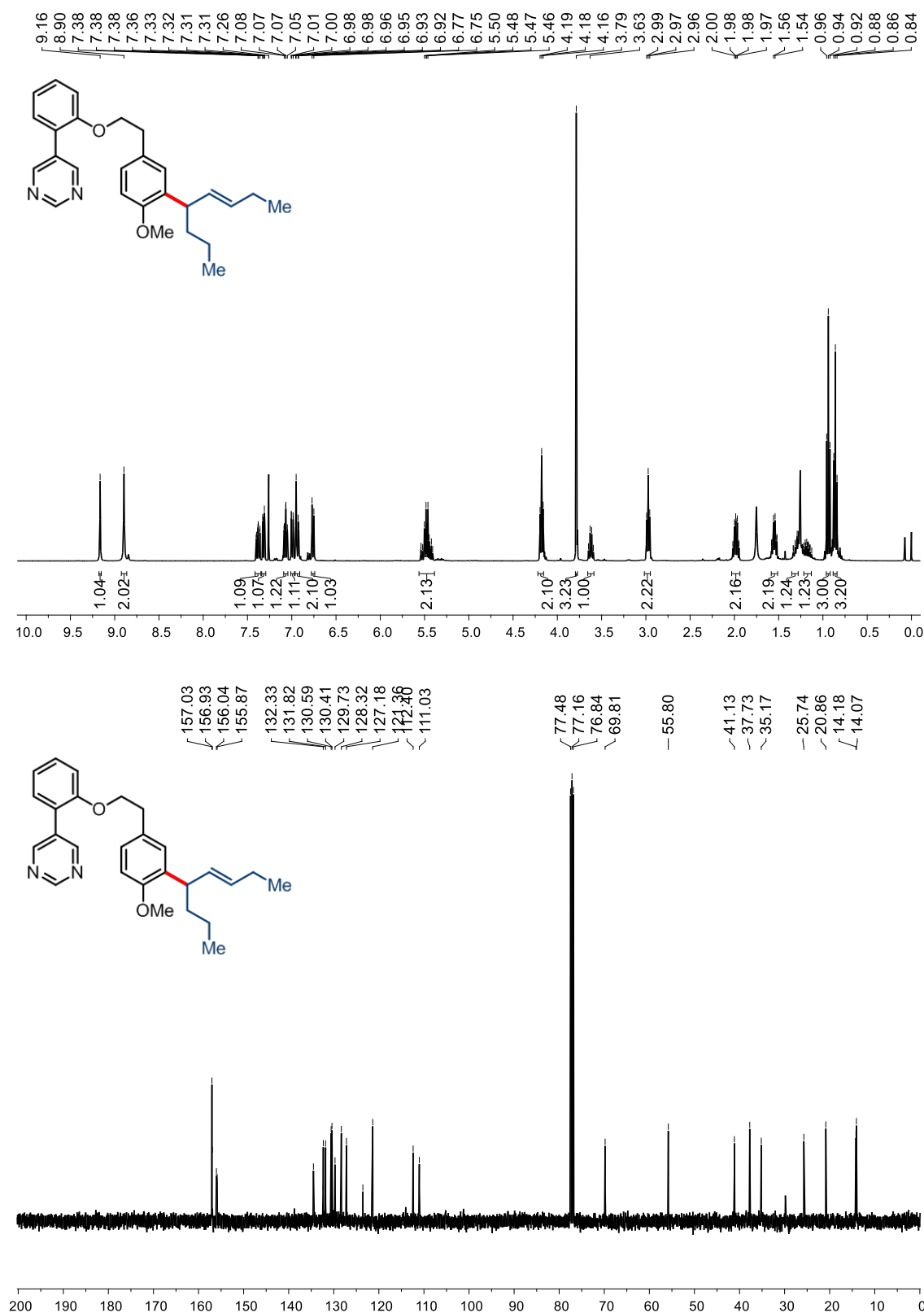


Figure S63. ¹H (top) and ¹³C (bottom) NMR of **5k**

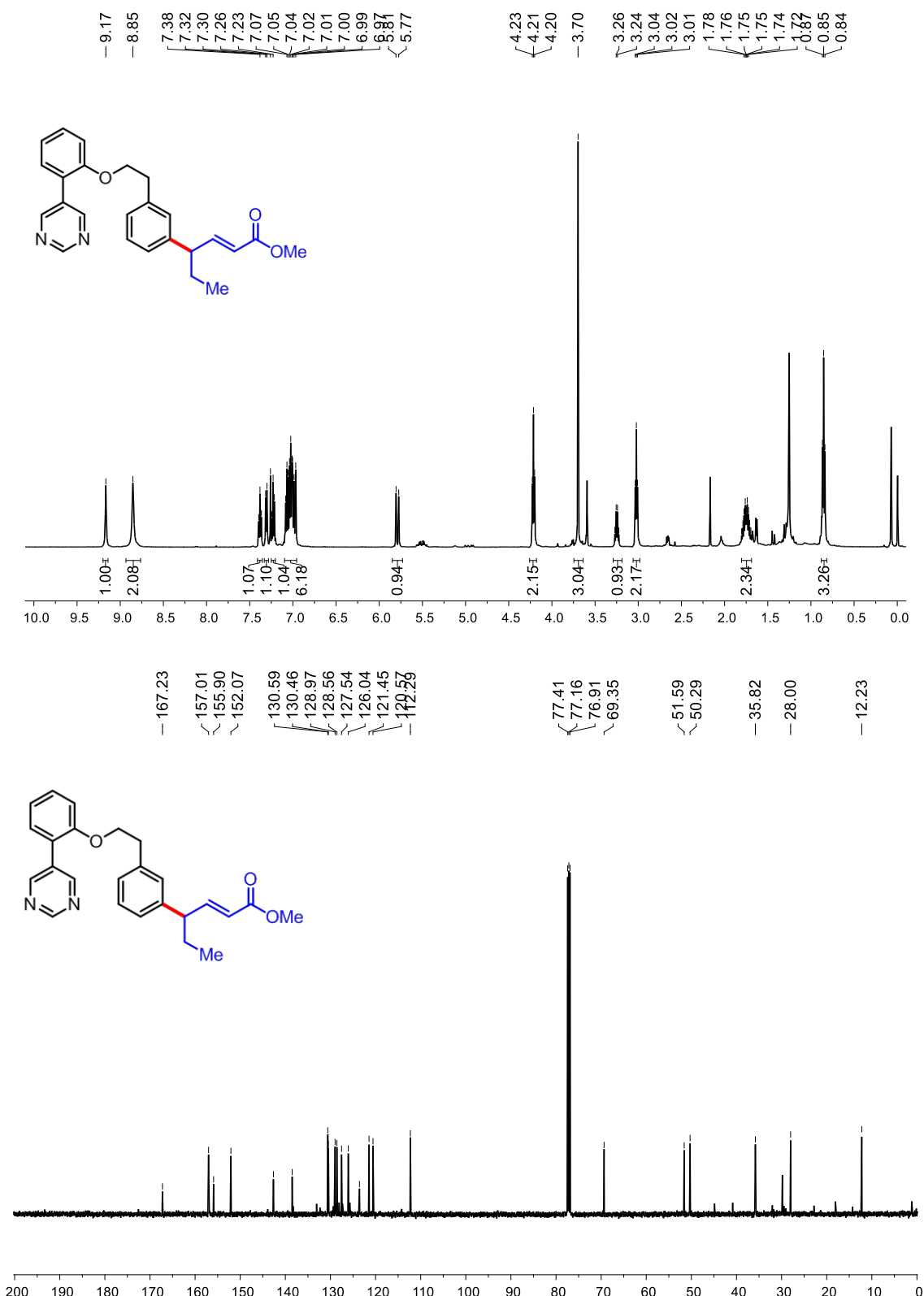


Figure S64. ¹H (top) and ¹³C (bottom) NMR of **5l**

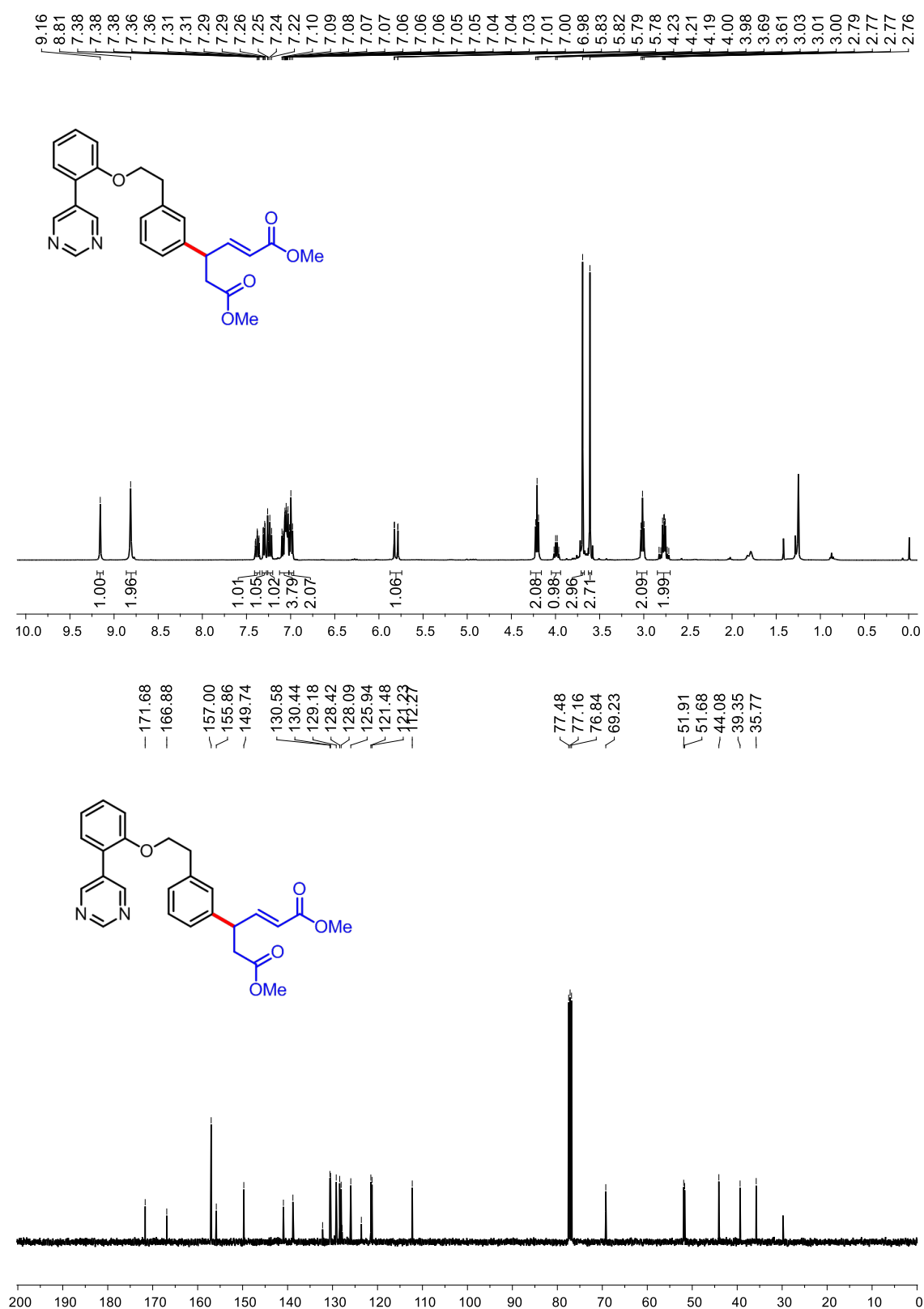
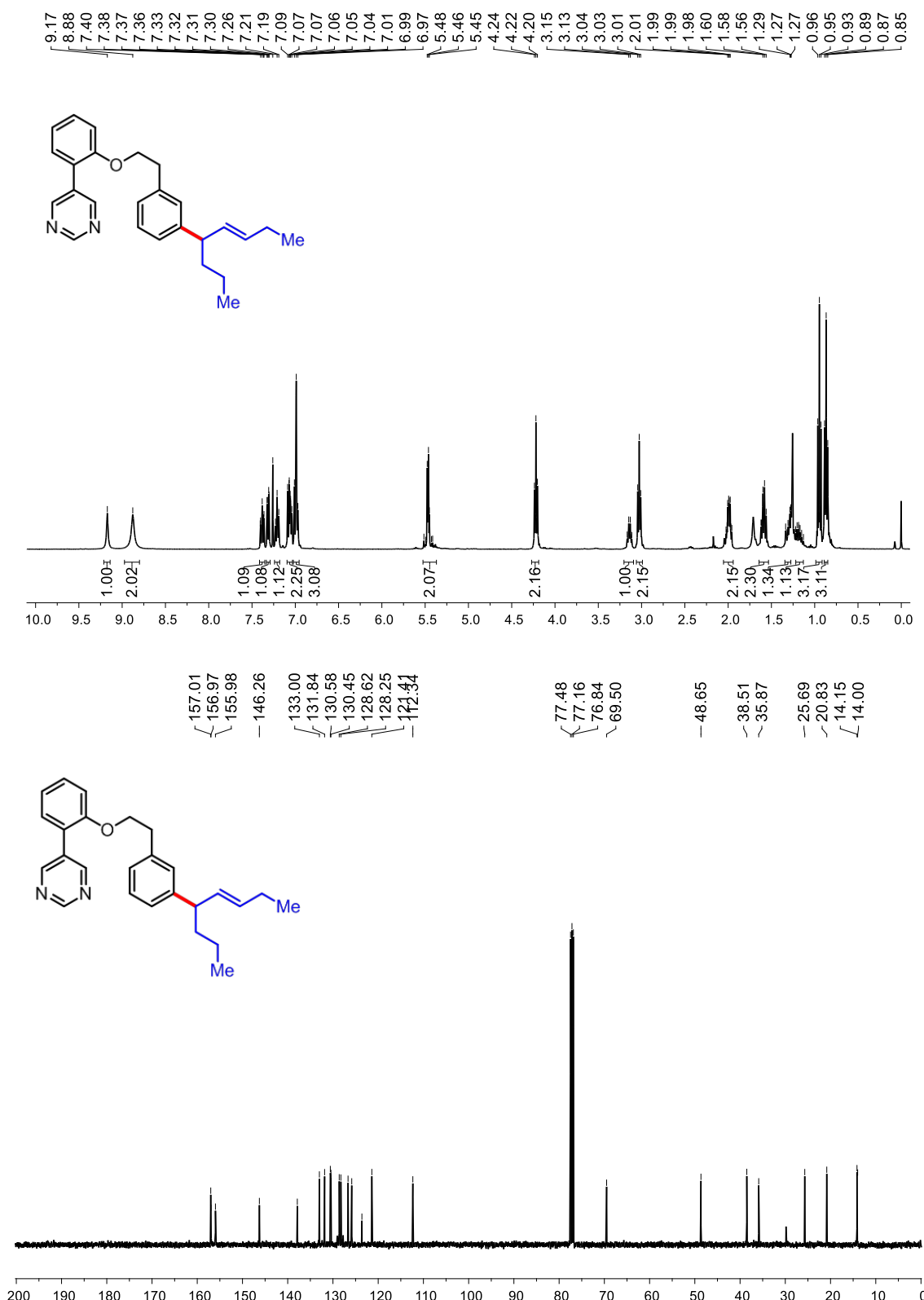
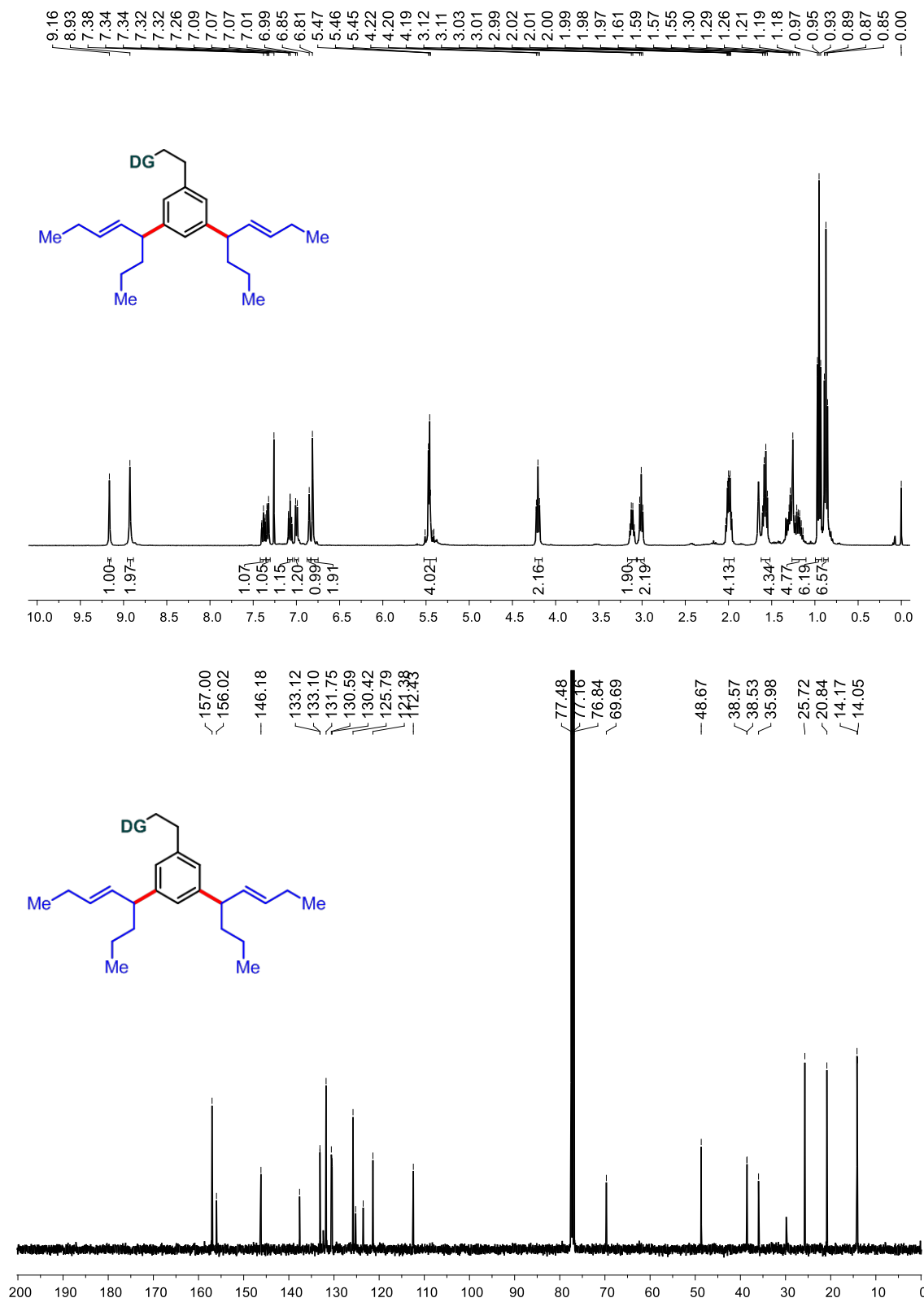


Figure S65. ¹H (top) and ¹³C (bottom) NMR of **5m**

**Figure S66.** ¹H (top) and ¹³C (bottom) NMR of **5n**

**Figure S67.** ¹H (top) and ¹³C (bottom) NMR of **5n'**

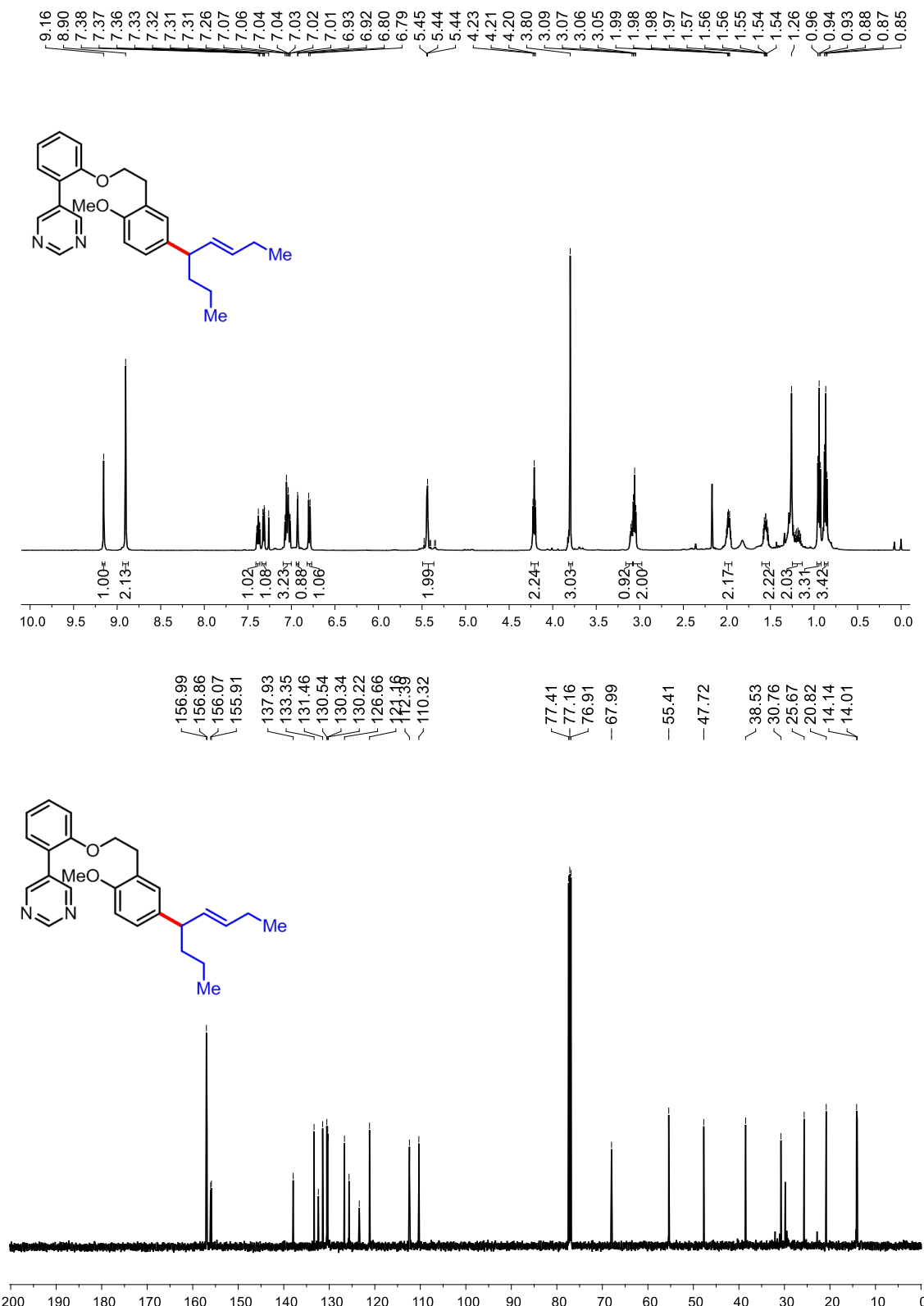


Figure S68. ^1H (top) and ^{13}C (bottom) NMR of **5o**

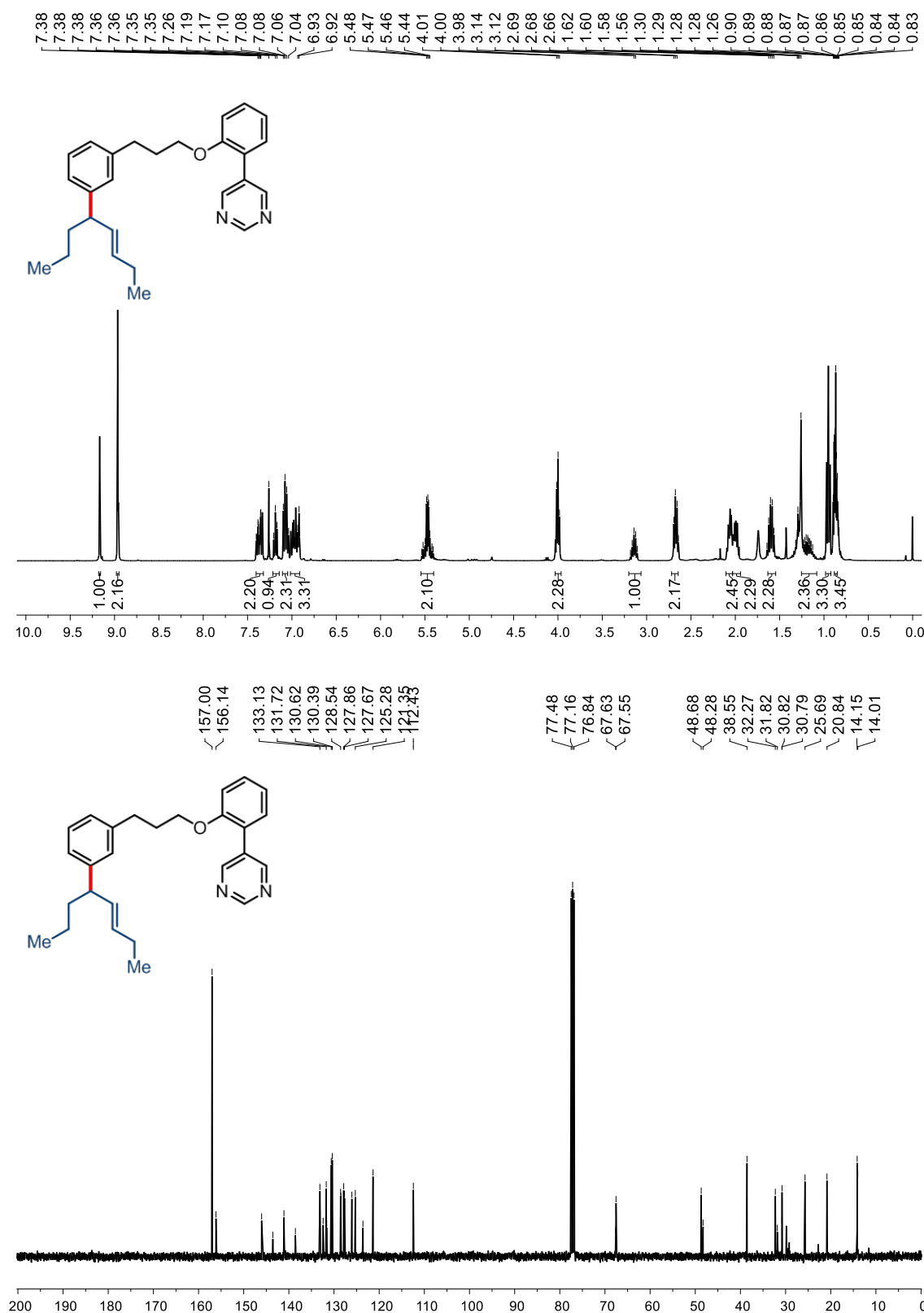
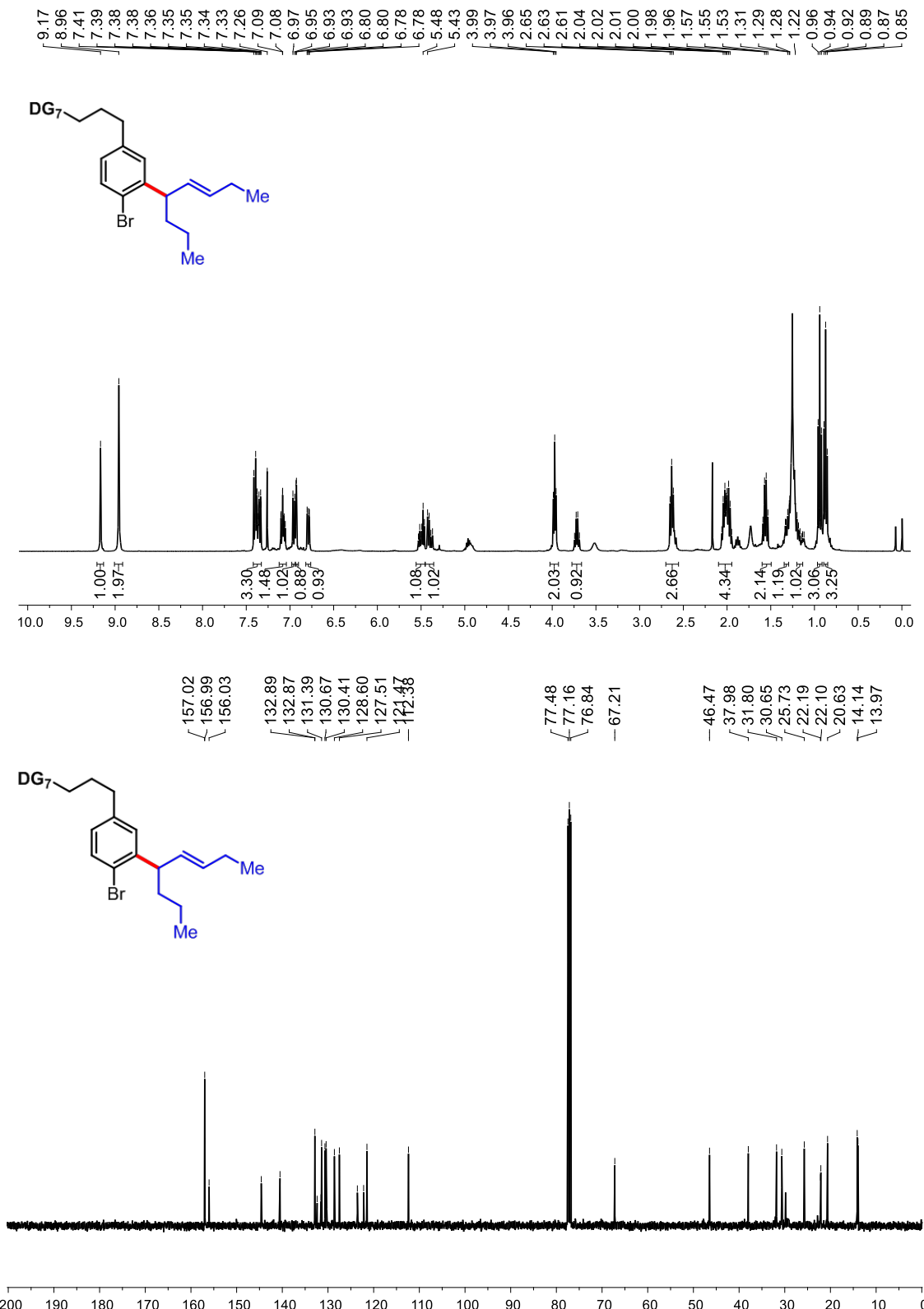


Figure S69. ¹H (top) and ¹³C (bottom) NMR of **5p**

**Figure S70.** ¹H (top) and ¹³C (bottom) NMR of **5q**

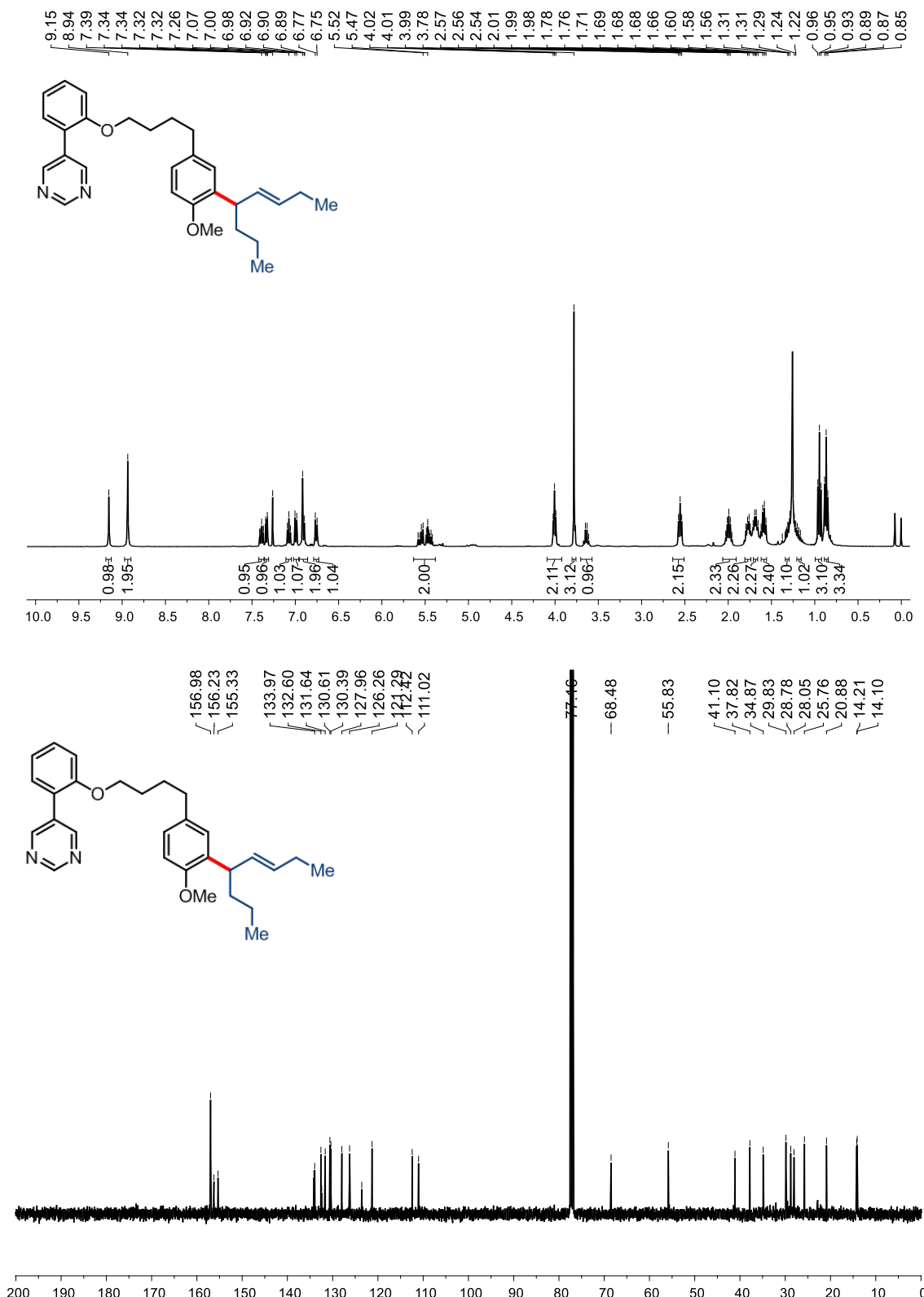


Figure S71. ¹H (top) and ¹³C (bottom) NMR of **5r**

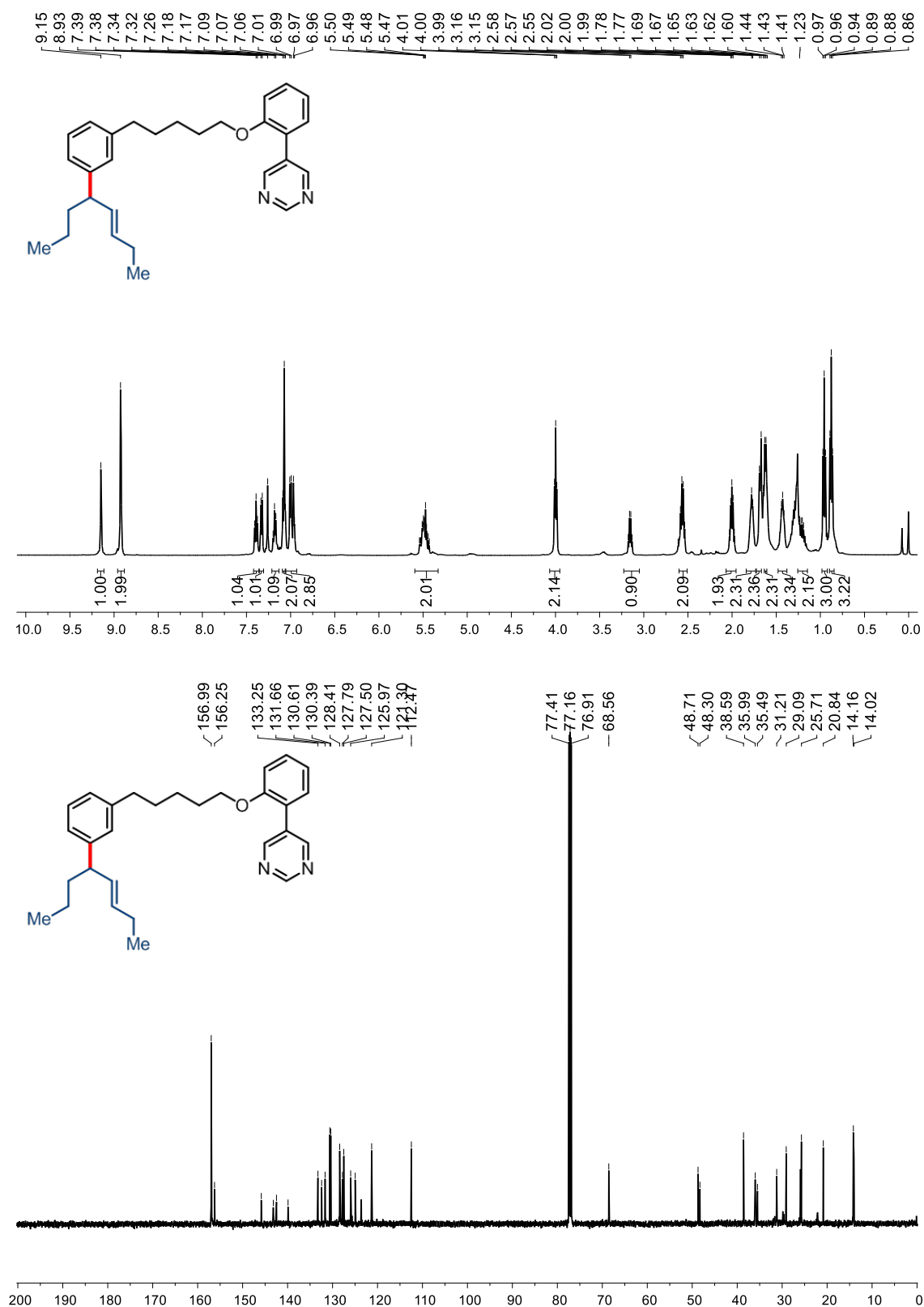


Figure S72. ¹H (top) and ¹³C (bottom) NMR of **5s**

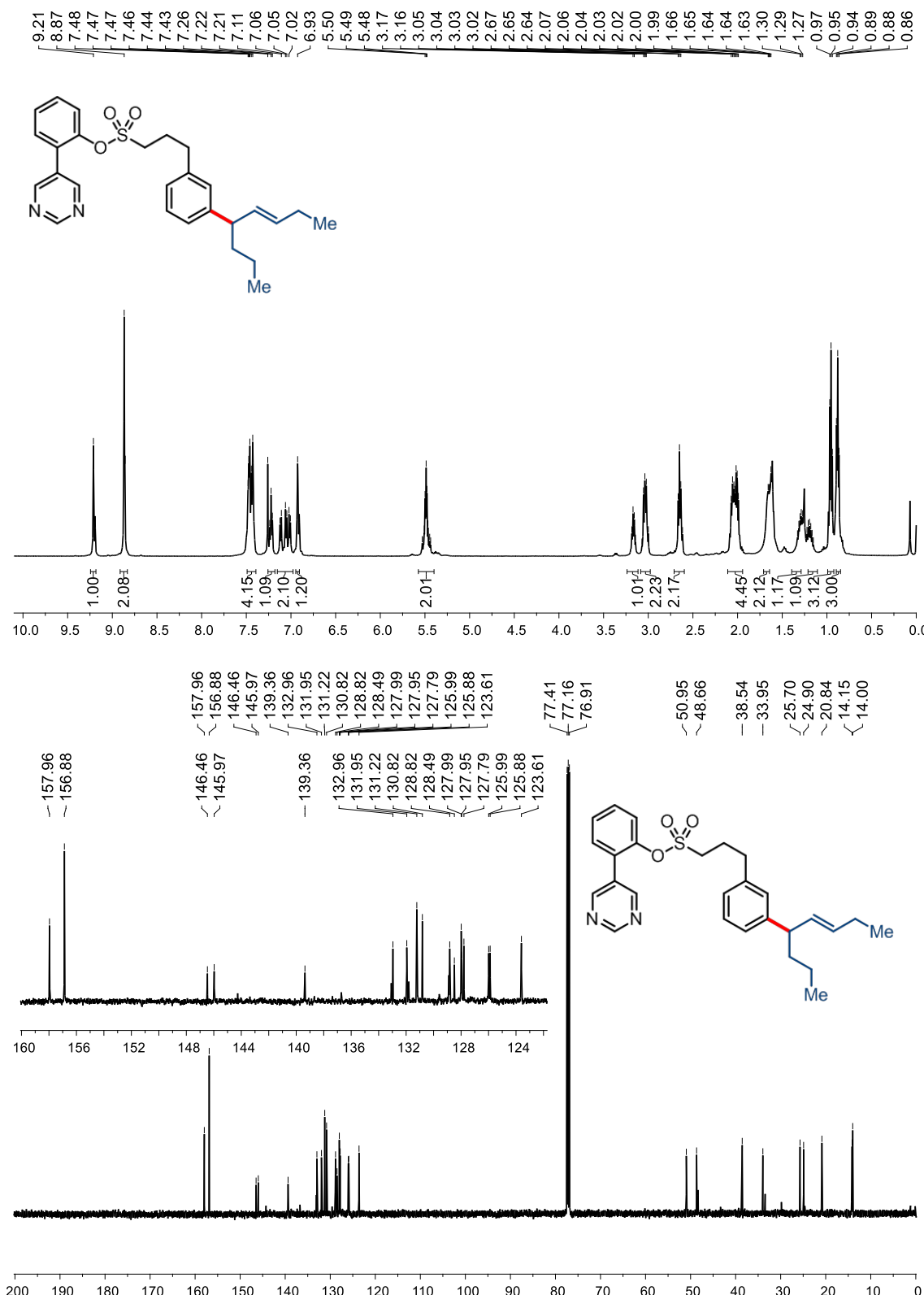
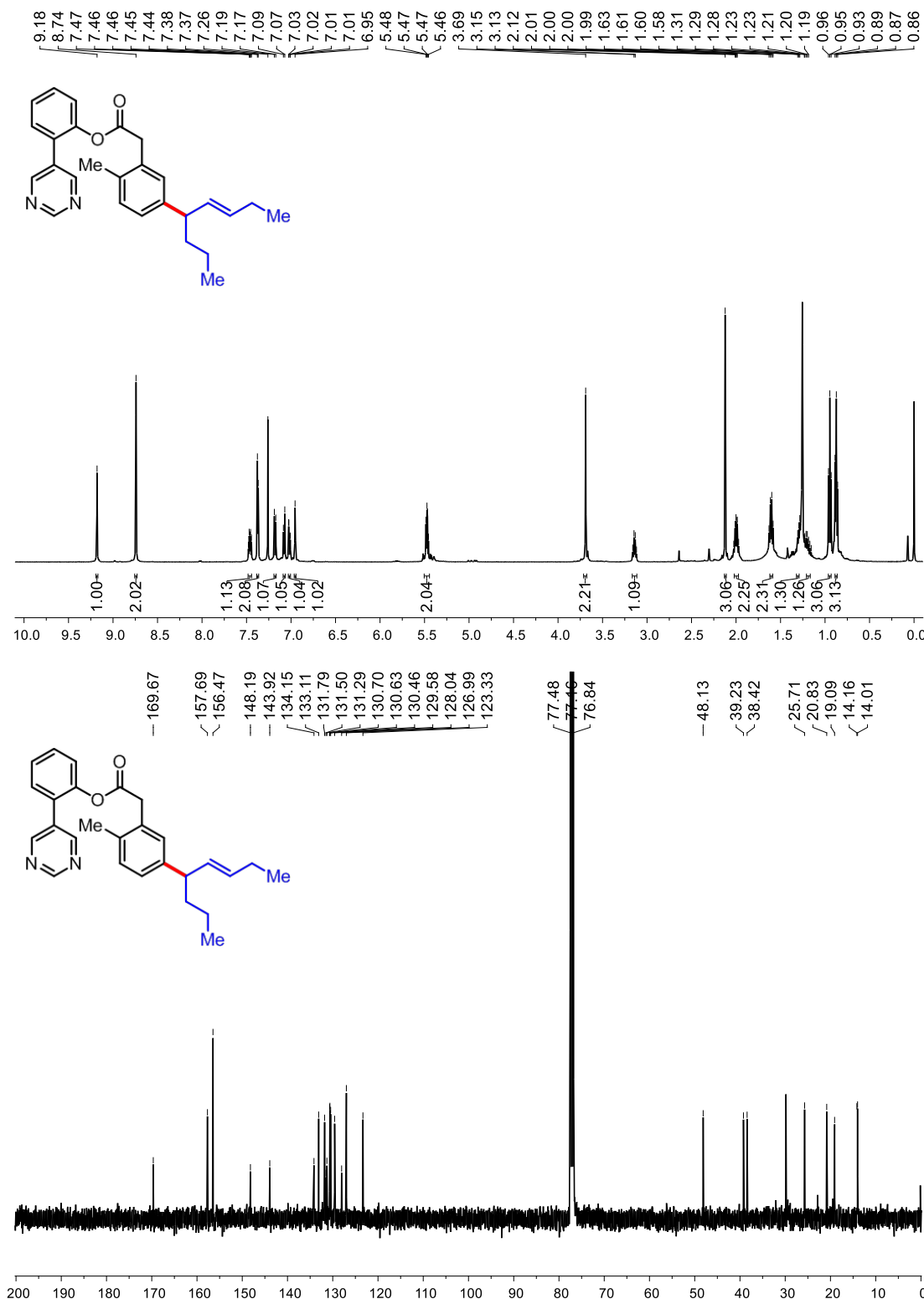


Figure S73. ^1H (top) and ^{13}C (bottom) NMR of **3aa**

**Figure S74.** ^1H (top) and ^{13}C (bottom) NMR of **7a**

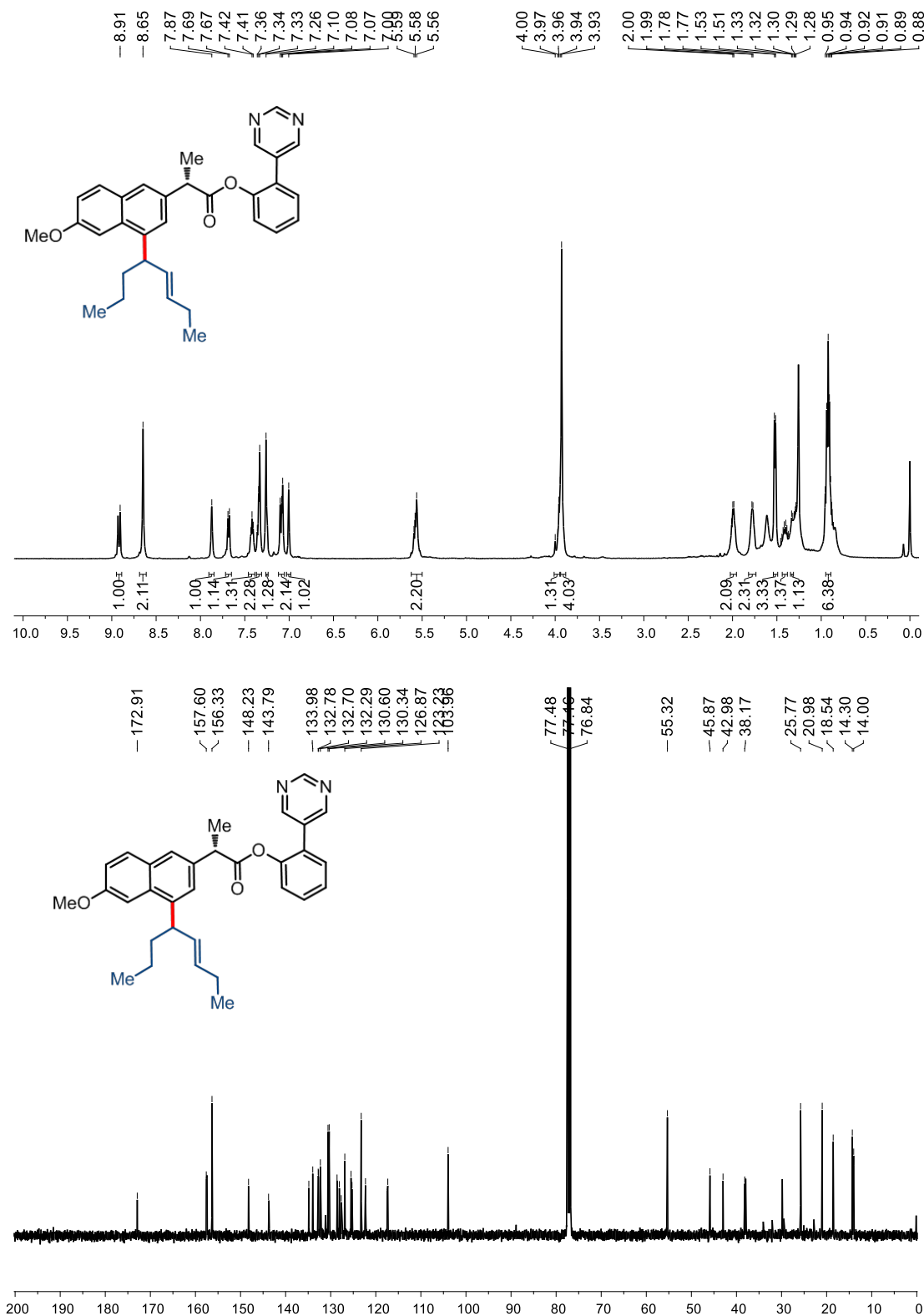
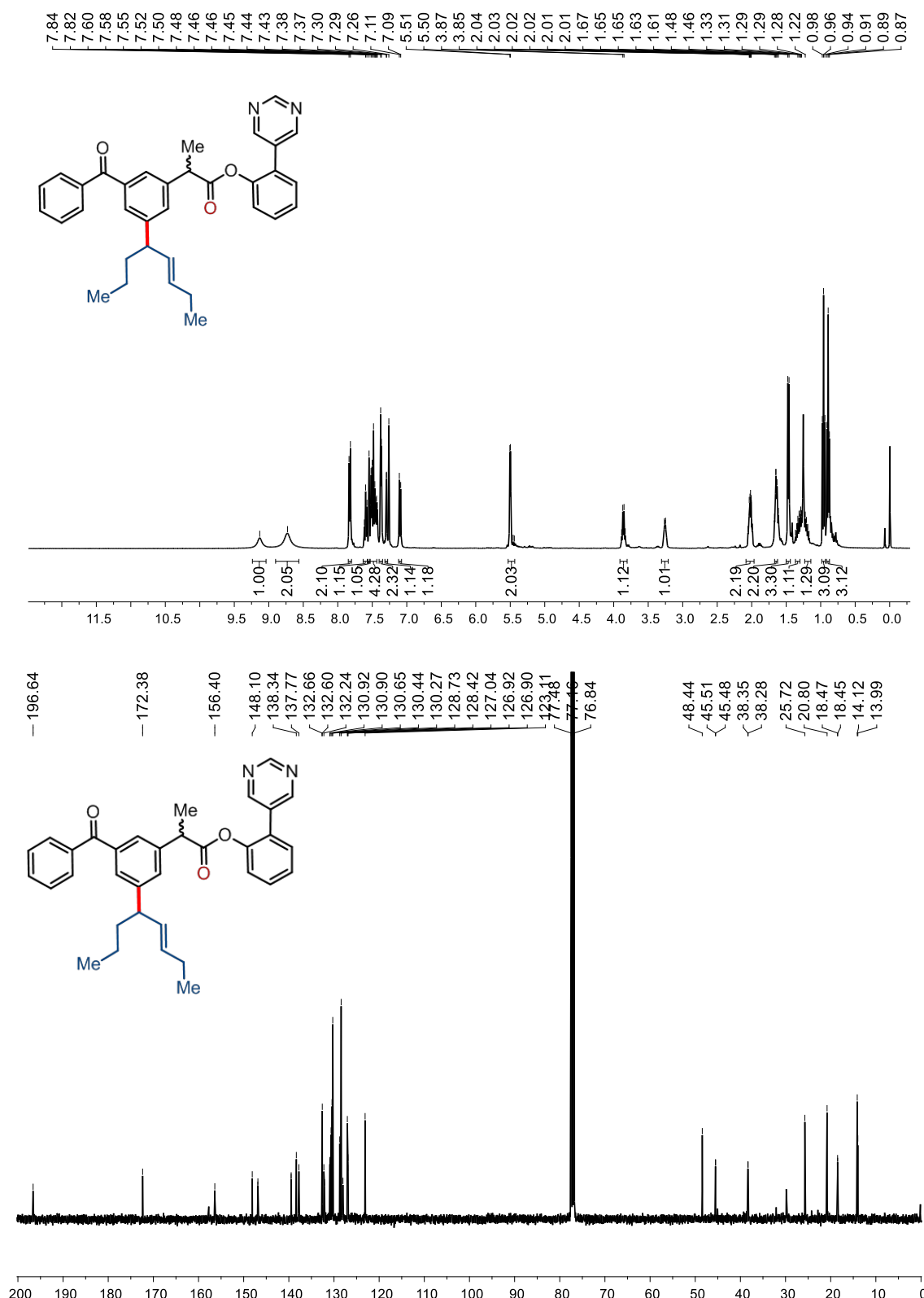


Figure S75. ^1H (top) and ^{13}C (bottom) NMR of **7b**

**Figure S76.** ¹H (top) and ¹³C (bottom) NMR of **7c**

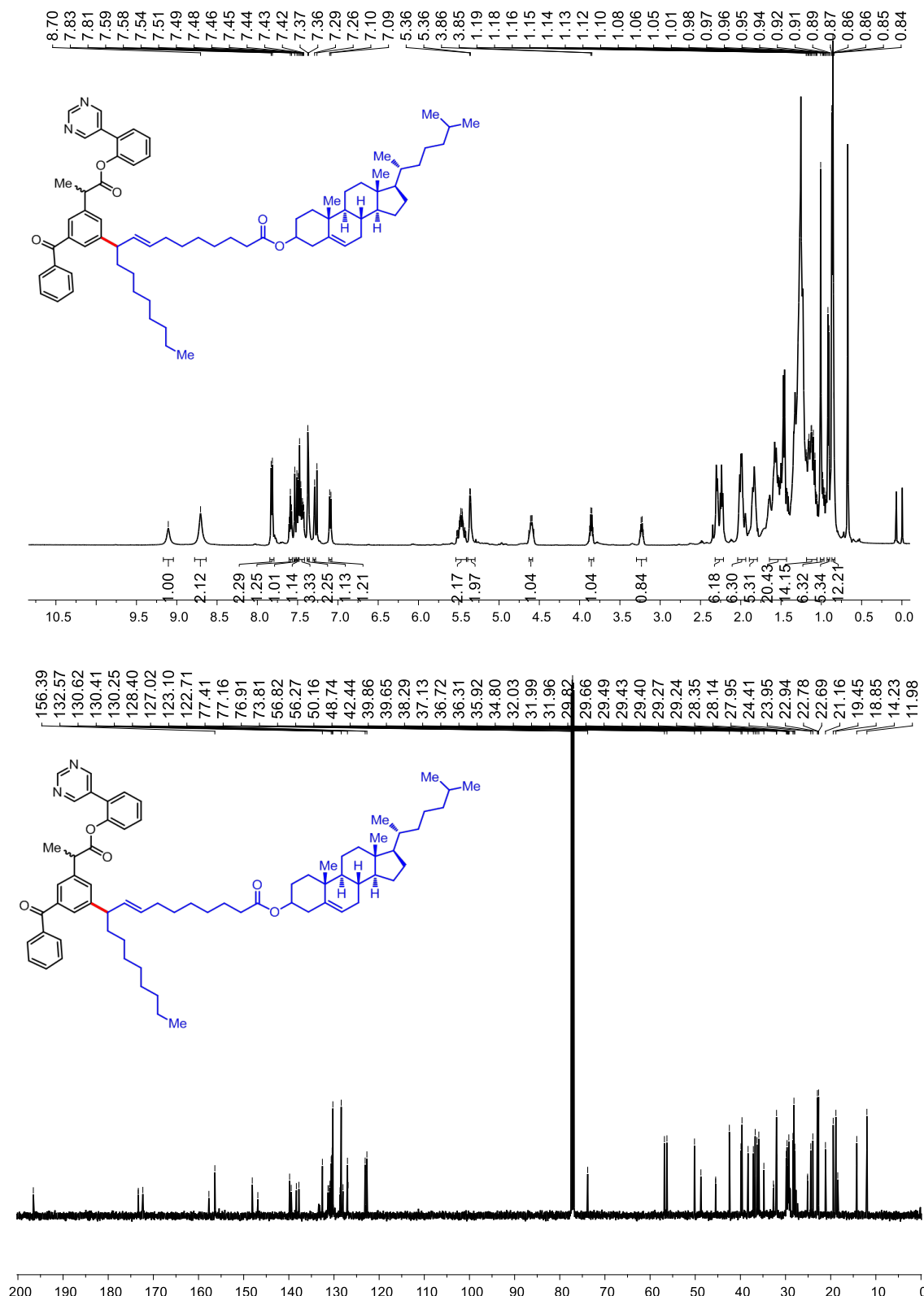


Figure S77. ^1H (top) and ^{13}C (bottom) NMR of **7d**

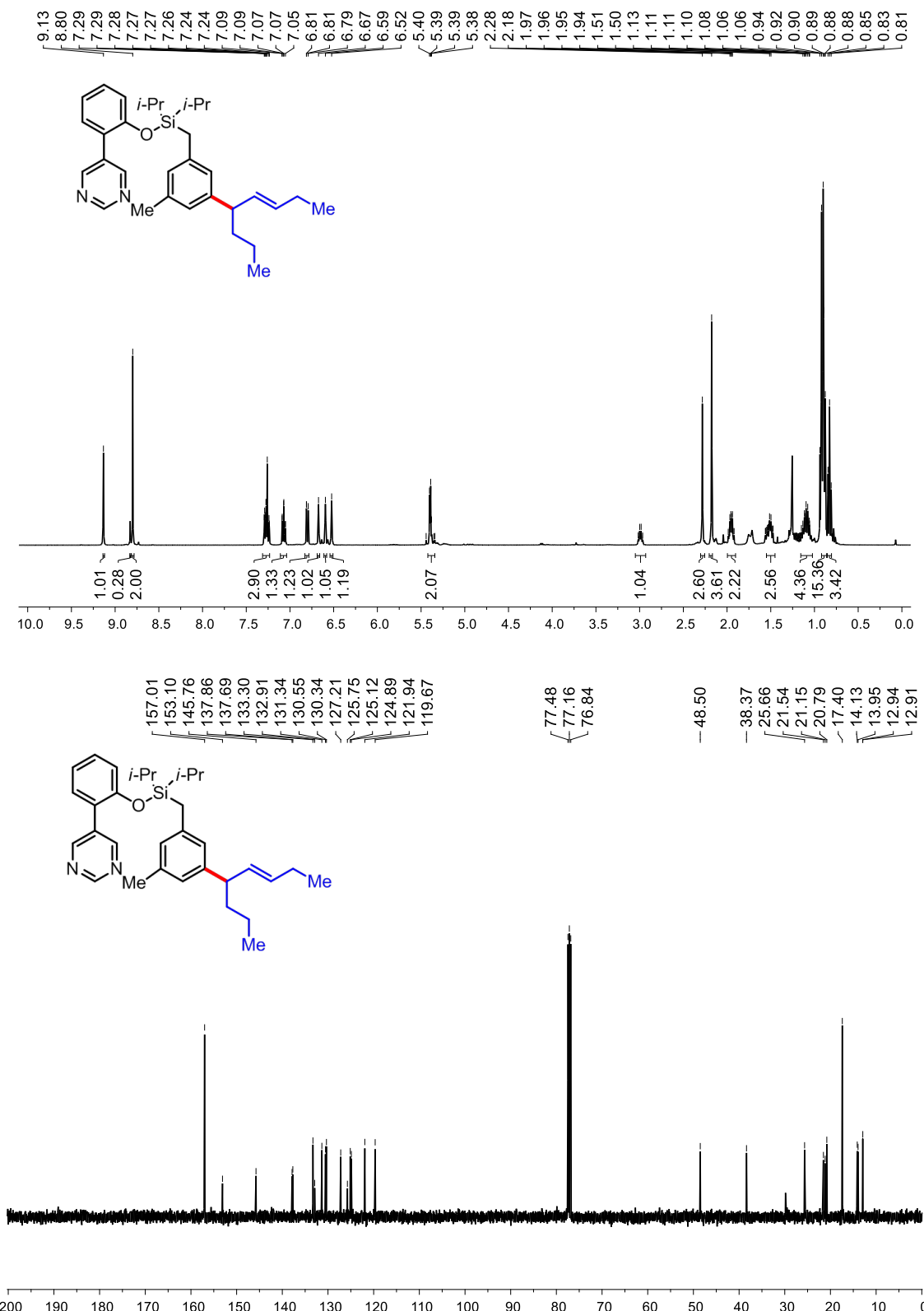
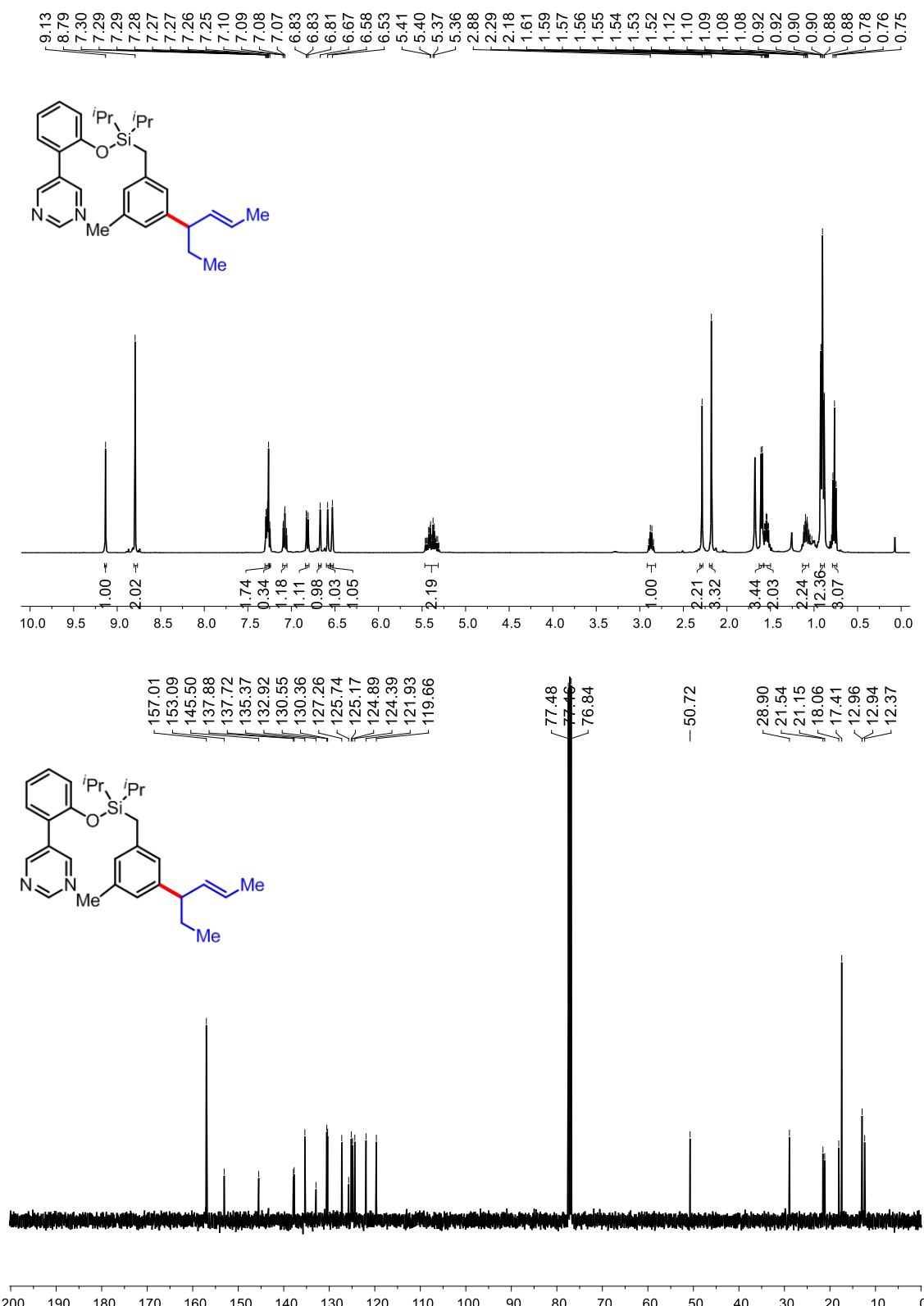


Figure S78. ^1H (top) and ^{13}C (bottom) NMR of **9a**

**Figure S79.** ¹H (top) and ¹³C (bottom) NMR of **9b**

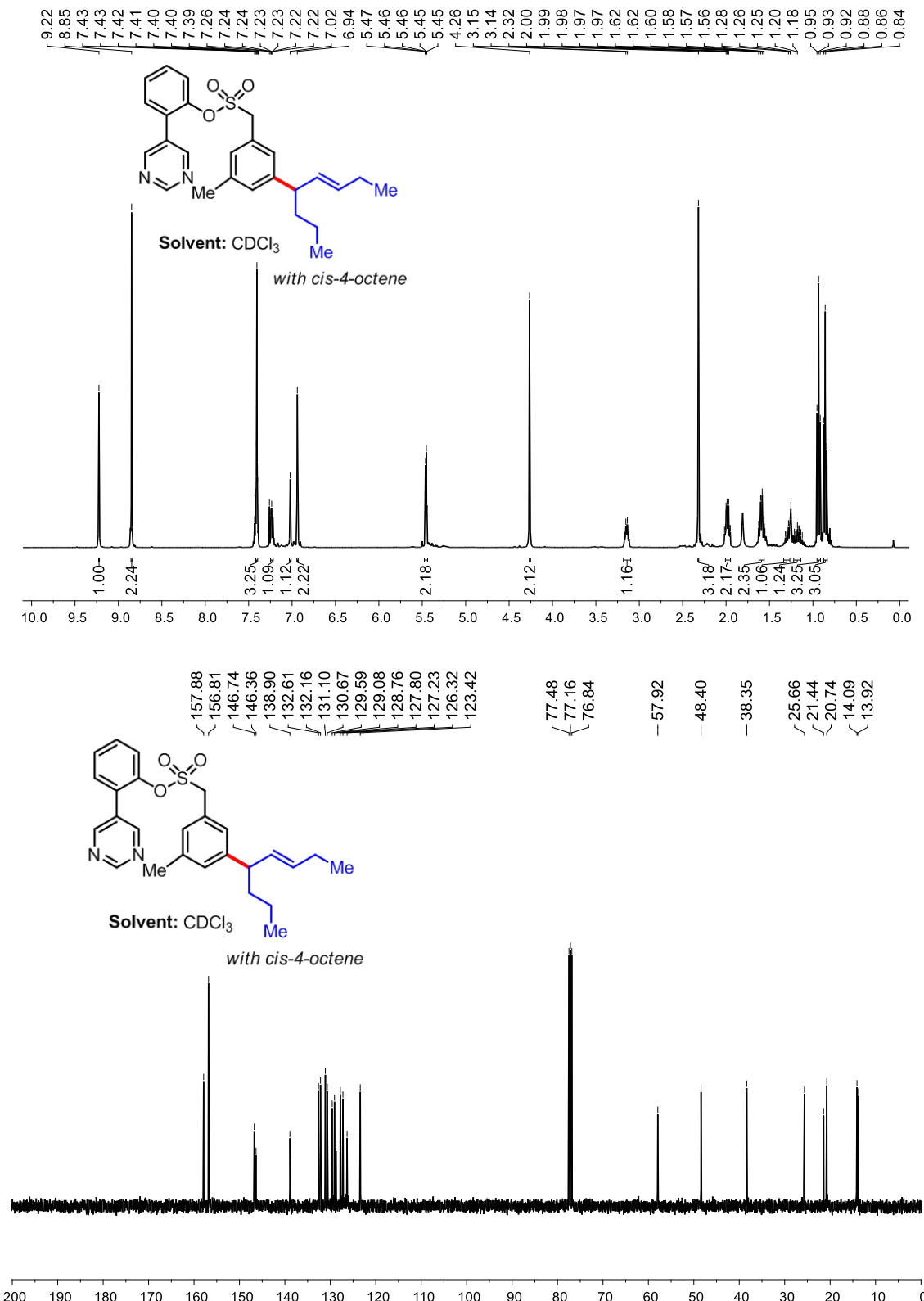


Figure S80. ^1H (top) and ^{13}C (bottom) NMR of **3a** (with *cis*-4-octene)